

**The characterisation of Late Embryogenesis Abundant 5 and Ethylene
Responsive Factor 109 functions in plants growth and stress tolerance**

Daniel Steven Shaw

Submitted in accordance with the requirements for the degree of Doctor of Philosophy

The University of Leeds

September 2016

The candidate confirms that the work submitted is their own, except where work which has formed part of jointly authored publications has been included. The contribution of the candidate and the other authors to this work has been explicitly indicated below. The candidate confirms that appropriate credit has been given within the thesis where reference has been made to the work of others.

Shaw, D.S., Meitha, K., Considine, M.J. and Foyer, C.H. Mitochondrial respiration and oxygen tension. *in press*. 2016.

This copy has been supplied on the understanding that it is copyright material and that no quotation from the thesis may be published without proper acknowledgement.

© 2016 The University of Leeds and Daniel Steven Shaw

Acknowledgements

Firstly, I give thanks to my supervisor, Christine H. Foyer, for her guidance throughout my studentship. I also give thanks to all members of the research groups that I had the privilege to spend time with while working in Leeds. I particularly thank group members James Cooper and Ambra de Simone who provided interesting discussions and joyous times filled with laughter.

I extend my gratitude to the BBSRC and to Bayer CropScience for funding my research and for their support; I especially thank Korneel Vandenbroucke who was a great supervisor and colleague at Bayer CropScience in Ghent, Belgium.

Many thanks go to the Geert De Jaeger lab group at VIB for their guidance, and support in performing the tandem affinity purifications and analysis of the purified protein complexes.

Above all, I would like to thank my family, my friends, and Victoria Bueno Gonzalez for all the love and support they have provided me with.

“Science, my lad, is made up of mistakes, but they are mistakes which it is useful to make, because they lead little by little to the truth”.

-Jules Verne

Abstract

Understanding plant responses to environmental stresses is a key strategy to meet the challenges of food security, adequate nutrition and sustainable agriculture. Environmental stresses limit plant growth and crop yields. In this thesis, the roles of Late Embryogenesis Abundant 5 (LEA5) and Ethylene Responsive Factor 109 (ERF109) in plant growth and stress tolerance were investigated. These two genes are involved in the regulation of plant redox processes. LEA5 was previously shown to provide tolerance to oxidative stress. Furthermore, previous studies using transgenic *A. thaliana* found that the over-expression of *LEA5* resulted in plants with a greater biomass. However, the precise functions of *LEA5* in these processes are unknown. In this thesis, genetic and protein interaction approaches were used to investigate the role of *LEA5*. Protein interaction studies, which used tandem affinity purification (TAP) of protein complexes combined with mass-spectrometry revealed several *LEA5* interacting partners, including genes associated with stress tolerance. Transgenic crops provide a promising avenue to reduce yield losses, improve growth. Homozygous transgenic barley plants expressing *LEA5* were found to have an altered shoot phenotype compared to WT barley plants.

ERF109 is part of a regulatory network that has a major role in the adjustment of *A. thaliana* leaves to reach homeostasis after high-light stress. Understanding the roles of transcriptional regulatory networks and their effects on downstream target genes will aid in the development of stress tolerant crops. Phenotype analysis of *erf109* mutants presented here suggest that *ERF109* has a role in the control of shoot growth in the absence of stress. Moreover, protein interactions of *ERF109* were elucidated using TAP, a number of which might explain the phenotypic characteristics of the *erf109* mutants. Taken together, this information could be used in breeding programmes to improve the predictability and sustainability of crop yields by enhancing stress tolerance.

Contents

Chapter 1. Introduction	1
1.1. The challenge.....	1
1.2. Stress tolerance of plants	1
1.3. LEA proteins.....	2
1.3.1. LEA protein structures	2
1.3.2. LEA proteins can protect enzymes in non-optimal metabolic conditions	3
1.4. LEA5	3
1.5. Mitochondria	5
1.5.1. Mitochondrial targeting signals.....	7
1.5.2. Protein insertion into the inner mitochondrial membrane.....	7
1.6. Respiration.....	9
1.6.1. Respiration: Step 1 - Glycolysis.....	9
1.6.2. Respiration: Step 2 - The Krebs cycle.....	11
1.6.3. Respiration: Step 3 - The electron transport chain.....	11
1.6.4. Respiration: Step 4 - ATP synthesis.....	13
1.7. Reactive Oxygen Species	15
1.8. Mitochondria-to-nucleus communication.....	15
1.9. Chloroplast to nucleus communication	16
1.10. Transcription factors of the ethylene responsive factor family	16
1.11. ERF109	17
1.12. Summary	18
1.13. Aims and objectives.....	19
Chapter 2. Materials and Methods	20
2.1. Arabidopsis plant material and growth analysis	20
2.1.1. Plant material.....	20
2.1.2. <i>In vitro</i> shoot growth and stress treatments.....	20
2.1.3. Shoot growth on soil and drought experiments.....	21
2.1.4. Determination of rosette area	21
2.1.5. Measuring the efficiency of photosystem II.....	21

2.1.6.	Photosynthetic CO ₂ assimilation measurements	21
2.1.7.	Chlorophyll measurements.....	22
2.1.8.	Anthocyanin measurements	22
2.1.9.	Root analysis	22
2.2.	Barley plant material and growth analysis	23
2.2.1.	Plant material.....	23
2.2.2.	Selection	23
2.2.3.	Phenotype analysis	23
2.3.	General molecular biology protocols	24
2.3.1.	Standard PCR reaction	24
2.3.2.	Agarose gel electrophoresis	24
2.3.3.	Gel extraction	24
2.4.	Gene transcript analysis.....	25
2.4.1.	Production of plants	25
2.4.2.	Harvest	25
2.4.3.	RNA extraction	25
2.4.4.	Synthesis of cDNA.....	26
2.4.5.	Quantitative real-time PCR	26
2.5.	Mitochondria respiration assays	27
2.5.1.	Isolation of intact mitochondria	27
2.5.2.	Verifying mitochondrial integrity by measuring cytochrome <i>c</i> oxidase latency	28
2.5.3.	Complex I respiratory control ratio.....	28
2.5.4.	Complex II respiratory control ratio.....	29
2.6.	Production of plants expressing reduction-oxidation sensitive GFP.....	29
2.6.1.	Amplification of roGFP DNA using <i>E. coli</i>	29
2.6.2.	Preparation and transformation of <i>Agrobacterium</i>	30
2.6.3.	<i>Agrobacterium</i> -mediated transformation of <i>Arabidopsis thaliana</i>	30
2.6.4.	Selection of transformants.....	31
2.7.	Protein-protein interaction analysis by tandem affinity purification (TAP).....	33
2.7.1.	Primer design and amplification of <i>LEA5</i>	33
2.7.2.	Cloning of constructs containing <i>LEA5</i> used in TAP	33
2.7.3.	Cloning of constructs containing <i>ERF109</i> used in TAP	34
2.7.4.	Cell culture cultivation	36
2.7.5.	Cell culture transformation.....	36

2.7.6.	Protein extract preparation	36
2.7.7.	Western blots.....	37
2.7.8.	Tandem affinity purification	37
2.7.9.	Sample preparation.....	38
2.7.10.	Acquisition of mass spectra.....	38
2.7.11.	Mass spectra-based protein homology identification	38
2.7.12.	Data analysis.....	39
2.8.	Protein-protein interaction analysis by split-YFP	39
2.8.1.	Construction of the LEA5-YFPc and LEA5-YFPn vectors	39
2.8.2.	Construction of the RH22-YFPc and RH22-YFPn vectors	39
2.8.3.	Isolation of protoplasts	40
2.8.4.	Transient gene expression in protoplasts	40
2.8.5.	Visualisation of interactions.....	41
Chapter 3.	Characterisation of the phenotype of <i>Arabidopsis thaliana</i> with modified expression of <i>LEA5</i>	42
3.1.	Introduction	42
3.2.	Results: Shoot phenotype	44
3.2.1.	Rosette growth in the absence of stress.....	44
3.2.2.	Rosette growth in the presence of stress	46
3.3.	Results: Root phenotype in optimal conditions.....	53
3.3.1.	Analysis of root phenotypes for plants grown on ½ MS media.....	53
3.3.2.	Analysis of root phenotypes for plants grown on ATS media	56
3.4.	Discussion.....	58
Chapter 4.	The identification of the effects of <i>LEA5</i> expression on mitochondrial respiration and redox state.....	60
4.1.	Introduction	60
4.2.	Results: <i>LEA5</i> transcript expression	62
4.3.	Results: Mitochondrial respiration	64
4.3.1.	The protein basis of mitochondria.....	64
4.3.2.	The integrity of mitochondria and maximal cytochrome <i>c</i> oxidase activity.....	64
4.3.3.	Respiratory control assays.....	65
4.4.	Results: Transformation of <i>Arabidopsis thaliana</i> to express roGFP in the cytosol or mitochondria.....	69
4.5.	Discussion.....	73

Chapter 5.	The identification of proteins that interact with LEA5	74
5.1.	Introduction	74
5.2.	Results: TAP.....	78
5.2.1.	Constructs for TAP experiments	78
5.2.2.	The growth of <i>Arabidopsis thaliana</i> cell suspension cultures	83
5.2.3.	The effect of light on LEA5 protein expression.....	83
5.2.4.	The effect of H ₂ O ₂ on LEA5 protein expression.....	84
5.2.5.	Identification of purified proteins from TAP with LEA5 as bait protein.....	89
5.3.	Results: Split-YFP	93
5.3.1.	Production of constructs for split-YFP experiments	93
5.3.2.	Confirmation of interaction	93
5.4.	Discussion.....	102
Chapter 6.	Production and phenotype of transgenic barley expressing <i>LEA5</i>	104
6.1.	Introduction	104
6.2.	Results	105
6.2.1.	The selection of transgenic barley plants	105
6.2.2.	Shoot phenotypes	111
6.3.	Discussion.....	114
Chapter 7.	Characterisation of phenotype of <i>Arabidopsis thaliana erf109</i> mutant plants.	115
7.1.	Introduction	115
7.2.	Results - Shoot phenotype	117
7.2.1.	Rosette growth in the absence of stress.....	117
7.2.2.	Rosette growth in the presence of stress	117
7.2.3.	Anthocyanin content of leaves	126
7.3.	Results - Root phenotype.....	128
7.4.	Discussion.....	131
Chapter 8.	The identification of proteins that interact with ERF109.....	133
8.1.	Introduction	133
8.2.	Results	134
8.2.1.	Constructs for TAP experiments	134
8.2.2.	The growth of <i>Arabidopsis thaliana</i> cell suspension cultures	137
8.2.3.	The effect of H ₂ O ₂ on ERF109 protein expression in the light and dark.....	137
8.2.4.	Identification of purified proteins from TAP with ERF109 as bait protein	140
8.3.	Discussion.....	143

Chapter 9. General discussion and conclusions	146
9.1. The challenge.....	146
9.2. The role of LEA5 in plant growth and stress responses	147
9.3. Future prospects for LEA5	150
9.4. The role of EFR109 in plant growth and stress responses	150
9.5. Future prospects for ERF109.....	152
9.6. Conclusion.....	152
Chapter 10. References	153

List of Figures

Figure 1-1: A diagram of mitochondria and the sub-compartments contained within.	6
Figure 1-2: Sorting pathways of inner membrane proteins.....	8
Figure 1-3: Glycolysis.....	10
Figure 1-4: The mitochondrial electron transport chain.....	14
Figure 2-1: Plasmid map of pCAMBIA1304.....	32
Figure 2-2: Plasmid map of pDONR201.....	35
Figure 3-1: A comparison of the rosette areas wild-type (WT) <i>A. thaliana</i> and transgenic lines that either over-express <i>LEA5</i> (OEX2-2, OEX 2-5 and OEX-YFP), or express antisense <i>LEA5</i> (AS2 & AS8).....	45
Figure 3-2: The effects of abiotic stress treatments (mannitol, salt, and sorbitol) on the rosette area of wild-type (WT) <i>A. thaliana</i> and on transgenic lines that either over-express <i>LEA5</i> (OEX2-2, OEX2-5 and OEX-YFP) or produce antisense transcripts (AS2 & AS8) in comparison to plants grown in the absence of stress.	49
Figure 3-3: The effects of high-light treatment on the shoot phenotype (A) and rosette area (B) of 21-day-old wild-type (WT) <i>A. thaliana</i> and transgenic lines that either over-express <i>LEA5</i> (OEX2-2, OEX2-5 and OEX-YFP) or produce antisense transcripts (AS2 & AS8) in comparison to plants grown in the absence of stress.	50
Figure 3-4: The effects of oxidative stress treatments (menadione and paraquat) on the rosette area of wild-type (WT) <i>A. thaliana</i> and on transgenic lines that either over-express <i>LEA5</i> (OEX2-2, OEX2-5 and OEX-YFP) or produce antisense transcripts (AS2 & AS8) in comparison to plants grown in the absence of stress.	51
Figure 3-5: Anthocyanin concentration ($\mu\text{g/g}$ FW) in the leaves of four-week-old wild-type (WT) <i>A. thaliana</i> and transgenic <i>LEA5</i> over-expressing (OEX 2-5) and <i>LEA5</i> antisense lines (AS2) grown on soil.	52
Figure 3-6: The root architecture of seven-day-old wild-type (WT) <i>A. thaliana</i> and transgenic <i>LEA5</i> over-expressing (OEX2-2, OEX2-5) and <i>LEA5</i> antisense (AS2, AS8) lines grown on $\frac{1}{2}$ MS.	54

Figure 3-7: The root architecture of ten-day-old wild-type (WT) <i>A. thaliana</i> and transgenic <i>LEA5</i> over-expressing (OEX2-2, OEX2-5) and <i>LEA5</i> antisense (AS2, AS8) lines grown on ½ MS.	55
Figure 3-8: The root architecture of seven-day-old wild-type (WT) <i>A. thaliana</i> and transgenic <i>LEA5</i> over-expressing (OEX2-5) and <i>LEA5</i> antisense (AS2) lines grown on ATS media.....	57
Figure 4-1: Diurnal changes in <i>LEA5</i> transcript abundance.	63
Figure 4-2: Protein standard curve used to determine the protein basis of mitochondria.....	66
Figure 4-3: Determinations of the latency of cytochrome <i>c</i> oxidase (COX) in mitochondrial preparations.	67
Figure 4-4: The naming policy for the selection of transgenic plants.....	70
Figure 4-5: Selection for transformants on media containing Hygromycin B.	71
Figure 4-6: PCR genotyping of transgenic plants	72
Figure 5-1: Strategy followed to clone, express, purify, and identify tagged proteins and their interacting partners.	77
Figure 5-2: Identification of <i>LEA5</i> DNA subcloned from plasmid DNA by PCR.	79
Figure 5-3: Identification of the <i>LEA5+attB</i> DNA fragment.	80
Figure 5-4: Analysis of pDONR201 plasmid containing <i>LEA5</i> DNA.	82
Figure 5-5: Western blot - expression of <i>LEA5</i> in the light and the dark at different time points.	85
Figure 5-6: Western blot - expression of <i>LEA5</i> in response to H ₂ O ₂ in the light and the dark.	86
Figure 5-7: Western blot - expression of <i>LEA5</i> over time in response to treatment with H ₂ O ₂	87
Figure 5-8: Western blot - expression of <i>LEA5</i> over time in response to treatment with 2mM H ₂ O ₂	88
Figure 5-9: SDS-PAGE of purified protein complexes.	92
Figure 5-10: Analysis of pDH51-GW-YFPc and pDH51-GW-YFPn plasmid containing either <i>LEA5</i> or <i>RH22</i> DNA.	95
Figure 5-11: Light microscopy images of mesophyll protoplasts.....	96
Figure 5-12: Confocal microscopy images of an intact mesophyll protoplast transiently expressing APP1-GFP.....	97
Figure 5-13: Confocal microscopy images of an intact mesophyll protoplast transiently expressing APP2-GFP.....	98

Figure 5-14: Confocal microscopy images of mesophyll protoplasts autofluorescence (negative control).	99
Figure 5-15: Confocal microscopy images of an intact mesophyll protoplast transiently expressing LEA5-YFPc and RH22-YFPn.....	100
Figure 5-16: Confocal microscopy images of an intact mesophyll protoplast transiently expressing LEA5-YFPn and RH22-YFPc.....	101
Figure 6-1: The naming policy for the selection of transgenic barley plants from callus.....	106
Figure 6-2: Segregation analysis.	107
Figure 6-3: PCR genotyping of T ₂ transgenic barley plants.	109
Figure 6-4: PCR genotyping of T ₃ transgenic barley plants.	110
Figure 6-5: The effects of <i>LEA5</i> expression on the phenotype of barley plants.	112
Figure 6-6: The effects of <i>LEA5</i> expression on the phenotype of barley plants.	113
Figure 7-1: The effects of abiotic stress treatments (mannitol, salt, and sorbitol) on the rosette area of wild-type (WT) <i>A. thaliana</i> and <i>erf109</i> mutants in comparison to plants grown in the absence of stress (control).	118
Figure 7-2: The effects of drought on the growth of wild-type (WT) <i>A. thaliana</i> and <i>erf109</i> mutant plants.	120
Figure 7-3: Photosynthetic CO ₂ assimilation of 4-week-old wild-type (WT) <i>A. thaliana</i> and <i>erf109</i> mutant plants in optimal and restricted watering regimes.	121
Figure 7-4: The rosette area of wild-type (WT) and <i>erf109</i> mutant plants grown under standard (control) light conditions for 11 days and then either under standard light conditions or high-light for 10 days.....	123
Figure 7-5: The effects of paraquat on rosette area on wild-type (WT) <i>A. thaliana</i> and <i>erf109</i> mutant plants.	124
Figure 7-6: The effects of menadione on the rosette area of wild-type (WT) <i>A. thaliana</i> and <i>erf109</i> mutants.....	125
Figure 7-7: Anthocyanin concentration (µg/g FW) in 4-week-old wild-type (WT) <i>A. thaliana</i> and <i>erf109</i> mutant plants grown on soil under standard (control) light conditions for 3 weeks and then either under standard light conditions or high-light for 1 week.	127
Figure 7-8: The root architecture of 7-day-old wild-type (WT) <i>A. thaliana</i> and <i>erf109</i> mutant plants.	129
Figure 7-9: The root architecture in 10-day old wild-type (WT) and <i>erf109</i> mutant plants grown on ½ MS.	130

Figure 8-1: Linear plasmid map and sequence alignment of the pENTR221 plasmid containing <i>ERF109</i> DNA.....	135
Figure 8-2: Circular plasmid map and sequence of pENTR221 plasmid containing <i>ERF109</i> DNA.	136
Figure 8-3: Western blots – expression of ERF109 after one hour treatment with H ₂ O ₂ in the light and the dark.....	138
Figure 8-4: Western blots – expression of ERF109 in the light and the dark when treated with 1 mM H ₂ O ₂ for up to 1 hour.....	139
Figure 8-5: SDS-PAGE of purified protein complexes.	141
Figure 9-1: Plant compara gene tree of all known orthologues of LEA5 in Ensembl Plants (plants.ensembl.org).....	149

List of Tables

Table 1: PCR Primers for amplification of the Hygromycin B resistance and the <i>LEA5-YFP</i> sequences.....	23
Table 2: PCR Primers for amplification <i>LEA5</i> (without stop codon)	33
Table 3: PCR Primers for amplification <i>RH22</i> (without stop codon)	40
Table 4: Percentage of plants with inflorescences 24 days after germination	44
Table 5: Oxygen consumption (nmol O ₂ .min ⁻¹ .mg protein ⁻¹) at maximal COX activity and percentage intact mitochondria	68
Table 6: Oxygen consumption (nmol O ₂ .min ⁻¹ .mg protein ⁻¹) when assaying complex I respiratory control	68
Table 7: Oxygen consumption (nmol O ₂ .min ⁻¹ .mg protein ⁻¹) when assaying complex II respiratory control	68
Table 8: Proteins that interact with LEA5 in either the light or dark.....	90
Table 9: Selected proteins that interact with LEA5 either in the light or dark	91
Table 10: Segregation analysis of T ₂ plants	108
Table 11: Segregation analysis of T ₃ plants	108
Table 12: Proteins that interact with ERF109 in the light when either untreated or treated with 1mM H ₂ O ₂	142

List of abbreviations

ABA	Abscisic acid
ABI1	ABA INSENSITIVE 1
ADP	Adenosine diphosphate
AOX	Alternative oxidase
AP2	APETALA2
APP	Amino peptidase P
AS	Anti-sense orientation
ATP	Adenosine triphosphate
ATS	<i>A. thaliana</i> growth medium with sucrose
BLAST	Basic local alignment search tool
BN	Blue Native
BSA	Albumin from bovine serum
CBP	Calmodulin binding peptide
COX	Cytochrome <i>c</i> oxidase
Ct	Cycle threshold
DNA	Deoxyribonucleic acid
DREB	Dehydration Responsive Element
ERF	Ethylene Responsive Factor
ETC	Electron transport chain
EV	Empty Vector

FAD	Flavin adenine dinucleotide
FADH ₂	Reduced flavin adenine dinucleotide
FCCP	Carbonyl cyanide-p-trifluoromethoxyphenylhydrazone
Fm	Maximal fluorescence
Fv	Variable fluorescence
GFP	Green fluorescent protein
GUS	β-glucuronidase
IDP	Intrinsically disordered proteins
IgG	Immunoglobulin G
IMS	Intermembrane space
JA	Jasmonic acid
LB	Lysogeny broth
LEA	Late embryogenesis abundant
MS	Murashige and Skoog
MSMO	Murashige and Skoog basal salts with minimal organics
mtROS	ROS formation by the mitochondrial electron transport chain
MW	Molecular weight
NAD ⁺	Oxidised nicotinamide adenine dinucleotide
NADH	Reduced nicotinamide adenine dinucleotide
OEX	Over-expressing / Over-expressor
ORF	Open Reading Frame
Oxa1	Oxidase assembly 1
PAGE	Polyacrylamide gel electrophoresis

PAP	Peroxidase anti-peroxidase
PCR	Polymerase chain reaction
ProtA	Protein A of <i>Staphylococcus aureus</i>
PVP	Polyvinylpyrrolidone
QPCR	Quantitative real-time PCR
QY	Quantum yield
RD17	Responsive to Dehydration 17
Redox	Reduction-oxidation
RH	Dead(D/H)-box RNA helicase family protein
RNA	Ribonucleic acid
roGFP	Reduction-oxidation sensitive green fluorescent protein
ROS	Reactive oxygen species
SDS	Sodium dodecyl sulfate
TAP	Tandem affinity purification
TBT	Tris-buffered tween
TEV	Tobacco (<i>Nicotiana tabacum</i> L.) etch virus
TIM	Transporter Inner Membrane
TOM	Transporter Outer Membrane
UV	Ultra violet
VIB	Vlaams Instituut voor Biotechnologie
WT	Wild-type
YFP	Yellow fluorescent protein

Chapter 1. Introduction

1.1. The challenge

The challenges of food security, adequate nutrition and sustainable agriculture require innovative approaches to crop improvement. Environmental stresses limit plant growth and crop yields. Next generation crops are needed to mitigate future food shortages and to make agricultural industries more competitive. This requires a greater understanding of the processes that control growth and productivity, particularly under stress conditions. Research of this kind is of great interest for biotechnology companies [1]. Organelles that drive cellular metabolism, such as chloroplasts and mitochondria, play important roles in both growth and stress responses. This project focuses on gaining an improved understanding of how plants cope with stress.

1.2. Stress tolerance of plants

Plants are sessile organisms that can be regularly exposed to varying environmental conditions. Environmental factors deviating from the optimal intensity or quantity for the plant are called stress factors. Environmental stress can be categorised as biotic and abiotic stresses. Biotic stress results from interactions with other organisms, such as herbivory, pathogens, and parasitism. Abiotic stresses are defined as the negative impacts of non-living factors on living organisms. These can include factors such as extremes of temperature, drought or excess water, high-light intensity, and mineral deficiencies. It is not unusual for an organism to be subject to several stresses at once, for example high temperatures could cause a drought and therefore there is both heat-stress as well as a lack of water. It is also possible for a secondary stress factor to follow the primary one: for example, a plant might close its stomata in response to a lack of water which can result in an internal CO₂ deficiency due to photosynthesis, and as a further consequence this could cause oxidative stress [2]. However, plants are extremely flexible and their metabolic processes continuously acclimate to accommodate changes in the environment. The perception of environmental change and associated signalling pathways are crucial to orchestration of an appropriate response. Late embryogenesis abundant (LEA) proteins are frequently associated with cellular dehydration as well as other stresses [3, 4].

1.3. LEA proteins

LEA proteins were first identified in the seeds of cotton (*Gossypium hirsutum*) and wheat (*Triticum aestivum*) [5, 6]. Proteins homologous to prototypical LEAs have since been identified in the seeds of other plants, as well as in other plant tissues. LEA proteins are not plant specific and have been detected in other organisms, including archaea, protozoa, yeast and nematodes [7-11]. It has been proposed that many LEA proteins have functional roles in stress tolerance as their genes are often induced by stresses such as temperature, salt and osmotic stress. LEA proteins are frequently associated with cellular dehydration tolerance due to the accumulation of LEA proteins when presented with dehydration, salinity, or chilling stresses [12, 13]. The expression of LEA proteins in transgenic plants has been shown to be able to confer stress tolerance to drought, cold and freezing. There are many examples of this: in rice and wheat, the expression of a barley LEA protein, improved drought tolerance [14, 15]; the expression of a citrus LEA in tobacco bestowed cold tolerance [16]; and the freezing tolerance of strawberry leaves was increased by the expression of a wheat LEA [17]. However, the expression of LEA proteins does not always have these effects, for example, cold tolerance did not improve in tobacco with the expression of cold-induced spinach LEA proteins [18].

In *Arabidopsis thaliana*, LEA proteins consist of a family of 51 members that can be subdivided into nine groups [19]. Typically, LEA proteins are small and highly hydrophilic [20, 21]. Most LEA proteins contain high amounts of amino acid residues glycine, alanine, and glutamic acid and are poor in cysteine and tryptophan. There is a substantial overlap in proteins classified as hydrophilins with LEA proteins due to their tendency to be hydrophilic. However, not all LEA proteins are highly composed of glycine and not all LEA proteins are hydrophilins. Many non-hydrophilin LEAs are essential for desiccation tolerance in yeast [20]. The mechanism by which LEA proteins protect organisms in response to environmental stresses is yet to be defined.

1.3.1. LEA protein structures

Many members of the major LEA protein groups lack conventional secondary structures and are included in a class of proteins called intrinsically disordered proteins (IDP) [22-24]. However, some LEA proteins exhibit the notable ability to become more ordered and to develop secondary structure as dehydration proceeds, which may have significance to their proposed functions during dehydration [4, 25-33]. For example, a plant group-3 LEA protein from the pollen of *Typha latifolia* became more ordered and developed a secondary structure in response to dehydration [25]. Drying the protein slowly led to both α -helical and intermolecular extended

β -sheet structures, which suggested that the final protein conformation was not predetermined [25]. Similar results have also been found for animal LEA proteins [29, 32], where the LEA proteins were unstructured in the fully-hydrated state but upon dehydration the protein became folded into an α -helical conformation. LEA protein folding during dehydration could be functionally important in dry viable seeds but it should be noted that LEA proteins accumulate in the vegetative organs of plants under mild stress conditions and so the functional relevance of protein folding under partially dehydrated conditions is uncertain.

1.3.2. LEA proteins can protect enzymes in non-optimal metabolic conditions

After desiccation, proteins may form aggregates and enzymes can lose their catalytic activities, however it has been shown that LEA proteins can protect against both aggregation and inactivation [27, 34-36]. Many LEA proteins do not aggregate upon dehydration, freezing or boiling due to their hydrophilic and unstructured nature. Group-3 LEA proteins from *A. thaliana* [37, 38], pea [39], and *Aphelenchus avenae* [30] were shown to be effective in protecting enzymes such as lactate dehydrogenase, malate dehydrogenase, citrate synthase, fumarase, and rhodanese against partial dehydration. Furthermore, LEA proteins from the green alga *Chlorella vulgaris* [40] and from the anhydrobiotic nematode *A. avenae* [27] prevented enzyme inactivation in freeze-thaw assays. LEA proteins can have a wide range of functional properties but the structural features of LEA proteins in relation to their function or their interaction with target peptides have not been elucidated [3, 41]. To date there are few studies indicating the induction of LEA proteins in response to oxidative stress but many highlighting their involvement in other environmental stresses. However, a novel LEA protein, LEA5, was induced in response to oxidative stress.

1.4. LEA5

LEA5 (At4g02380; also known as Senescence Associated Gene 21 [42, 43], and LEA38 [41, 44]) is a member of the LEA protein family and belongs to the LEA-3 group [41]. *LEA5* is unique in its responses to oxidation. The YAP1 transcription factor controls the expression of an array of anti-oxidative defensive components in yeast. The expression of LEA5 in a *yap1* mutant strain of *Saccharomyces cerevisiae* increased tolerance to oxidative stress [43]. These mutants have previously been used to identify novel genes associated with oxidative stress tolerance [45-48]. Furthermore, expression of *LEA5* in *A. thaliana* was shown to be up-regulated with the addition of H₂O₂ to wild-type (WT) *A. thaliana* cells in culture [49] and in mutants defective in antioxidants [50].

LEA5 mRNA is expressed in leaves with transcripts having a diurnal pattern of regulation, being abundant in the dark but suppressed in the light [43]. However, in the presence of biotic and abiotic stresses *LEA5* is expressed in leaves even in the light. Unlike canonical LEAs, *LEA5* is constitutively expressed in roots and reproductive organs but not in seeds. Although first identified as a senescence-associated gene, *LEA5* is expressed only briefly, early in leaf senescence, as the leaves begin to yellow [42]. The abundance of *LEA5* transcripts was significantly increased in *A. thaliana* tissues exposed to a range of biotic and abiotic stresses that cause enhanced cellular oxidation and alter stress hormone signalling [43, 51].

Arabidopsis thaliana plants with constitutive over-expression (OEX) of *LEA5* accumulated more biomass than WT plants, while conversely, plants that expressed *LEA5* in the anti-sense orientation (AS) had a dwarfed phenotype with restricted shoot and root growth [51]. The *LEA5* AS plants notably had significantly fewer lateral roots and poorly formed root hairs [51]. These studies demonstrate that *LEA5* has a role in the control of plant growth. Additionally, the growth of a fungal (*Botrytis cinerea*), and a bacterial pathogen (*Pseudomonas syringae* pv. Tomato) was altered in *LEA5* over-expression lines [51].

Database evidence (from publicly available microarrays) [52], shows that *LEA5* is up-regulated in response to exposure to many stresses including ozone [53], cold [54], low nitrate [55] and infection by *Colletotrichum higginsianum* [56]. It is also expressed in response to sugar signalling [57] and to hormones such as ethylene [42, 58], jasmonate [59] and abscisic acid (ABA) [43]. ABA is a hormone that has functions in many plant developmental processes. Moreover, ABA-mediated signalling plays an important part in plant responses to environmental stress and plant pathogens. [43, 60, 61]. ABA induces the expression of over half of the *A. thaliana* LEA genes [41]. However, *LEA5* induction was found to be independent of ABI1 (ABA INSENSITIVE 1; a protein phosphatase that participates in ABA signalling) [43], suggesting that the signalling pathway converging on *LEA5* is not exclusively via ABA dependent reactive oxygen species (ROS) production. Analogous to other LEA proteins, *LEA5* is induced in leaves by dehydration [43], suggesting that it has a role in the response to stress. In support of this view, a genome wide association study to map local adaptation in *Arabidopsis* identified *LEA5* as being likely to be a key component underpinning plant stress tolerance in field conditions [62]. A single nucleotide polymorphism at position 1046738 (A/T), which is in the first exon of *LEA5*, was associated with local adaptation to temperature stress [62]. The T allele, which is the less frequent allele across *Arabidopsis* ecotypes, was associated with poor survival in Finland, due to low-temperature stress [62].

LEA5 was found to be localised to mitochondria of *A. thaliana* cells using a yellow fluorescent protein (YFP) fusion [51], and separately to the mitochondrial matrix using a green fluorescent protein (GFP) fusion [44]. As LEA proteins appear to have a role in protecting plants against stresses [13-18], it is possible that LEA5 has a role in the protection of mitochondrial functions in plants exposed to stress. Expression of LEA5 is strongly regulated by oxidants [43], leading to the hypothesis that LEA5 fulfils functions related to respiration and associated oxidative stress tolerance or signalling in mitochondria.

1.5. Mitochondria

Mitochondria are organelles, each of which is about 0.5 to 1.0 μm in diameter, found in eukaryotic cells [63]. Mitochondrial respiration generates most of the cell's supply of adenosine triphosphate (ATP) which is used as a source of chemical energy to drive metabolism, growth and biomass production. Mitochondria also participate in multiple cellular signalling pathways, and are involved in processes as diverse as cell cycle regulation, cellular differentiation and apoptosis [64]. The number of mitochondria in a cell can vary depending upon the tissue type [65]. Mitochondria have an outer and inner membrane, which are composed of phospholipid bilayers and embedded proteins. This double membrane organisation provides four distinct areas to a mitochondrion; these are the outer mitochondrial membrane, the inter-membrane space, the inner mitochondrial membrane, and the matrix (Figure 1-1).

The assembly of a mitochondrion necessitates the co-operation of several processes which include the transcription of mitochondrial-associated genes, the translocation and targeting of newly synthesised proteins and the assembly of those proteins into a functional unit [66, 67]. Mitochondria have their own DNA but require the input of the nuclear genome to encode most of the protein complement that constitute a mitochondrion [68, 69]. Mitochondrial biogenesis therefore requires coordination in the expression of the two genomes which is achieved by signalling between the nucleus and mitochondria. This coordination is also essential to ensure that mitochondria can respond to the changes in the physiological milieu of the cell [69]. The synthesis of some proteins destined to reside in mitochondria can occur on polysomes bound to mitochondria [70-74]. The localised synthesis of mitochondrial proteins is thought to promote their efficient import and assembly [67]. The trafficking of nuclear-transcribed and cytosol-synthesised proteins into the mitochondria is carried out by mitochondrial protein import machinery [75]. Mitochondrial protein import machinery is a collective term for several translocation processes, each consisting of a distinct network of multi-subunit proteins.

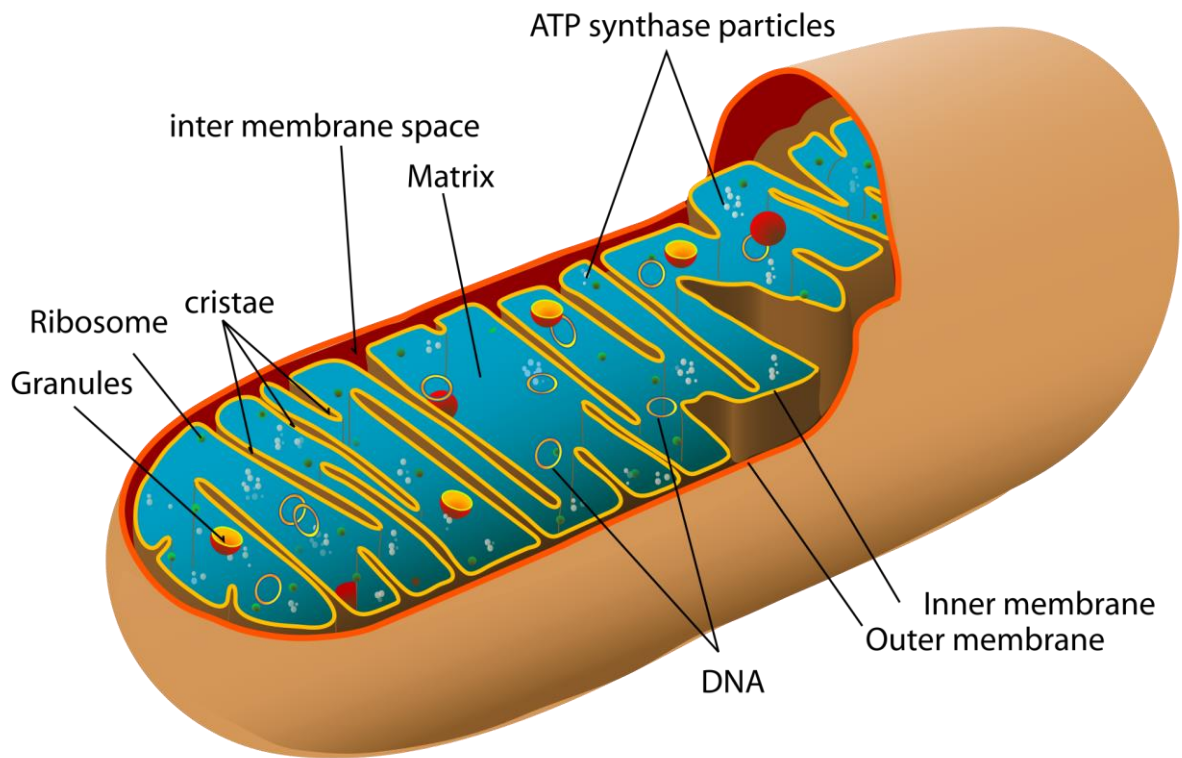


Figure 1-1: A diagram of mitochondria and the sub-compartments contained within.

(http://en.wikipedia.org/wiki/File:Animal_mitochondrion_diagram_en.svg)

1.5.1. Mitochondrial targeting signals

Precursors of mitochondrial proteins that are present in the cytosol contain information to direct them to the mitochondria. This information is often available as a cleavable sequence at the N terminus. The N-terminal targeting sequences, in the absence of further sorting information, direct proteins into the matrix and are cleaved from the precursors by mitochondrial-processing peptidase in most cases. These targeting sequences, which in some cases can co-target proteins to both chloroplasts and mitochondria, allow the passage of proteins into the organelles via highly conserved import and incorporation machinery [68, 76]. Most mitochondrial proteins reside in the matrix of the mitochondria. Cytosolic precursors of mitochondrial proteins are imported into this innermost sub-compartment of mitochondria via the Transporter Outer Membrane (TOM) complex in the outer membrane [77, 78] and the Transporter Inner Membrane (TIM) 23 complex in the inner membrane [79]. This is not always the case as many precursors lack such a sequence and instead contain internal targeting signals. There are internal signals that direct the precursors to all mitochondrial subcompartments.

1.5.2. Protein insertion into the inner mitochondrial membrane

The inner mitochondrial membrane has a variety of proteins embedded within it. Most of these proteins are imported from the cytosol, although some are synthesised by mitochondrial ribosomes in the matrix. For proteins of a cytosolic origin, there are three import routes identified. One mechanism uses the TIM22 complex (Figure 1-2 a), in which proteins with internal signals are inserted into the inner mitochondrial membrane. The TIM22 pathway uses three mitochondrial protein complexes to facilitate the import and membrane insertion of proteins. These complexes are the TOM complex in the outer membrane [77, 78], complexes of small Tim proteins in the inter membrane space, and the TIM22 translocase in the inner membrane [68]. Another method of insertion involves the arrest of preproteins at the level of the TIM23 complex where they are laterally integrated into the inner membrane. This route is often referred to as the stop-transfer pathway [80] (Figure 1-2 b). The third method is called the conservative sorting pathway as it reflects that of the prokaryotic ancestors of mitochondria [81, 82](Figure 1-2 c). In this method, inner membrane proteins are initially translocated into the matrix and, from there, they are inserted in to the inner membrane in an export-like step [68]. During translocation to the matrix, some proteins using this pathway are bound by Hsp70 [68]; which is thought to prevent degradation and aggregation, and remodel folding pathways [83]. The Oxa1 complex then facilitates the insertion of these proteins in to the membrane [84, 85].

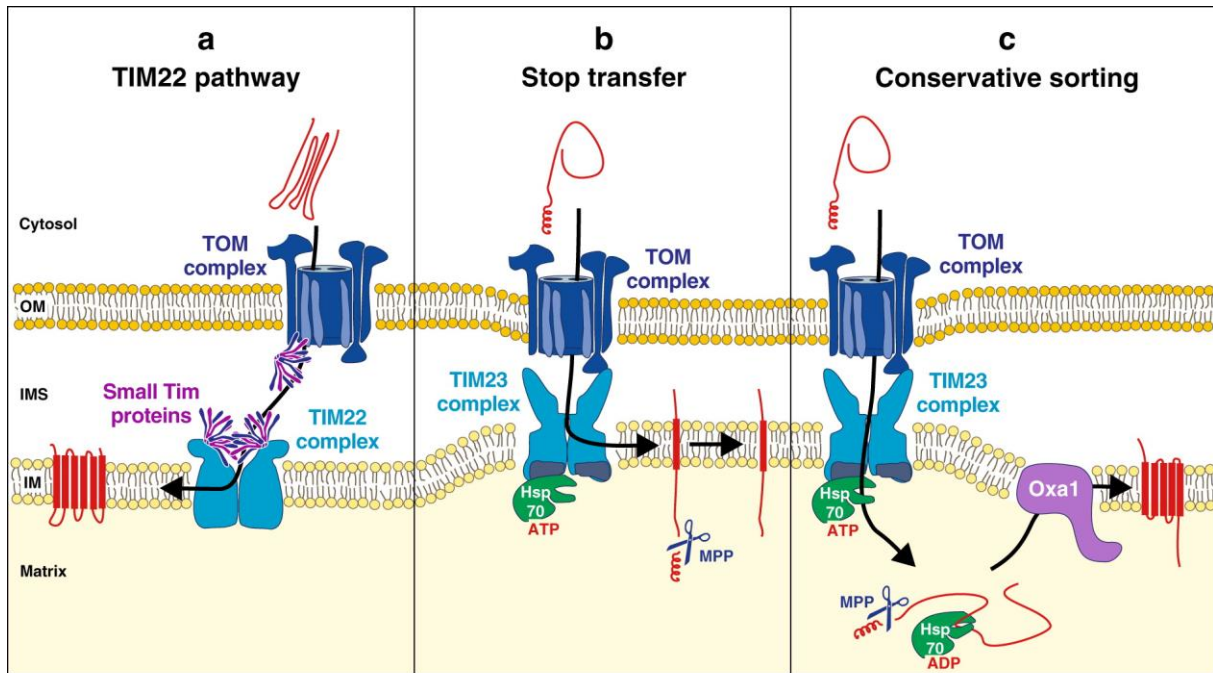


Figure 1-2: Sorting pathways of inner membrane proteins

a: Solute carriers and hydrophobic TIM subunits are inserted into the inner membrane by a dedicated inner membrane complex, the TIM22 translocase. Small Tim proteins in the intermembrane space (IMS) are assumed to function as chaperones, which guide the hydrophobic precursors across the IMS. **b:** Inner membrane proteins containing only one transmembrane span are arrested at the level of the TIM23 complex and are integrated into the inner membrane by lateral exit. **c:** A class of inner membrane proteins are sorted via soluble translocation intermediates in the matrix. Membrane insertion occurs here from the matrix side and, at least in certain cases, is facilitated by the Oxa1 (oxidase assembly) complex of the inner membrane. Figure taken from Neupert and Herrmann, 2007 [68].

1.6. Respiration

Respiration can be divided into three main pathways: glycolysis (Section 1.6.1), the Krebs cycle (Section 1.6.2) and the mitochondrial electron transport chain (Section 1.6.3). Cells use these pathways to harvest chemical energy by degrading complex organic compounds containing potential energy into products that have less energy. Through oxidation, of glucose for example, respiration makes energy available for ATP synthesis [86]. The energy stored in ATP can then be used to drive processes requiring energy, such as biosynthesis, or transportation of molecules across cell membranes. Plants respiratory metabolism has unique features, including multiple entry points from sucrose and starch [86, 87], complementation between the cytosol, plastid and mitochondria [86, 87], and the presence of non-phosphorylating transport systems [86].

1.6.1. Respiration: Step 1 - Glycolysis

The glycolytic pathway oxidises hexose sugars (e.g. glucose) to generate ATP, reductant, and pyruvate. Glycolysis does not occur in a single step; rather is the linear sequence of 10 enzymatic reactions occurring in the cytosol [87]. In glycolysis, glucose is converted into fructose 1, 6-biphosphate (F1, 6BP; Figure 1-3), consuming 2 ATP in three separate enzymatic reactions [87]. Fructose 1, 6-biphosphate is split into two molecules of glyceraldehyde 3-phosphate (GADP; Figure 1-3). These three-carbon sugars are then oxidised and their remaining atoms rearranged to form two molecules of pyruvate (Figure 1-3), a process that yields 2 ATP per sugar (net yield 4 ATP) [87]. However, plants can use sucrose and starch as substrates for glycolysis; the products of sucrose and starch breakdown are metabolised via the classic intermediates of glycolysis. If O₂ is present, the pyruvate is transported to mitochondria where it is converted to acetyl-coenzyme A (CoA), an enzyme used to provide acetate to the Krebs cycle for further oxidation, through a process called pyruvate decarboxylation.

Glycolysis is an anaerobic reaction. In conditions of oxygen deprivation, such as when excessive rainfall has caused soil waterlogging or even the complete submergence of plants, plants rely on the ATP produced through glycolysis. This is because in anaerobic conditions, ATP production by the mitochondrial electron transport chain is compromised due to oxygen being the final acceptor of electrons. However, the absence of NADH oxidation by the mitochondrial electron transport chain puts glycolysis at risk of stopping as oxidised nicotinamide adenine dinucleotides (NAD⁺) are used in glycolysis to oxidise GADP [87]. However, plants can respond to low oxygen by shifting from aerobic mitochondrial respiration to fermentation in which NADH is oxidised by pyruvate which then forms lactate [88, 89].

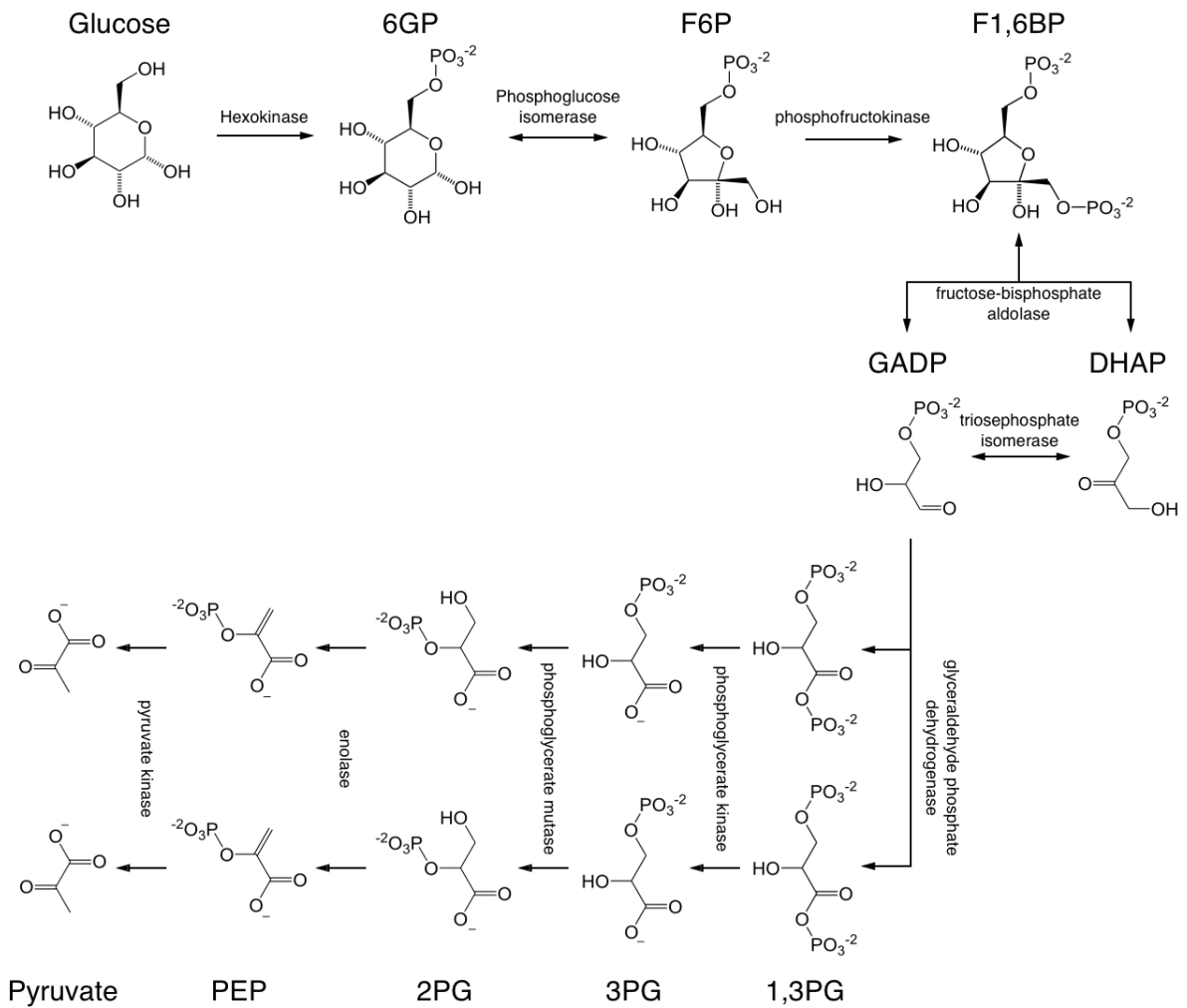


Figure 1-3: Glycolysis

The metabolic pathway of glycolysis converts glucose to pyruvate via intermediate metabolites. Each chemical modification is performed by a different enzyme. The steps performed by hexokinase and phosphofructokinase consume ATP. The steps performed by phosphoglycerate kinase and pyruvate kinase produce ATP. Since the steps performed by phosphoglycerate kinase and pyruvate kinase occurs twice per glucose molecule there is a net production of ATP.

1.6.2. Respiration: Step 2 - The Krebs cycle

The respiratory process continues with the mitochondrial reactions of the Krebs cycle [90] (also known as the citric acid cycle, and the tricarboxylic acid cycle). Pyruvate, either entering the mitochondria from the cytosol or generated within the matrix via the malic enzyme, is first oxidized by pyruvate dehydrogenase complex to form acetyl-CoA [86]. The acetate entering the cycle is oxidized in a series of reactions carried out by 8 enzymes. The first reaction is the enzymatic addition of the two-carbon acetyl group from acetyl-CoA to the four-carbon acceptor oxaloacetate, forming citrate, a six-carbon compound, and coenzyme A [91]. The coenzyme A component of acetyl coenzyme A can be reused in acetyl coenzyme A formation. Subsequent steps revert the citrate back into oxaloacetate, producing CO₂. For each acetate that enters the cycle, three molecules of NAD⁺ are reduced to NADH. In the sixth step of the cycle, catalysed by succinate dehydrogenase, electrons are transferred to flavin adenine dinucleotide (FAD) producing the reduced form of FADH₂ [92]. Both FADH₂ and NADH donate their electrons to the electron transport chain (ETC). One molecule of ATP is also formed in the Krebs cycle, but most of the ATP output of respiration occurs from oxidative phosphorylation which utilises the electrochemical proton gradient produced by the ETC for ATP synthesis.

1.6.3. Respiration: Step 3 - The electron transport chain

The ETC is an enzymatic series of electron donors and acceptors comprised of four large protein complexes (I, II, III, IV), the coenzyme ubiquinone, and the protein cytochrome *c*, residing in the inner mitochondrial membrane and inter membrane space (Figure 1-4). The electrons used in the ETC come from the NADH and FADH₂ generated in the first two stages of respiration (glycolysis and the Krebs cycle). Each electron donor passes electrons to a more electronegative acceptor, which in turn donates these electrons to another acceptor, a process that continues until electrons are passed to oxygen, the most electronegative and terminal electron acceptor in the chain. The transfer of electrons between donors and acceptors during passage through the ETC releases energy which is used to generate an electrochemical proton gradient across the mitochondrial inner membrane by actively moving protons into the intermembrane space from the mitochondrial matrix. This electrochemical proton gradient allows ATP synthase to use the flow of H⁺ through the enzyme back into the matrix to generate ATP from adenosine diphosphate (ADP) and inorganic phosphate.

Complex I (NADH dehydrogenase) is an initial electron acceptor. It transfers two electrons from NADH to ubiquinone, via an Fe-S cluster [93], in an exergonic process that is tightly

coupled to the endergonic translocation of four protons across the inner mitochondrial membrane into the inter membrane space [94]. In addition to the Complex I found in many organisms, plants have alternative NADH and NADPH dehydrogenases [95]. These dehydrogenases do not contribute to the electrochemical potential difference of protons across the inner mitochondrial membrane but still reduce ubiquinone. This provides a mechanism for plants to remove excess reducing power and balance the reduction-oxidation (redox) poise of the cell. Another initial electron acceptor is Complex II (succinate dehydrogenase), participating in both the Krebs cycle and the ETC [96]. Complex II reduces ubiquinone to ubiquinol by transferring electrons from FADH₂ derived from the oxidation of succinate to fumarate in the Krebs cycle [93, 96]. However, unlike complex I, complex II is does not pump protons in to the intermembrane space [96].

Ubiquinone is an electron carrier that is reduced to form ubiquinol upon accepting electrons from complexes I and II. Ubiquinol freely diffuses within the inner mitochondrial membrane to deliver electrons to complex III (cytochrome *bc₁*). Ubiquinol is oxidised by complex III which sequentially transfers electrons to cytochrome *c* [97, 98], a water-soluble electron carrier located within the intermembrane space [99]. The electrons are utilised by complex III for proton motive force generation through the Qcycle mechanism in a bifurcated fashion [97]. Four H⁺ ions are pumped across the mitochondria inner membrane during this process [98].

Complex IV (cytochrome *c* oxidase; COX) is a terminal oxidase of the ETC. Complex IV accepts electrons from cytochrome *c* and reduces molecular oxygen to water [99]. The residual energy from this reduction is used to pump 2 H⁺ ions across the inner membrane into the intermembrane space [100, 101]. Therefore, for every two NADH molecules, one O₂ is reduced to two molecules of water. The electrochemical gradient produced by this process is utilised in oxidative phosphorylation to produce ATP [101]. As oxygen is the terminal electron acceptor in the chain, each acceptor molecule in the chain retains its electrons if it is not present. ATP synthesis will stop if the H⁺ gradient equilibrates as oxidative phosphorylation requires an electrochemical proton gradient. Inhibitors of the ETC components also constrain ATP synthesis.

The plant ETC is highly branched and contains a second terminal oxidase in addition to Complex IV, known as alternative oxidase (AOX). The quinol-oxidizing AOX directly couples the oxidation of ubiquinol with the reduction of O₂ to produce H₂O and heat [102]. The presence of AOX in the mitochondrial ETC allows electron flow from ubiquinol to be diverted from the

cytochrome *c* pathway (complex III, cytochrome *c*, complex IV) to AOX to prevent the over reduction of the ubiquinone pool. The regulation of the redox state of the ubiquinone pool is particularly important because the ubisemiquinone intermediate formed at complexes I and III can act as an electron donor to oxygen forming superoxide [103]. The major sites of superoxide production are complexes I [104] and III [105-107]. By removing electrons from the ubiquinone pool that would reduce components of complex III, AOX minimises the likelihood of univalent oxygen reduction by complex III.

1.6.4. Respiration: Step 4 - ATP synthesis

Embedded in the inner membrane of the mitochondria are many copies of a protein complex called ATP synthase (Complex V; F₀F₁-ATP synthase). ATP synthase is the site of oxidative phosphorylation, which accounts for almost 90% of the ATP generated by respiration. The F₀F₁-ATP synthase consists of 2 domains: the F₀ portion (its name derives from the fact that this fraction binds to oligomycin [108, 109]) which resides within the mitochondrial inner membrane, and the F₁ portion of the ATP synthase, which projects out of the inner membrane into the matrix of the mitochondria [110]. ATP synthesis by the F₀F₁-ATP synthase is powered by a proton-motive force, which is generated by the electrochemical potential difference of protons across the inner mitochondrial membrane [111] formed by the electron flow through the ETC [101]. The flow of protons through the inner mitochondrial membrane drives the rotation of ATP synthase components causing conformational changes in the catalytic sites of the F₁ domain resulting in the synthesis and release of ATP [112].

The simplest known ATP synthase consists of 8 subunits; the F₀ domain consists of subunits *ab*₂*c*_{*n*} while subunits $\alpha_3\beta_3\gamma\delta\epsilon$ comprise the F₁ domain [109]. Subunits *a* and *b* form the proton conducting half channels that end on either side of the inner mitochondrial membrane. Driven by the proton motive force, protons flow through the F₀ portion of the enzyme [113]. This transfer drives the rotation of a ring of *c* subunits (*c*-ring) in the F₀ domain relative to the subunits *a* and *b* [113, 114]. The *c*-ring is also attached to an asymmetric central stalk consisting primarily of the γ subunit [115] with subunit ϵ attached [116]. The rotation of the *c*-ring is passed to the $\gamma\epsilon$ central stalk of the F₁ region. The rotation of $\gamma\epsilon$ causes conformational changes in the catalytic sites on the three β subunits of the F₁ motor, resulting in the synthesis and release of ATP [112]. A narrow (45 Å) peripheral stator stalk, composed of a β dimer and subunit δ in most bacterial enzymes fixes the major F₁ subunits, $\alpha_3\beta_3$, to the static portions of the F₀ domain preventing the $\alpha_3\beta_3$ ring following the rotation of the γ subunit [117-120].

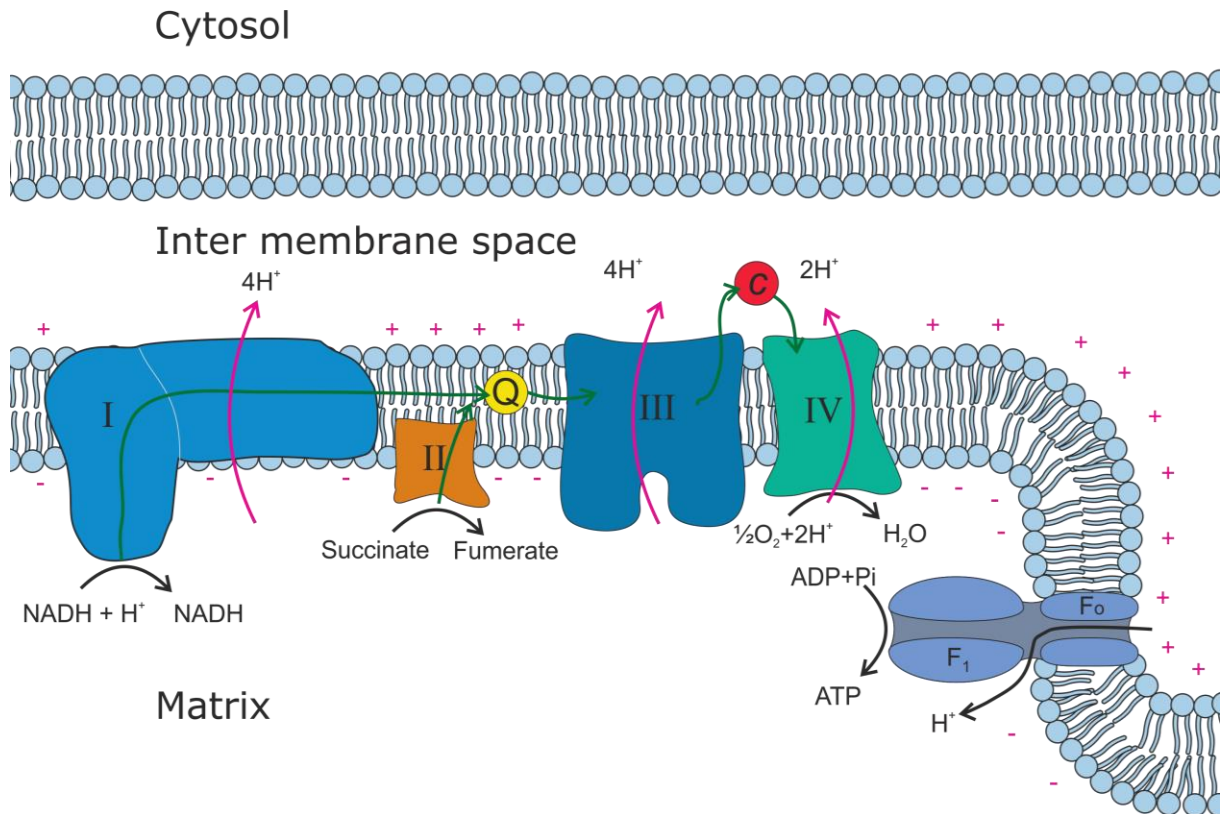


Figure 1-4: The mitochondrial electron transport chain.

The electron transport chain couples electron transfer between an electron donor (such as NADH) and an electron acceptor (such as O_2) with the transfer of H^+ ions across the inner membrane and into the intermembrane space. The passage of protons through the F_0 domain of ATP synthase is coupled with a conformational change in the ATP synthase which is used to generate chemical energy in the form of ATP.

1.7. Reactive Oxygen Species

ROS are chemically reactive molecules containing oxygen. Molecular oxygen has two unpaired electrons in its outer electron shell which makes oxygen reactive. More reactive species such as superoxide ($^{\cdot}\text{O}_2$) and hydrogen peroxide (H_2O_2) can be derived from molecular oxygen during metabolism. Plants produce ROS in chloroplasts, mitochondria, and peroxisomes, as well as other sites of the cell because of their metabolic processes such as photosynthesis and respiration [121]. ROS formation in mitochondria occurs under optimal conditions but can be increased with exposure to stress [122]. Most of the oxygen used in the ETC is reduced to water by complex IV but about 1–2% of the oxygen molecules are converted to the superoxide anion radical ($\text{O}_2^{\cdot-}$) [123], mostly via complex I [104], and complex III [105-107]. The primary determinant of mitochondrial ROS production is the ubiquinone pool as the ubisemiquinone intermediate formed at complexes I and III is the principal electron donor to oxygen [103].

ROS fulfil multiple functions in cells but excessive amounts can be detrimental to cells. ROS generated in the pathogen-induced oxidative burst play a key role in the elicitation of defence responses [124]. They are involved in multiple signalling pathways [125, 126] leading to alterations in gene expression and at high levels they can trigger programmed cell death. The lifetime of ROS is determined by the antioxidant network which prevents uncontrolled oxidation. Moreover, pathways such as the alternative oxidase pathway are considered to attenuate ROS formation by the mitochondrial electron transport chain (mtROS) by diverting electron flow from complex III, a major site of ROS formation [104, 106, 107], to AOX.

1.8. Mitochondria-to-nucleus communication

Plant cell function is dependent upon the regulated and reciprocal interaction between its different compartments [127]. This requires communication between the nucleus, mitochondria, and chloroplasts. Plant hormones are the major signalling components regulating cellular functions and are used for communication between the nucleus and mitochondria [127]. These signals can directly regulate nuclear gene expression (anterograde signalling; nucleus-to-organelle) to adjust the protein composition of the mitochondria to the needs of the cell [127]. The mitochondria can also communicate their functional status to the nucleus (retrograde signalling; organelle-to-nucleus) to prompt adjustment of gene expression in the nucleus [127, 128]. Intricate signalling pathways are needed as the nuclear genome encodes the majority of mitochondrial proteins which then have to be imported into the mitochondria [68, 69]. This coordinated regulation is essential for appropriate responses to changes in the environment e.g.

temperature [129]. This mechanism may be used in response to the loss of mitochondrial function caused by a deficit in the electrochemical potential (uncoupling) of oxidative phosphorylation subunits [130], or by the accumulation of unfolded proteins in the organelle [131]. As well as direct mitochondria-to-nucleus signalling, it is plausible that mtROS produces secondary signals from local ROS detection mechanisms which then alter nuclear gene expression [132-135]. These responses enable mitochondria to recover from stress [129].

1.9. Chloroplast to nucleus communication

The photosynthetic apparatus is composed of proteins encoded by genes from both the nucleus and chloroplast [136, 137], similar to mitochondria [68, 69]. For example, in the photosynthetic ETC of the thylakoid membrane, the core subunits are encoded by the chloroplast genome, and the peripheral subunits are encoded by the nuclear genome. In the stroma, the large subunit of ribulose-1,5-bis-phosphate carboxylase/oxygenase (Rubisco) is encoded by the chloroplast [138], whereas the small subunit is encoded by the nucleus [139]. To ensure the complexes are assembled stoichiometrically and to enable responses to changes in the environment, the plastids emit signals that are able to regulate nuclear gene expression [140-144]. Several plastid processes produce signals that influence nuclear photosynthetic gene expression [144, 145]. Moreover, different signals are produced at different developmental stages [146]. In this way, retrograde signalling is able to coordinate the expression of nuclear genes encoding plastid proteins with the metabolic and developmental state of the plastid [143, 147].

1.10. Transcription factors of the ethylene responsive factor family

Elaborate mechanisms exist to buffer the cellular redox state in plants to prevent excessive oxidation or reduction that would impair metabolic functions. Increases in the levels of ROS, which can occur in cells exposed to stress, lead to oxidative signals that modify growth, development and defence responses [148, 149]. The type and extent of these modifications depends greatly on the nature of the stimulus, as well as its strength, and the exposure time of the tissue to the stimulus. The orchestration of these changes is brought about by the redox regulation of many proteins including transcription factors of the *Ethylene Responsive Factor* (*ERF*) family. ERFs are characterised by a common ‘GCC’ DNA binding domain. These bind directly to the cis-element called a GCC-box containing the core 5’-GCCGCC-3’ sequence [150]. These transcription factors are able to regulate primary and secondary metabolism as well as plant growth and defence responses [151]. The expression of ERFs in *A. thaliana* is inducible with biotic and abiotic stresses, and many have roles in the regulation of gene

expression in stress conditions. For example, by binding to GCC boxes in the promoters of target genes, such as the *Dehydration Responsive Element 2A* (*DREB2A*; At5g05410), ERFs are able to confer drought tolerance in *A. thaliana*; in this case by controlling the expression of the *Responsive to Dehydration 17* (*RD17*; At1g20440) gene [148, 152]. However, the precise functions of many ERFs such as *ERF109* (At4g43310) remain to be characterised.

1.11. ERF109

ERF109 (also known as Redox Responsive Transcription Factor 1) is a member of the ERF/APETALA2 (AP2; At4g36920) transcription factor superfamily and contains only one AP2 domain, which binds to the promoters of downstream target genes [150, 153, 154]. The role performed by *ERF109* may be unique and without genetic redundancy to other ERF family members as it has a low homology with other members of the superfamily and within the AP2 domain [155]. The transcription factor, *ERF109*, was identified as being part of a regulatory network that has a major role in the adjustment of leaves to reach homeostasis after high-light stress [156]. Analysis of an *erf109* mutant found that 30 genes were differentially expressed in the vicinity of *ERF109*, many of which have roles in stress responses [156].

ERF109 transcripts increase in leaves that are directly exposed to high-light. The extent of transcript accumulation depends on the intensity of light that the leaves are exposed to [157]. Furthermore, *ERF109* transcripts also accumulate in leaves that have not experienced high-light as a result of systemic signalling from leaves exposed directly to high-light [158]. Oxidative stress is an inescapable consequence when plants are exposed to high-light as singlet oxygen ($^1\text{O}_2$) is produced in energy transfer reactions from the excited triplet state of chlorophyll molecules or their precursors to molecular oxygen [159, 160]. *ERF109* expression is induced by singlet oxygen but not by hydrogen peroxide [161]. Singlet oxygen-dependent activation of jasmonic acid (JA) and oxylipin signalling pathways may also be important in the activation of *ERF109* expression in systemic leaves [161]. The lack of functional *ERF109* restricted ROS accumulation in response to stress in mutant plants and conversely overexpression of *ERF109* resulted in an accumulation of ROS [162]. *ERF109* is therefore considered to propagate ROS accumulation in response to ROS-producing abiotic and biotic stress signals. This is perhaps why *ERF109* mRNAs accumulate in aphid-infested leaves [163].

Transgenic lines that overexpress *ERF109* were impaired in root and shoot development [155, 162], and showed increased light sensitivity [162]. *ERF109* is expressed in low levels in roots [155] but transcripts are upregulated in response to JA [164]. JA is an endogenous hormone

that can be generated in response to many environmental stimuli. It activates a variety of transcription factors in order to mediate responses to biotic and abiotic stresses [164, 165]. ERF109 was shown to mediate cross-talk between JA signalling and auxin biosynthesis in the regulation of lateral root formation in *A. thaliana* [155]. Notably, *ERF109* was significantly induced by methyl jasmonate but not by ABA [155], which has been shown to interact with JA to regulate plant responses to water stress conditions [166, 167]. The *erf109* mutants have fewer lateral roots under methyl jasmonate treatments compared with WT. The shoots of these mutants have no visible phenotypic differences to the WT when grown under low-light [157]. However, they show a markedly different phenotype when grown for two weeks under high-light as the leaves of WT plants appear visibly darker than those of the *erf109* mutants [157].

1.12. Summary

The functional integrity of mitochondria is vital to the sustained production of ATP and survival of the cell. Exposure to stress can cause the processes that facilitate mitochondrial energy conversion to malfunction, leading to the generation of signals that are transmitted to the nucleus to mitigate harmful effects [127]. Despite intensive research efforts in recent years, very little is known about the mitochondrial signalling pathways that play central roles in the control of plant growth and stress responses. LEA5 is a protein that localises to mitochondria [44, 51] and was shown to protect against oxidative stress [43, 51]. There is the intriguing possibility that LEA5 has a role in mitochondrial ROS signalling, which in turn, impacts on root development and pathogen responses. The root and shoot development and response to biotic stress in *LEA5* OEX and AS lines has been characterised [43, 51]. Primary root length was found to be shorter in AS lines, which also had fewer laterals relative to the primary root [51]. *LEA5* AS genotypes also had a less shoot biomass and flowered earlier [51]. OEX lines had longer root hairs than WT [51]. These results suggest that LEA5 is an oxidation-responsive mitochondrial protein that is involved in growth and biotic and abiotic stress responses. Furthermore, the transcription factor ERF109 is considered to propagate ROS accumulation in response to ROS-producing stress signals [162] and is part of a regulatory network that has a major role in the adjustment of *A. thaliana* leaves to reach homeostasis after high-light stress [156]. ERF109 was shown to mediate cross-talk between JA signalling and auxin biosynthesis in the regulation of lateral root formation in *A. thaliana* [155].

1.13. Aims and objectives

The aim of these studies was to characterise LEA5 functions in mitochondria, in order to determine the effects LEA5 has on respiration and respiratory regulation and to determine whether the interactions between LEA5 and other proteins are important in the control of growth and stress tolerance. An understanding of LEA5 function in mitochondria will provide insights into the control of plant growth and stress tolerance. This information could be used in future breeding programs to improve the predictability and sustainability of cereal crop yields by enhancing environmental stress tolerance. A further aim was to characterise the phenotypes of *erf109* mutants and to determine whether the interactions between ERF109 and other proteins are important to stress tolerance and root architecture.

The specific objectives of this study were as follows:

1. To characterise the phenotypes of *A. thaliana* plants that either overexpress *LEA5* or express *LEA5* in the anti-sense orientation in the absence and presence of stress.
2. To investigate the role of LEA5 in respiration and redox homeostasis.
3. To identify proteins that interact with LEA5.
4. To characterise the phenotypes of barley plants that overexpress *LEA5*.
5. To characterise the phenotypes of *A. thaliana erf109* mutant plants.
6. To identify proteins that interact with ERF109.
7. To identify homologues of LEA5 in crop species.

Chapter 2. Materials and Methods

2.1. Arabidopsis plant material and growth analysis

2.1.1. Plant material

Wild-type (WT) *Arabidopsis thaliana* seeds (Col-0) were obtained from Bayer (Crop Science Division - Trait Research Innovation Centre, Ghent, Belgium). Transgenic *A. thaliana* plants that over-express *LEA5* under the control of the Cauliflower mosaic virus (CaMV) 35S promoter (*LEA5*-OEX) that were produced by Dr. Shaheen Mowla, University of Cape Town (Cape Town, South Africa) [43], and transgenic *A. thaliana* plants that express *LEA5* in the anti-sense (AS) orientation or with a YFP fusion (OEX-YFP), described by Dr. Faezah Mohd Salleh, Cardiff University (Cardiff, UK) [51], were provided by Dr. Hilary Rogers, Cardiff University. The *erf109* mutant line was provided by Prof. Peter Meyer, University of Leeds (Leeds, UK) and is a Salk T-DNA insertion line (SALK_150614; containing an insertion in exon of At4g34410) [156]. All lines had a Col-0 background and were homozygous for the gene of interest.

2.1.2. *In vitro* shoot growth and stress treatments

Seeds were sown in plates on half-strength Murashige and Skoog 1% agar medium (½ MS; 2.2 g/l Murashige and Skoog basal medium (Sigma-Aldrich Company Ltd. Dorset, UK), 0.5 g/l MES, 0.1 g/l Myoinositol, 10 g/l sucrose, dissolved in deionised H₂O, adjusted to pH 5.7 with 1 M KOH, 10 g/l agar, and autoclaved at 121°C for 20 minutes) supplemented with 1.2% glucose. Control plates contained media alone. Stress conditions were achieved by adding sodium chloride (75 mM), mannitol (50 mM), sorbitol (100 mM) paraquat (N,N'-dimethyl-4,4'-bipyridiniumdichloride; 0.1 µM), or menadione (0.1 mM) to the media. Once sown, seeds were stored at 4°C for 3 days and then moved to a controlled environment and arranged in a random-block design. Plants were grown under an irradiance of 100 µmol.m⁻².s⁻¹ with a 16 hour photo period, a constant temperature of 22 ± 2°C, and a relative humidity of 60% for 21 days.

2.1.3. Shoot growth on soil and drought experiments

In the drought experiments, seeds were sown on to ½ MS and stratified at 4°C for 3 days. Seedlings were then grown in a controlled environment with an irradiance of 200 $\mu\text{mol.m}^{-2}.\text{s}^{-1}$, a photo period of 8 hours, and a constant temperature of $20 \pm 2^\circ\text{C}$ for two weeks. Two-week-old seedlings were transplanted to soil and grown for a further 10 weeks. In this experiment water was withheld after 5 weeks of plant growth. Watering was reinitiated after 2 weeks of the water being withheld. Measurements taken included rosette area, leaf count, biomass, and water content. The fresh and dry weights of plant and soil samples were measured to calculate the percentage water content.

2.1.4. Determination of rosette area

Total rosette surface area measurements of plants grown on media were performed using RosettR (github.com/hredestig/rosettR). RosettR is open-source software that performs a protocol for a high-throughput phenotyping assay for *Arabidopsis* implemented as an R-package. For plants grown on soil, photographs of the plants were used to measure the total rosette surface area using Fiji Image J (v1.46r) [168]. Statistical analysis was performed with the program R studio [169]. The total rosette surface area, measured here, is highly correlated with the fresh weigh of the plant (usually $r = 0.9\text{--}0.95$).

2.1.5. Measuring the efficiency of photosystem II

A Flourpen FP100 was used to measure the Quantum Yield (QY), which is a measure of the efficiency of photosystem II, of all plants. In light-adapted leaf QY is equivalent to F_v'/F_m' (Variable Fluorescence (the difference between minimal and maximal fluorescence) / maximal fluorescence). Measurements of F_v'/F_m' were taken from light-adjusted plants.

2.1.6. Photosynthetic CO₂ assimilation measurements

A LI-COR LI-6400XT Portable Photosynthesis System and a 6400-17 Whole Plant Arabidopsis Chamber (LI-COR Biotechnology UK Ltd, Cambridge, UK) was used to measure the photosynthetic CO₂ capacity of *A. thaliana* plants. Plants were dark adjusted for 30 minutes before measurement. CO₂ was kept constant at 400 $\mu\text{mol.s}^{-1}$ and the temperature was maintained at 20°C. Measurements of CO₂ assimilation by plants were taken at light intensities from 0 to 1600 $\mu\text{mol.m}^{-2}.\text{s}^{-1}$. Measurements were adjusted to account for the rosette area.

2.1.7. Chlorophyll measurements

Chlorophyll *a*, *b* and carotene, were extracted by homogenising weighed plant material in liquid N₂ using a mortar using a pestle and suspending in 95% ethanol. The homogenate was then centrifuged at 10000 × *g* for 10 minutes at 4°C. If the pellet was not white, the supernatant was removed and the pellet re-suspended in 400 µl of ethanol 95% and centrifuged again using the same settings. 200 µl of sample was used to assay pigment absorbance at 470 nm, 649 nm, and 664 nm with a spectrophotometer. A blank of 95% ethanol was made for each wavelength.

The pigment concentrations were calculated using the following equations [170]:

$$\text{Chlorophyll } a = 13.36A_{664.2} - 5.19A_{646.6} ;$$

$$\text{Chlorophyll } b = 27.43A_{648.6} - 8.12A_{664.2} ;$$

$$\text{Carotene} = (1000A_{470} - 2.13\text{Chlorophyll } a - 97.64\text{Chlorophyll } b)/209.$$

2.1.8. Anthocyanin measurements

Leaf material (100 mg) was ground to a fine powder in liquid N₂. 300 µl methanol and 1% HCl were added to the homogenate and incubated overnight at 4°C. Subsequently, 200 µl of deionised H₂O and 500 µl of chloroform were added to the homogenate which was then centrifuged at 14000 × *g* for 5 minutes. After centrifugation, two different fractions were obtained. The bottom fraction contained chlorophylls and other pigments, and the upper fraction contained anthocyanin [171]. The upper fraction was used for spectrophotometric quantification of total anthocyanin. The absorbance at wavelengths 530 nm and 657 nm was measured. The total anthocyanin content of leaves was expressed as A₅₃₀–A₆₅₇ / g FW⁻¹.

2.1.9. Root analysis

Seeds were sown onto *A. thaliana* growth medium with sucrose (ATS; 5 mM KNO₃, 2.5 mM KPO₄ (adjusted to pH 5.5), 2 mM MgSO₄, 2 mM Ca(NO₃)₂, 70 µM H₃BO₃, 50 µM Fe-EDTA, 14 µM MnCl₂, 10 µM NaCl, 1 µM ZnSO₄, 0.5 µM CuSO₄, 0.2 µM Na₂MoO₄, 0.01 µM CoCl₂, 10 g/l sucrose, 8 g/l Agar, dissolved in deionised H₂O, and autoclaved) or ½ MS plates and stratified for 3 days in the dark at 4°C. Plants were then grown in a controlled environment with an irradiance of 200 µmol.m⁻².s⁻¹, a photo period of 8 hours, and a constant temperature of 20 ± 2°C. Images of plants were captured at different time points and a scale was included for comparison. The length of the primary roots and total length including lateral roots was measured using imageJ (v1.46r), and the number of lateral roots were counted.

2.2. Barley plant material and growth analysis

2.2.1. Plant material

Barley (Golden Promise) was transformed in our lab by Gloria Comadira (University of Leeds, Leeds, UK) with the assistance of Jennifer Stephens (University of Dundee, Dundee, UK).

2.2.2. Selection

T₂ WT and transgenic barley seeds were sterilised and sown on to ½ MS media containing 100 mg/ml Hygromycin B to select for transformants containing the *LEA5-YFP* constructs. Seeds were kept in the dark at 4°C for 3 days to stratify them. Stratified seeds were moved to the light for 8 hours at a constant temperature of 20 ± 2°C to stimulate germination. The seeds were then moved to the dark for 4 days at a temperature of 20 ± 2°C. Transformants identified as Hygromycin B resistant seedlings were standing tall like dark grown plants with long blades. Hygromycin B sensitive plants were bleached with short hypocotyls. The plates were kept in weak light for 2 days to allow the Hygromycin B resistant plants to become green without bleaching them. Hygromycin B resistant plants were then grown in standard conditions for 1 week until green and the number of resistant and sensitive plants was recorded. T₃ WT and transgenic barley seeds were sown following the same procedure and the ratio of resistant to sensitive plants was recorded. Plants were selected for homozygosity. DNA was extracted from these plants and a PCR reaction (section 2.3.1), using primers targeting either the Hygromycin B resistance or the *LEA5-YFP* DNA sequences (Table 1), was performed to confirm the presence of the gene of interest.

Table 1: PCR Primers for amplification of the Hygromycin B resistance and the *LEA5-YFP* sequences

Primer	Sequence
Hygromycin B Forward	5' - ACTCACCGCGACGTCTG -3'
Hygromycin B Reverse	5' - GCGGTCTGCTGCTCCATA -3'
<i>LEA5-YFP</i> Forward	5' - GAGCTGTTGCTTGGCTGTGA -3'
<i>LEA5-YFP</i> Reverse	5' - ATGCCGTTCTTCTGCTTGTGC -3'

2.2.3. Phenotype analysis

Barley seeds were sown on soil containing 10% perlite in pots with a 1 L volume (10 cm diameter base, 13 cm diameter top, 10.8 cm depth). Pots were placed in trays and arranged in a random-block design. Plants were grown in greenhouses under an irradiance at soil level of

250 $\mu\text{mol}\cdot\text{m}^{-2}\cdot\text{s}^{-1}$, a 16 hour photoperiod, and a constant temperature of $22 \pm 2^\circ\text{C}$. Plants were watered twice per week. The length of the longest leaf was measured from the base of the plant to the tip of the leaf, the number of leaves counted and the QY measured each week for 8 weeks. At the end of the experiment (week 25), the number of tillers were counted, and the flower head weight, seed weight, and shoot biomass was measured.

2.3. General molecular biology protocols

2.3.1. Standard PCR reaction

Polymerase chain reaction (PCR) amplification of DNA fragments was conducted using BioMix™ Red (Bioline, London, UK) with a 1x final working concentration. PCR was performed in 0.2 ml PCR tubes with the final volumes of the reaction mix typically at 20 μl . Oligonucleotide primers were typically designed to have 25 bp homology with the sequence to be amplified. A 100 μM stock of each oligonucleotide primer was made in TE from which a 10 μM working solution was made in deionised H_2O . All PCRs contained a final concentration of 1 μM of the forward and reverse primer and typically 100 ng DNA. Reactions were run in a thermal cycler with the following conditions: an initial denaturation step was performed at 95°C for 5 minutes, followed by 34 cycles of amplification consisting of a denaturation step at 95°C for 30 seconds, an annealing step at 56°C for 30 seconds, and an extension step at 72°C for 30 seconds. This was followed by a final extension step at 72°C for 5 minutes.

2.3.2. Agarose gel electrophoresis

Agarose gel electrophoresis was used to separate fragments according to their size to determine if gene inserts were present, whether vectors and gene inserts had been correctly digested, and to verify ligation reactions. Agarose gels were prepared by dissolving agarose in 1x Tris-acetate-EDTA (TAE) buffer (40 mM Tris, 20 mM acetic acid, and 1 mM EDTA) by heating. 1x SYBR® safe DNA gel stain (Qiagen nv, Hilden Germany) was added to allow DNA visualisation under ultra violet (UV) light. Samples loaded on the gel were treated with 1x loading buffer (0.05% (w/v) bromophenol blue, 0.05% (w/v) xylene cyanol, 3% (w/v) Ficoll) before loading. Electrophoresis was performed at a constant voltage of 100 V in 1x TAE buffer.

2.3.3. Gel extraction

Gel extraction was performed using a QIAquick Spin Column (Qiagen) according to the manufacturer's instructions. The protocol uses a spin column combined with a silica membrane

to which DNA can bind to purify the DNA. The DNA fragment was excised from the agarose gel and weighed in a 1.5 ml microcentrifuge tube. The binding and solubilisation buffer, buffer QG, was added to the gel (300 μ l per 100 mg of gel fragment) and incubated at 50°C until the gel was dissolved. The DNA was bound to a QIAquick spin column silica membrane by centrifugation for 1 minute at 12100 $\times g$. The silica membrane was then washed with buffer PE and centrifuged for 1 minute at 12100 $\times g$. Residual PE buffer was removed by a second centrifugation for 2 minutes at 12100 $\times g$. The DNA was eluted from the column in 40 μ l deionised H₂O by centrifugation for 2 minutes at 12100 $\times g$.

2.4. Gene transcript analysis

2.4.1. Production of plants

Seeds were germinated and plants grown on soil under 150 μ mol.m⁻².s⁻¹ irradiance with an 8 hour photoperiod at 22°C \pm 2°C. Plants were grown under a propagator cover for 1 week after which the cover was removed and plants were grown until four weeks old.

2.4.2. Harvest

Four-week-old plants were harvested by cutting the shoot just above the soil, taking care not to take any soil with it. For diurnal experiments, plants were harvested over a period of 24 hours and 3 plants were collected for each time point. Each plant was wrapped in foil, labelled and placed in liquid N₂. Samples were stored at -80°C.

2.4.3. RNA extraction

RNA was extracted from plant samples using a NucleoSpin® RNA Plant kit following the standard protocol as follows. The rosettes of 4-week-old *A. thaliana* were homogenised under liquid N₂. The cells were then lysed in 350 μ l Buffer RA1 and 3.5 μ l β -mercaptoethanol and vortexed vigorously. To reduce viscosity and clear the lysate the homogenate was filtered through a NucleoSpin® Filter by centrifugation 11000 $\times g$ for 1 minute. 350 μ l ethanol (70%) was added to the homogenised lysate and mixed to adjust binding conditions. The preparation was added to a NucleoSpin® RNA Plant Column placed in a collection tube which was centrifuged for 30 seconds at 11000 $\times g$ to bind DNA to the column. The silica membrane was desalted using 350 μ l of membrane desalting buffer and centrifuged at 11000 $\times g$ for 1 minute to wash the column. DNA was digested using rDNase which was incubated on the column at room temperature for 15 minutes. The silica membrane and bound RNA was then washed with

200 μ l Buffer RA2 and dried by centrifugation for 30 seconds at $11000 \times g$, washed with 600 μ l Buffer RA3 and dried by centrifugation for 30 seconds at $11000 \times g$ and had a final wash with 250 μ l Buffer RA3 after which the membrane was thoroughly dried by centrifugation for 2 minutes at $11000 \times g$. RNA was eluted in 60 μ l RNase-free deionised H₂O which passed through the column by centrifugation at $11000 \times g$ for 1 minute. RNA was stored at -80°C .

2.4.4. Synthesis of cDNA

RNA was quantified using a Nanodrop (ND-1000 Spectrophotometer, Labtech International, UK). The ratio of absorbance at 260 nm and 280 nm was used to assess the purity of RNA. A ratio of at least 2.0 was accepted as “pure” for RNA. The ratio of absorbance at 260 nm and 230 nm used as a secondary measure of nucleic acid purity. The 260/230 values of RNA used were in the range of 2.0-2.2. 1 μ g of RNA was used to synthesise cDNA using a QuantiTect Reverse Transcription Kit (QIAGEN) following the manufacturer’s protocol. The reverse transcription step was also performed in the absence of reverse transcriptase as a no reverse transcriptase control. This control was to assess the amount of DNA contamination present in the RNA preparation.

2.4.5. Quantitative real-time PCR

Quantitative real-time PCR (QPCR) was performed on cDNA synthesised from the RNA of harvested samples. The cDNA was used in a reaction containing 10 μ l 2x QuantiFast® SYBR® Green PCR master mix (provided by a QuantiFast SYBR Green PCR Kit – QIAGEN), 1 μ M (final concentration) forward and reverse primers, and 20 ng of DNA. The reaction mixture was made to 20 μ l with RNase-free H₂O. At least three technical replicates were performed for each reaction. A no template control which omitted cDNA from the reaction was used as a control for extraneous nucleic acid contamination. This control also served as a control for primer dimer formation. Reactions were performed in skirted, low-profile 96-well PCR plates (STARLAB, Milton Keynes, UK). The reaction mix was used in a two-step cycling protocol. This reaction started with an initial incubation step at 95°C for 5 minutes to activate HotStarTaq Plus DNA Polymerase. This was followed by 40 cycles of amplification consisting of a denaturation step at 95°C for 10 seconds, and a combined annealing and extension step at 60°C for 30 seconds. Fluorescence data was collected during the combined annealing and extension step. Finally, a melting curve analysis was performed to monitor possible mispriming or primer dimer artefacts.

2.5. Mitochondria respiration assays

2.5.1. Isolation of intact mitochondria

The shoots of four-week-old *A. thaliana* plants (50 g), grown on soil with an irradiance of $200 \mu\text{mol}\cdot\text{m}^{-2}\cdot\text{s}^{-1}$, a photo period of 8 hours, and a constant temperature of $20 \pm 2^\circ\text{C}$, were harvested. The following steps were performed at 4°C , where possible. Samples were homogenised in 200 ml Grinding Medium (0.3 M sucrose, 25 mM $\text{Na}_4\text{P}_2\text{O}_7$, 10 mM KH_2PO_4 , 2 mM EDTA disodium, 1% PVP-40 (Polyvinylpyrrolidone MW 40000), 1% BSA (Albumin from bovine serum), 18 mM sodium L-Ascorbate, 20 mM L-Cysteine, dissolved in deionised H_2O and adjusted to pH 7.5 with HCl) using a mortar and pestle at 4°C . Homogenised material was filtered through miracloth into a conical flask sat in ice to remove cell debris. Filtrate was transferred into cooled 50 ml centrifuge tubes (Nalgene). Cell debris and nuclei were pelleted by centrifugation at $2500 \times g$ at 4°C for 5 minutes with slow deceleration. The supernatant was transferred to clean pre-cooled centrifuge tubes, balanced by weight and then the mitochondria, chloroplasts and peroxisomes were pelleted by centrifugation at $17500 \times g$ at 4°C for 20 minutes with slow deceleration. Once pelleted the supernatant was aspirated and discarded. The pellets were resuspended in 1 ml of 1x wash buffer (0.3 M Sucrose, 10 mM TES (2-[(2-Hydroxy-1,1-bis(hydroxymethyl) ethyl) amino] ethanesulfonic acid, N-Tris (hydroxymethyl) methyl] -2-aminoethanesulfonic acid), 0.1% BSA, dissolved in deionised H_2O and adjusted to pH 7.5 with NaOH) and pooled into one 50 ml centrifuge tube using a sterile pipette. The centrifuge tube was filled to 50 ml with 1x wash buffer and again cell debris and nuclei were pelleted to ensure purity ($2500 \times g$ at 4°C for 5 minutes with slow deceleration). The supernatant was transferred to a clean centrifuge tube and centrifuged at $17500 \times g$ at 4°C for 20 minutes to re-pellet mitochondria and peroxisomes. The supernatant was aspirated and discarded and the pellet was resuspended in 1ml 1x wash buffer. A 0-4% PVP-40 gradient was formed using a BioRAD Gradient Former 485. A heavy gradient fraction (17.5 ml 2x Wash buffer, 9.8 ml Percoll, and 7.7 ml 20% PVP-40) and a light gradient fraction (17.5 ml 2x Wash buffer, 9.8 ml Percoll, and 7.7 ml H_2O) were prepared and poured into the BioRAD Gradient Former 485. The two fractions formed a gradient as the solutions were drawn from the BioRAD Gradient Former 485 by a peristaltic pump, into 50 ml centrifuge tubes (Nalgene). Crude mitochondria were carefully layered on top of the gradient. Gradients were centrifuged at $40000 \times g$ at 4°C for 40 minutes with no brakes. The mitochondria formed a light-yellow band low in the tube. Layers above the mitochondria were removed by aspiration. The remaining solution was washed in 1x wash buffer and centrifuged at $31000 \times g$ at 4°C for 15 minutes. The supernatant was removed and

the pellet was resuspended and washed as previously. After this wash, most of the supernatant was removed and the pellet was resuspended in the residual 1x wash buffer. The concentration of mitochondria was determined with a Bradford assay (the BSA in the wash buffer was accounted for by subtracting 1 mg/ml from the determined concentration of protein).

2.5.2. Verifying mitochondrial integrity by measuring cytochrome *c* oxidase latency

A Clark-type oxygen electrode with a 2.5 ml chamber was calibrated and the chamber was filled with 2 ml Mitochondrial Reaction Buffer (0.3 M Mannitol, 10 mM TES-KOH pH 7.5, 3 mM MgSO₄, 10 mM NaCl, 5 mM KH₂PO₄, 0.1% BSA, and dissolved in deionised H₂O) and warmed to 25°C. 500 µg of mitochondria was added (in a volume of 10-40 µl) to the Mitochondrial reaction buffer and the chamber was closed ensuring that no bubbles remained in the chamber. Any substrates added after was through a pore in the chamber using a Hamilton syringe. Respiration rates were calculated by measuring oxygen saturation of buffer and dividing by time. Once a base respiration rate was established 40 µl of 0.5 M ascorbate was added using a 50 µl Hamilton syringe to reduce endogenous cytochrome *c*. 2-3 minutes later 20 µl 5 mM cytochrome *c* was added. 2-3 minutes later 10 µl 10% Triton X-100 (C₁₄H₂₂O(C₂H₄O)_{*n*}) was added to solubilise mitochondrial membranes. Cytochrome *c* cannot traverse an intact outer mitochondrial membrane and so if the outer membrane is intact, COX will be 100% latent. Thus, by comparing COX activity in the absence and presence of Triton X-100, an estimation of the percentage of mitochondria with an intact outer membrane can be obtained. The following equation was used to calculate the proportion of intact mitochondria:

$$100 - \left(\frac{(\text{COX activity with cyt } c - \text{COX activity with ascorbate})}{(\text{COX activity with Triton X100} - \text{COX activity with ascorbate})} \right) * 100$$

2.5.3. Complex I respiratory control ratio

The reaction chamber of the oxygen electrode was prepared with 2 ml of fresh reaction medium at 25°C with the stirrer on. A known concentration of mitochondria was added to the chamber (in a volume of 10-40 µl) so that the final concentration in the chamber was 100 µg/ml. The chamber was closed and any substrates added after was through a pore in the chamber using a Hamilton syringe. 8 µl of 500 mM pyruvate, 12 µl of 500 mM Thiamine pyrophosphate (TPP) and 8 µl of 800 mM Malate was added to the chamber so that the final concentration in the chamber was 2 mM, 3 mM and 2 mM, respectively. Typically, one or two minutes passed before adding 20 µl of 100 mM ADP to the chamber. After a further two minutes had passed, the reaction was stopped with the addition of 2.5 µl of 5 mg/ml Oligomycin to the chamber

(2 µg/ml final concentration). Oligomycin should block the F₀ domain of ATP synthase and thus inhibit respiration. Subsequently, 1 µl of 1 mM of the ionophore FCCP (Carbonyl cyanide-p-trifluoromethoxyphenylhydrazone) was added to the chamber (0.5 µM final concentration).

2.5.4. Complex II respiratory control ratio

The reaction chamber of the oxygen electrode was cleaned and filled with 2 ml of reaction medium at 25°C with the stirrer on. A known concentration of mitochondria was added to the chamber (in a volume of 10-40 µl) so that the final concentration in the chamber was 100 µg/ml. The chamber was closed while ensuring that no bubbles remained in the chamber. Any substrates added after this step were added through a pore in the chamber using a Hamilton syringe. 20 µl of 1 M succinate was added to the chamber using a 50 µl syringe so that the final concentration in the chamber was 10 mM. This step reduces complex II. One minute later, 1 µl of 1 mM rotenone was added to the chamber using a 10 µl syringe (final concentration in chamber is 0.5 µM) which inhibited complex I activity. Two minutes passed before adding 2 µl of 100 mM ADP to the chamber using a clean 10 µl syringe. After a further two minutes had passed 2.5 µl of 5 mg/ml Oligomycin was added to the chamber using a clean 10 µl syringe (2 µg/ml final concentration). Subsequently 1 µl of 1 mM of the ionophore FCCP was added to the chamber (concentration in chamber: 0.5 µM).

2.6. Production of plants expressing reduction-oxidation sensitive GFP

Plasmids (pCAMBIA-1304; Figure 2-1) containing a roGFP2 sequence that was either targeted to the mitochondria (mitochondrial-roGFP) or without a targeting sequence (cytosolic-roGFP) were obtained from Prof. Ulrike Zentgraf (Universität Tübingen, Tübingen, Germany). These constructs were produced as in Wierer *et al.*, 2012 [172]. A mitochondrial targeting sequence had been inserted before the roGFP sequence to produce roGFP targeted to the mitochondrion.

2.6.1. Amplification of roGFP DNA using *E. coli*

Ultra-competent *E. coli* were produced using a protocol by Inoue *et al.*, 1990 [173]. 1µl (150 ng/µl) of each of the modified pCAMBIA1304 vectors was added to separate aliquots of ultra-competent 200 µl *E. coli* (DH5α) cells. The cells were left on ice for 5 minutes. 10 µl of cells were then spread onto LB plates containing 50 µg/ml kanamycin (Fisher Scientific), covered and incubated at 37°C overnight. Individual colonies were selected from the plates and cultured in 10ml LB medium containing 50 µg/ml Kanamycin. A sterile pipette tip was touched to a transformed colony and put into the culture medium. The culture was then incubated at

37°C with shaking at 200 rpm overnight. Cultures were grown to an OD₆₀₀ of approximately 1.6. Plasmids were extracted from cultured *E. coli* using the QIAGEN plasmid mini kit following the manufacturer's protocol. Plasmids were stored at -20°C.

2.6.2. Preparation and transformation of Agrobacterium

To generate electro-competent *Agrobacterium tumefaciens* (strain: GV3101 (*rhoH⁺ hrcA⁺*)), an overnight culture of *Agrobacterium* in 100 ml YEB medium (1 g/l Yeast Extract, 5 g/l Beef extract, 5 g/l Sucrose, 5 g/l Bacto-peptone, 0.5 g/l Magnesium sulphate, dissolved in deionised H₂O, adjusted to pH 7 and autoclaved) was prepared and grown at 28°C with agitation. The overnight culture was used to inoculate 1 L YEB. This was grown overnight at 28°C to an OD₆₀₀ of approximately 1.5. This culture was centrifuged at 2400 × *g* for 15 minutes at room temperature and resuspended in 1 L ice-cold deionised H₂O. The suspension was pelleted by centrifugation at 2400 × *g* for 15 minutes. This pellet was resuspended in 2 x 20 ml aliquots of ice-cold 10% glycerol and centrifuged for 15 minutes at 3500 × *g*. The cells were then resuspended in 1 ml ice-cold glycerol, aliquoted into 100 µl and frozen in liquid nitrogen. Electro-competent cells were stored at -80°C.

Aliquots of electrocompetent *Agrobacterium* were thawed on ice and the electroporator was set up to use 50 µF, 1.8 kV, 150 Ω. The plasmids were diluted to 40 ng/µl and 2 µl was added to 100 µl of *Agrobacterium*, mixed briefly and placed in a pre-chilled electroporation cuvette. The mixture was then pulsed by the electroporator. 1 ml of pre-chilled YEB was added to the bacteria and the mixture was transferred to a sterile test tube. The bacteria were incubated at 28°C for 2 hours. Cells were then plated out onto YEB-agar plates containing 50 µg/ml Kanamycin (to select for the construct), 50 µg/ml Gentamycin (to select for the Ti Helper plasmid) and 100 µg/ml Rifampicin (to select for *Agrobacterium*).

2.6.3. Agrobacterium-mediated transformation of *Arabidopsis thaliana*

A single colony of *Agrobacterium* harbouring the gene of interest in a binary vector was used to inoculate 5 ml liquid LB medium containing the appropriate antibiotics for binary vector selection. The liquid culture was grown at 28°C for 2 days with shaking. This feeder culture was used to inoculate 500 ml LB with the appropriate antibiotics and the bacteria were grown at 28°C for 16–24 hours to reach the stationary phase (OD 1.5–2.0). *Agrobacterium* cells were harvested by centrifugation at 4000 × *g* for 10 minutes at room temperature, the supernatant was discarded and the cells gently resuspended in 1 volume of freshly made 5% (wt/vol) sucrose

solution with a stirring bar. Silwet L-77 (a surfactant) was added to a concentration of 0.02% (vol/vol) and mixed well immediately before floral dipping the plants. The *Agrobacterium* cell suspension was transferred to a 500 ml beaker and plants were inverted and their flowers dipped in the *Agrobacterium* cell suspension for 10 seconds with gentle agitation. Care was taken to also dip the shorter axillary inflorescences. Plants were removed from the solution and drained for 10 seconds. Dipped plants were covered with a plastic cover and laid on their sides for 16–24 hours to maintain high humidity. The cover was removed the next day and treated plants were grown normally for 1 month. Water was withheld when the siliques turned brown. Dry seeds were collected using a sieve mesh.

2.6.4. Selection of transformants

Transformed *Arabidopsis* seeds were sterilised in 10% bleach, with a wash of 70% EtOH and 5 washes of sterile H₂O. Seeds were sown on to ½ MS media containing 20 µg/ml Hygromycin B. Seeds were kept in the dark at 4°C for 3 days to stratify them. Stratified seeds were moved to the light for 8 hours at a constant temperature of 20 ± 2°C to stimulate germination. The seeds were then moved to the dark for 4 days at a temperature of 20 ± 2°C. Transformants identified as Hygromycin B resistant seedlings were standing tall like normal dark grown seedlings with long hypocotyls and closed cotyledons. Hygromycin B sensitive seedlings were lying on medium with very short hypocotyls. The seedlings were kept in weak light for 2 days to allow the Hygromycin B resistant seedlings to become green without bleaching the etiolated seedlings. Hygromycin B resistant seedlings were transferred to soil and grown to seed. Plants were selected for homozygosity. DNA was extracted from transgenic plants and a PCR was used to confirm the presence of the transgene. Primers that amplified the sequence encoding the mitochondrial targeting peptide and roGFP were used to confirm the presence of mitochondrial-roGFP. Primers that amplified roGFP were used to confirm the presence of cytosolic-roGFP.

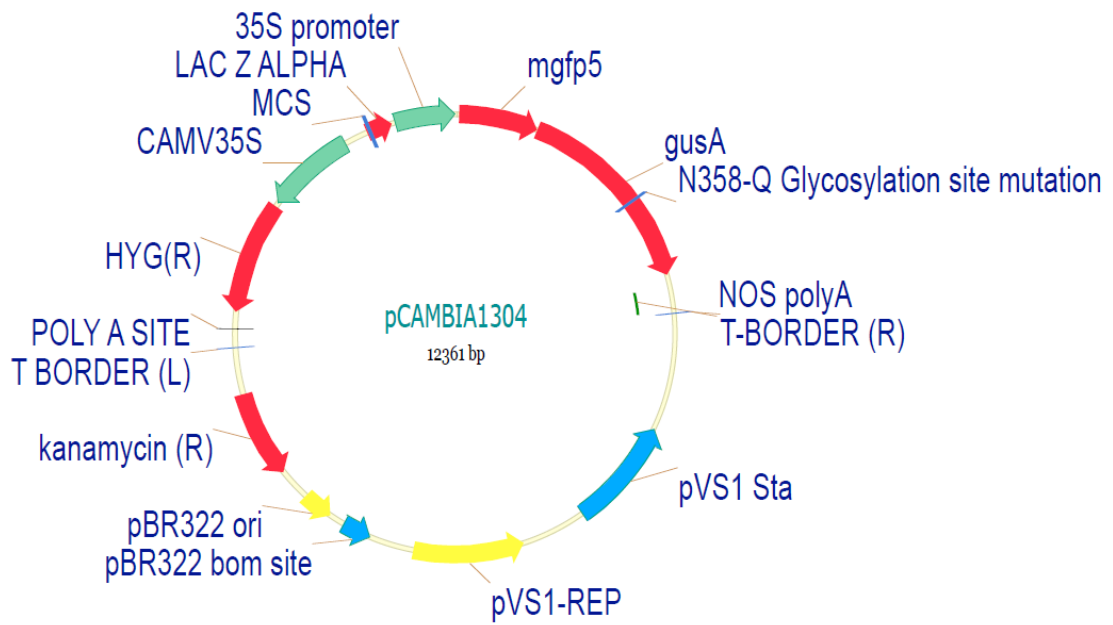


Figure 2-1: Plasmid map of pCAMBIA1304

2.7. Protein-protein interaction analysis by tandem affinity purification (TAP)

2.7.1. Primer design and amplification of *LEA5*

Primers were designed to amplify *LEA5* from the start codon to the last nucleotide before the stop codon (Table 2: *LEA5* Forward and *LEA5* (no stop codon) Reverse, respectively). A standard PCR (Section 2.3.1) was performed to amplify the target gene. Once amplified the gene was purified and sequenced.

A PCR reaction was then performed to add *attB* sites to the 5' and 3' ends of the *LEA5* sequences using primers that target *LEA5* and contain overhangs for *attB1* and *attB2* sites (Table 2: *LEA5-attB1* Forward and *LEA5-attB2* Reverse, respectively). The forward primer was designed to contain the Kozak sequence which plays a major role in the initiation of the translation process [174]. The reverse primer was designed without a stop codon to perform a C-terminal fusion. The product was produced using a standard PCR (Section 2.3.1) with minor changes - the first 5 cycles had an annealing temperature of 45°C and the next 29 cycles had an annealing temperature of 58°C. The PCR products were separated by 1.5% agarose gel electrophoresis, and then purified and sequenced. The product identified as *LEA5* without the stop codon and with *attB* ends was then used to produce constructs for TAP using the Gateway® Technology cloning method.

Table 2: PCR Primers for amplification *LEA5* (without stop codon)

Primer	Sequence
<i>LEA5</i> Forward	5' - ATGGCTCGTTCTATCTCTA ACG -3'
<i>LEA5</i> (no stop codon) Reverse	5' - CTGCTTGTTGTTCAAGAGAGC -3'
<i>LEA5-attB1</i> Forward	5' - GGGGACAAGTTTGTACAAAAAAGCAGGCT <u>CCACC</u> ATGGCTCGTTCTATCTCTA ACG -3'
<i>LEA5-attB2</i> Reverse	5' - GGGGACCACTTTGTACAAGAAAGCTGGGT <u>CCTGCTTGTTGTTCAAGAGAGCTGC</u> -3'

Kozak sequence (underlined). *LEA5* sequences (**bold**).

2.7.2. Cloning of constructs containing *LEA5* used in TAP

Once amplified and sequenced, 100 fmol of PCR product and 100 fmol of pDONR201 (Figure 2-2) was placed in a 10 µl BP reaction containing 2 µl 5x BP-clonase™ II enzyme mix and made to 10 µl with TE buffer. The reaction was left for 4 hours after which 1 µl 10x Proteinase K was added and incubated for 10 minutes at 37°C to stop the reaction.

One Shot® OmniMAX™ 2 T1 Phage-Resistant Cells were transformed 5 µl of the recombined plasmid by heat-shock of the cells to facilitate uptake of the DNA. The cells were then incubated in Lysogeny Broth (LB; 10 g/l Tryptone, 5 g/l Yeast extract, 10 g/l NaCl, dissolved in deionised

H₂O, adjusted to pH 7 with NaOH, and autoclaved) for one hour and then spread onto plates containing LB agar and 50 µg/ml kanamycin. Kanamycin resistant colonies were identified on the plates after 16 hours. A single colony was used to inoculate LB medium containing 50 µg/ml kanamycin. After 16 hours, these cells were pelleted and the plasmid was extracted using the QIAGEN plasmid mini kit following the manufacturer's protocol. The plasmid was quantified using a Nanodrop.

Finally, the *LEA5* fragment, contained in the pDONR201 vector (Figure 2-2), was assembled in to a pKCTAP destination vector during a single MultiSite LR Clonase reaction to produce an expression clone. This procedure was performed at VIB following an established procedure [175]. The pKCTAP destination vector contained the improved TAP tag [176] on the C terminus of *LEA5*, a kanamycin resistance gene for selection of transformed cells, and a green fluorescent protein (GFP) expression cassette for use as a visible marker for transformation.

2.7.3. Cloning of constructs containing *ERF109* used in TAP

ERF109 flanked by *attB1* and *attB2* sites was ordered as a gBlocks® Gene Fragment (double-stranded, sequence-verified genomic DNA) from Integrated DNA Technologies Inc (Integrated DNA Technologies, BVBA, Leuven, Belgium). The *ERF109* flanked by *attB1* and *attB2* DNA was cloned in to pDONR221 in a BP reaction using the Gateway® Technology cloning method, as in section 2.7.2. Subsequently the *ERF109* fragment, contained in the pDONR221 vector, was assembled in to pKNTAP destination vector during a single MultiSite LR Clonase reaction to produce an expression clone. Assembly in to the pKNTAP destination vector was performed at VIB following an established procedure [175]. The pKNTAP destination vector contained the improved TAP tag [176] on the N terminus of *ERF109*.

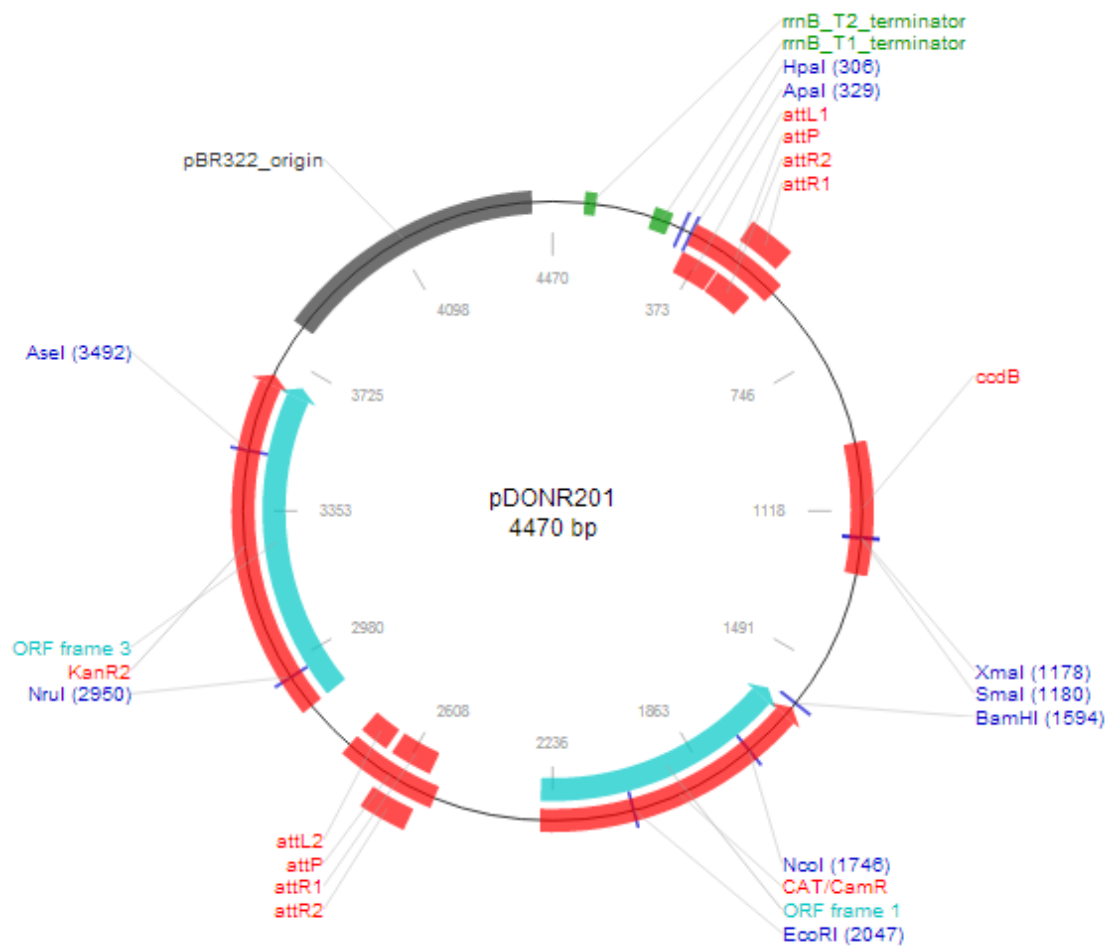


Figure 2-2: Plasmid map of pDONR201

2.7.4. Cell culture cultivation

Arabidopsis thaliana (ecotype Landsberg *erecta*) cell suspension cultures (Plant Systems Biology; PSB-L and PSB-D), originally derived from MM1 and MM2d cultures [177], were obtained from Geert De Jaeger (VIB, Ghent, Belgium). Cultures were maintained in 50 ml Murashige and Skoog basal salts with minimal organics (MSMO) medium (4.43 g/l MSMO, 30 g/l sucrose, 0.5 mg/l α -naphthaleneacetic acid, 0.05 mg/l kinetin, adjusted to pH 5.7 with 1 M KOH) at 25°C in the dark, with agitation (130 rpm). Subcultures were established every 7 days in fresh medium at a 1:10 dilution.

2.7.5. Cell culture transformation

Agrobacterium tumefaciens (strain: GV3101 (*rhoH*⁺ *hrcA*⁺)), were transformed by electroporation with appropriate plasmids. Transformed *Agrobacterium* were grown in YEB medium until they reached an OD₆₀₀ between 1.0 and 1.5. The *Agrobacterium* culture was then washed three times by centrifugation (10 minutes at 3050 × g) with an equal volume MSMO medium. Washed *Agrobacterium* was resuspended in MSMO medium to an OD₆₀₀ of 1. Two days after the sub-cultivation of an *Arabidopsis thaliana* cell suspension culture, 3 ml was incubated with 200 μ l washed *Agrobacteria* and 200 μ M acetoseringone at 25°C in the dark with agitation (130 rpm) for 48 hours. Two days after co-cultivation, 7 ml MSMO containing a mix of three antibiotics (25 μ g/ml kanamycin, 500 μ g/ml carbenicillin, and 500 μ g/ml vancomycin) was added to the cell cultures and grown for 11 days under standard conditions. The stable transgenic cultures were selected by 1:5 dilution in 50 ml fresh MSMO medium with antibiotics 11 days after inoculation, and then with a sequential 1:10 dilution in to 50 ml fresh MSMO medium with antibiotics 18 days post inoculation. The transgenic cells were subcultured at a 1:5 ratio in 50 ml MSMO medium containing 25 μ g/ml kanamycin once per week for 2 more weeks. Cell cultures were then scaled up to 200 ml (1:5 dilution) in a 500 ml conical flask and then after 1 week scaled up to 2x 1 L (1:10 dilution) in 2 L Erlenmeyer flasks.

2.7.6. Protein extract preparation

Cell material from cell cultures (1:5 dilution) was grown for 3 days, harvested on a sintered glass filter, wrapped in foil, frozen in liquid nitrogen and stored at -80°C. 2.5 g of cell culture was homogenised by grinding in liquid nitrogen. Crude protein extracts were mixed with 1.67 ml extraction buffer (25 mM Tris/HCL pH 7.6, 15 mM MgCl, 150 mM NaCl, 15 mM pNO₂Phenyl PO₄, 60 mM β -glycerophosphate, 0.1% NP-40, 0.1 mM Na₃VO₄, 1 mM PMSF,

1 μ M E64, EDTA-free Ultra Complete tablet (1 per 10 ml), 0.1% benzonase nuclease (Novagen), 5% ethyleenglycol) with an Ultra-Turrax T25 mixer (IKA Works, Wilmington, NC) and then incubated at 4°C for 30 minutes. The soluble protein fraction was obtained by centrifugation at $36900 \times g$ for 20 minutes, transference of the supernatant to a clean microcentrifuge tube and another centrifugation at $36900 \times g$ for 20 minutes. The protein concentration was quantified using a Bradford assay.

2.7.7. Western blots

To decide on the conditions for TAP, first it was important to understand how the protein responded to oxidants. Cultures were treated with 0, 1, 2, 5, 10, & 20 mM H₂O₂ for 1 hour, and separately with either 1 mM or 2 mM H₂O₂ and samples were collected between 0 and 60 minutes. Protein extractions were acquired as in section 2.6.5.

Samples were transferred to Nitrocellulose membranes (N-2639, Sigma) by semi-dry western blotting after sodium dodecyl sulfate (SDS) polyacrylamide gel electrophoresis (PAGE). The transfer was performed for 60-70 minutes in electrophoresis buffer containing 20% methanol, at a constant current of 1.1 mA times the area of the gel in cm². The membrane was blocked in 5% skimmed milk in Tris-Buffered Tween (TBT: 6 mM Tris base, 19 mM Tris HCl, 150 mM NaCl, 0.1% (v/v) Tween® 20 Chemiluminescence solution: 100 mM Tris/HCl pH 8.5, 1.25 mM luminol, 68 μ M p-Coumaric acid, 0.01% H₂O₂) for 45-60 minutes at room temperature or overnight at 4°C. Once blocked the membrane was incubated with the primary antibody (PAP) in a 1:2500 dilution in 5% skimmed milk in TBT for 2 hours at room temperature. The membrane was then washed in TBT for 15 minutes, and then washed a further three times for 5 minutes each time (total = 30 minutes). The chemiluminescence emitted by the antibody in the respective solutions was detected by Super RX films (Fuji).

2.7.8. Tandem affinity purification

Purifications were performed as described by Van Leene *et al.*, 2007 [175] with some modifications. In the binding step, 25 mg of total protein extract was incubated with 500 μ l IgG Sepharose 6 Fast Flow beads (GE-Healthcare, UK), pre-equilibrated with 3 x 1 ml extraction buffer with gentle rotation in a DNA LoBind Eppendorf for 1 hour at 4°C. The IgG Sepharose beads were transferred to a 1 mL Mobicol column (MoBiTec, Germany) and washed with 3.75 ml (150 x V: 5x750 with rotation) tobacco (*Nicotiana tabacum* L.) etch virus (TEV) buffer (10 mM Tris-HCl, pH 8.0, 150 mM NaCl, 0.1% [v/v] NP-40, 0.5 mM EDTA, 1 mM PMSF,

1 μ M E64, 5% [v/v] ethylene glycol). In the first elution step, 100 μ l TEV buffer + 5 μ l (10U) Rhinovirus protease (GE Healthcare) was added to the column and incubated at 4°C for 1 hour. After 30 minutes, an addition 5 μ l (10 U) Rhinovirus protease was added. The eluate was collected in a microcentrifuge tube by centrifugation at 150 \times g at 4°C for 1 minute. The eluate was then washed with an addition 100 μ l TEV buffer (10 mM Tris/HCl pH 7.6, 150 mM NaCl, 0.1% NP-40, 0.5 mM EDTA, 1 μ M E64, 1 mM PMSF, 5% ethylene glycol) on a Mobicol spin column and again the eluate was collected by centrifugation at 150 \times g at 4°C for 1 minute (total volume collected 210 μ l). In the second binding step, the TEV-eluate was incubated with TEV-buffer (1 ml) equilibrated 100 μ l Streptavidin Sepharose High Performance (Amersham) beads at 4°C on a rotating mixing device for 1 hour. The mix was transferred to a mobicol column and the Streptavidin beads were washed with 2.5 ml (100 CV) (3x833 μ l) TEV buffer. In the second elution step, bound complexes were eluted with 30 μ l 1x NuPAGE sample buffer containing 20 mM Desthiobiotin, incubated for 5 minutes with regular mixing. The beads were separated from eluate on a Mobicol spin column and the eluate was stored at -70°C.

2.7.9. Sample preparation

Sample preparation was performed by the Geert De Jaeger lab at VIB, Ghent, Belgium. Purified protein complexes were concentrated by trichloroacetic acid precipitation, resolved by NuPAGE electrophoresis, and visualised by Coomassie Brilliant Blue G-250 staining as described by Van Leene *et al.*, 2011 [178]. Protein gels were cut to isolate complete lanes, and single protein bands were excised and collected in microtiter plates. These were further processed for mass spectrometry analysis as described by Shevchenko *et al.*, 1996 [179], with minor modifications.

2.7.10. Acquisition of mass spectra

Single protein bands excised from gel were analysed by VIB Proteomics Expertise Center, Ghent University (Ghent, Belgium). Peptide mass fingerprints and subsequent 1 kV CID fragmentation spectra of selected peptides were acquired using a MALDI-tandem-mass spectrometry instrument (4700 Proteomics Analyzer; Applied Biosystems).

2.7.11. Mass spectra-based protein homology identification

Protein homology identification was performed by Dominique Eeckhout (VIB, Ghent, Belgium). GPS Explorer 3.5 (Applied Biosystems) was used to process the peptide mass fingerprints and peptide sequence spectra of each sample. Data search files were generated and

submitted for protein homology identification by using a local database search engine, Mascot v 2.4.01 (Matrix Science, London, UK). The database, SNAPS (Simple Non redundant Assembly of Protein Sequences; version 0.4) for *Arabidopsis*, compiled from multiple public databases, was searched for homologous proteins. A decoy database from the SNAPS for *Arabidopsis* database was generated to approximate the false positive rate of the protein homology data set. Each protein amino acid sequence was shuffled with the EMBOSS shuffle tool [180]. False positives were excluded from the results.

2.7.12. Data analysis

The BLAST (Basic Local Alignment Search Tool) and PSI (Position Specific Iterative)-BLAST algorithms were used to search for homologues of the identified proteins. The Arabidopsis Information Resource database (<http://www.Arabidopsis.org>) was used for gene ontology annotation searches.

2.8. Protein-protein interaction analysis by split-YFP

2.8.1. Construction of the LEA5-YFPc and LEA5-YFPn vectors

The pDONR201+*LEA5* plasmid (constructed in 2.7.2) was used in an LR reaction with N9842 to produce LEA5-YFPc plasmid, and used in an LR reaction with N9843 to produce the LEA5-YFPn plasmid. The LR recombination reaction was performed as in the handbook (ThermoFisher Gateway® Technology manual). 2 µl (300 ng/reaction) of the entry clone, 2 µl (300 ng/reaction) of the destination vector, along with 4 µl of 5 x LR Clonase Reaction buffer, 8 µl TE buffer pH 8.0 and 4 µl of LR Clonase™ and mixed briefly. The reaction as incubated at 25°C for 1 hour. The reaction was stopped by the addition of 2 µl Proteinase K and incubation at 37°C for 10 minutes. The reaction was stored at -20°C and used to transfect protoplasts.

2.8.2. Construction of the RH22-YFPc and RH22-YFPn vectors

Primers were designed to amplify the ORF of *DEA(D/H)-box RNA helicase 22 (RH22)* from the start codon to the last nucleotide before the stop codon (Table 3). *RH22* was amplified from genomic DNA extracted from *A. thaliana* using a standard PCR reaction. The PCR products were separated by agarose gel electrophoresis. The band representing *RH22* was excised and purified. Primers were designed to extend the *RH22* gene with *attB* sites (Table 3; *RH22-attB1* Forward and *RH22-attB2* Reverse, respectively). The ORF of *RH22* was used in a PCR reaction with *attB* primers (Table 3) in a standard PCR reaction. PCR products were separated by

agarose gel electrophoresis and the band representing *RH22* with *attB* ends was excised, purified and sequenced. The sequenced PCR product representing *RH22* with *attB* ends was then used in a BP reaction, as in Section 2.7.2.

Table 3: PCR Primers for amplification *RH22* (without stop codon)

Primer	Sequence
<i>RH22</i> Forward	5' - ATGATTCTCTCACGCTCTGTCTCC -3'
<i>RH22</i> Reverse	5' - ATATCTCACAGCTTGAGGCTCCTC -3'
<i>RH22-attB1</i> Forward	5' - GGGGACAAGTTTGTACAAAAAAGCAGGCT <u>CCACC</u> ATGATTCTCTCACGCTCTGTCTCC -3'
<i>RH22-attB2</i> Reverse	5' - GGGGACCACTTTGTACAAGAAAGCTGGGT CATATCTCACAGCTTGAGGCTCCTC -3'

Kozak sequence (underlined). *RH22* sequences (**bold**).

2.8.3. Isolation of protoplasts

Protoplasts were isolated from *A. thaliana* following the protocol of Wu *et al.*, 2009 [181] with minor modifications, and the assistance of Nurhayati Razak. Plants were grown on soil in standard conditions for 4 weeks. Leaves were taken from these plants and the upper epidermal layer was affixed to Time tape (Time Med, Burr Ridge, IL) to support the leaf. The lower epidermal surface was affixed to a strip of Magic tape (3M, St. Paul, MN) which was then carefully pulled away removing the lower epidermal surface cell layer. Several leaves (~2 g) while still adhered to the Time tape were transferred to a Petri dish containing a 10 ml enzyme solution (1% cellulose 'Onozuka' R10 (Yakult, Tokyo, Japan), 0.25% macerozyme 'Onozuka' R10 (Yakult), 0.4 M mannitol, 10 mM CaCl₂, 20 mM KCl, 0.1% BSA and 20 mM MES, pH 5.7). The leaves were agitated on a platform shaker at 70 rpm for 30 minutes, releasing the protoplasts in to the solution. The solution was placed in to a centrifuge tube and the protoplasts were centrifuged at 100 × *g* for 3 minutes. The supernatant was removed and the protoplasts were washed with 50 ml of pre-chilled modified W5 solution (154 mM NaCl, 125 mM CaCl₂, 5 mM KCl, 5 mM glucose, and 2 mM MES, pH 5.7), and incubated on ice for 30 minutes. After 30 minutes the protoplasts were centrifuged again at 100 × *g* for 3 minutes, the supernatant was removed and the protoplasts were resuspended in MMg solution (0.4 M mannitol, 15 mM MgCl₂, and 4 mM MES, pH 5.7) to a final concentration of 2 to 5 × 10⁵ cells/ml.

2.8.4. Transient gene expression in protoplasts

DNA was transiently expressed in Arabidopsis mesophyll protoplast using the method described by Yoo *et al.*, 2007 [182], with minor modifications. Approximately 10 µg (8 to 12 µg) of plasmid DNA was mixed with 200 µl of approximately 5 × 10⁴ protoplasts (2 × 10⁴ to 1 × 10⁵) in MMg solution at room temperature. Prepared fresh, a 200 µl of a solution of 40%

(w/v) PEG (MW 4000; Fluka), 0.1 M CaCl₂, and 0.2 M mannitol was added to the protoplasts, and the mixture was incubated at room temperature for 5 minutes. Once incubated, the protoplasts were washed with 3 ml of W5 solution. The protoplasts were then pelleted by centrifugation at 100 × *g* for 1 minute. This wash step was repeated twice. Pelleted protoplasts were gently resuspended in 1 ml W5 solution and finally incubated in 6-well plates coated with 1% BSA at room temperature for 16 hours in the light.

2.8.5. Visualisation of interactions

Protoplasts were observed with a Zeiss LSM700 laser scanning confocal microscope using 20×/0.8 Plan-Apochromat, 40×/1.2 W C-Apochromat or 63×/1.4 Oil Plan-Apochromat in multi-track channel mode. Excitation wavelengths and emission filters were 488 nm/bandpass 505-530 nm for YFP, and with simultaneous excitation at 488 nm with a band-pass 650-710 nm for detection of chloroplast auto-fluorescence. Image processing was performed using Zeiss ZEN 2011 (black edition) v7.1, and ImageJ v1.46r. Translational research

The bioinformatics resources at Bayer (Crop Science Division - Trait Research Innovation Center in Ghent, Belgium) were leveraged to find crop homologues. A tree of orthologous genes was produced using Ensembl. Using the OMA browser [183] candidate genes identified in the TAP tag experiments were used to find homologous genes from key monocot species for each of those candidate genes. The protein sequences found were extracted *in silico* from genomic sequences and are sometimes truncated and/or absent due to the incompleteness of the original DNA molecule and/or genome. The same tool was used for expression analysis of candidates in wheat. Swiss model was used to produce 3D protein models.

Chapter 3. Characterisation of the phenotype of *Arabidopsis thaliana* with modified expression of *LEA5*

3.1. Introduction

The expression of LEA proteins in transgenic plants has been shown to be able to confer stress tolerance to drought [14, 15], cold [16], and freezing [17]. *LEA5* is distinctive as it provided *Saccharomyces cerevisiae* tolerance to a range of oxidants including H₂O₂, menadione, and paraquat [43]. Previous studies have shown that plants with constitutive expression of *LEA5* accumulated more biomass than wild-type (WT) plants [43, 51]. Transgenic plants overexpressing *LEA5* also demonstrated a higher tolerance to H₂O₂ by sustaining a higher root and shoot growth rate than WT plants when exposed to comparable levels of H₂O₂ [43]. The expression of *LEA5* in leaves is suppressed in the light [43], unless in the presence of biotic and abiotic stresses [43]. This could be due to enhanced cellular oxidation - a common feature in the responses of plants to stress - as *LEA5* is up-regulated by a range of oxidants [43]. Moreover, plants that expressed *LEA5* in the anti-sense orientation (AS) accumulated less shoot biomass, and had shorter primary roots with fewer lateral roots and poorly formed root hairs [51]. The *LEA5* AS plants also had earlier flowering and senescence [51]. However, the constitutive over-expression of *LEA5* did not confer drought tolerance in *A. thaliana* which could have been expected from its up-regulation during dehydration stress [43]. Interestingly, plants over-expressing *LEA5* in drought conditions were assimilated less CO₂ [43]. A *LEA5* - yellow fluorescent protein (YFP) fusion was localised to mitochondria [51]. For this reason, it was suggested that there is possibility that *LEA5* interacts with proteins involved in mitochondrial ROS signalling, which could impact on root development [51].

The following studies focus on the role of *LEA5* in growth and stress tolerance of *A. thaliana*. Three lines that over-express *LEA5* (OEX2-2, OEX2-5 [43], and a line expressing *LEA5* fused to *YFP* - OEX-YFP [51]), and two *LEA5* AS lines (AS2 and AS8 [51]) were compared to WT type plants in a range of conditions to observe any phenotypical affects that *LEA5* has on the

plants. The OEX2-5 line was reported to have a moderately increased expression of the transgene [43]. In contrast, the AS lines had about five-fold lower transcript levels [51].

An *in vitro* setup was used as a proxy for field environments to study the effects of abiotic stress on plants. These experimental setups are based on the addition of compounds to the growth medium or exposure of the *in vitro* setup to controlled environmental conditions. Drought was simulated by adding osmotica - mannitol and sorbitol [184, 185] - to lower the water potential of the medium. Similarly, the addition of NaCl to the medium was used to expose plants to a combination of osmotic stress and Na⁺ toxicity [186]. The *in vitro* setup was also exposed to various light intensities. The production of ROS is an inescapable consequence of oxygenic photosynthesis. However high-light can result in the production of excessive amounts of ROS such as singlet oxygen (¹O₂) which is believed to be the main ROS produced in the chloroplasts under excess light. It is produced in energy transfer reactions from the excited triplet state of chlorophyll molecules or their precursors to molecular oxygen. It is a highly reactive species that engages readily with a variety of biomolecules, especially those containing double bonds [159], and results in reduced photosynthetic efficiency and ultimately cell death in photosynthetic tissues exposed to excess light [160]. The medium was also separately supplemented with hydrogen peroxide (H₂O₂), menadione, and paraquat to induce ROS formation in plant tissues. Paraquat, for example, accepts electrons from the photosystem I and transfers them to molecular oxygen to generate ROS. The use of *in vitro* setups offers practical advantages, such as control of stress level, low variability, and the ability to grow many plants in a limited space [184, 187]. Much of our current knowledge on stress physiology in *A. thaliana* is based on artificial stress conditions, and resulted in the identification of many genes that enhance stress tolerance [186, 188, 189]. The studies on shoot phenotypes were performed in the controlled environment facilities at Bayer (Crop Science Division, Trait Research Innovation Centre, Ghent, Belgium). The controlled environment facilities at the University of Leeds were also used to study the root phenotypes of these plants.

The aim of the studies described in this chapter was to gain an insight in to the role of *LEA5* in plant development and responses to abiotic stresses.

3.2. Results: Shoot phenotype

3.2.1. Rosette growth in the absence of stress

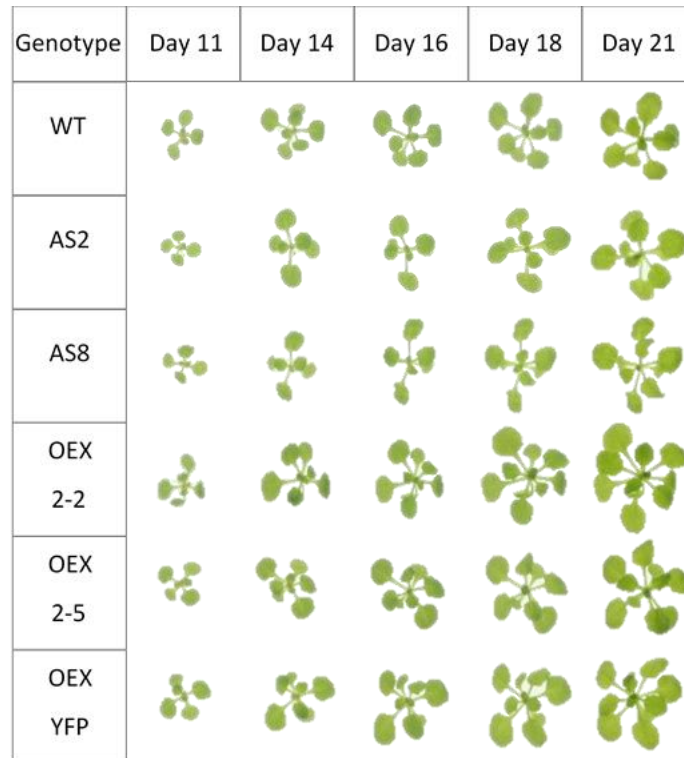
In the following studies, transgenic *A. thaliana* plant with either increased expression or anti-sense expression of *LEA5* (characterised previously [43, 51]) were grown on ½ MS media in the absence of stress to test if phenotypes were similar to those grown on soil described in previous studies [43, 51]. The rosette area and relative growth rates were determined in plants grown for 21 days *in vitro* under growth conditions described in the Materials and Methods chapter. The overall germination rate for these experiments was 94.8%. A total of 960 plants per genotype were analysed in the absence of stress. Measurements were taken on seedlings that had been sown on to ½ MS agar and stratified for 3 days before transferring to the growth chambers for germination and growth. Plants were grown for a period of 21 days with measurements taken on the 11th, 14th, 16th, 18th, and 21st day after transfer to the growth chamber. Representative shoot phenotypes of the different lines on days 11, 14, 16, 18 and 21 are shown in Figure 3-1 A. Although the shoot phenotypes are visually similar in all lines, analysis revealed that the rosette area of AS2 and AS8 plants were significantly smaller early in the growth period – days 11 (P<0.001 for both genotypes), 14 (P<0.001 for both genotypes), and 16 (P<0.001 for AS2 plants), whereas the rosette area of OEX lines was similar to WT plants at these stages (Figure 3-1 B). Later in the growth period (days 18 and 21), the rosette areas of AS plants had grown to a similar size of the WT plants (Figure 3-1 B). Interestingly, more AS plants had inflorescences than the WT plants at 24 days whereas fewer OEX plants had committed to inflorescence at this age (Table 4).

Table 4: Percentage of plants with inflorescences 24 days after germination

Genotype	WT	AS2	AS8	OEX2-2	OEX2-5	OEX-YFP
Percentage with inflorescences	22.5	48.4	50.8	22.5	17.5	15

Plants were also grown in stress conditions and a total of 20,160 plants were analysed. 8,640 were analysed in drought stress experiments, another 8,640 were analysed in oxidative stress experiments, and 2,880 were analysed in light stress experiments. 360 plants per genotype were analysed in each condition.

A



B

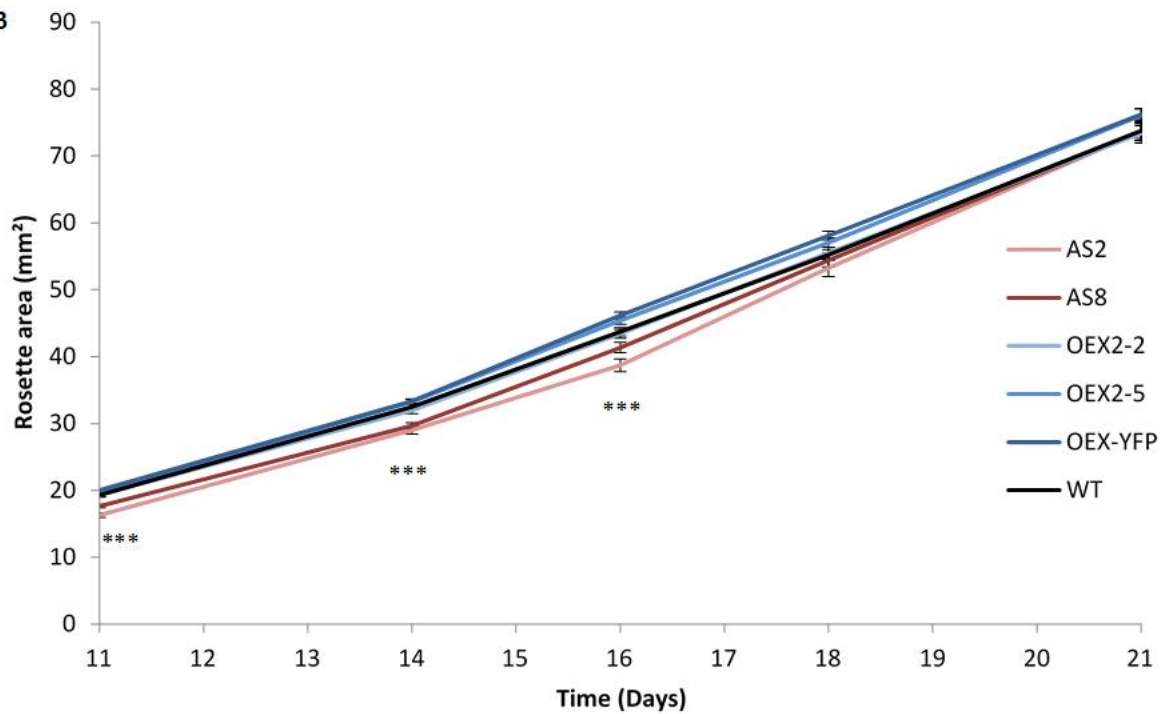


Figure 3-1: A comparison of the rosette areas wild-type (WT) *A. thaliana* and transgenic lines that either over-express *LEA5* (OEX2-2, OEX 2-5 and OEX-YFP), or express antisense *LEA5* (AS2 & AS8)

Plants were grown under $150 \mu\text{mol}\cdot\text{m}^{-2}\cdot\text{s}^{-1}$ irradiance with a 16 hour photoperiod at $22^\circ\text{C} \pm 2^\circ\text{C}$. Rosette areas were measured at 11, 14, 16, 18 and 21 days in the absence of stress. **A:** Representative phenotypes. Scale bar represents 10 mm. **B:** Rosette area (mm^2) over 21 days. Error bars represent mean \pm standard error. The asterisks indicate significant differences to WT plants (***) $P < 0.001$; ANOVA). $N=960$.

3.2.2. Rosette growth in the presence of stress

Drought, salt and osmotic stress

In these experiments, plants were grown in the absence of stress (control) or in the presence of 50 mM mannitol, 75 mM sodium chloride (NaCl), or 100 mM sorbitol which was added to the ½ MS media to simulate drought stress. The aim of these experiments was to gain an insight in to the role of *LEA5* in responses to abiotic stresses. The effects of the osmotica on WT and transgenic plants that either over-express *LEA5* (OEX2-2, OEX 2-5 and OEX-YFP), or express antisense *LEA5* (AS2 & AS8) were determined over 21 days. A total of 8640 plants were sown for these experiments and the germination rate was 93.5%. 8076 plants were assessed.

Representative shoot phenotypes of plants from each of the different lines grown in each treatment condition 21 days after being moved into the growth chamber are shown in Figure 3-2 A. The rosettes of plants grown in all stress treatments were visibly smaller than those grown in the absence of stress (Figure 3-2 A), with plants grown on media containing sodium chloride (salt stress) being the smallest at this point. The shoot phenotypes of plants grown in the control condition are visually similar in all lines, and analysis revealed that in the absence of stress, the rosette area of all lines was similar to WT plants after 21 days (Figure 3-2 B).

The rosette areas of all genotypes were significantly smaller in all the stress treatments compared to the control condition (Figure 3-2 B, C, D & E; $P < 0.001$). No effect of *LEA5* expression on the rosette area was observed when plants were grown in the presence of mannitol. In the salt stress treatment, the rosette area of AS8 plants was significantly smaller than WT plants (Figure 3-2 D; $P < 0.001$); however, there were no significant differences between WT plants and the other lines. The OEX-YFP plants had significantly larger rosette areas than WT plants when grown on ½ MS media containing sorbitol (Figure 3-2 E; $P < 0.001$).

High-light stress

In these experiments, WT and transgenic plants with altered expression of *LEA5* were grown for 11 days under $100 \mu\text{mol.m}^{-2}.\text{s}^{-1}$ irradiance with a 16 hour photoperiod. At this point plants in the high-light treatment were transferred to a comparable chamber but grown with an irradiance of $600 \mu\text{mol.m}^{-2}.\text{s}^{-1}$. All plants were grown for a further 10 days. Measurements of the rosette area were taken on day 7, 8, 9, 10, 11, 14, 16, 18 and 21. For simplicity however, data shown in Figure 3-3 are for day 21 only. A total of 2880 plants were sown, with a germination rate of 98.5%. 2837 plants were measured.

The rosettes of all genotypes were generally visibly smaller when grown for 10 days in the high-light condition compared to the control condition (Figure 3-3 A). Growth of WT plants under high-light resulted in plants with significantly smaller rosette areas than those grown in control conditions (Figure 3-3 A, B; $P < 0.001$). WT plants grown under high-light were 14.3% smaller than those grown in control conditions. Furthermore, after 10 days of growth under high-light, the rosette areas of AS2 plants were significantly smaller than that of the WT plants (Figure 3-3 B; $P < 0.001$). However, there was no uniform effect of *LEA5* expression on the rosette area when plants were grown in the under high-light: AS2 and AS8 plants were 22.8% and 13% smaller, respectively, than control plants, while OEX lines 2-2, 2-5 and YFP were 12.7%, 16.5%, and 20% smaller, respectively (Figure 3-3 B).

Oxidative stress

In these experiments, plants were grown in the absence (controls) or presence of oxidative stress caused by addition of H_2O_2 , paraquat, and superoxide generating agent menadione to the growth media. A total of 8640 plants were sown directly on to $\frac{1}{2}$ MS plates that either had no added chemicals or contained 10 mM H_2O_2 , 0.1 mM menadione or 0.1 μ M paraquat with 2160 in each treatment condition. The germination rates of all genotypes sown on H_2O_2 were very low (25.6%) compared to the germination rates in the absence of added oxidants – the control condition (98.5%). Those that did germinate struggled to thrive. No further experiments were therefore conducted on the seedlings grown in the presence of H_2O_2 . Seed germination rates were lower in the menadione condition (80.7%) than in the control condition. However, germination rates on paraquat condition were little affected (96.8%).

In these experiments, the rosette area of OEX-YFP plants after 21 days in the control condition was significantly larger than that of WT plants (Figure 3-4 B: $P < 0.001$). Notably, in these experiments, the rosette areas of 21-day-old AS2 and AS8 plants grown in the control condition were also significantly larger than those of WT plants ($P < 0.001$ for both genotypes).

The rosettes of all genotypes were visibly smaller when grown with menadione or paraquat compared to those grown in the absence of oxidative stress after 21 days (Figure 3-4 A). Moreover, the rosette area of all genotypes grown in the presence of either menadione or paraquat were significantly smaller than those in the absence of oxidative stress after 21 days ($P < 0.001$ for all genotypes in both conditions). Both AS2 and AS8 lines as well the OEX-YFP line were significantly smaller than WT plants when grown on 0.1 mM menadione (Figure 3-4 A & C: $P = 0.023$ for AS8, $P < 0.001$ for AS2 & OEX-YFP).

The mean rosette areas of plants were smallest when grown on media containing paraquat. The inhibition of photosynthetic electron transport by paraquat resulted in the rosette area of WT, OEX2-2, and OEX-YFP plants being between 54 and 62% smaller than those in the control condition with OEX2-5 being 40% smaller. In contrast, the paraquat-dependent decrease in rosette area was only 35% and 39% in AS lines, AS2 and AS8, respectively. The mean rosette areas of *LEA5* AS2 and AS8 plants were significantly larger than WT plants after 21 days grown in the presence of paraquat (Figure 3-4: $P < 0.001$ for both AS2 and AS8). However, the mean rosette area of OEX2-5 plants was also significantly larger than WT plants when grown in the presence of paraquat ($P < 0.001$).

Anthocyanin content of leaves

The shoots of plants, grown on soil for 4 weeks in standard conditions, were homogenised and anthocyanins were extracted. WT plants had an average of 2.6 $\mu\text{g/g}$ FW of anthocyanin (Figure 3-5). There was no significant difference in the concentration of anthocyanins between WT plants and OEX2-5 plants which had 3.3 $\mu\text{g/g}$ FW anthocyanin content. However, the leaves of AS2 plants had 0.6 $\mu\text{g/g}$ FW anthocyanin content ($P < 0.001$) which was significantly less anthocyanin content than in WT leaves.

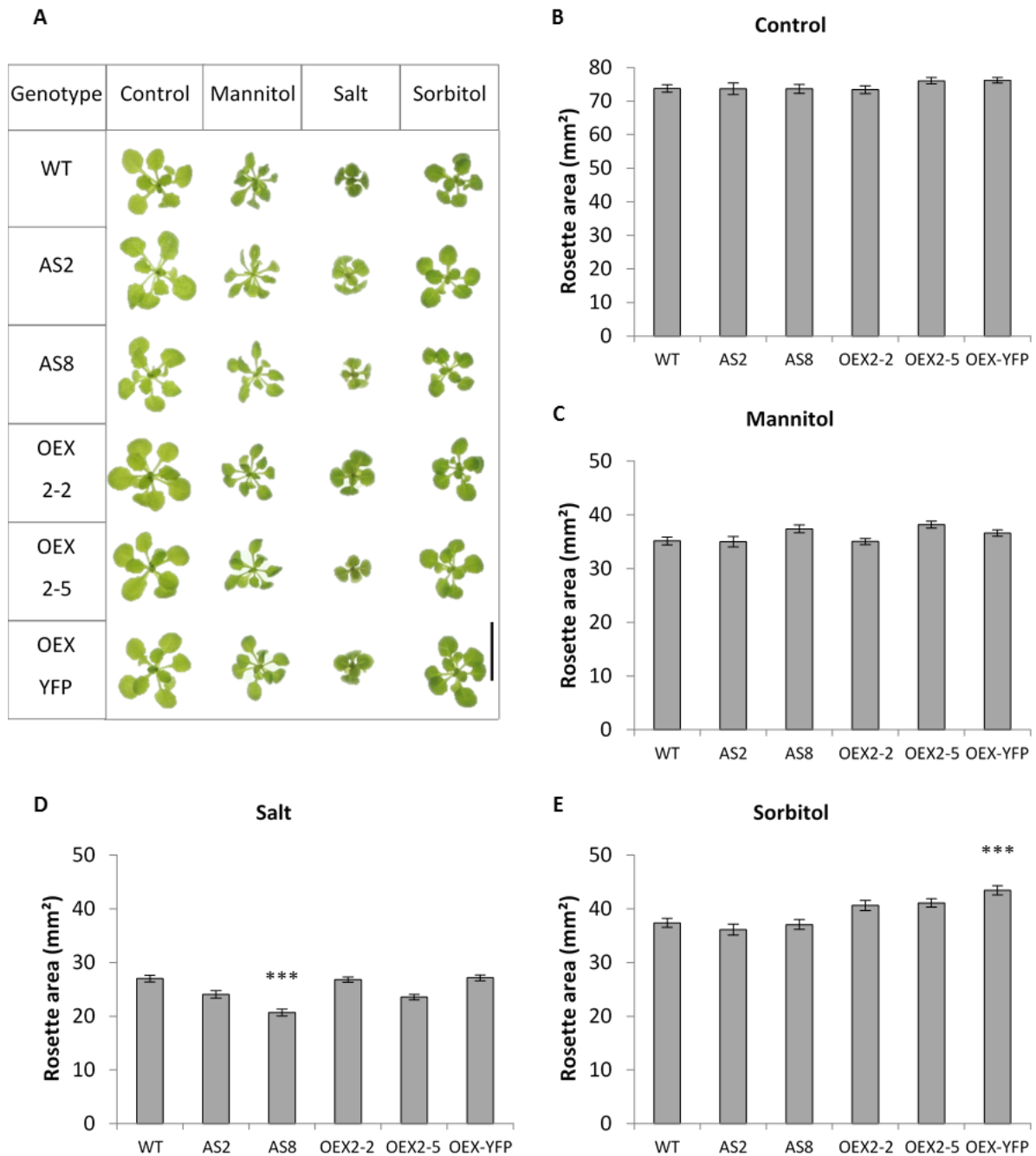


Figure 3-2: The effects of abiotic stress treatments (mannitol, salt, and sorbitol) on the rosette area of wild-type (WT) *A. thaliana* and on transgenic lines that either over-express *LEA5* (OEX2-2, OEX2-5 and OEX-YFP) or produce antisense transcripts (AS2 & AS8) in comparison to plants grown in the absence of stress.

Plants were grown under $150 \mu\text{mol}\cdot\text{m}^{-2}\cdot\text{s}^{-1}$ irradiance with a 16 hour photoperiod at $22^\circ\text{C} \pm 2^\circ\text{C}$ for 21 days. Representative phenotypes are shown in **A**. Scale bar represents 10 mm. The rosette area (mm^2) for plants grown in the absence of stress (control) is shown in **B**, and in the presence of stress caused by addition of 50 mM mannitol, 75 mM salt (NaCl), or 100 mM sorbitol to the growth media are shown in **C**, **D** and **E**, respectively. Error bars represent mean \pm standard error. The asterisks indicate significant differences ($P < 0.001$; ANOVA). $N = 360$.

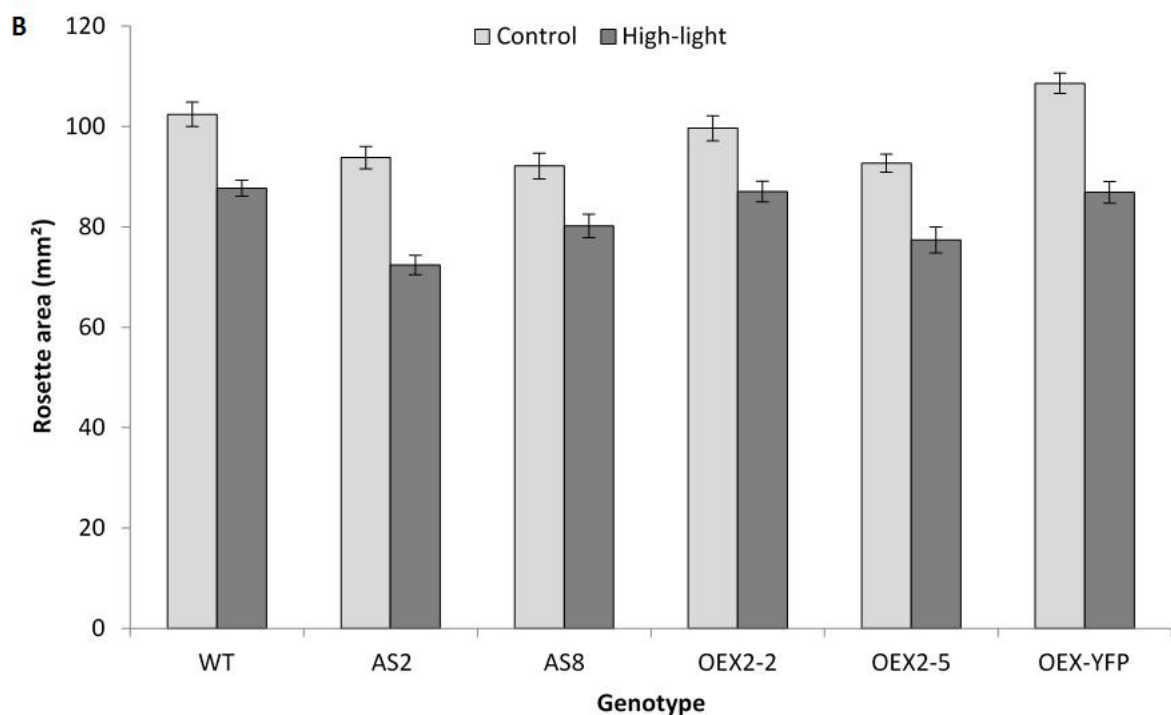
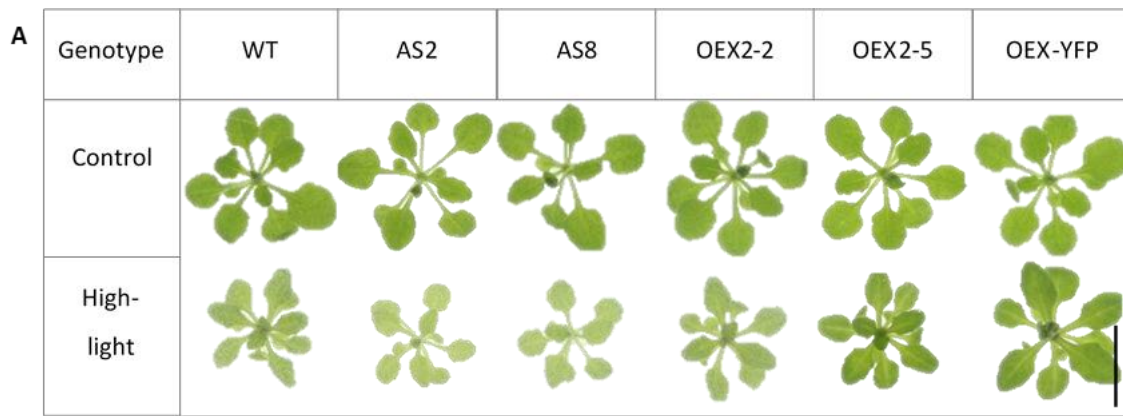


Figure 3-3: The effects of high-light treatment on the shoot phenotype (A) and rosette area (B) of 21-day-old wild-type (WT) *A. thaliana* and transgenic lines that either over-express *LEA5* (OEX2-2, OEX2-5 and OEX-YFP) or produce antisense transcripts (AS2 & AS8) in comparison to plants grown in the absence of stress.

Plants were grown for 11 days under $100 \mu\text{mol}\cdot\text{m}^{-2}\cdot\text{s}^{-1}$ irradiance with a 16 hour photoperiod, at which point half were grown under high-light ($600 \mu\text{mol}\cdot\text{m}^{-2}\cdot\text{s}^{-1}$) for the remaining 10 days. All plants were grown for 21 days at $22^\circ\text{C} \pm 2^\circ\text{C}$. A: Representative phenotypes at 21 days. Scale bar represents 10 mm. B: The rosette area (mm^2) of plants grown in the absence of stress and under high-light. Error bars represent mean \pm standard error. N=360.

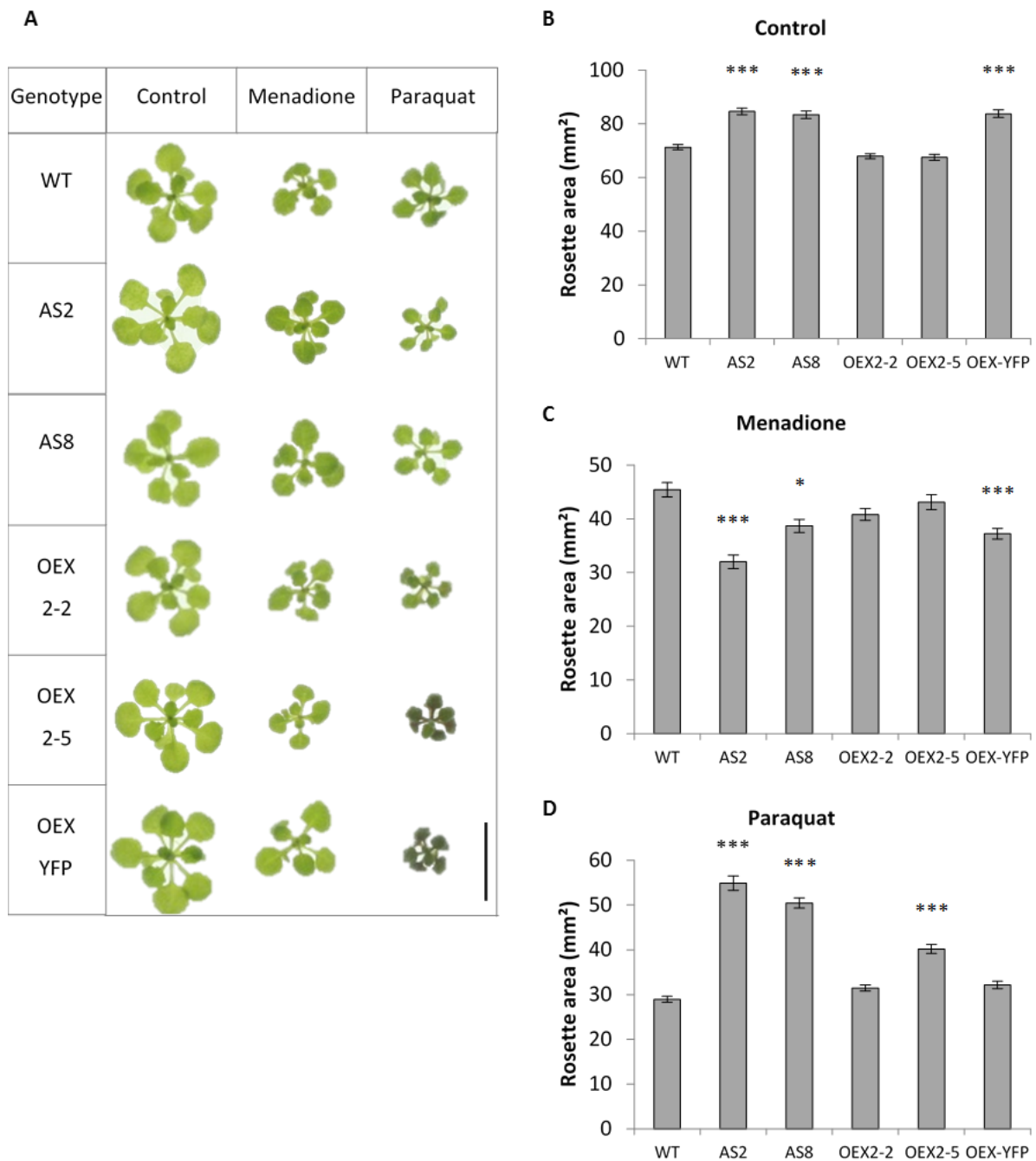


Figure 3-4: The effects of oxidative stress treatments (menadione and paraquat) on the rosette area of wild-type (WT) *A. thaliana* and on transgenic lines that either over-express *LEA5* (OEX2-2, OEX2-5 and OEX-YFP) or produce antisense transcripts (AS2 & AS8) in comparison to plants grown in the absence of stress.

Plants were grown under $150 \mu\text{mol}\cdot\text{m}^{-2}\cdot\text{s}^{-1}$ irradiance with a 16 hour photoperiod at $22^\circ\text{C} \pm 2^\circ\text{C}$ for 21 days. Representative phenotypes are shown in A. Scale bar represents 10 mm. The rosette area (mm^2) for plants grown in the absence of stress (control) is shown in B, and in the presence of stress caused by addition of 0.1 mM menadione, or 0.1 μM paraquat to the growth media are shown in C and D, respectively. Error bars represent mean \pm standard error. The asterisks indicate significant differences (* $P < 0.05$, *** $P < 0.001$; ANOVA). $N = 360$.

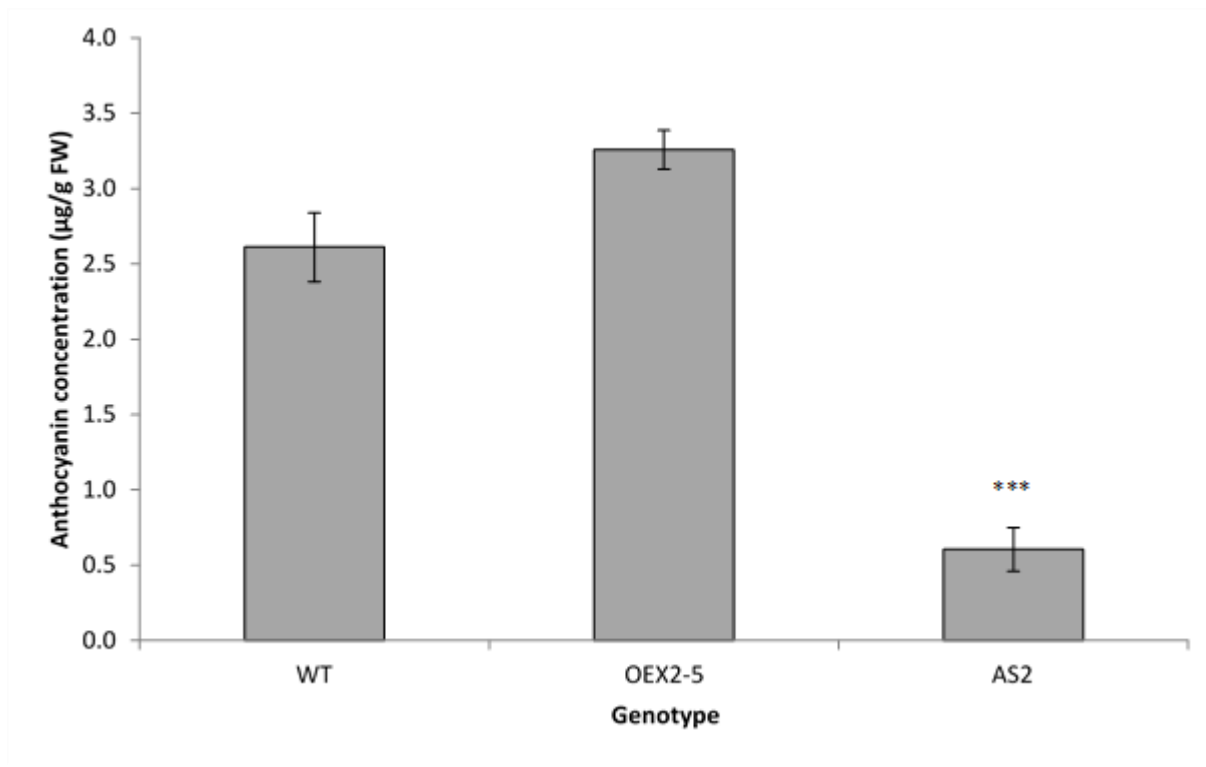


Figure 3-5: Anthocyanin concentration ($\mu\text{g/g FW}$) in the leaves of four-week-old wild-type (WT) *A. thaliana* and transgenic *LEA5* over-expressing (OEX 2-5) and *LEA5* antisense lines (AS2) grown on soil.

Plants were grown on soil under $150 \mu\text{mol.m}^{-2}.\text{s}^{-1}$ irradiance with a 16 hour photoperiod at $22^\circ\text{C} \pm 2^\circ\text{C}$ for four weeks. Error bars represent mean \pm standard error. The asterisks indicate significant differences to WT plants (***) $P < 0.001$; ANOVA). $N > 30$.

3.3. Results: Root phenotype in optimal conditions

3.3.1. Analysis of root phenotypes for plants grown on ½ MS media

The aim of these experiments was to investigate the role of *LEA5* in root development. The AS2 and OEX2-5 have been reported to have a marked effect on root phenotype when grown on ½ MS media for 20 days [51]. However, the AS8 and OEX2-2 lines had not been described. The objective of these experiments was to determine the root phenotypes of the AS8 and OEX2-2 lines as well as to confirm the previously observed phenotypes of the AS2 and OEX2-5 lines. After 7 and 10 days of growth (Figure 3-6 & Figure 3-7, respectively), the primary root lengths, the number of lateral roots and lateral root densities were determined. Root architecture was determined in a total of 244 plants.

The root architecture of the AS2 and AS8 plants appeared visually different to WT plants 7 days after germination (Figure 3-6 A), while both of the OEX lines were visually similar to the WT. Analysis of the roots revealed that the AS2 & AS8 plants had similar mean primary root lengths to the WT plants (Figure 3-6 B). In contrast, the OEX2-2 plants had significantly longer primary roots than the WT seedlings (Figure 3-6 B; $P=0.009$). However, there was no significant difference between OEX2-5 plants and the WT plants. Furthermore, there was no significant differences in the number of lateral roots (Figure 3-6 C) or the lateral root density between any of the transgenic lines and the WT plants after 7 days (Figure 3-6 D).

After 10 days, AS2 and AS8 plants had similar primary root lengths to the WT plants (Figure 3-7 B), as did OEX2-5 plants. However, OEX2-2 plants had significantly longer primary roots ($P=0.0075$; Figure 3-7 B), as well as significantly more lateral roots than WT plants ($P=0.03$; Figure 3-7 C). Lateral root density was similar to WT plants for all genotypes (Figure 3-7 D).

Notably, the angle of root growth differed significantly in AS2 and AS8 lines which showed a preference for growing at angles 42° and 47° whilst WT grew at 20° ($P<0.001$ for both genotypes) and the primary roots of both OEX2-2 and OEX2-5 lines grew at 13° (Figure 3-7 A & E).

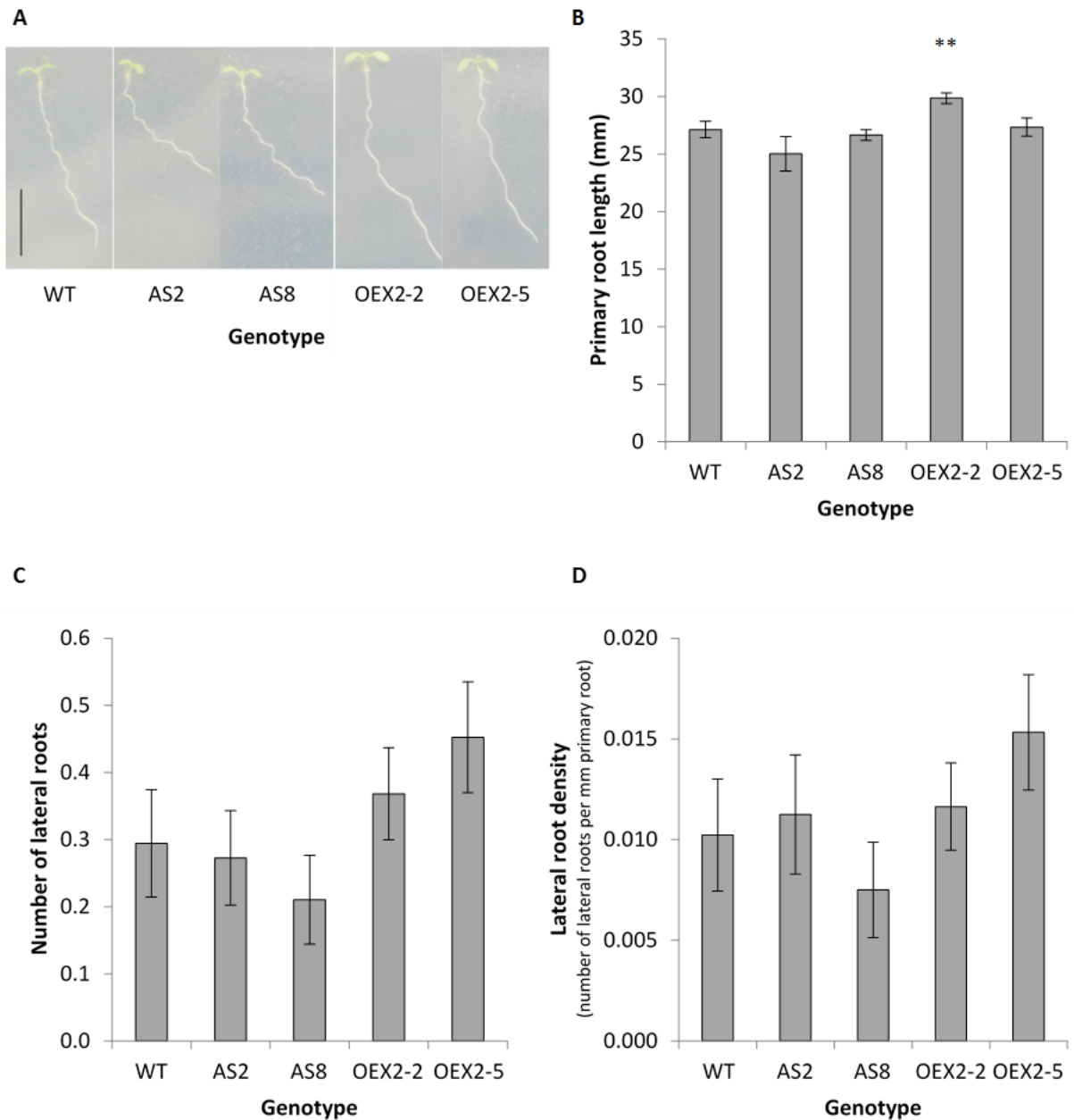


Figure 3-6: The root architecture of seven-day-old wild-type (WT) *A. thaliana* and transgenic *LEA5* over-expressing (OEX2-2, OEX2-5) and *LEA5* antisense (AS2, AS8) lines grown on ½ MS.

A: Representative phenotypes on day 7. Scale bar represents 10 mm. **B:** Primary root length (mm). **C:** The number of lateral roots. **D:** The lateral root density (number of lateral roots per mm primary root). Error bars represent mean +/- standard error. The asterisks indicate significant differences to WT plants (** P<0.01; ANOVA). N=48.

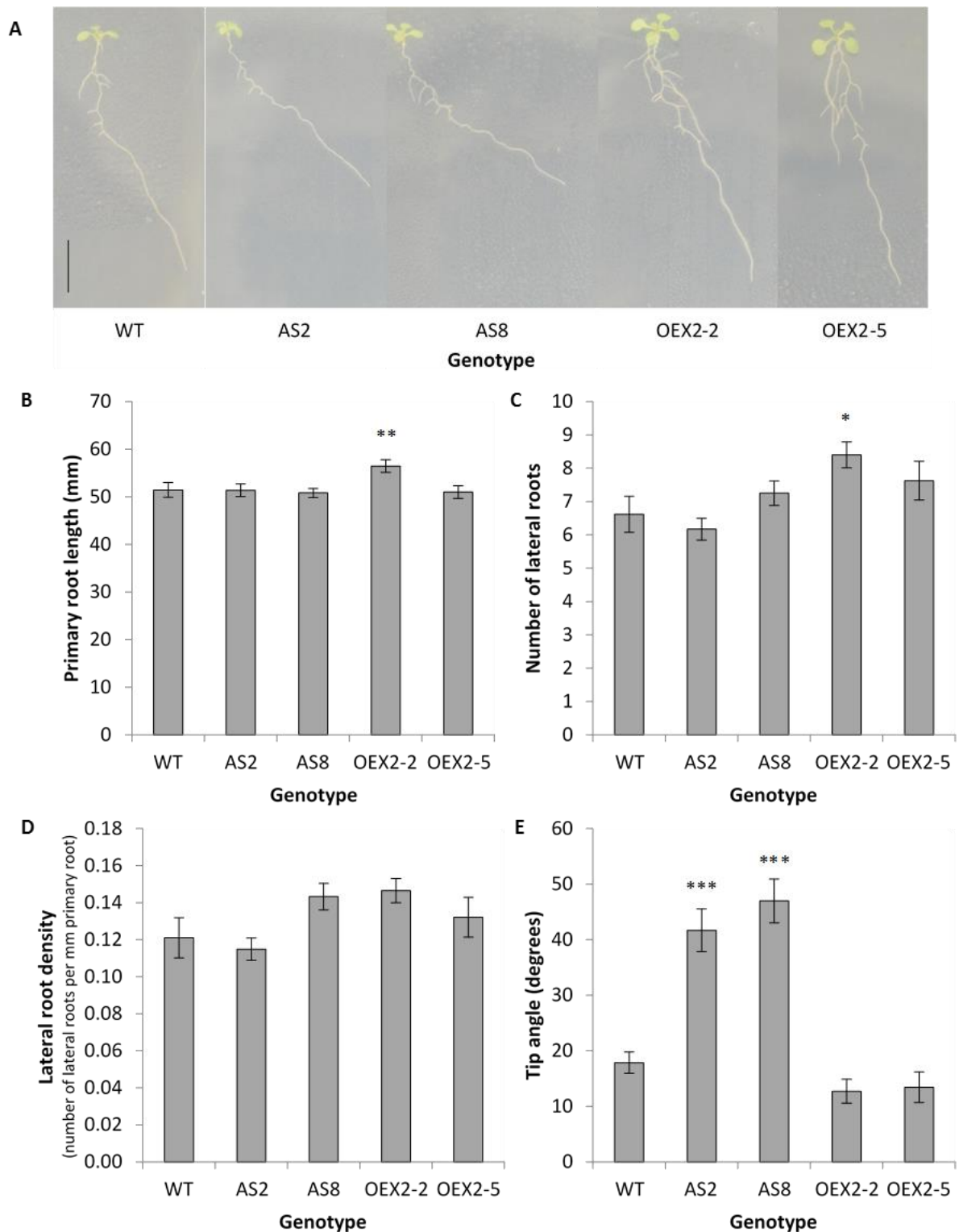


Figure 3-7: The root architecture of ten-day-old wild-type (WT) *A. thaliana* and transgenic *LEA5* over-expressing (OEX2-2, OEX2-5) and *LEA5* antisense (AS2, AS8) lines grown on ½ MS.

A: Representative phenotypes on day 10. Scale bar represents 10 mm. **B:** Primary root length (mm). **C:** The number of lateral roots. **D:** The lateral root density (number of lateral roots per mm primary root). **E:** The primary root tip angle (degrees). Error bars represent mean +/- standard error. The asterisks indicate significant differences to WT plants (* $P < 0.05$, ** $P < 0.01$, *** $P < 0.001$; ANOVA). $N = 48$.

3.3.2. Analysis of root phenotypes for plants grown on ATS media

In the second root phenotype investigation, the roots of 7-day-old WT *A. thaliana* and transgenic *A. thaliana* seedlings that express *LEA5* in the sense (OEX2-5) or antisense (AS2) orientations grown on ATS media were compared (Figure 3-8 A). These experiments were performed in the same way as those performed with ½ MS media (Section 3.3.1) except that these seedlings were grown on ATS media. After 7 days of growth, the primary root lengths, the number of lateral roots and lateral root densities were measured. The roots had reached the bottom of the media by day 10 and so no measurements were made on this day.

After 7 days of growth on ATS, the root phenotypes of OEX2-5 and AS2 seedlings were visually like those of the WT plants (Figure 3-8 A). Under these conditions the primary root lengths of WT and OEX2-5 lines were similar (Figure 3-8 B). In contrast, the AS2 seedlings had significantly shorter primary roots than WT seedlings (Figure 3-8 B: P=0.022). There were no significant differences in the number of lateral roots per plant between WT and transgenic plants (Figure 3-8 C). Likewise, the abundance of lateral roots relative to the primary root length was similar in WT, OEX2-5 and AS2 seedlings (Figure 3-8 D).

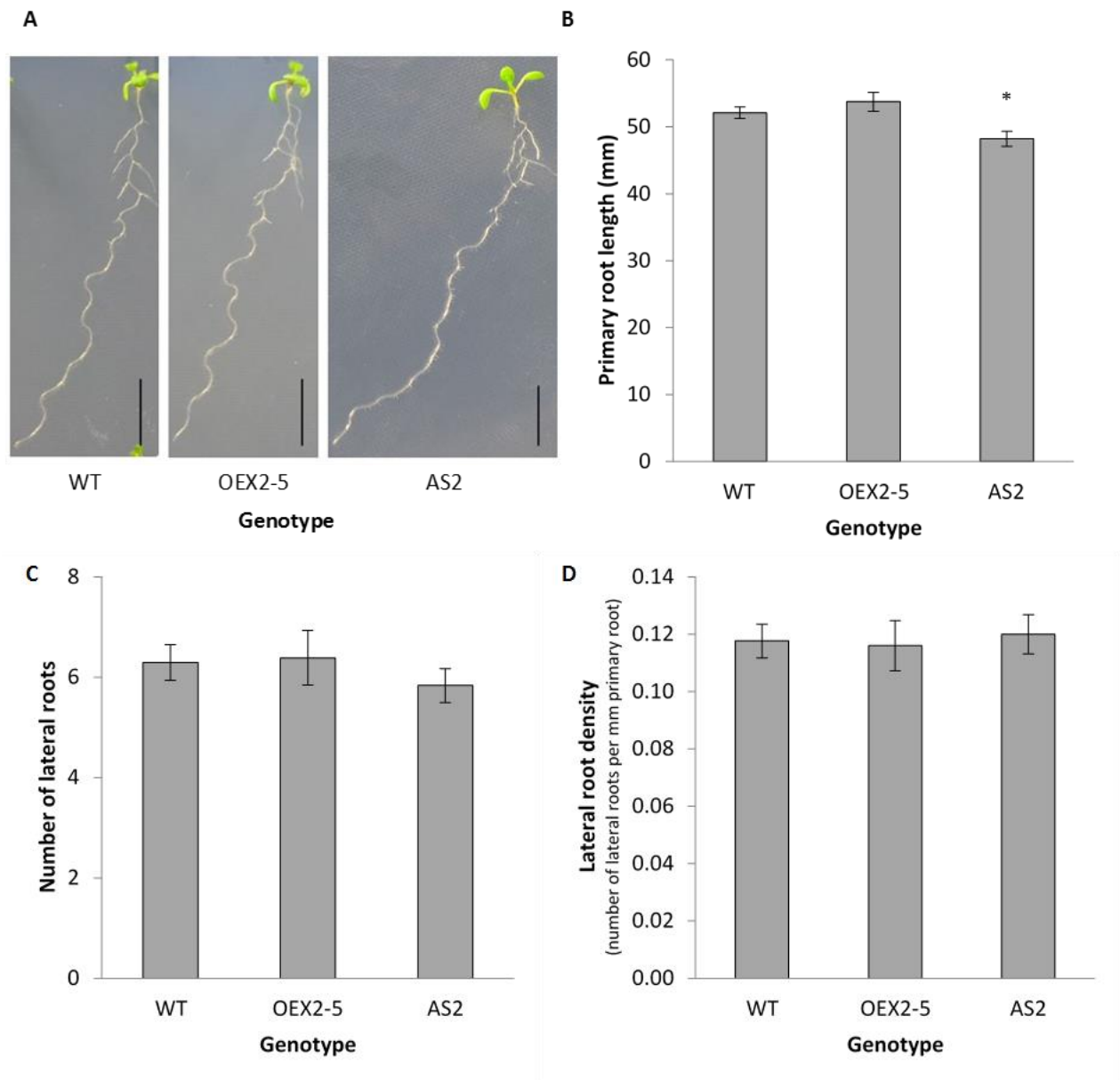


Figure 3-8: The root architecture of seven-day-old wild-type (WT) *A. thaliana* and transgenic *LEA5* over-expressing (OEX2-5) and *LEA5* antisense (AS2) lines grown on ATS media.

A: Representative phenotypes at 7 days. Scale bar represents 10 mm. **B:** Primary root length (mm). **C:** The number of lateral roots. **D:** The lateral root density (number of lateral roots per mm primary root). Error bars represent mean +/- standard error. The asterisks indicate significant difference to WT plants (* $P < 0.05$; ANOVA). $N = 45$.

3.4. Discussion

The aim of these studies was to characterise the shoot and root phenotypes of *A. thaliana* lines with altered expression levels of *LEA5*. The data presented in Figures 3-1 to 3-4 show no consistent effects of the level of *LEA5* expression on shoot development as determined by rosette area. Furthermore, the root phenotypes were largely the same in all lines. These data are in marked contrast to previous studies [43, 51]. While in some experiments the rosette area reflect results published previously [43, 51], no consistent differences were observed between the experiments. The experiments performed in this chapter involved thousands of plants and the data is therefore arguably robust. The reasons for the apparent discrepancy in the results presented here and those reported previously [43, 51] are unknown. Seedlings were confirmed to contain the Kanamycin resistance gene by PCR and are thus transgenic. Furthermore, all plants grown on media containing Kanamycin were resistant and did not segregate which suggests they are homozygous for the gene of interest. However, expression of *LEA5* in these lines (data not shown) was not as previously described [43, 51]. This could be due to the seeds being of a different generation to those used previously, and so some silencing of the transgene may have occurred.

LEA proteins have frequently been associated with drought stress [13]. Plants over-expressing *LEA5* were previously shown to be less able to assimilate CO₂ in drought conditions [43]. For this reason, the effects of water deficiency on the rosette area of plants with altered *LEA5* expression were determined. A total of 8640 plants were assessed in the drought experiments. Rosette areas were significantly decreased following the drought stress treatments in all genotypes. The rosette areas of *LEA5* OEX plants were similar to WT plants in most treatments with the exception of the treatment with sorbitol, in which OEX-YFP plants had a significantly larger rosette area than WT plants (Figure 3-2 A, E). Furthermore, the rosette areas of the *LEA5* AS plants were similar to WT plants when grown on media containing mannitol and sorbitol. However, the rosette areas of plants from the AS8 line were significantly smaller when grown on media containing salt (Figure 3-2 A & D). These findings as a whole do not suggest that the expression of *LEA5* adjusts plant tolerance to drought stress.

High-light led to a significant decrease in overall rosette size in all genotypes tested relative to the same genotypes in control conditions. This observation implies that an irradiance of 600 $\mu\text{mol}\cdot\text{m}^{-2}\cdot\text{sec}^{-1}$ is sufficient to elicit photoinhibitory effects and inhibit growth in *A. thaliana*. While all plants showed inhibited growth under high-light, there was no clear effect

of *LEA5* expression on the rosette area (Figure 3-3). Expression of *LEA5* is usually downregulated in the light [51]. However, it appears from this data that constitutive expression of *LEA5* is not preventing the plants coping with high-light stress.

LEA5 is up-regulated by a range of oxidants [43] including both H₂O₂ and superoxide (O₂⁻) generating agents such as menadione and paraquat. The effects of continuous exposure to oxidative stresses on transgenic *A. thaliana* plants were also analysed in this study. It was found that 10 mM H₂O₂ was too strong a concentration for all plants tested to survive post germination. Any that did manage to germinate bleached and died soon after. All genotypes had a smaller rosette area when grown on media containing 0.1 mM menadione. Both AS lines were found to be significantly more sensitive to menadione than the WT plants. However, this effect was also observed in OEX-YFP plants. The greatest reduction in rosette area was observed in plants grown on media containing 0.1 μM paraquat. As expected, all genotypes had a smaller rosette area in this condition, however *LEA5* AS plants were not as sensitive as the OEX lines and their rosette areas were larger than WT plants (Figure 3-4).

The effects of *LEA5* on root architecture reported previously [43] were also found to be less dramatic in this study. However, *LEA5* OEX2-2 plants had a significantly longer primary root (Figure 3-7 B) and more lateral roots (Figure 3-7 C) after 10 days on ½ MS media. Moreover, the primary roots of *LEA5* AS2 plants were significantly shorter than WT plants (Figure 3-8 B) when grown on ATS media. However, then root architecture of all other lines was like that of WT plants. While in some experiments, the data reflect results published previously, no consistent differences were observed between the experiments. The discrepancies between this and the previous studies could be due to subtle differences in growth conditions. However, it would appear that the expression of *LEA5* in these plants does not match those used in previous studies, possibly due to silencing of the transgene.

Chapter 4. The identification of the effects of *LEA5* expression on mitochondrial respiration and redox state

4.1. Introduction

LEA proteins are typically intrinsically-disordered proteins that seem to have roles in protecting plants against a range of stresses [13-18], although their precise cellular functions remain largely unknown [3]. There are 51 genes encoding LEA proteins in *A. thaliana* and they are clustered into nine families. Of these, 36 are localised to the cytosol, and 29 of these have a dual cytosolic-nuclear localisation [44]. Three proteins localised exclusively to the plastids or mitochondria, and two others are dually targeted to these organelles [44]. One of the LEA proteins found to be localised to mitochondria was LEA5, which appeared to localise in the mitochondrial matrix [44, 51]. As LEA proteins appear to have a role in protecting plants against stresses [13-18], it is possible that LEA5 has a role in the protection of mitochondrial functions in plants exposed to stress. LEA5 is unique among LEA proteins, in that its expression is strongly regulated by oxidants [43]. Furthermore, plants over-expressing *LEA5* had a reduced sensitivity to H₂O₂ [43, 51]. It is possible that LEA5 fulfils functions related to respiration and associated oxidative stress tolerance or signalling in mitochondria.

Plant cell function is dependent upon the regulated and reciprocal interaction between its different compartments. Retrograde signalling from the mitochondria to the nucleus has been proposed to mediate abiotic stress perception [190]. Many abiotic stress conditions will influence mitochondrial metabolism and could generate signals by the over-reduction of the ETC, enhanced accumulation of ROS, or altered redox potential that will, in turn, trigger nuclear gene expression and acclimation responses. This co-ordinated regulation is essential for appropriate responses to changes in the environment e.g. temperature [129].

Intact plant mitochondria can be isolated from plant tissues and organs such as potato tubers, pea shoots and soybean cotyledons and roots [191-193] where mitochondria are abundant and tissues are relatively free of compounds such as lignins, polysaccharides and other cellular components. To perform the experiments described in this chapter, mitochondria were isolated

from the shoots of *A. thaliana* and purified by density gradient centrifugation using Percoll and PVP. The Percoll/PVP gradient separated the intact mitochondria from other cell components such as chloroplasts and thylakoids [191]. The integrity of the isolated mitochondria were determined, and respiratory electron transport rates were then assayed by measuring O₂ consumption in a Clark-type oxygen electrode [194, 195]. The respiration rates of mitochondria isolated from the shoots of 4-week-old WT *A. thaliana*, as well as from a transgenic line that over-expresses *LEA5* characterised in Chapter 3, were measured to determine whether altered *LEA5* expression alters respiration rates. In addition, transgenic plants were produced that express a reduction-oxidation sensitive Green Fluorescent Protein (roGFP) targeted to either the mitochondria or the cytosol [172]. The roGFP emission spectrum changes in a more reduced environment [172]. These transformations were made on plants that were either WT, or transgenic and either over-express *LEA5* or express *LEA5* in the anti-sense (AS) orientation. Homozygous lines were produced to observe if the expression of *LEA5* alters the redox state of mitochondria and the cytosol. An understanding of how *LEA5* functions in mitochondria could provide insights into plant growth and stress tolerance.

4.2. Results: *LEA5* transcript expression

To verify that *LEA5* mRNA expression in leaves is abundant in the dark but suppressed in the light – shown previously by Northern blotting [43] – transcripts were quantified by QPCR. The shoots of four-week-old plants were harvested over a period of 24 hours. RNA was extracted from the plant samples, the concentration was measured, and 1 µg of RNA was used to synthesise cDNA. QPCR was then performed on the cDNA to determine *LEA5* transcript abundance over the light/dark cycle (Figure 4-1).

LEA5 transcripts were abundant in the shoots of WT plants at the 0 hour time point, when the plants had experienced 16 hours of darkness (Figure 4-1 A). The quantity of *LEA5* transcripts decreased rapidly upon illumination, such that levels had almost halved after 1 hour of illumination (Figure 4-1 A). Levels of *LEA5* mRNAs remained low throughout the light period and only accumulated once illumination was removed at the end of the photoperiod (Figure 4-1). These results demonstrate that *LEA5* mRNAs are most abundant in darkness. Therefore, all procedures undertaken to isolate mitochondria were performed on leaves harvested in the dark period.

The melting temperatures of the target amplicons for the reference gene, *UBC37*, and for *LEA5* was 82°C and 81°C, respectively (Figure 4-1 B). A single peak can be seen in each curve indicating that primers amplified only one product. No products could be seen in the non-template control which indicates a lack of contamination and primer dimers. Taken together this data implies that the cycle threshold (Ct) values i.e. the number of cycles required for the fluorescent signal to exceed background level, are valid and not due to nonspecific products.

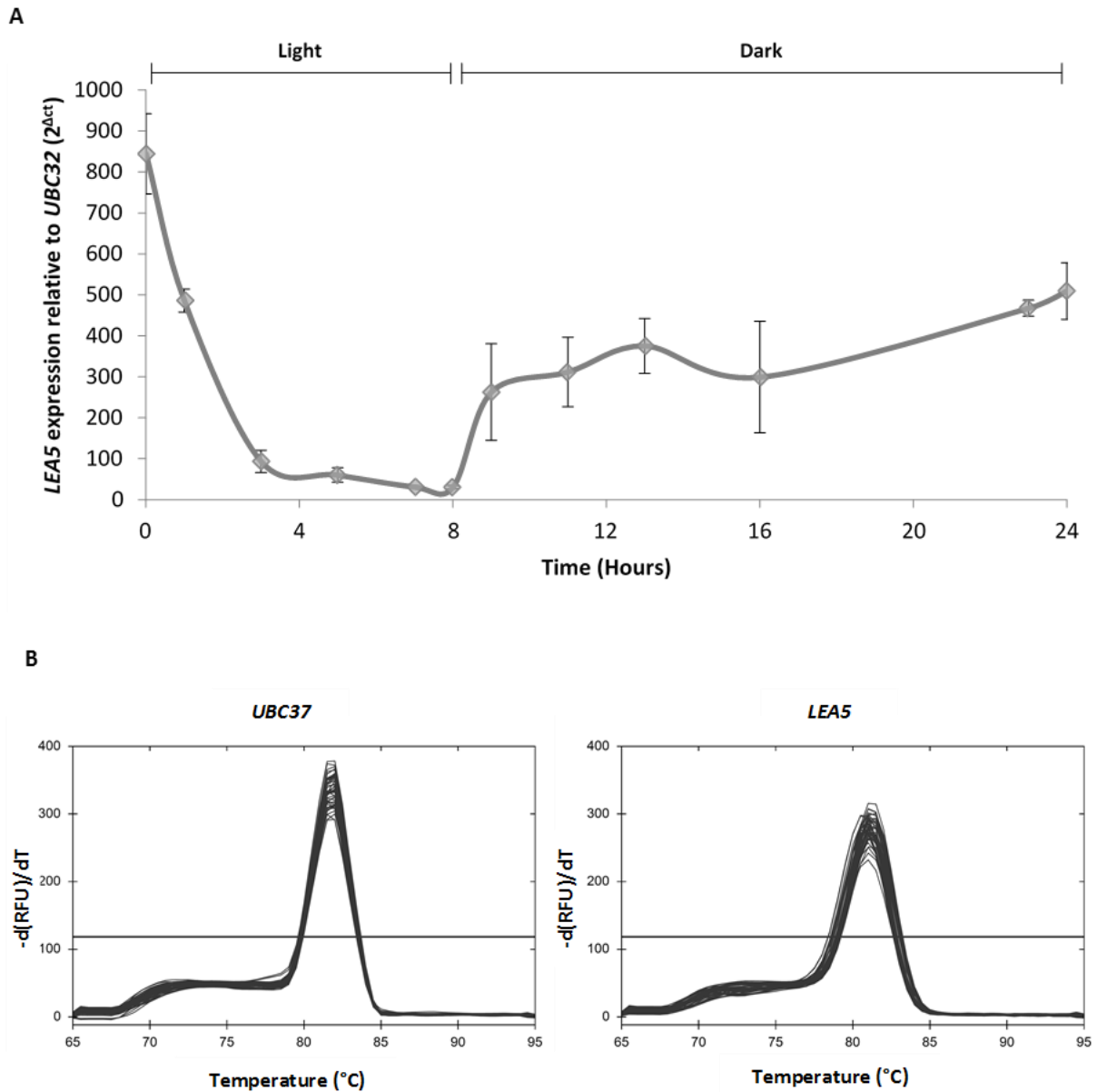


Figure 4-1: Diurnal changes in *LEA5* transcript abundance.

Plants were grown under $150 \mu\text{mol m}^{-2} \text{s}^{-1}$ irradiance with an 8-hour photoperiod at $22^\circ\text{C} \pm 2^\circ\text{C}$ for 28 days.

A: QPCR was used to quantify *LEA5* transcripts relative to transcripts encoding a ubiquitin-conjugating enzyme (*UBC37*) in the rosettes of 4-week-old WT plants. The light period was from 0 to 8 hours as indicated by the bars above the graph. Error bars are means \pm standard error.

B: Dissociation curves illustrating the specificity of QPCR primers. The specific melting temperature of a product indicates its size, and a pure product gives one clear peak. Data are the mean of 3 biological replicates, each with 3 technical replicates.

4.3. Results: Mitochondrial respiration

Mitochondria were isolated from the shoots of four-week-old WT and *LEA5*-OEX2-5 plants grown on soil under an irradiance of $150 \mu\text{mol.m}^{-2}.\text{s}^{-1}$ with a photo period of 8 hours and a constant temperature of $22 \pm 2^\circ\text{C}$, in order to determine whether the *LEA5* protein alters respiratory functions in mitochondria. The method of isolating intact mitochondria from soil grown *A. thaliana* was first optimised (as described in Chapter 2 and in Shaw *et al.*, 2016 [196]). Parameters such as the age of the plants, the biomass:grinding buffer ratio and other factors were found to influence the amount and quality of the mitochondrial preparations [196]. The procedures used to establish (i) the proportion of intact mitochondria in the isolation, (ii) the mass (protein basis) of mitochondria required to give a linear respiratory response to substrate concentration and (iii) the optimal concentrations of additional substrates, cofactors and inhibitors for subsequent assays are described in Shaw *et al.*, 2016 [196].

4.3.1. The protein basis of mitochondria

The mass (protein basis) of mitochondria was determined using a Bradford assay (Figure 4-2). The standard curve produced had a coefficient of determination (R^2) at 0.9982 (Figure 4-2). A R^2 value this close to 1 indicates that the data points fit very closely to the line of best fit. It is therefore acceptable to use this curve to calculate unknown protein concentrations from the equation of this line. Respiration assays used $100 \mu\text{g}$ of mitochondria (in a volume of 10-40 μl).

4.3.2. The integrity of mitochondria and maximal cytochrome *c* oxidase activity

The maximal activity of cytochrome *c* oxidase (COX: Complex IV) was used as a measure of the integrity of isolated mitochondria [197]. These assays utilised a Clark-type oxygen electrode. COX is bound within the inner mitochondrial membrane and oxidises the electron carrier cytochrome *c*, located within the inter membrane space. The basis of these measurements is that cytochrome *c* cannot traverse the outer mitochondrial membrane, so the addition of cytochrome *c* to a preparation of mitochondria should only increase the COX activity if mitochondria with broken outer membranes are present. Representative traces are shown in Figure 4-3 A & B. The oxygen consumption rate in the absence and presence of a detergent that should disrupt the membranes was used to calculate the percentage of intact mitochondria. Preparations of mitochondria were used if over 75% were intact (Table 5). The maximal COX activity of mitochondria isolated from the leaves of WT plants was $142.9 \text{ nmol O}_2.\text{min}^{-1}.\text{mg protein}^{-1}$ (Figure 4-3 C; Table 5). The maximal COX activity of mitochondria

isolated from the leaves of OEX2-5 plants was $166.2 \text{ nmol O}_2 \cdot \text{min}^{-1} \cdot \text{mg protein}^{-1}$ (Figure 4-3 D; Table 5). There was no significant difference in the COX activity of mitochondria isolated from the leaves of WT plants and those isolated from OEX2-5 plants (Table 5).

4.3.3. Respiratory control assays

Assays were performed to investigate complex I and complex II respiratory control. Respiration measurements were performed on mitochondria that are >80% intact. To assay complex I respiratory control, the substrates pyruvate, tetrasodium pyrophosphate and malate were added to the chamber once a base respiration rate was established. Once a stable respiration rate had been established ADP was added to the chamber. After a further two minutes had passed, the reaction was stopped with the addition of oligomycin to the chamber. Oligomycin should block the F_0 domain of ATP synthase and thus inhibit respiration. Subsequently, the ionophore FCCP was added to the chamber thus negating this inhibition. FCCP is a mobile ion carrier that makes membranes selectively leaky to H^+ , and can dissipate the H^+ electrochemical gradient across the mitochondrial inner membrane. There was no significant difference in complex I respiratory control between WT and OEX2-5 plants (Table 6).

To assay complex II respiratory control, succinate was added to the chamber to reduce complex II and rotenone was added to inhibit complex I activity. Once a stable respiration rate was established ADP was added to the chamber. Following this oligomycin was added to the chamber inhibiting respiration. Finally, FCCP was added to the chamber negating this inhibition by dissipating the H^+ electrochemical gradient across the mitochondrial inner membrane. There was no significant difference in complex II respiratory control between WT and OEX2-5 plants (Table 7).

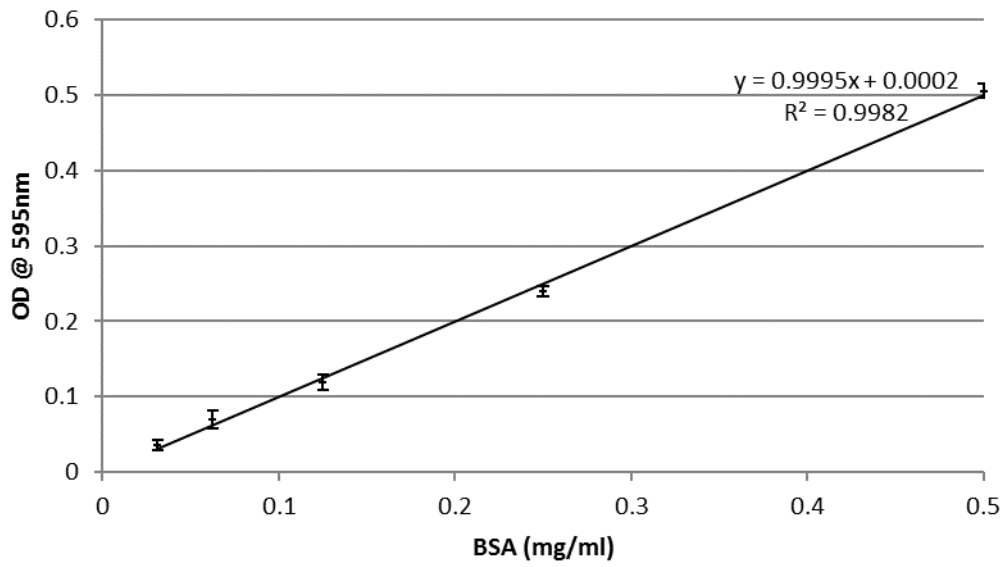


Figure 4-2: Protein standard curve used to determine the protein basis of mitochondria.

$R^2 = 0.9982$

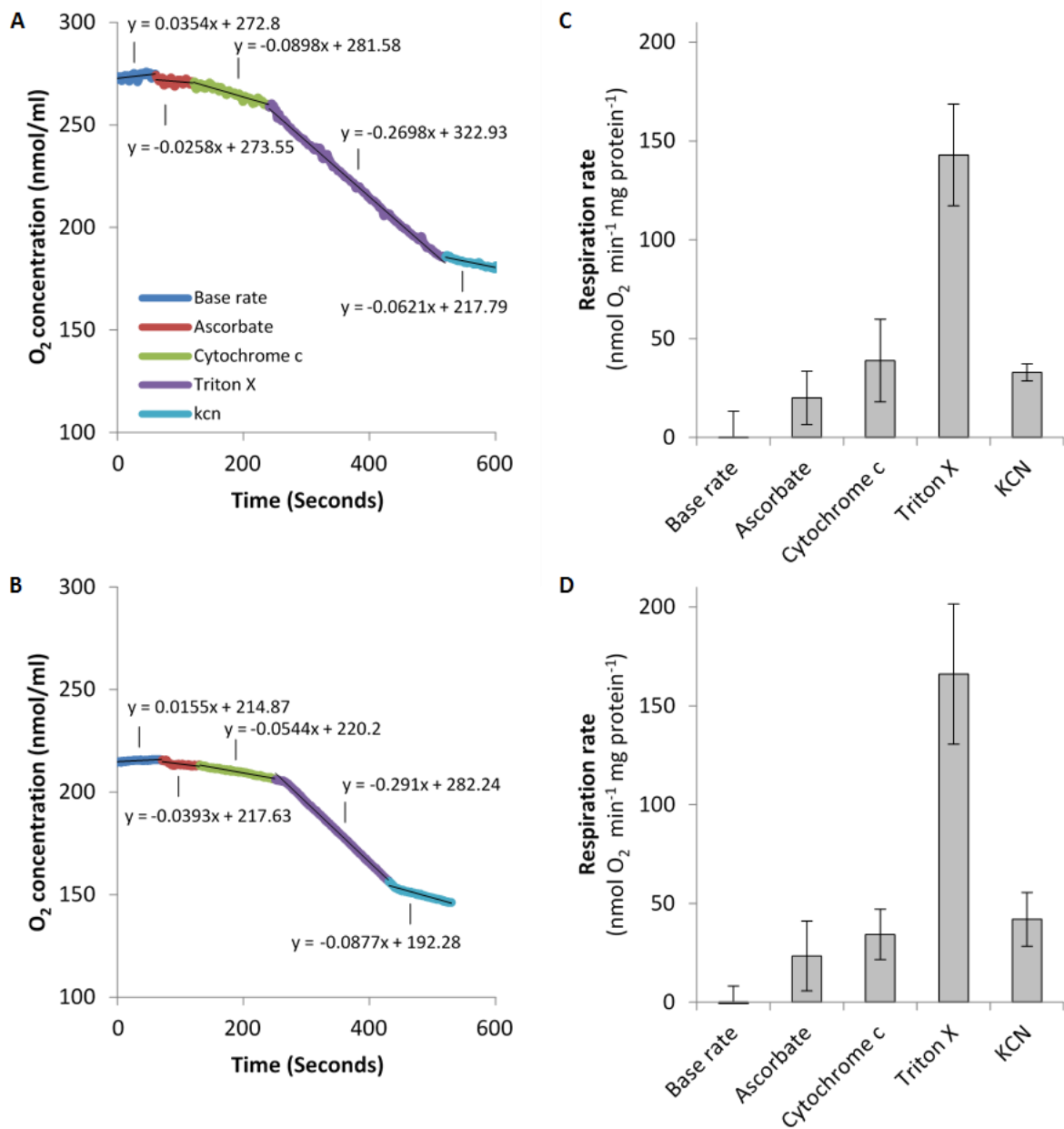


Figure 4-3: Determinations of the latency of cytochrome c oxidase (COX) in mitochondrial preparations.

Representative trace of oxygen uptake by mitochondria extracted from **A**: WT and **B**: OEX2-5 plants. Average oxygen consumption rate (nmol O₂.min⁻¹.mg protein⁻¹) by mitochondria extracted from **C**: WT and **D**: OEX2-5 plants.

Table 5: Oxygen consumption (nmol O₂.min⁻¹.mg protein⁻¹) at maximal COX activity and percentage intact mitochondria

Genotype	Maximal COX activity		Percentage (%) of intact mitochondria	
	WT	OEX2-5	WT	OEX2-5
Average	142.9	166.2	85.4	89.8
+/- SE	+/- 7.9	+/- 9.8	+/- 3.2	+/- 1.3

N=24

Table 6: Oxygen consumption (nmol O₂.min⁻¹.mg protein⁻¹) when assaying complex I respiratory control

Genotype	CI Substrates	ADP	Oligomycin	FCCP
WT	23.0 +/- 2.5	18.6 +/- 1.1	1.0 +/- 0.5	20.4 +/- 3.8
OEX2-5	22.0 +/- 2.5	22.5 +/- 5.2	1.4 +/- 0.3	14.0 +/- 4.1

N=4

Table 7: Oxygen consumption (nmol O₂.min⁻¹.mg protein⁻¹) when assaying complex II respiratory control

Genotype	Succinate	Rotenone	ADP	Oligomycin	FCCP
WT	23.1 +/- 3.4	26.2 +/- 3	41.0 +/- 3.3	26.2 +/- 4.6	32.6 +/- 3.4
OEX2-5	22.8 +/- 4.2	24.2 +/- 2.6	33.4 +/- 3.9	27.5 +/- 3.5	24.3 +/- 4.6

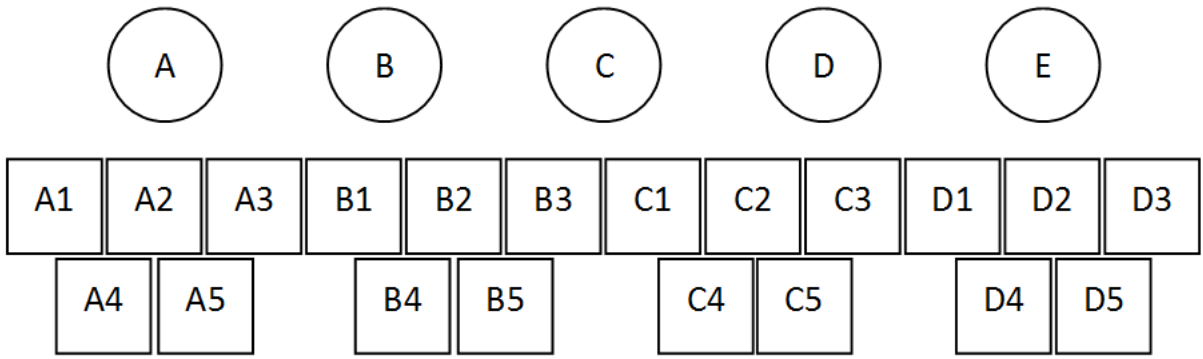
N=15

4.4. Results: Transformation of *Arabidopsis thaliana* to express roGFP in the cytosol or mitochondria

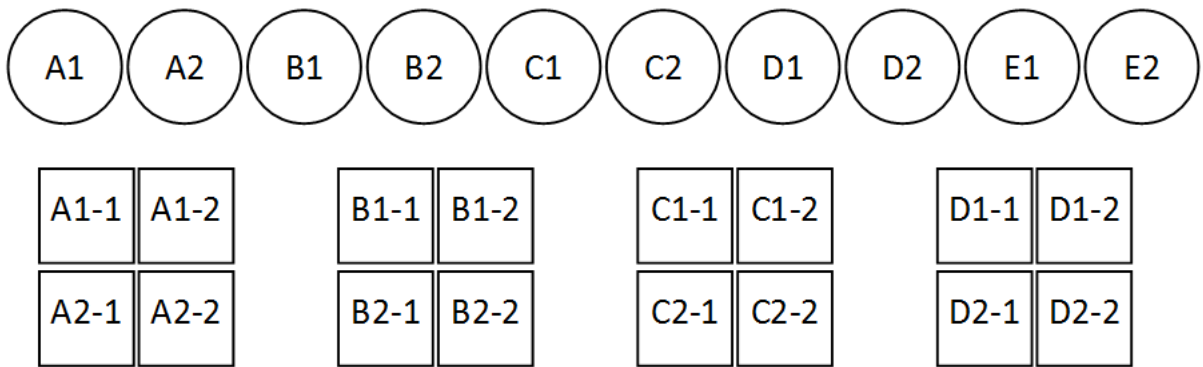
Arabidopsis thaliana plants with a WT background, and the transgenic lines *LEA5*-OEX(2-2), *LEA5*-OEX(2-5), *LEA5*-AS(2), and *LEA5*-AS(8) were transformed by Agrobacterium-mediated transformation with constructs containing roGFP that was either targeted to the mitochondria (mitochondrial-roGFP) or without a targeting sequence (cytosolic-roGFP). The naming policy for the selection of transgenic plants is shown in Figure 4-4. The seeds of independently transformed lines (T₁) were harvested and 3% were found to be resistant to Hygromycin B (Figure 4-5 A). The seedlings that were resistant to Hygromycin B were transplanted from the selection media onto soil where they were grown to seed (T₂). T₂ seeds were harvested and sown onto ½ MS agar containing Hygromycin B. About 75% of the seedlings that germinated on selection media were found to be resistant to Hygromycin B (Figure 4-5 B). The other 25% were sensitive to the antibiotic and did not grow. Deviations from the 3:1 ratio of antibiotic resistant to sensitive can indicate multiple insertions of the gene. One line was found to be 100% resistant to Hygromycin B. Plants were selected for homozygosity. Seeds with a segregation ratio of 3:1, resistant: sensitive were selected and grown to seed (T₃). The T₃ generation was 100% resistant to Hygromycin B, suggesting that the plants were homozygous for the insert. The phenotypes of these plants appeared no different from WT plants.

DNA was extracted from the plants of each generation and a PCR was used to confirm the presence of the transgene. Primers that amplified the sequence encoding the mitochondrial targeting peptide and roGFP were used confirm the presence of mitochondrial-roGFP (Figure 4-6). Primers that amplified roGFP were used to confirm the presence of cytosolic-roGFP (Figure 4-6). The sequence encoding the mitochondrial targeting peptide was not amplified from plants transformed with cytosolic-roGFP as expected (Figure 4-6). This indicates that the plants are correctly transformed with either roGFP targeted to the mitochondria or roGFP without a targeting peptide (Figure 4-6).

T₁



T₂



T₃

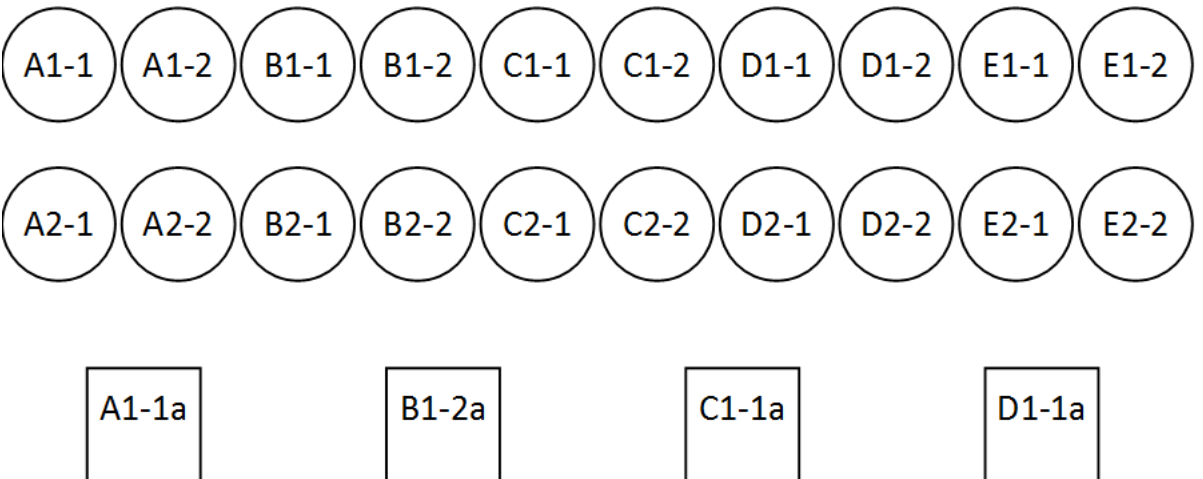


Figure 4-4: The naming policy for the selection of transgenic plants.

Seeds are shown in circles and plants are shown in squares

A



B

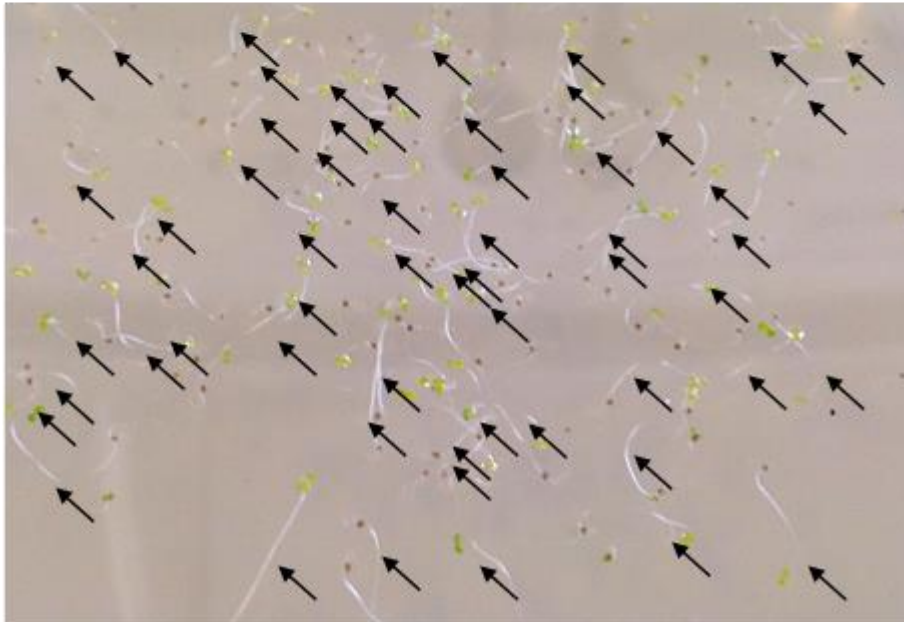


Figure 4-5: Selection for transformants on media containing Hygromycin B.

Seedlings resistant to Hygromycin B stand tall like normal dark grown seedlings with long hypocotyls and closed cotyledons and are indicated by arrows, whereas seedlings sensitive to Hygromycin B lay on the medium with very short hypocotyls and open cotyledons. **A:** T₁ seedlings. **B:** T₂ seedlings.

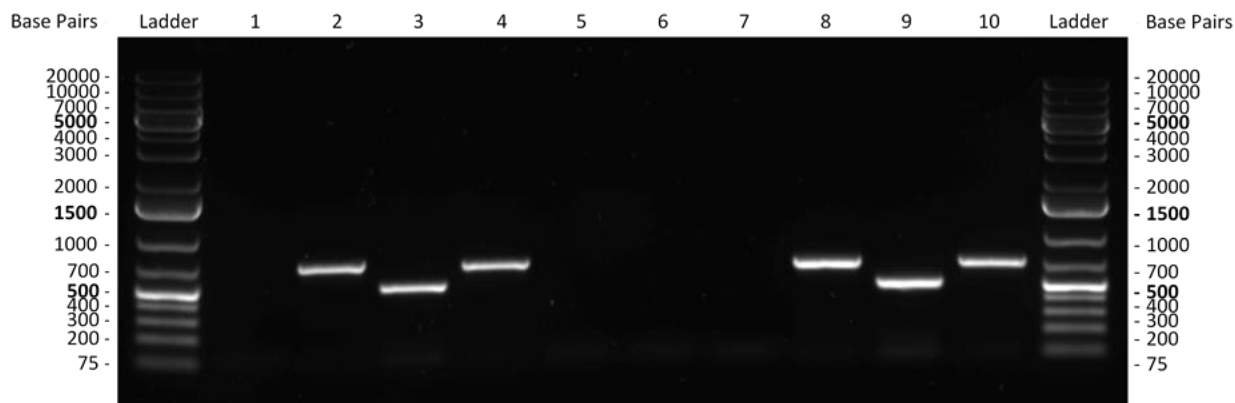


Figure 4-6: PCR genotyping of transgenic plants

DNA was extracted from plants expressing cytosolic roGFP (lanes 1 and 2) and mitochondrial roGFP (lanes 3 and 4). Lanes 5 and 6 were the non-template control. Lanes 7 and 8 contained plasmid containing cytosolic roGFP and lanes 9 and 10 contained the plasmid containing mitochondrial roGFP to act as a positive control. Primers targeted the mitochondrial targeting peptide in lanes 1, 3, 5, 7, and 9. Primers targeted roGFP in lanes 2, 4, 6, 8, and 10.

4.5. Discussion

The aim of the studies performed in this chapter was to gain greater insights in to the functions of LEA5 in plant mitochondria, and to determine if the abundance of LEA5 affects respiration and respiratory regulation. The rationale for these studies is that LEA5 was found to be localised to the mitochondria [51], and *LEA5* transcripts were found to be abundant in the dark (Figure 4-1), consistent with previous studies [43], therefore it is plausible that LEA5 has functions related to mitochondrial functions, such as dark respiration. The mitochondria used in these studies were therefore harvested from leaves during the dark period.

The data presented here show that while maximal COX activity in mitochondria from WT leaves was on average lower than in the mitochondria from OEX2-5 leaves, there was no significant difference between the two. Further studies using Blue-Native Polyacrylamide Gel Electrophoresis could determine the composition of respiratory complexes, and if the abundance of COX is altered by the levels of *LEA5*. A change in the abundance of the COX protein in transgenic plants that either overexpress *LEA5* or express *LEA5* in the antisense orientation would indicate that LEA5 stimulates respiratory functions in mitochondria.

Respiratory control ratios were also measured for complex I and for complex II. However, no differences were apparent in respiratory control. The absence of differences between these lines is possibly due to the expression of *LEA5* in the OEX2-5 line not being as previously described [43, 51]. This could be due to the seeds being of a different generation to those used previously, and so some silencing of the transgene has occurred. However, the optimisation of a method of isolating intact mitochondria from soil grown *A. thaliana in vitro* is still a considerable feat.

Transgenic plants expressing either mitochondrial-roGFP or cytosolic-roGFP were produced in the WT background and in the transgenic lines of *LEA5*-OEX(2-2), *LEA5*-OEX(2-5), *LEA5*-AS(2), and *LEA5*-AS(8) in order to explore the effects of altered LEA5 abundance on the redox state of the cytosol and mitochondria. Homozygous T₃ generation lines expressing either mitochondrial-roGFP or cytosolic-roGFP were produced for each genotype and seeds of these lines are now available for further study.

In the next chapter *A. thaliana* ecotype Landsberg *erecta* cell suspension cultures were transformed to express a tagged *LEA5* protein in order to identify proteins that interact with LEA5 through the use of tandem affinity purification and mass spectrometry. Verification of these interactions utilised transfected protoplasts in a split-YFP system.

Chapter 5. The identification of proteins that interact with LEA5

5.1. Introduction

Many members of the major LEA protein groups lack conventional secondary structures and are included in a class of proteins called “intrinsically disordered” proteins [22-24]. It is possible for a transition from a disordered to an ordered state to occur under certain conditions, for example a transition in protein conformation of ASR1 was induced by desiccation [33]. The ability to attain an ordered structure in conditions of water limitation [25-28] presumably allows LEA proteins to recognize their target molecules under stress situations. Typically Group 3 LEA proteins, of which LEA5 is a member, have been shown to prevent aggregation caused by drought and chilling. However, LEA5 has not been shown to have these functions. *LEA5* is unusual as it is inducible by oxidative stress, as well as phytohormones, and a range of biotic and abiotic stresses.

The interactome has been defined as “the complete repertoire of interactions” in a cell [198]. Analysing protein complexes and protein-protein networks allows the functional annotation of gene products, and is therefore of central importance in biological research. In the previous chapters, studies were presented concerning the role of *LEA5*, explored using transgenic lines with either sense or antisense expression of the gene. Unfortunately, these studies did not reveal new information concerning *LEA5* functions. Since it was not possible to predict the functions of *LEA5* from sequence and structural information, deducing the interactome of this protein might yield some results. Many methods have been developed to study protein-protein interactions; some are based on genetic approaches, while others rely on biochemical approaches, and more recently, computational methods have proven their utility in predicting protein-protein interactions. Comparing results obtained with different methods requires careful consideration as some methods only allow mapping of binary interactions whilst others can study protein complexes and are able to delineate both direct binary and indirect interactions.

A tandem affinity purification (TAP) approach was used in the following studies to identify proteins that interact with LEA5. TAP is a purification technique for studying protein-protein interactions. One-step purification methods have low purification levels, and so a method that isolates native protein complexes was developed. This method, named tandem affinity purification, was named due to its two consecutive affinity purification steps [199]. The use of two independent affinity steps enhances the specificity of the method. The original method used two Immunoglobulin G (IgG)-binding units of protein A of *Staphylococcus aureus* (ProtA) and the calmodulin binding peptide (CBP). While the CBP tag allowed for efficient elution under close to physiological conditions, ProtA release from the IgG matrix required denaturing conditions at relatively low pH levels. This problem was solved by the addition of the specific Tobacco (*Nicotiana tabacum*) Etch Virus (TEV) cleavage site which allowed proteolytic release under mild conditions, keeping the eluted complexes intact. Using this method, purification steps were optimized to recover high levels of protein while maintaining protein complex integrity [200]. However, the TAP approach in plants was not as well established until methods were optimised for plants. Most protein complex purifications from plants were, until recently, performed using the classical TAP tag, with two IgG-binding units of Prot A, or with a plant-adapted version, named the improved TAP tag [201]. Both the classical TAP tag and the improved TAP tag have been used to purify protein complexes from *A. thaliana* [175, 201]. Further optimisation of the purification method was necessary to improve the efficacy of this approach in plants. The use of the GS tag, which consists of two IgG-binding domains with a streptavidin-binding peptide that are separated by two TEV cleavage sites [200], was adapted for use in TAP of protein complexes in plants [175]. The GS tag outperformed the classical TAP tag in plant cells in both specificity and complex yield [202]. Furthermore this method was improved with the replacement of the TEV protease cleavage sites in the GS tag with the rhinovirus 3C cleavage site, improving protein complex stability during purification [202]. The rhinovirus 3C cleavage site is more specific and low-temperature active [203].

In the following experiments, plant cell suspension cultures were used to overexpress tagged LEA5 protein because they are fast growing and protein complexes can be rapidly isolated after homogenisation [175]. *Arabidopsis thaliana* (ecotype Landsberg *erecta*) cell suspension cultures (Plant Systems Biology; PSB-L and PSB-D), originally derived from MM1 and MM2d cultures [177], were used in these studies. The success of the TAP approach depends on the amount of protein complexes purified and the sensitivity of mass spectrometry. We therefore used TAP eluates from parallel purifications to overcome this problem. The approaches and

strategies used in these studies are summarised in Figure 5-1, which is taken from Van Leene *et al.*, (2007) [175]. The tagged protein is recovered from the host by breaking the cells, and retrieving it and associated components through affinity selection. Once isolated, the protein complex was identified using mass-spectrometry analysis [204]. Comprehensive protein sequence repositories were then used to identify purified protein complexes [205].

Split-YFP was also used in these studies to validate protein-protein interactions. In split-YFP, unfolded complementary fragments of the enhanced yellow fluorescent protein (YFP) are fused to two proteins that are postulated to interact, and expressed in live cells. If there is no interaction, then there is no fluorescence. If these proteins interact with one another then the fluorescent fragments will be brought within proximity to each other, which allows the YFP protein to form into its native three-dimensional structure and, upon excitation, emit a fluorescent signal. This assumes that the two fragments can fold properly. One major advantage of split-YFP is that, while initially the proteins fused to the YFP fragments may interact reversibly, once the YFP fragments associate, the complex is stabilised, facilitating visualisation of an interaction. However, a major drawback of split-YFP is that the fluorescent protein halves may self-assemble independent of a protein interaction event [206]. Split-YFP also has the advantage that it can show the intracellular locations where the protein association occurs. Furthermore, visualising protein-protein interactions occurs *in vivo* which has the advantage that it is possible to observe interactions dependent on post-translational modification. Split-YFP is now a well-established procedure, with many groups having used it in plants [207-211].

The following experiments were performed to identify protein candidates that interact with LEA5 through the use of TAP and mass spectrometry, and verify these interactions by using split-YFP.

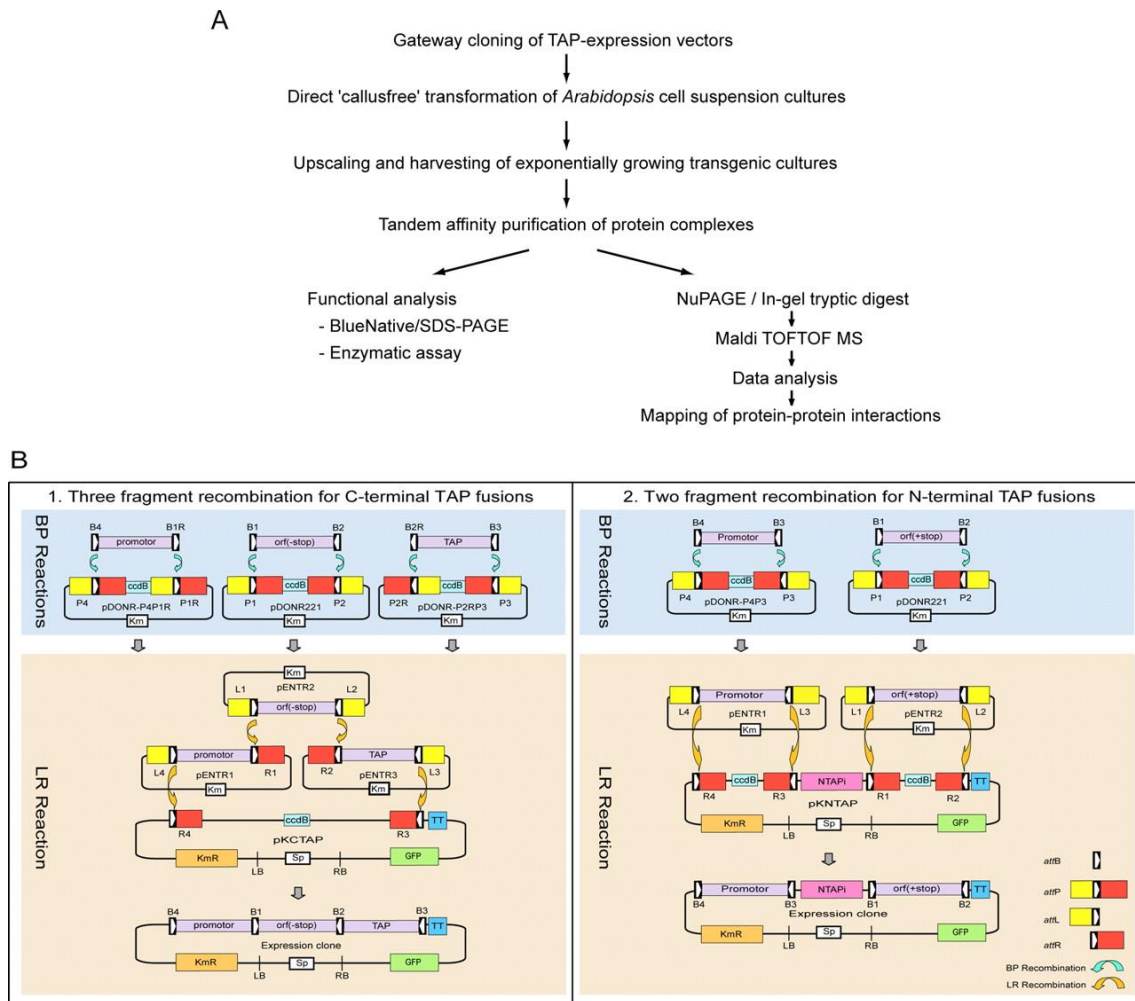


Figure 5-1: Strategy followed to clone, express, purify, and identify tagged proteins and their interacting partners.

A: Summary of the technology platform implemented for screening of protein-protein interactions in plant cells.

B: Overview of the TAP construct cloning strategy.

For C-terminal TAP fusions, a three-fragment recombination strategy was used. Three entry vectors were produced in a BP Clonase reaction that transferred a PCR amplicon (promoter, ORF without stop codon, and TAP tag) flanked by the appropriate *att* sites in to a compatible donor vector (e.g. pDonr221). The three fragments are then assembled into the pKCTAP destination vector in a single MultiSite LR Clonase reaction to produce an expression clone.

For N-terminal TAP fusions, a two-fragment recombination strategy was used. The promoter was cloned by BP Clonase reaction in pDonrP4P3, and the ORF (plus stop codon) was cloned in to pDonr221. Subsequently the two fragments were assembled into the pKNTAP destination vector, which contained the NTAPi tag [176], in a single MultiSite LR Clonase reaction to produce an expression clone.

The pKCTAP vectors contained a kanamycin resistance gene for selection of transformed cells and a GFP expression cassette as a visible marker for transformation between the left (LB) and right (RB) T-DNA border sequences.

Figure taken from Van Leene *et al.*, 2007 [175].

5.2. Results: TAP

5.2.1. Constructs for TAP experiments

A plasmid containing *LEA5-YFP* was obtained from Dr. Hilary Rogers (Cardiff University, UK). *LEA5* was subcloned from this plasmid by PCR using primers that amplified from the start codon to the stop codon of *LEA5*. The PCR products were separated by 1.5% agarose gel electrophoresis (Figure 5-2 A). The PCR product with the most intense band illustrated in Figure 5-2 A was at ~300 bp (*LEA5* is 291 nucleotides long). This was extracted from the gel and sequenced. The DNA sequence (Figure 5-2 B) of this PCR product and its translated amino acid sequence (Figure 5-2 C) was found to be identical to the genome sequence open reading frame (ORF) of *LEA5*. The *attB* sites were added to the 5' and 3' ends of the *LEA5* sequences by PCR. The primers used in this reaction amplified *LEA5* and contained overhangs with the *attB* sites. These PCR products were separated using a 1.5% agarose gel electrophoresis (Figure 5-3 A). The predicted size for a DNA product comprising *LEA5* and the *attB* DNA sequences is 352 bp. The DNA band between 300 bp and 400 bp on the gel (Figure 5-3 A) was excised from the gel and the DNA was extracted and sequenced (Figure 5-3 B). The sequence of PCR product matched the genomic sequence of *LEA5* with the addition of the *attB* ends in the correct orientation (Figure 5-3 B). The DNA sequence of the PCR product was translated in to the amino acid sequence (Figure 5-2 C) and found to be identical to the ORF of *LEA5*.

A BP reaction was performed with pDONR201 vector and the *LEA5+attB* PCR product to swap out the DNA cassette containing the *ccdB* gene in the pDONR201 with the gene of interest. The *ccdB* protein interferes with *E. coli* DNA gyrase inhibiting growth in most *E. coli* strains thereby facilitating recovery of only the desired clones. One Shot® OmniMAX™ 2 T1 Phage-Resistant Cells were transformed with the BP reaction by heat-shock of the cells to facilitate uptake of the DNA. The transformed cells were incubated in SOC for one hour. Cells were then streaked onto a LB plate containing 50 µg/ml kanamycin. The transformation was deemed to be successful as colonies were present on the plates after 16 hours. A single colony was selected and used to inoculate LB medium containing 50 µg/ml kanamycin. After 16 hours, the cells were pelleted and the plasmid was extracted from the cells. The plasmid was quantified using a Nanodrop at 140 ng/µl. 1µg of DNA was used in both a single and a double digest. The digested DNA was separated by 1% agarose gel electrophoresis (Figure 5-4 A). The single enzyme digest (Figure 5-4 A – lane 2) produced a single product between 2000 bp and 3000 bp, close to 2800 bp. The double digest (Figure 5-4 A – lane 4) produced two products, one at ~ 2300 bp and another at ~400 bp. These values are similar to the predicted sizes of the digested plasmid. 100 ng of plasmid was sequenced using primers that covered the *attL1* region of the vector and provided complete coverage of the plasmid insert (*LEA5*). The sequenced *LEA5* region of the plasmid shared 100% identity with the *LEA5* ORF minus the stop codon (Figure 5-4 B & C). Furthermore, this result was verified by sequencing using *LEA5* primers.

Finally, the *LEA5* fragment, contained in the pDONR201 vector, was assembled in to pKCTAP destination vector during a single MultiSite LR Clonase reaction to produce an expression clone. This procedure was performed at VIB following the strategy outlined by Van Leene *et al.*, 2007 [175]. The pKCTAP destination vector contained the improved TAP tag [176] on the C terminus of *LEA5*, a kanamycin resistance gene for selection of transformed cells, and a GFP expression cassette as a visible marker for transformation.

5.2.2. The growth of *Arabidopsis thaliana* cell suspension cultures

Arabidopsis cell suspension cultures were transformed with the pKCTAP-*LEA5* expression vector. The cultures were sub-cultured every 7 days. Growth curves for the cultures grown in the light or in the dark were the same; the exponential phase occurring between 3 and 7 days, after which the cells enter the stationary phase (data not shown). The presence of the tagged *LEA5* protein was detected in extracts of the cell cultures harvested at the beginning of the exponential growth phase by western blotting. The western blot used a peroxidase anti-peroxidase (PAP) antibody that binds to the ProtG domains of the GS-tag. For these experiments, cells were harvested on a sintered glass pore filter with a paper filter disc. The tissue was homogenized in extraction buffer. This material was centrifuged, and the supernatant fraction was resolved using a western blot. The PAP antibody identified a protein band at 31.3 kDa (as in Figure 5-5). The *LEA5* protein has a molecular weight of 10.3 kDa and the GS tag has a molecular weight of 21 kDa. Hence the size of the tagged *LEA5* protein is 31.3 kDa.

5.2.3. The effect of light on *LEA5* protein expression

The cell cultures expressing the tagged *LEA5* protein were grown either in the dark or in the light with $100 \mu\text{mol}\cdot\text{m}^{-2}\cdot\text{s}^{-1}$ irradiance and a 16 hour photoperiod. In these experiments, samples were harvested immediately upon exposure to light (time point 0) or after 1 day or 3 days of exposure to the light (Figure 5-5 A). Samples were also harvested from dark grown cultures at the same time points (Figure 5-5 B). All samples were harvested on three days after sub-culturing. Western blot analysis resolved a 31.3 kDa band that was present in both the light and dark grown cultures at all time points (Figure 5-5). An 18 kDa band, similar in size to the peroxidase product was also present in the western blots of samples harvested from both the light and dark grown cultures. This band was particularly prominent in cells harvested after 3 days of exposure to light. In cultures grown in the light for 1 day, the 18 kDa protein was less abundant than those grown in the light for 3 days. Another band, representing a protein with a molecular weight of 50 kDa was present on the blots representing cultures grown in the light for 3 days (Figure 5-5 A). The 50 kDa protein was absent in cultures grown in the light for 1 day. Furthermore, when cultures were placed in the light at the onset of the experiment, there was no noticeable difference between cultures introduced to the light to cultures kept in the dark.

It should be noted that in contrast to cultures grown only in the dark, the *LEA5* expressing cultures grown in the light over a 3-week period were no longer viable.

5.2.4. The effect of H₂O₂ on LEA5 protein expression

The cell cultures were treated with various concentrations of H₂O₂ for different time periods. In the first experiment, concentrations of H₂O₂ up to 20 mM were added to dark-grown cultures or cultures grown in the light for 3 days. Samples were harvested after 1 hour (Figure 5-6). Western blot analysis showed that a 31.3 kDa band was present in both the light and dark grown cultures at all concentrations of H₂O₂. However, the intensity of this band was greatly decreased in the presence of 20 mM H₂O₂, relative to cells not treated with H₂O₂ (Figure 5-6). In contrast, the intensity of the 18 kDa band was increased in the presence of 20 mM H₂O₂, relative to cells not treated with H₂O₂, particularly in the light (Figure 5-6 A). Other bands were also present in the light grown cultures at all concentrations of H₂O₂ (Figure 5-6 A). There was a 50 kDa band which had an increased intensity in the presence of 20 mM H₂O₂, in the cultures grown in the light but not in the dark (Figure 5-6 B). Furthermore, a band with a molecular weight slightly greater than 31.3 kDa was also apparent in cells treated with H₂O₂ (Figure 5-6 A).

In the second series of experiments, cell cultures were treated with 1 mM H₂O₂ either upon exposure to light or after 1 day of exposure to light. Samples were harvested over a period of 1 hour (Figure 5-7 and Figure 5-8). The pattern of bands observed in the dark-grown cultures or exposed to light at the onset of the experiment was similar at all harvest points (Figure 5-7). However, when cell cultures were exposed to 1 mM H₂O₂ having been exposed to light for 1 day, the presence of the H₂O₂ and/or light had a marked effect on the proteins observed on the western blots (Figure 5-8). The 31.3 kDa band was predominant in both the light and dark grown cultures at all the harvest points in the absence or presence of H₂O₂ (Figure 5-8). However, the 31.3 kDa band was more intense in cultures grown in the light compared to dark grown cultures, particularly at the later harvest points (Figure 5-8). The intensity of the 18 kDa band also increased with the time of incubation in presence of H₂O₂, and was most intense in the light after 60 minutes (Figure 5-8). Moreover, the band with a molecular weight slightly greater than 31.3 kDa was observed in the cells treated with 1 mM H₂O₂, being most prominent in the light-grown cells at the later harvest points (Figure 5-8 A).

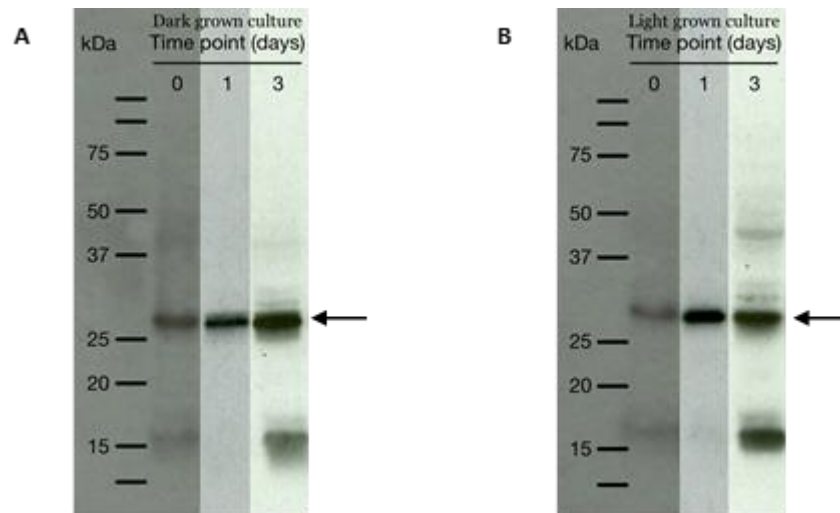


Figure 5-5: Western blot - expression of LEA5 in the light and the dark at different time points.

Three-day old *Arabidopsis thaliana* (ecotype *Landsberg erecta*) cell suspension cultures (Plant Systems Biology), either grown in the dark or exposed to light at sample collection, for 1 day, or for 3 days. **A:** Cultures grown in the light. **B:** Culture grown in the dark. LEA5 with the GS tag is 31.5 kDa and indicated on the blots with arrows.

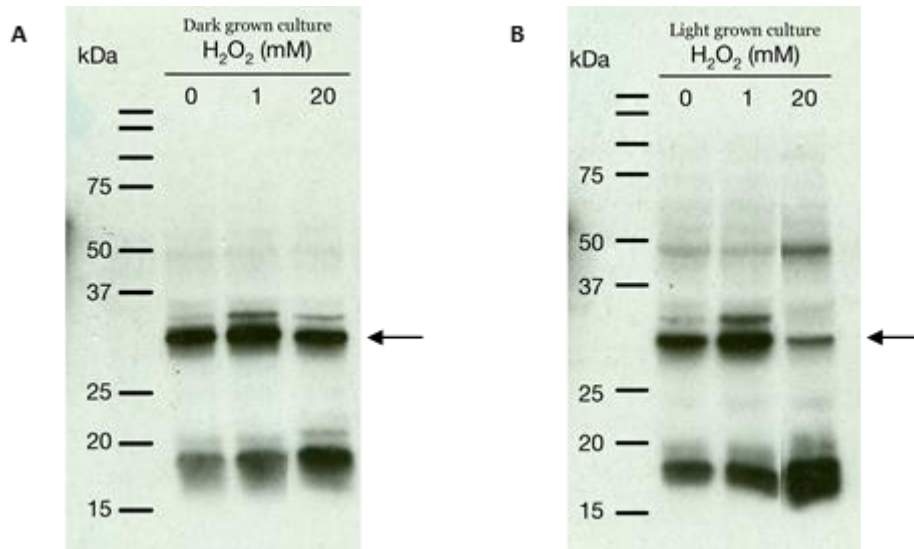


Figure 5-6: Western blot - expression of LEA5 in response to H₂O₂ in the light and the dark.

Arabidopsis thaliana (ecotype *Landsberg erecta*) cell suspension cultures (Plant Systems Biology), either grown in the light for 3 days or in the dark, were treated for 1 hour with 0, 1, or 20 mM H₂O₂. **A:** Culture grown in the light. **B:** Culture grown in the dark. LEA5 with the GS tag is 31.5 kDa and indicated on the blots with arrows.

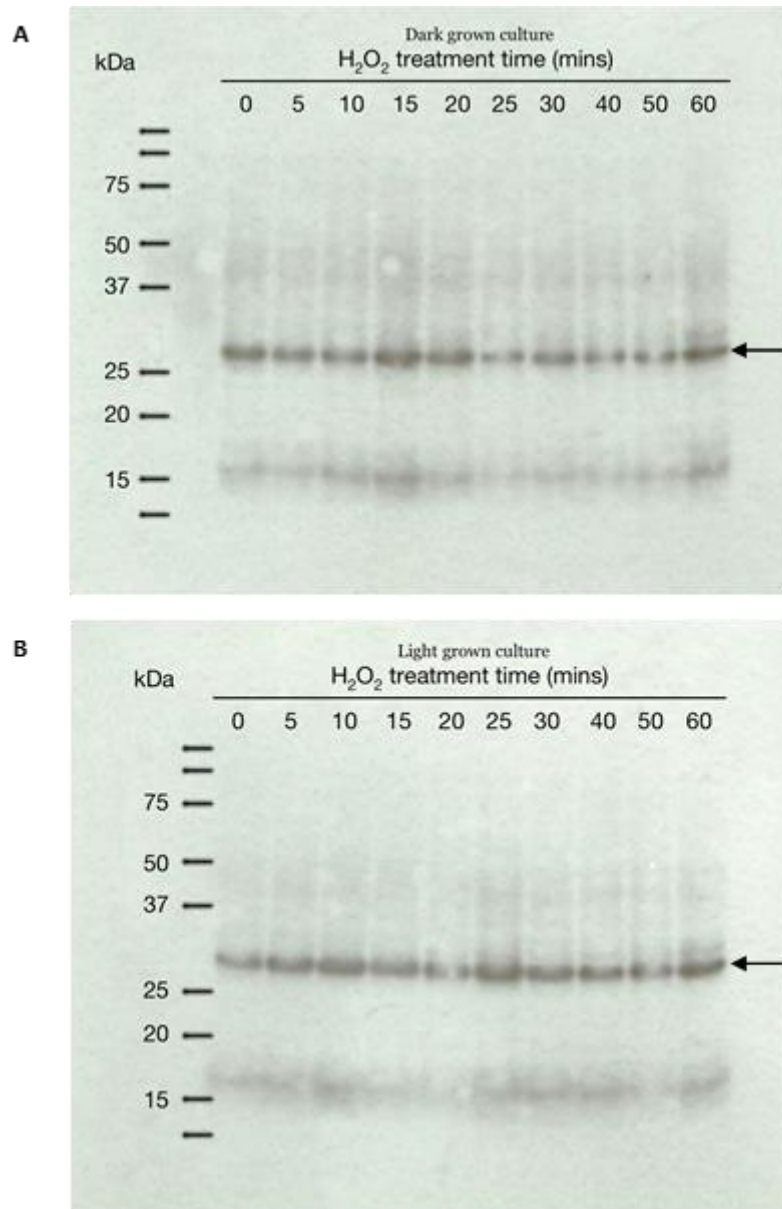


Figure 5-7: Western blot - expression of LEA5 over time in response to treatment with H₂O₂.

Arabidopsis thaliana (ecotype *Landsberg erecta*) cell suspension cultures (Plant Systems Biology), grown in the dark, were treated for 1 hour with 1 mM H₂O₂ and either kept in the dark or exposed to light from the onset of the treatment. Cultures were harvested over a period of 1 hour. **A:** Culture kept in the light. **B:** Culture exposed to the dark. LEA5 with the GS tag is 31.5 kDa and indicated on the blots with arrows.

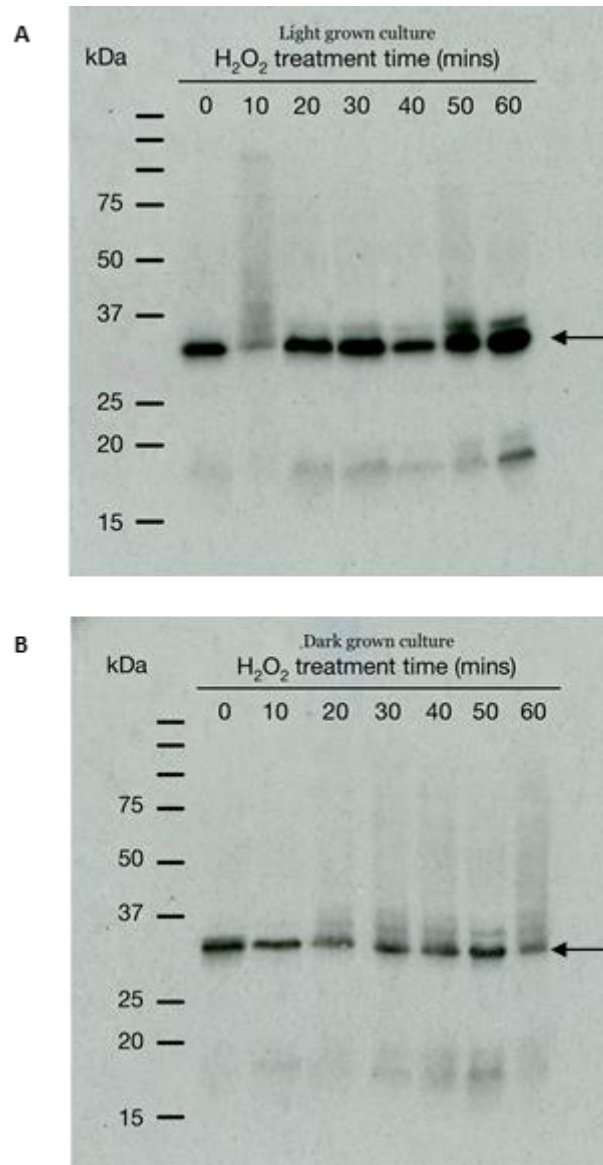


Figure 5-8: Western blot - expression of LEA5 over time in response to treatment with 2mM H₂O₂.

Three-day-old *Arabidopsis thaliana* (ecotype Landsberg *erecta*) cell suspension cultures (Plant Systems Biology), either grown in the light for one day or in the dark, were treated for 1 hour with 1 mM H₂O₂. Cultures were harvested over a period of 1 hour. **A:** Culture grown in the light. **B:** Culture grown in the dark. LEA5 with the GS tag is 31.5 kDa and indicated on the blots with arrows.

5.2.5. Identification of purified proteins from TAP with LEA5 as bait protein

The conditions selected for analysis by TAP were based on the western blot data. For these experiments, cultures grown in either the dark or the light for 3 days were treated with 1 mM H₂O₂ for 1 hour. The cells were harvested and homogenised, and protein complexes were extracted and purified by TAP. Protein complexes were then separated by SDS PAGE (Figure 5-9) and analysed using mass spectrometry. Identified proteins were first checked against a list of proteins known to interact with the GS tag [212]. Proteins that interact with the GS tag were excluded from the list presented in Table 8. In total, 27 interacting proteins were identified in at least one replication of the experiment (Table 8). It is interesting to note that the LEA5 interactome largely consists of proteins involved DNA or RNA processing and associated transport rather than metabolism (Table 8). Five LEA5-interacting proteins were identified in more than one replicate (Table 9). These are encoded by the following genes At1g59990, At3g16810, At1g55150, At2g02100, At2g36200.

A Dead(D/H)-box RNA helicase family protein, RH22 (encoded by At1g59990) interacted with LEA5 in cells grown either in the dark or the light (Table 9). Pumilio 24 (encoded by At3g16810), also interacted with LEA5 in both conditions (Table 9). Another Dead(D/H)-box RNA helicase family protein, RH20 (encoded by At1g55150) interacted with LEA5 in the dark but not in the light (Table 9). At2g02100 encodes defensin like protein, PDF2.2, which is located in the cell wall and is often used a marker for ethylene and jasmonate dependent pathogen defence induction. PDF2.2 interacted with LEA5 in cells grown either in the dark or the light (Table 9). At2g36200 encodes a kinesin family protein that is involved in microtubule motor activity and translocation. This protein also interacted with LEA5 in cells grown either in the dark or the light but only in one instance of each (Table 9).

Table 8: Proteins that interact with LEA5 in either the light or dark

Each experiment was repeated twice in the dark and twice in the light. A tick indicates that an interaction was observed. A cross indicates no interaction.

Protein accession	Protein description	Dark 1	Dark 2	Light 1	Light 2	YAP1A background
At1g59990	RH22 DEA(D/H)-box RNA helicase family protein 22	✓	✓	✓	✓	0
At3g16810	PUM24 pumilio 24	✓	✓	✓		0
At1g55150	RH20 DEA(D/H)-box RNA helicase family protein 20	✓	✓			0
At2g02100	PDF2.2 low-molecular-weight cysteine-rich 69		✓	✓		0
At2g36200	P-loop containing nucleoside triphosphate hydrolases superfamily protein		✓	✓		0
At1g22730	MA3 domain-containing protein			✓		0
At1g23280	MAK16 protein-related			✓		0
At1g24290	AAA-type ATPase family protein			✓		0
At1g26830	CUL3A, ATCUL3A, ATCUL3, CUL3 cullin 3		✓			0
At1g48900	Signal recognition particle, SRP54 subunit protein		✓			0
At1g50920	Nucleolar GTP-binding protein		✓			0
At1g72440	EDA25, SWA2 CCAAT-binding factor			✓		0
At2g02090	CHR19, CHA19, ETL1 SNF2 domain-containing protein / helicase domain-containing protein			✓		0
At2g31660	SAD2 ARM repeat superfamily protein	✓				0
At2g34357	ARM repeat superfamily protein		✓			0
At3g06400	CHR11 chromatin-remodeling protein 11		✓			0
At3g08947	ARM repeat superfamily protein			✓		0
At3g15590	Tetratricopeptide repeat (TPR)-like superfamily protein			✓		0
At3g19820	DWF1, DIM, EVE1, DIM1, CBB1 cell elongation protein / DWARF1 / DIMINUTO (DIM)		✓			0
At3g58660	Ribosomal protein L1p/L10e family		✓			0
At3g60240	EIF4G, CUM2 eukaryotic translation initiation factor 4G			✓		0
At4g12420	SKU5 Cupredoxin superfamily protein		✓			0
At5g10470	KCA1, KAC1 kinesin like protein for actin based chloroplast movement 1			✓		0
At5g18620	CHR17 chromatin remodeling factor17			✓		0
At5g45550	Mob1/phocein family protein			✓		0
At5g51570	SPFH/Band 7/PHB domain-containing membrane-associated protein family		✓			0
At5g64420	DNA polymerase V family			✓		0

Table 9: Selected proteins that interact with LEA5 either in the light or dark

Each experiment was repeated twice in the dark and twice in the light. A tick indicates that an interaction was observed. A cross indicates no interaction.

Protein accession	Protein description	Dark 1	Dark 2	Light 1	Light 2
At1g59990	RH22 DEA(D/H)-box RNA helicase family protein 22	✓	✓	✓	✓
At3g16810	PUM24 pumillio24	✓	✓	✓	
At1g55150	RH20 DEA(D/H)-box RNA helicase family protein 20	✓	✓		
At2g02100	PFD2.2 low molecular-weight cysteine-rich 69		✓	✓	
At2g36200	P-loop containing nucleoside triphosphate hydrolases superfamily protein		✓	✓	

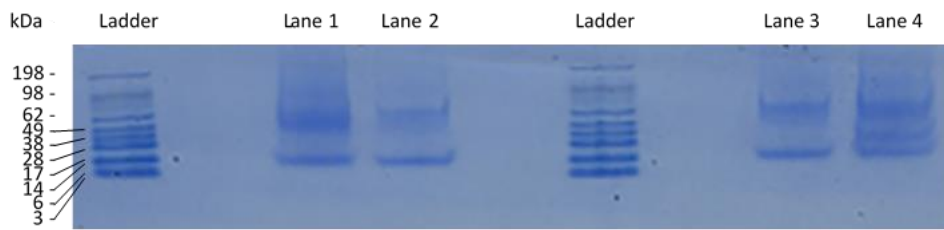


Figure 5-9: SDS-PAGE of purified protein complexes.

Proteins purified by TAP were separated by SDS-PAGE. The MW ladder is SeeBlue Plus2 (Invitrogen). Lane 1: 35S-LEA5-GSrhino Light replicate 1. Lane 2: 35S-LEA5-GSrhino Light replicate 2. Lane 3: 35S-LEA5-GSrhino Dark replicate 1. Lane 4: 35S-LEA5-GSrhino Dark replicate 2.

5.3. Results: Split-YFP

The results of the TAP experiments demonstrated that LEA5 interacted with RH22. Since this interaction was observed in all the TAP experiments, this part of the LEA5 interactome was investigated in more detail. A split-YFP method was used to attempt to verify this interaction. To perform this analysis, constructs for split-YFP analysis were first produced.

5.3.1. Production of constructs for split-YFP experiments

Plasmids containing *LEA5* fused to either the YFPc or YFPn halves of YFP were produced by recombining the pDONR201+*LEA5* construct (produced previously for TAP tagging) with either the pDH51-GW-YFPc (NASC code: 9843, Accession number: AM773754) or the pDH51-GW-YFPn (NASC code: 9842, Accession number: AM773753) plasmid in an LR reaction. Plasmids containing *RH22* fused to either YFPc or YFPn were produced in a similar manner. All plasmids were sequenced and confirmed to contain the genes of interest fused to either YFPc or YFPn (Figure 5-10).

Plasmids containing either amino peptidase P1 (APP1; At4g36760) or amino peptidase P2 (APP2; At3g05350) fused to GFP were used as transformation controls. As a negative control, protoplasts were transfected with two constructs containing the same half of YFP.

5.3.2. Confirmation of interaction

Protoplasts were successfully isolated from 3-week-old *A. thaliana* following the protocol of Wu *et al.*, 2009 [181] with minor modifications (described in the Materials and Methods chapter). Protoplasts were viewed with a light microscope and a sufficient amount were deemed to be intact (Figure 5-11). These were transfected with constructs for the split-YFP experiments following the method of Yoo *et al.*, 2007 [182] with minor modifications (described in the Materials and Methods chapter).

Transfected protoplasts were observed with a Zeiss LSM700 laser scanning confocal microscope. Chloroplast autofluorescence was excited at 555 nm, and emission was 580 nm, the detection was 560-800 nm. Protoplasts transfected with control constructs, APP1, or APP2, indicated that transformation was successful. The APP1-GFP control was excited at 488 nm, and emission was 509 nm, the detection was 505-530 nm. The signal was detected in the cytoplasm (Figure 5-12). The APP2 control was excited at 488 nm, and emission was 509 nm, the detection was 505-530 nm. The signal was detected in the chloroplast (Figure 5-13). This

signal was similar to chlorophyll autofluorescence. Excitation at 488 nm can simultaneously excite enhanced GFP and chloroplast autofluorescence. As a negative control, protoplasts were transfected with two constructs, each containing the same half of YFP - LEA5-YFPc and RH22-YFPc (Figure 5-14). A relatively low signal was detected in the scan for YFP (Figure 5-14 A; excitation at 488 nm, and emission was 509 nm, the detection was 505-530 nm) which was determined to be background fluorescence.

To confirm LEA5 interaction with RH22, protoplasts were transfected with LEA5-YFPc and RH22-YFPn (Figure 5-15), or LEA5-YFPn and RH22-YFPc (Figure 5-16). If the LEA5 and RH22 proteins are able to interact with one another then the fluorescent fragments will be brought within proximity to each other, allowing the YFP protein to form into its native three-dimensional structure and, upon excitation, emit a fluorescent signal. Chloroplast autofluorescence was excited at 555 nm, and emission was 580 nm, the detection was 560-800 nm. YFP fluorescence was excited at 488 nm, and emission was 509 nm, the detection was 505-530 nm. A relatively low signal was detected in the scan for YFP (Figure 5-15 A), however this was deemed to be cell autofluorescence due to the pattern being similar to the negative control (Figure 5-14) and visible in all cells (transformation is unlikely to be 100% successful). Therefore, the YFP signal was not detected in protoplasts transformed with constructs containing *LEA5*-YFPc and *RH22*-YFPn (Figure 5-15). This was also the case for protoplasts transformed with constructs containing *LEA5*-YFPn and *RH22*-YFPc (Figure 5-16).

A: Amino acid sequence of LEA5 portion of plasmids aligned against ORF

ORF	1	MARSI SNVKIVSAFVSRELSNAIFRRGYAATAAQGSVSSGGRS GAVASAVM KKKGVEEST	60
LEA5-YFPc	1	MARSI SNVKIVSAFVSRELSNAIFRRGYAATAAQGSVSSGGRS GAVASAVM KKKGVEEST	60
LEA5-YFPn	1	MARSI SNVKIVSAFVSRELSNAIFRRGYAATAAQGSVSSGGRS GAVASAVM KKKGVEEST	60
ORF	61	QKISWVPDPKTYRYPETGSNEIDAAELRAALLNNKQ	97
LEA5-YFPc	61	QKISWVPDPKTYRYPETGSNEIDAAELRAALLNNKQ	97
LEA5-YFPn	61	QKISWVPDPKTYRYPETGSNEIDAAELRAALLNNKQ	97

B: Amino acid sequence of RH22 portion of plasmids aligned against ORF

ORF	1	MILSRSVSVLHLCGVSSSAPS KLLSQRFKVSFALAYGSSVSFRLSSLNRS DRKWVRFAS	60
RH22-YFPc	1	MILSRSVSVLHLCGVSSSAPS KLLSQRFKVSFALAYGSSVSFRLSSLNRS DRKWVRFAS	60
RH22-YFPn	1	MILSRSVSVLHLCGVSSSAPS KLLSQRFKVSFALAYGSSVSFRLSSLNRS DRKWVRFAS	60
ORF	61	ATEAEVEKKGNDTFFADHTVSWKSLGSLDNVSI ALRDSGFDRPSLTQAVCIP SILSGKDV	120
RH22-YFPc	61	ATEAEVEKKGNDTFFADHTVSWKSLGSLDNVSI ALRDSGFDRPSLTQAVCIP SILSGKDV	120
RH22-YFPn	61	ATEAEVEKKGNDTFFADHTVSWKSLGSLDNVSI ALRDSGFDRPSLTQAVCIP SILSGKDV	120
ORF	121	IVAAETGSGKTHGYLAPIIDQLTNTALDSEVTNREERPFPLKNI SLILCPNVMLCEQVVR	180
RH22-YFPc	121	IVAAETGSGKTHGYLAPIIDQLTNTALDSEVTNREERPFPLKNI SLILCPNVMLCEQVVR	180
RH22-YFPn	121	IVAAETGSGKTHGYLAPIIDQLTNTALDSEVTNREERPFPLKNI SLILCPNVMLCEQVVR	180
ORF	181	MVNGLVDEEDGNPLLRVEAVCGSQGWPDRLPDI IVSTPAALLNNI EPKRRRLEFLRCVKY	240
RH22-YFPc	181	MVNGLVDEEDGNPLLRVEAVCGSQGWPDRLPDI IVSTPAALLNNI EPKRRRLEFLRCVKY	240
RH22-YFPn	181	MVNGLVDEEDGNPLLRVEAVCGSQGWPDRLPDI IVSTPAALLNNI EPKRRRLEFLRCVKY	240
ORF	241	VVFDEADM LCGSFQNIIRLINMLRFDEKQVSR LAKSNLGRPMEIDASVPQIDLENE DD	300
RH22-YFPc	241	VVFDEADM LCGSFQNIIRLINMLRFDEKQVSR LAKSNLGRPMEIDASVPQIDLENE DD	300
RH22-YFPn	241	VVFDEADM LCGSFQNIIRLINMLRFDEKQVSR LAKSNLGRPMEIDASVPQIDLENE DD	300
ORF	301	AEFDEGSI SEEEDEEEYLD DIAQMP SVEAEAGSDTKKGWRRVRKIYTRSKQYIFIAA	360
RH22-YFPc	301	AEFDEGSI SEEEDEEEYLD DIAQMP SVEAEAGSDTKKGWRRVRKIYTRSKQYIFIAA	360
RH22-YFPn	301	AEFDEGSI SEEEDEEEYLD DIAQMP SVEAEAGSDTKKGWRRVRKIYTRSKQYIFIAA	360
ORF	361	TLPVNGKKTAGGILKHMFD AVWVSGNFLHRNSPRLKQKWVEVTVD SQVDALIEAVKNNN	420
RH22-YFPc	361	TLPVNGKKTAGGILKHMFD AVWVSGNFLHRNSPRLKQKWVEVTVD SQVDALIEAVKNNN	420
RH22-YFPn	361	TLPVNGKKTAGGILKHMFD AVWVSGNFLHRNSPRLKQKWVEVTVD SQVDALIEAVKNNN	420
ORF	421	NTNTERTMVFANTVEAVEAVADILEKASIQCYRYHKNHKLDERANILADFRETGGV FVCT	480
RH22-YFPc	421	NTNTERTMVFANTVEAVEAVADILEKASIQCYRYHKNHKLDERANILADFRETGGV FVCT	480
RH22-YFPn	421	NTNTERTMVFANTVEAVEAVADILEKASIQCYRYHKNHKLDERANILADFRETGGV FVCT	480
ORF	481	DAAARGVDVPNVSHVIQAD FASSAVDFLHRIGRTARAGQYGTVTSLYTEANRDLVEAIRE	540
RH22-YFPc	481	DAAARGVDVPNVSHVIQAD FASSAVDFLHRIGRTARAGQYGTVTSLYTEANRDLVEAIRE	540
RH22-YFPn	481	DAAARGVDVPNVSHVIQAD FASSAVDFLHRIGRTARAGQYGTVTSLYTEANRDLVEAIRE	540
ORF	541	AVKMGQPVETAFSRKRGFRNKVKKRAFLKAEAE EEPQAVRY	581
RH22-YFPc	541	AVKMGQPVETAFSRKRGFRNKVKKRAFLKAEAE EEPQAVRY	581
RH22-YFPn	541	AVKMGQPVETAFSRKRGFRNKVKKRAFLKAEAE EEPQAVRY	581

Figure 5-10: Analysis of pDH51-GW-YFPc and pDH51-GW-YFPn plasmid containing either LEA5 or RH22 DNA.

A: alignment of translated amino acid sequences of plasmids containing *LEA5*. **B:** alignment of translated amino acid sequences of plasmids containing *RH22*.

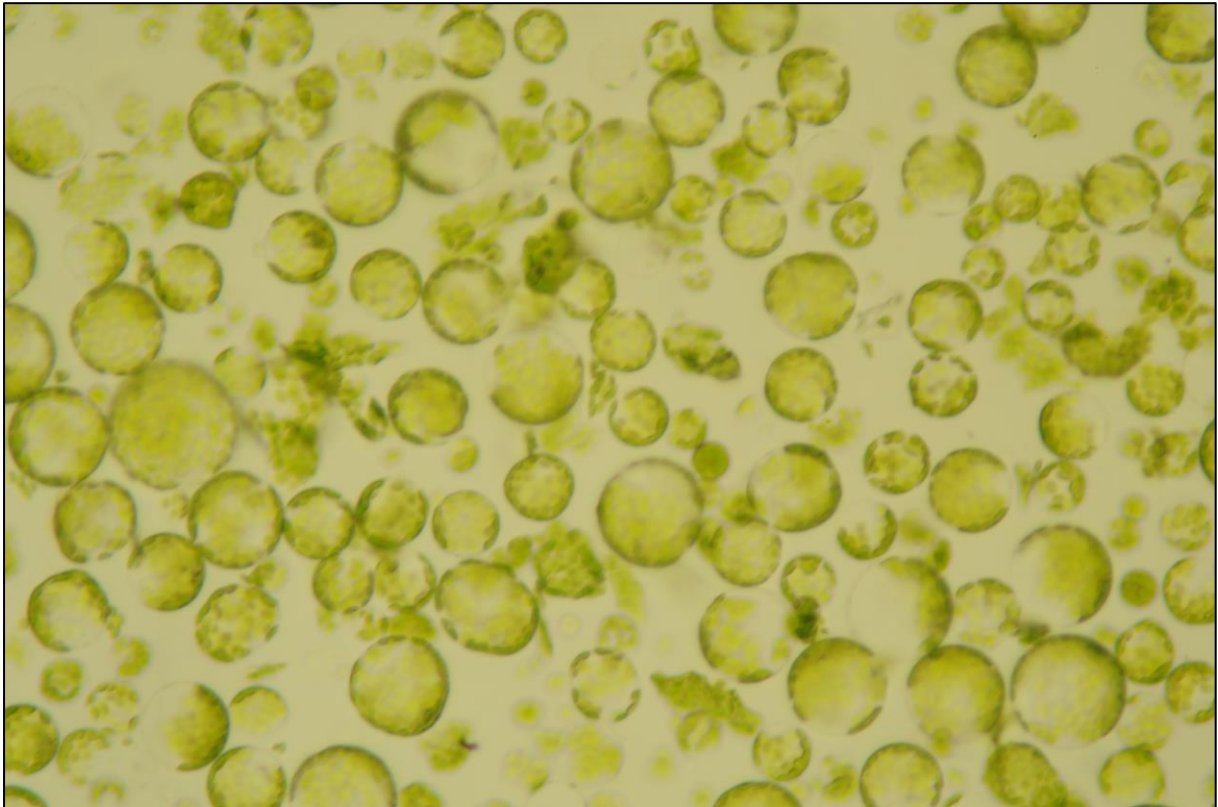


Figure 5-11: Light microscopy images of mesophyll protoplasts.

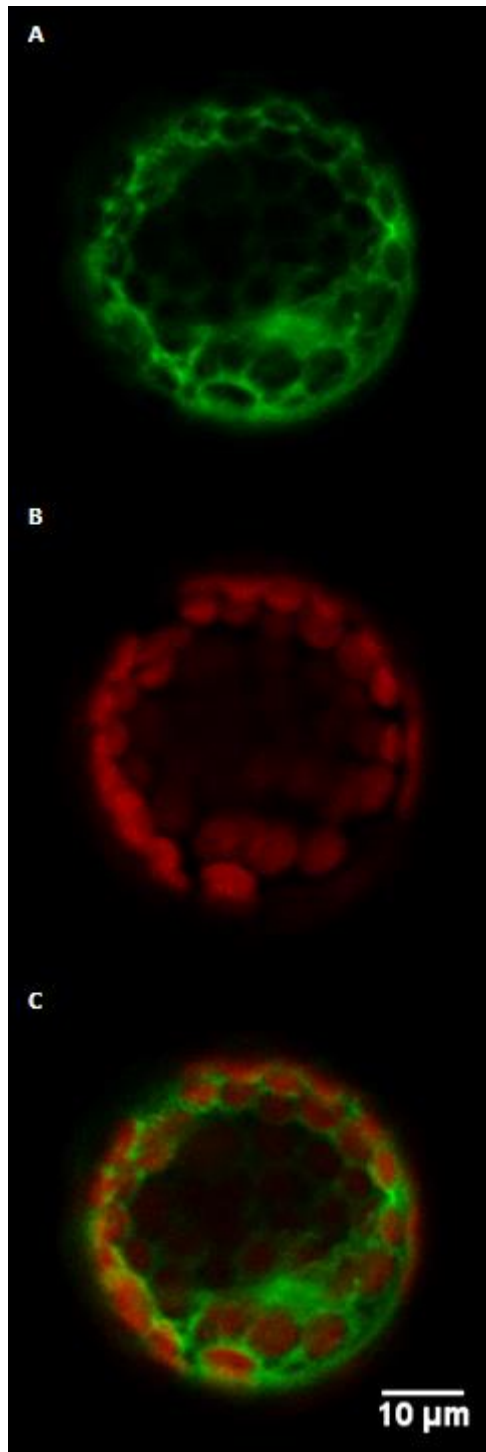


Figure 5-12: Confocal microscopy images of an intact mesophyll protoplast transiently expressing APP1-GFP.
A: APP1-GFP (Excitation 488 nm, Emission 518 nm, Detection 300-550 nm). **B:** Chlorophyll autofluorescence (Excitation: 555 nm, Emission 580 nm, Detection 560-800 nm). **C:** Merge of A and B.

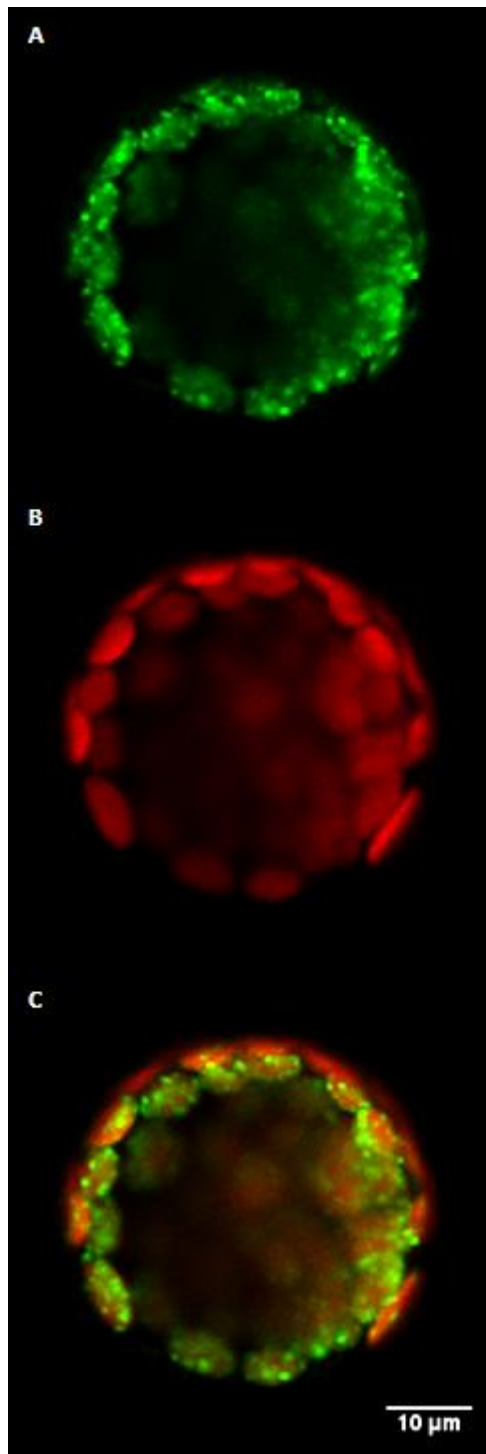


Figure 5-13: Confocal microscopy images of an intact mesophyll protoplast transiently expressing APP2-GFP.

A: APP2-GFP (Excitation 488 nm, Emission 518 nm, Detection 300-550 nm). **B:** Chlorophyll autofluorescence (Excitation: 555 nm, Emission 580 nm, Detection 560-800 nm). **C:** Merge of A and B.

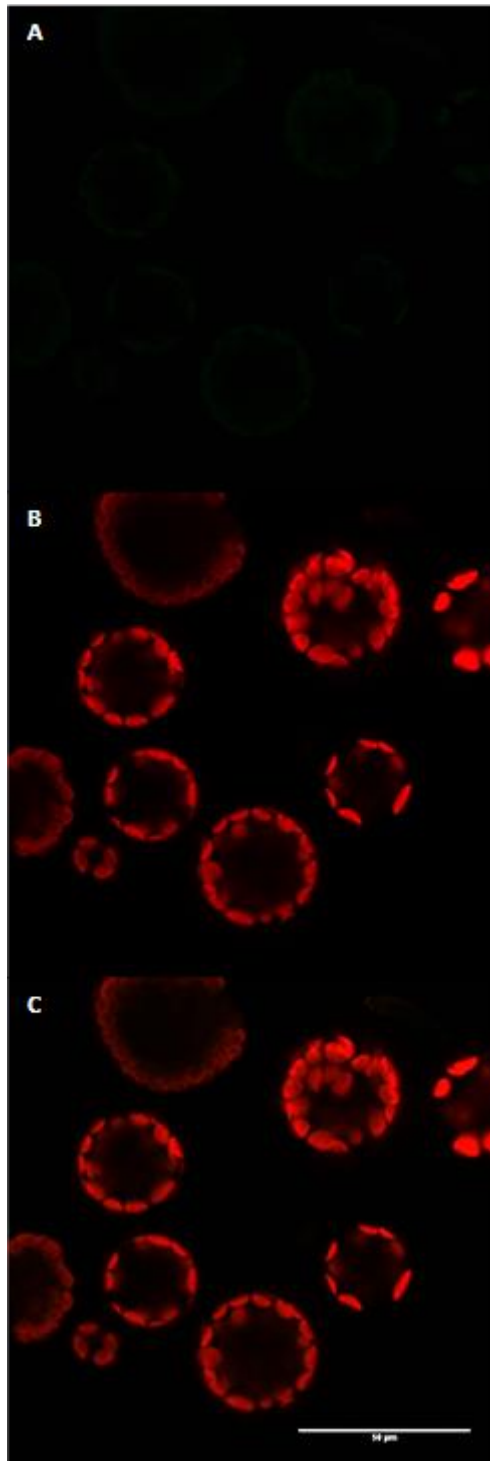


Figure 5-14: Confocal microscopy images of mesophyll protoplasts autofluorescence (negative control).

A: YFP negative (Excitation 488 nm, Emission 518 nm, Detection 300-550 nm). **B:** Chlorophyll autofluorescence (Excitation: 555 nm, Emission 580 nm, Detection 560-800 nm). **C:** Merge of A and B.

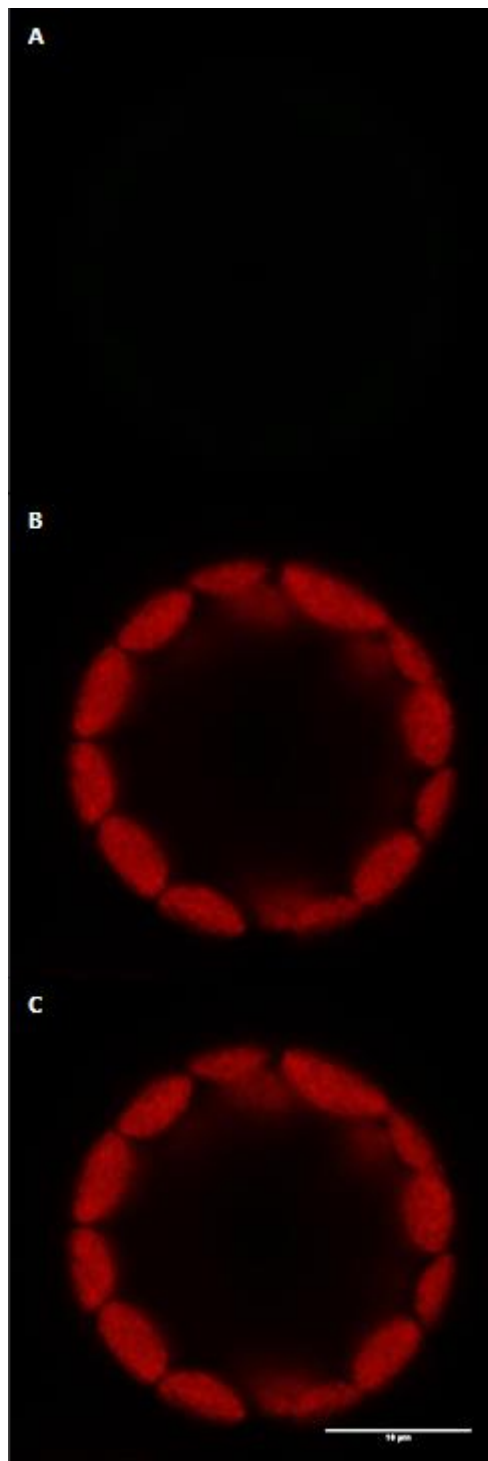


Figure 5-15: Confocal microscopy images of an intact mesophyll protoplast transiently expressing LEA5-YFPc and RH22-YFPn.

A: YFP (Excitation 488 nm, Emission 518 nm, Detection 300-550 nm). **B:** Chlorophyll autofluorescence (Excitation: 555 nm, Emission 580 nm, Detection 560-800 nm). **C:** Merge of A and B.

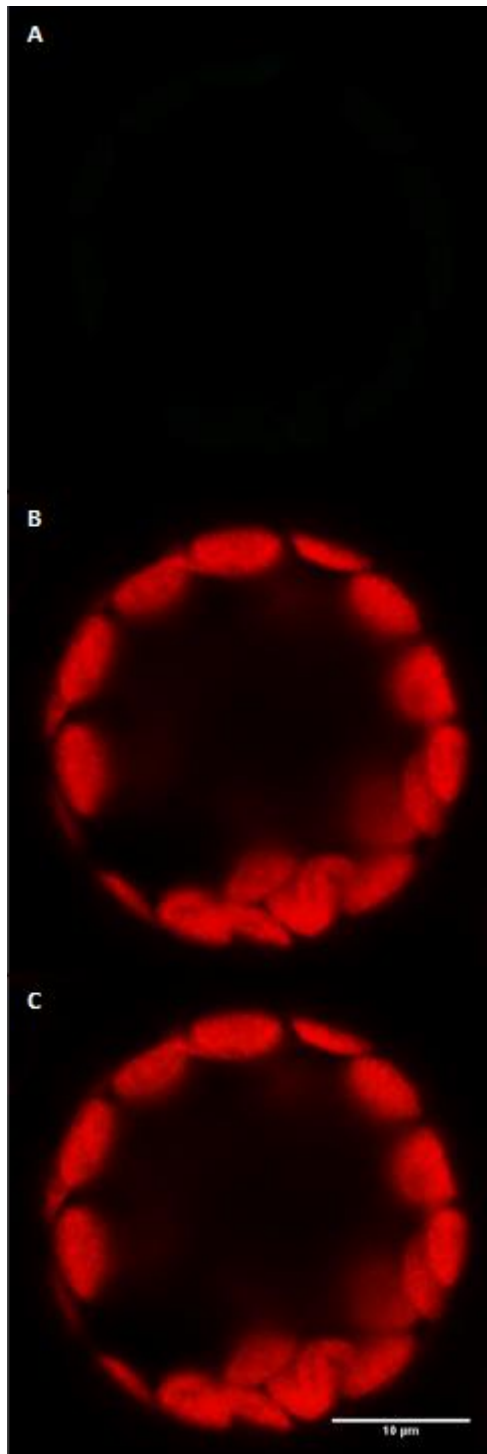


Figure 5-16: Confocal microscopy images of an intact mesophyll protoplast transiently expressing LEA5-YFPn and RH22-YFPc.

A: YFP (Excitation 488 nm, Emission 518 nm, Detection 300-550 nm). **B:** Chlorophyll autofluorescence (Excitation: 555 nm, Emission 580 nm, Detection 560-800 nm). **C:** Merge of A and B.

5.4. Discussion

The aim of the experiments reported in this chapter was to identify proteins that interact with LEA5. Through the use of an established tandem affinity purification procedure combined with mass spectrometry, a substantial list of proteins that interact with LEA5 was revealed. Previous studies have shown that LEA5 localises to the mitochondrion [51]. It was therefore predicted that many proteins that interact with LEA5 would also localise to the mitochondrion. However, no mitochondrial proteins were found to interact with LEA5 which was unexpected. The data presented here show that proteins localised to chloroplasts interacted with LEA5 in the TAP experiments. This finding is interesting as LEA5 was originally predicted to contain a putative chloroplast transit peptide [43, 213]. Of the proteins that interact in the TAP analysis, two are RNA helicases. These enzymes catalyse the unwinding and separation of double-stranded DNA or RNA during its replication. RH22 was shown to interact with LEA5 in all experiments and the functions of this protein therefore merit further consideration.

RH22 is localised to plastids [214]. The developing seedlings of *A. thaliana* plants defective in RH22 have a pale-green phenotype, however adult leaves were similar to WT plants [214]. *RH22* expression levels are high in developing seeds and seedlings compared to stems, and flowers. Plastid gene expression of the developing seeds and seedlings of *rh22* mutants differed from the WT [214]. The expression of several genes was decreased in developing *rh22* mutant seeds. For example, the expression of the gene encoding the β subunit of the carboxyltransferase, which is a component of acetyl-CoA carboxylase in the plastids, was decreased in *rh22* seeds. The β subunit of the carboxyltransferase is essential for acetyl-CoA carboxylase function [215-217]. The carboxylation of acetyl-CoA to malonyl-CoA by acetyl-CoA carboxylase is the first step in fatty acid biosynthesis [218]. Notably, the seeds of *rh22* mutants, which had a decreased expression of the gene encoding the β subunit of the carboxyltransferase, had a triacylglycerol content which was 10% lower than that of WT seeds, while the protein content was unchanged [214]. RH22 is essential for apposite accumulation of plastid mRNAs during seed development and seedling growth, ensuring seed oil biosynthesis by maintaining plastid mRNA levels. The strong evidence provided by the TAP analysis reported here suggests that RH22 interacts with LEA5 in both the light-grown and the dark-grown cultures. These findings might suggest that LEA5 interacts with RH22 to regulate plastid gene expression, a possibility that can be explored in future work.

Other data presented in this chapter suggest that LEA5 might influence cell viability and fate via effects on chloroplast function. Proliferating cells expressing LEA5 were viable in the dark, but not in the light. As the expression of LEA5 in light-grown cell cultures did not immediately lead to loss of the ability of the cultures to proliferate, the LEA5 protein would appear to have a progressive or accumulative influence on cell functions. This is an interesting observation as this was the first case where expression of a transgene led to the progressive loss of viability of the cell cultures. Cultures expressing LEA5 in the light lost chlorophyll and came to resemble the dark grown cultures, which might link LEA5 to RH22 in the regulation of plastid gene expression, a possibility that again should be explored in detail in future work.

Confirmation of RH22 interaction with LEA5 was attempted with a split-YFP approach. Split-YFP is now a well-established procedure in plants [207-211]. As well as its uses as a protein-protein interaction screening assay, split-YFP can also be used to show the intracellular locations where the protein association occurs. In the studies reported here, transfection of protoplasts with DNA control constructs was successful. APP1 was detected in the cytoplasm and APP2 was detected in the chloroplast. However, no signal was detected in the split-YFP verification of RH22-LEA5 interaction in the studies reported here. It could be possible that LEA5 interaction occurs in times of oxidative stress and so repeating the split-YFP experiments in the presence of H₂O₂ may yield more results. Given the rigour of the TAP tagging analysis, it is too soon to conclude that LEA5 does not interact with proteins localised to the chloroplasts, such as RH22. Similar experiments should also be performed to confirm other LEA5 protein interactions, such as those with PUM24, RH20, and PDF2.2.

The western blot analysis reported here, provides insights into the expression and stability of the tagged LEA5 protein. The tagged LEA5 protein was always detected in the cells, whether they were grown in the dark or the light, in the absence or the presence of oxidant. However, evidence of degradation of the tagged LEA5 protein was observed in the presence of hydrogen peroxide, particularly in cultures grown in the light. Moreover, other bands containing the tag were also apparent in blots of proteins extracted from cells incubated with H₂O₂, particularly in the light. These findings would suggest that the presence of light and oxidative stress alters features of the tagged protein, that appear to include, turnover, post-translational modification and binding properties. This data suggests that the LEA5 interactome is complex and highly dependent on environmental conditions, and that its expression has a profound influence on cell functions, particularly in the light.

Chapter 6. Production and phenotype of transgenic barley expressing *LEA5*

6.1. Introduction

Earlier studies on transgenic *A. thaliana* showed that the over-expression of *LEA5* resulted in plants with a greater biomass [43, 51]. Transferring this technology to a crop species, such as barley (*Hordeum vulgare* L.), could have a major effect in the agriculture industry. Research of this kind is of great interest for biotechnology companies [1]. Barley is a major cereal grain grown in temperate climates. In a 2007 ranking of cereal crops in the world, barley ranked fourth in quantity produced (136 million tons). Transgenic barley plants expressing *LEA5* have been produced as part of research within the EU CropLife program.

To produce the transgenic barley, *LEA5* fused to YFP was cloned in to the pBRACT214 vector using the Gateway® Technology cloning method. The *LEA5* gene was expressed with a 35S Ubi promoter. The golden promise cultivar - an English semi-dwarf, salt-tolerant variety, commonly used to make beer and whiskey - was transformed with the BRACT214_LeA5-YFP vector using Agrobacterium mediated transformation of embryos. The axis was removed from the barley embryos to stop development of root and shoot apices. Embryos were co-cultivated with Agrobacterium cells containing the transformation vector for 3 days in the dark. Embryos were then transferred to fresh media containing the antibiotic Timentin, used to kill the Agrobacterium; and Hygromycin B, used to select for transformants. Embryos were transferred to fresh media every two weeks and developed into callus over the following 4 weeks. Calluses were moved to regeneration media to produce shoots. Finally, transformed barley plants were confirmed by PCR using primers targeting the Hygromycin B resistance gene, and grown to seed in a glasshouse.

The aim of the studies described in this chapter was to produce homozygous transgenic barley plants expressing *LEA5* and to characterise the phenotype of these plants. In this chapter the effects of *LEA5* expression on barley shoot growth were determined in the absence of stress.

6.2. Results

6.2.1. The selection of transgenic barley plants

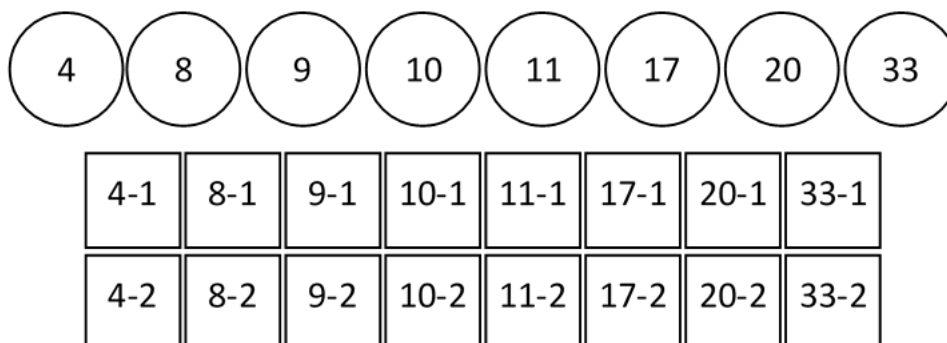
To select for homozygous plants, WT, and T₂ transgenic barley seeds that were either Empty Vector (EV) control, β-glucuronidase (GUS) control, or expressing *LEA5* were surface sterilised and sown on ½ MS media containing 100 mg/ml Hygromycin B to select for transgenic plants. The naming policy for the selection of transgenic plants is shown in Figure 6-1. Ten lines were sown for selection, which were previously shown to be following simple Mendelian inheritance with 75% of the plants having inherited resistance to Hygromycin B. The other 25% were sensitive to the antibiotic and did not grow. Deviations from this ratio can indicate multiple insertions of the gene. Sown seeds were kept at 4°C for 3 days to stratify them and then moved into the light at 20°C for 8 hours to stimulate germination before moving them back in to the dark at 20°C for 4 days. Transformants were identified as Hygromycin B resistant plants which were standing tall like normal dark grown plants with long stems and leaves. Hygromycin B sensitive plants were slightly bleached with short leaves (Figure 6-2 A). The plates were kept in weak light for 2 days before to allow the Hygromycin B resistant plants to become green without stressing the plants. Hygromycin B resistant plants were then grown in standard conditions for 1 week and numbers of resistant and sensitive plants were counted. As expected, no WT plants were resistant to Hygromycin B (Figure 6-2 A; Table 10). All of the EV and GUS control plants were resistant to Hygromycin B. Furthermore, all of plants from the transgenic *LEA5*-YFP lines, 4.1, 10.1, and 11.2, were resistant to Hygromycin B (Figure 6-2 B; Table 10). Plants were selected for homozygosity. DNA was extracted from these plants and a PCR reaction was performed using primers targeting the Hygromycin B resistance gene. The gene was confirmed to be present in the EV214 and GUS controls and *LEA5*-YFP lines, 4.1, 10.1, and 11.2 (Figure 6-3). Seeds from all lines were sown on to soil and grown until maturity at the James Hutton Institute, Dundee, for seed production. The phenotypes of these plants were analysed (data not shown). T₃ seeds were harvested from these plants.

Subsequently, seeds of WT, EV, GUS, and three T₃ lines expressing *LEA5*-YFP were sown on to ½ MS media containing 50 mg/ml Hygromycin B to select for transgenic plants. No WT plants were resistant to Hygromycin B. All of the EV and GUS control plants, and all of the plants from transgenic lines, 4.1.2, 10.1.1, and 11.2.2, were resistant to Hygromycin B (Table 11). DNA was extracted from these plants and a PCR reaction using primers targeting the *LEA5*-YFP sequence (Table 1) was performed to confirm the gene was present (Figure 6-4).

T₁ callus

1	2	3	4	5	6	7	8	9	10	11	12
13	14	15	16	17	18	19	20	21	22	23	24
25	26	27	28	29	30	31	32	33	34	35	36

T₂



T₃

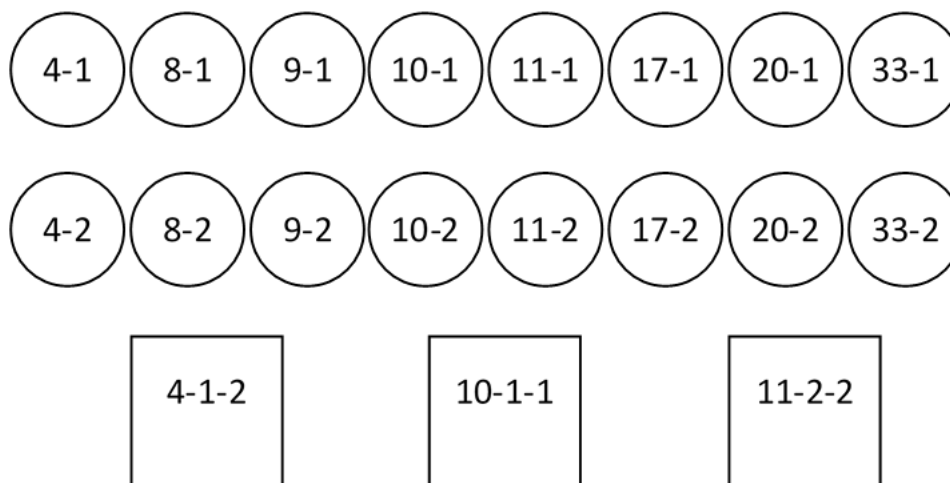


Figure 6-1: The naming policy for the selection of transgenic barley plants from callus.

Seeds are shown in circles and plants are shown in squares.

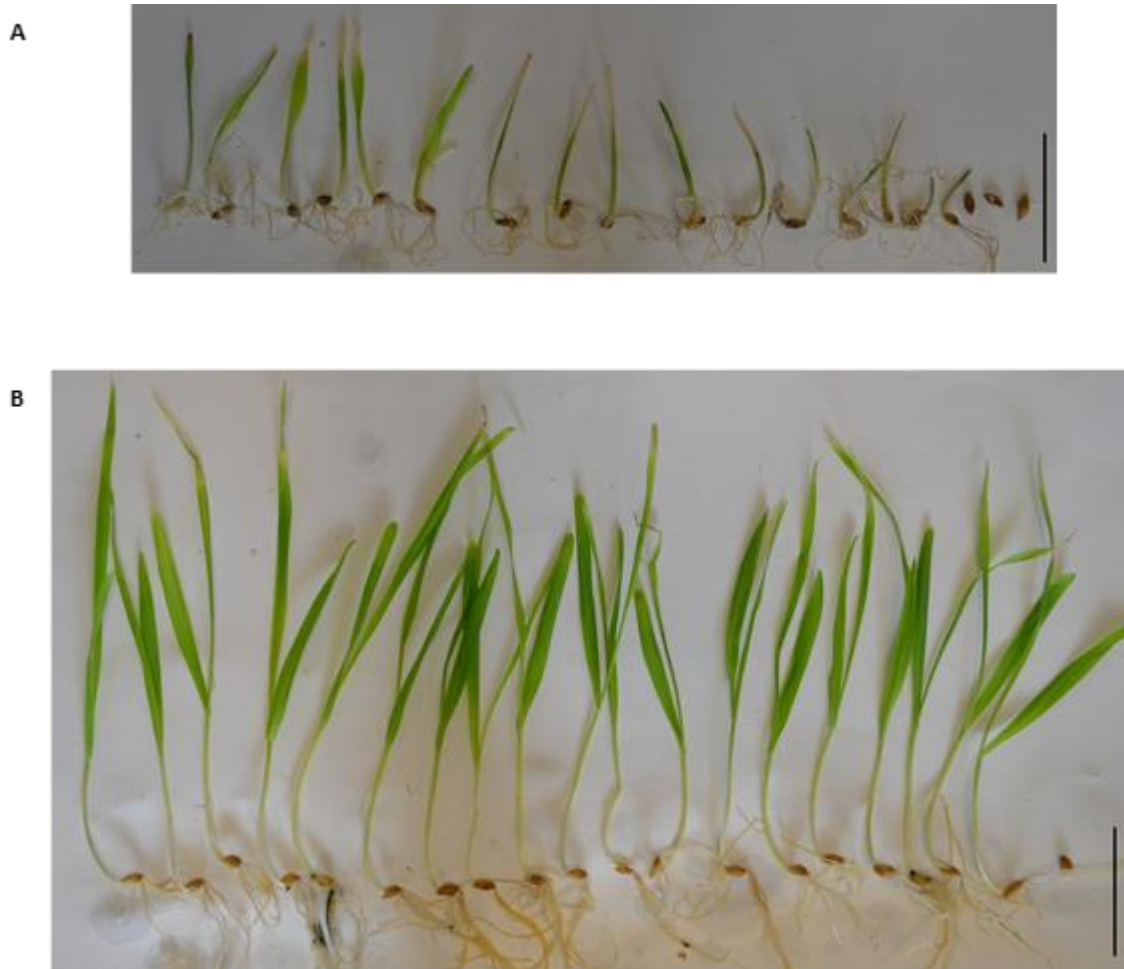


Figure 6-2: Segregation analysis.

A: WT barley plants with inhibited growth in the presence of Hygromycin B.

B: Transgenic barley plants that express *LEA5-YFP* (line 11.2.2) and have a Hygromycin B resistance gene presenting uninhibited growth in the presence of this antibiotic. The scale bar represents 5 cm.

Table 10: Segregation analysis of T₂ plants

Genotype	No germination	Sensitive	Resistant	% resistant	% germinated
WT	4	16	0	0.0	80.0
EV214 13.1	0	0	20	100.0	100.0
pBGUS 13.1	1	0	19	100.0	95.0
<i>LEA5-YFP</i> line 4.1	0	1	19	95.0	100.0
<i>LEA5-YFP</i> line 8.1	0	6	14	70.0	100.0
<i>LEA5-YFP</i> line 9.1	1	6	13	68.4	95.0
<i>LEA5-YFP</i> line 10.1	1	0	19	100.0	95.0
<i>LEA5-YFP</i> line 11.2	1	0	19	100.0	95.0
<i>LEA5-YFP</i> line 17.1	1	4	15	78.9	95.0
<i>LEA5-YFP</i> line 17.2	0	4	16	80.0	100.0
<i>LEA5-YFP</i> line 20.1	4	3	13	81.3	80.0
<i>LEA5-YFP</i> line 33.1	0	6	14	70.0	100.0

Table 11: Segregation analysis of T₃ plants

Genotype	No germination	Sensitive	Resistant	% resistant	% germinated
WT	1	19	0	0.0	95.0
EV214 13.1.1	0	0	20	100.0	100.0
pBGUS 13.1.1	11	0	9	100.0	45.0
<i>LEA5-YFP</i> line 4.1.2	17	0	3	100.0	15.0
<i>LEA5-YFP</i> line 10.1.1	7	0	13	100.0	65.0
<i>LEA5-YFP</i> line 11.2.2	8	0	12	100.0	60.0

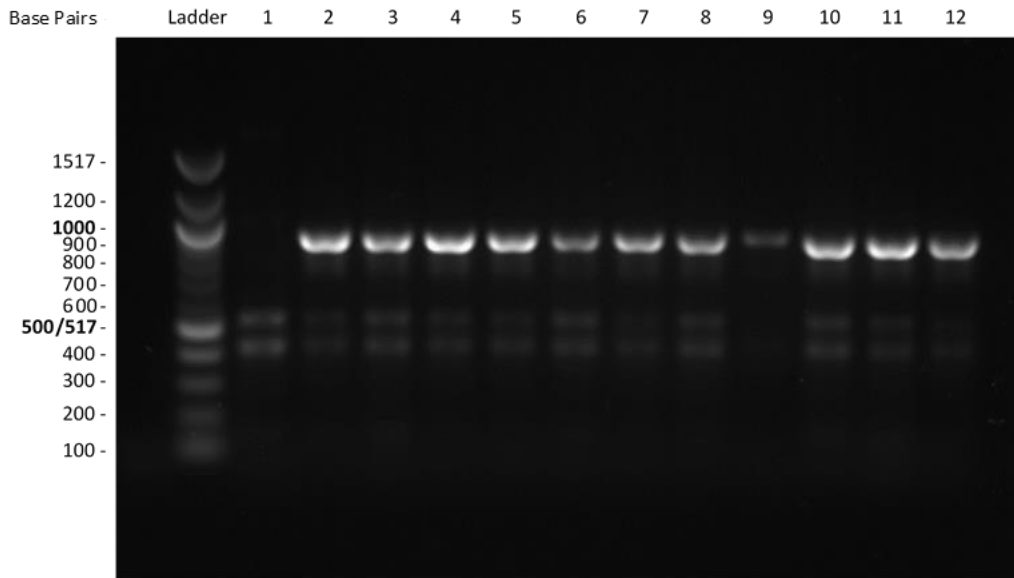


Figure 6-3: PCR genotyping of T₂ transgenic barley plants.

DNA was extracted from the leaves of WT, EV and GUS control plants as well as 9 independently transformed T₂ barley lines. A PCR using primers that amplify the Hygromycin B resistance gene was used to identify transgenic Barley. The ladder is Thermo Scientific GeneRuler 1 kb Plus DNA Ladder. Lane 1: WT, lane 2: EV214, lane 3: GUS, lane 4: LEA5-YFP line 4.1, lane 5: LEA5-YFP line 8.1, lane 6: LEA5-YFP line 9.1, lane 7: LEA5-YFP line 10.1, lane 8: LEA5-YFP line 11.2, lane 9: LEA5-YFP line 17.1, lane 10: LEA5-YFP line 17.2, lane 11: LEA5-YFP line 20.1, lane 12: LEA5-YFP line 33.1.

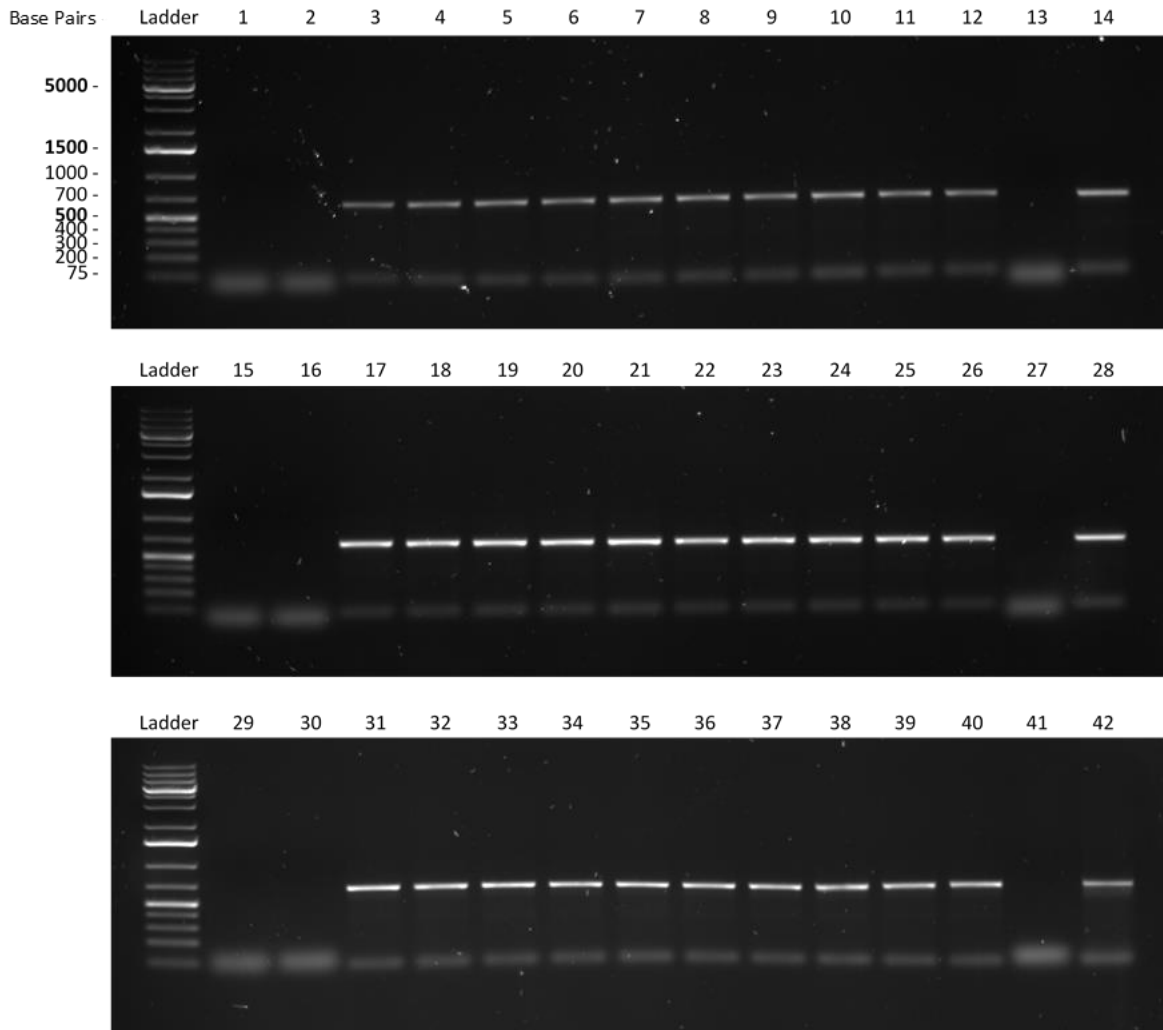


Figure 6-4: PCR genotyping of T₃ transgenic barley plants.

DNA was extracted from the leaves of WT and EV control plants as well as 3 independently transformed T₃ barley lines expressing LEA5. A PCR using primers that amplify the LEA5-YFP was used to identify transgenic Barley. The ladder is Thermo Scientific GeneRuler 1 kb Plus DNA Ladder. Lane 1: WT, lane 2: EV214, lanes 3-12: LEA5-YFP line 4.1.2, lane 13: Non-template control, lane 14: positive control. Lane 15: WT, lane 16: EV214, lanes 17-26: LEA5-YFP line 10.1.1, lane 27: Non-template control, lane 28: positive control. Lane 29: WT, lane 30: EV214, lanes 31-40: LEA5-YFP line 11.2.2, lane 41: Non-template control, lane 42: positive control.

6.2.2. Shoot phenotypes

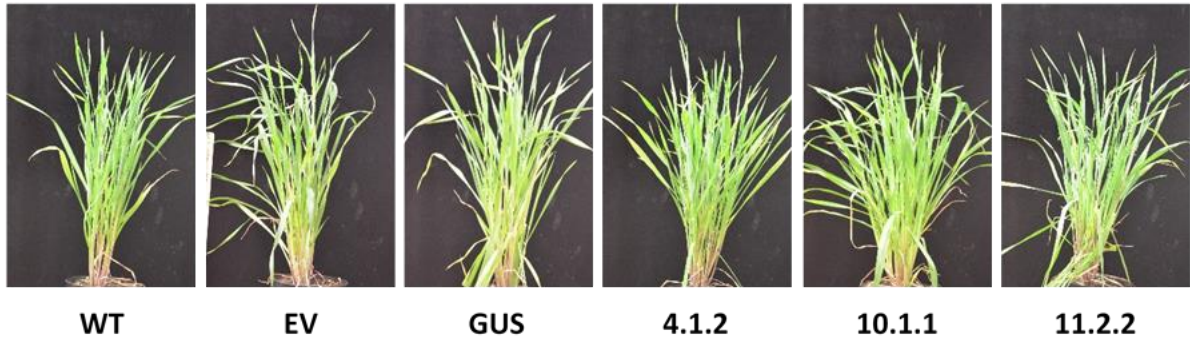
In the following study, the shoot growth of transgenic barley that expressed *LEA5-YFP* was compared to WT plants to characterise the effects of *LEA5* expression in barley. In addition, EV, and GUS control plants were also compared to WT plants. Measurements were taken each week for 8 weeks and then again on week 25. Representative shoot phenotypes of the different lines at week 8 are shown in Figure 6-5 A. Although the shoot phenotypes are visually similar in all lines, analysis revealed that after 8 weeks, *LEA5-YFP* line 11.2.2 had 96 leaves which was significantly more than WT plants which had 81 leaves ($P < 0.05$; Figure 5 B).

The plants were grown to produce seed and then dried in the controlled environment. Further measurements were taken on the 25th week; a few weeks after the plants had begun to turn brown. All lines were visually similar at week 25 (Figure 6-6 A). The dry shoot weight (without tillers) of *LEA5-YFP* expressing line 11.2.2 was significantly greater than WT plants ($P = 0.02$; Figure 6-6 B). However, there were no significant differences in total dry shoot weights (including tillers) between any of the *LEA5-YFP* expressing lines and WT plants (Figure 6-6 C).

LEA5-YFP line 4.1.2 produced an average of 32 tillers (Figure 6-6 D). This was significantly more tillers than WT plants which produced an average of 21 ($P = 0.025$; Figure 6-6 D). However, whilst not significant, the average weight of tillers produced by *LEA5-YFP* line 4.1.2 was 0.5 g which is noticeably less than WT plants which produced tillers with an average weight of 0.8 g (Figure 6-6 E). There was no significant difference in the number of tillers or the average tiller weight between WT plants and either *LEA5-YFP* line 10.1.1 or 11.2.2 (Figure 6-6 D & E).

At no point during the experiment was there a significant difference in the QY between any of the lines (data not shown).

A



B

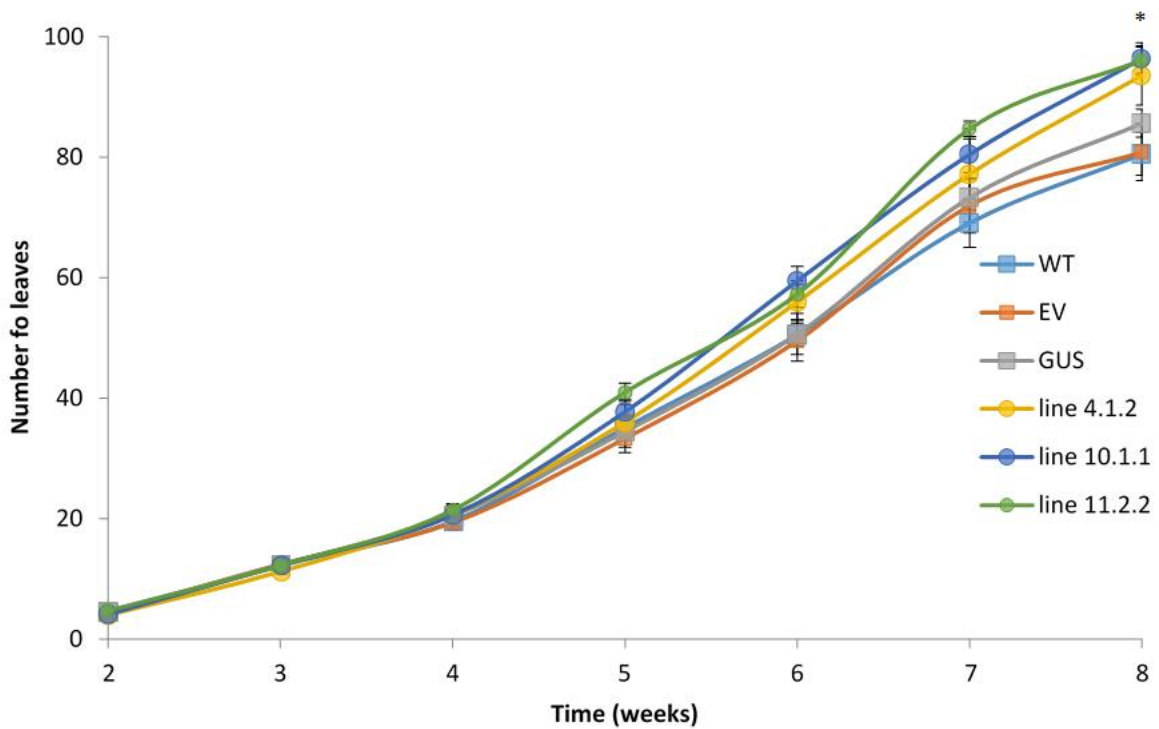


Figure 6-5: The effects of *LEA5* expression on the phenotype of barley plants.

Plants were grown under $400 \mu\text{mol}\cdot\text{m}^{-2}\cdot\text{s}^{-1}$ irradiance with a 16 hour photoperiod at $22^\circ\text{C} \pm 2^\circ\text{C}$. **A:** Representative phenotypes of WT and *LEA5-YFP* expressing plants. Scale bar represents 5cm. **B:** The number of leaves of control and *LEA5* expressing barley plants. Error bars represent mean \pm standard error. The asterisks indicate significant differences (* $P < 0.05$; ANOVA). $N=10$.

A

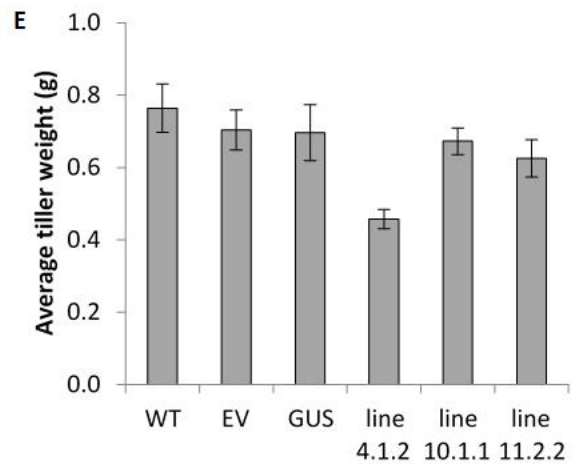
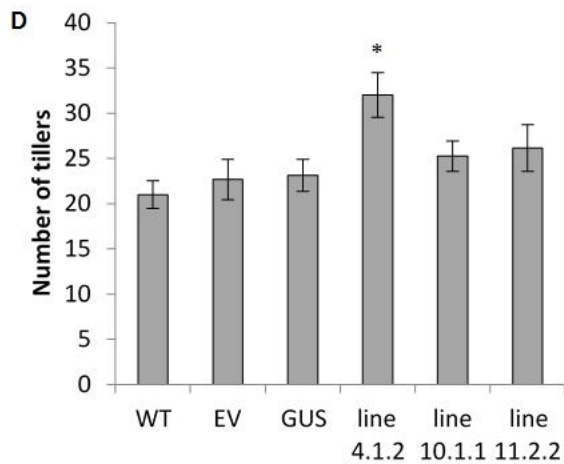
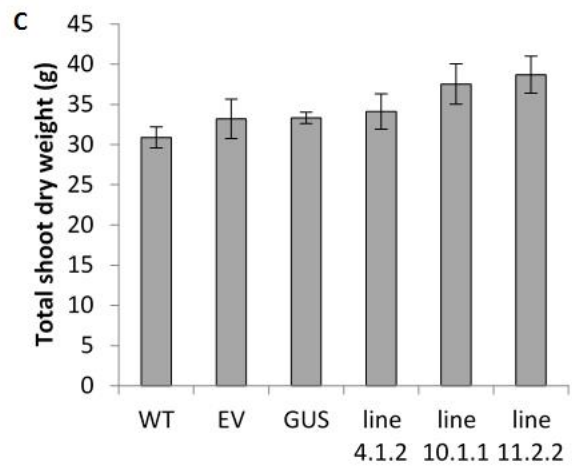
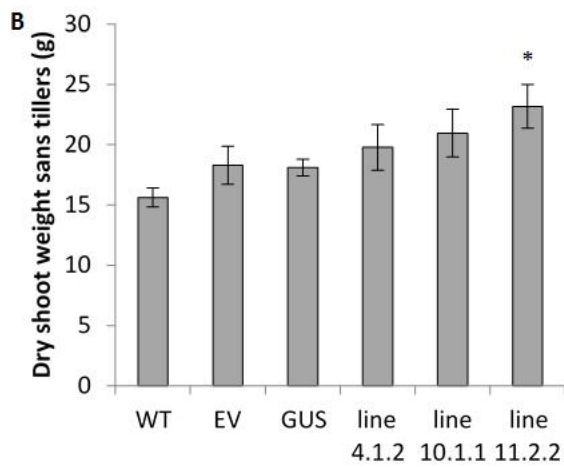
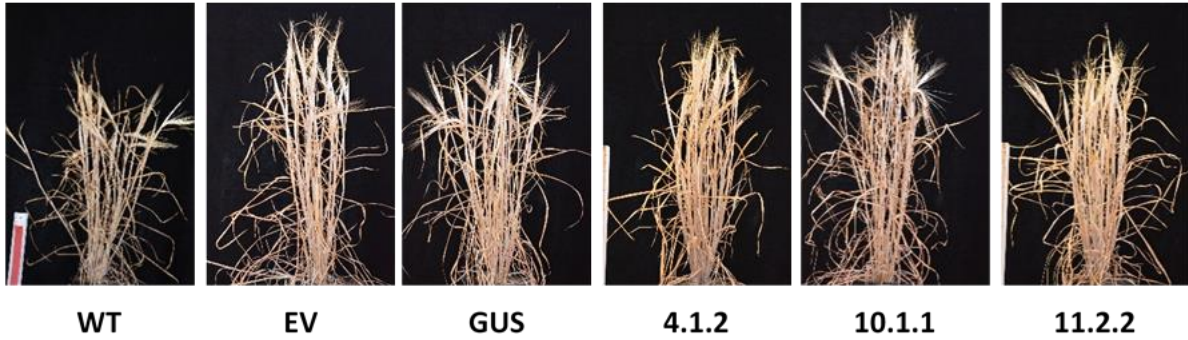


Figure 6-6: The effects of *LEA5* expression on the phenotype of barley plants.

Plants were grown under $400 \mu\text{mol}\cdot\text{m}^{-2}\cdot\text{s}^{-1}$ irradiance with a 16 hour photoperiod at $22^\circ\text{C} \pm 2^\circ\text{C}$. **A:** Representative phenotypes of WT and *LEA5-YFP* expressing plants. Scale bar represents 5cm. **B:** Dry weight (g) of shoot material without tillers. **C:** Total dry weight (g) of shoot material. **D:** Number of tillers. **E:** Average tiller weight (g). Error bars represent mean \pm standard error. The asterisks indicate significant differences (* $P < 0.05$; ANOVA). $N = 10$.

6.3. Discussion

The data described in this chapter demonstrate that transgenic homozygous lines transformed with *LEA5-YFP* can result in an altered shoot phenotype compared to WT barley plants. This was shown in two lines (4.1.2 and 11.2.2). This finding provides insight into the role of *LEA5* in plant growth.

Previous studies using transgenic *A. thaliana* found that the over-expression of *LEA5* resulted in plants with a greater biomass [43, 51]. The data presented here reflect results published by Mowla *et al.*, 2006 [43] and Mohd Salleh *et al.*, 2012 [51], albeit more subtly. Homozygous transgenic barley plants transformed with *LEA5-YFP* had significantly more biomass than WT plants in line 11.2.2. Furthermore, presence of the *LEA5-YFP* transgene resulted in *LEA5-YFP* line 11.2.2 resulted in those plants having significantly more leaves after 8 weeks than WT plants. Notably, the presence of the *LEA5-YFP* transgene in line 4.1.2 resulted in the production of significantly more tillers, however these tillers weighed less than those of WT plants. These findings support the view held previously that *LEA5* affects the growth of plants [43, 51].

The production of homozygous transgenic barley plants is a considerable feat. The analysis of barley plants transformed with *LEA5-YFP* under a range of biotic and abiotic stresses will allow the exploration of bestowed stress tolerance by *LEA5*. *LEA* proteins have been frequently been associated with providing protective functions [3, 4]. Some, for example, provide protections in dehydrated tissues, where they are thought to act as chaperones, protecting other proteins from aggregation or desiccation [13]. A reasonable starting point for further study of *LEA5* would be to investigate tolerance of these plants to H_2O_2 it has been shown to be upregulated by oxidants and provide tolerance to H_2O_2 [43]. Earlier studies also reported that *LEA5* is localised to the mitochondrial matrix [44, 51]. The inclusion of YFP, fused to *LEA5*, in these transgenic plants will allow confocal microscopy experiments to determine the cellular localisation of *LEA5* in barley. Moreover, *LEA5* was found to be involved in the control of root architecture [43, 51], and so the analysis of the effects of *LEA5* on barley roots could also provide further insights. Transferring results such as increased biomass, stress tolerance, and altered root structures into a crop species such as barley could have a major effect in the agriculture industry and be of substantial interest for biotechnology companies [1].

In the next chapter, the phenotype of *A. thaliana erf109* mutants is characterised in the absence and presence of different abiotic stresses to gain greater insights into the role of *ERF109* in plant development and in responses to abiotic stresses.

Chapter 7. Characterisation of phenotype of *Arabidopsis thaliana erf109* mutant plants

7.1. Introduction

Key processes in growth and development are regulated by the redox environment of the cell [148, 149]. *ERF109* (At4g43310), which is also known as *Redox Responsive Transcription Factor 1*, is part of a regulatory network that has a major role in the adjustment of *A. thaliana* leaves to reach homeostasis after high-light stress [156]. Transcripts of *ERF109* accumulate in leaves that are directly exposed to high-light, the extent to which depends on the intensity of light that the leaves are exposed to [157]. Furthermore, systemic signalling from leaves exposed directly to high-light results in the accumulation of *ERF109* transcripts in leaves that have not experienced high-light [158]. Exposure of leaves to high-light results in the production of singlet oxygen ($^1\text{O}_2$) due to energy transfer reactions from the excited triplet state of chlorophyll molecules or their precursors to molecular oxygen [159, 160]. *ERF109* expression is induced by singlet oxygen [161]. Moreover, singlet oxygen-dependent activation of JA and oxylipin signalling pathways may also be important in the activation of *ERF109* expression in systemic leaves [161]. The application of paraquat and inhibition of antioxidant enzymes by aminotriazole have also been found to induce *ERF109* expression [219].

Much of the current understanding of the functions of *ERF109* comes from the analysis of *A. thaliana erf109* mutants. These mutants have a markedly different phenotype when grown under high-light for two weeks as the leaves of WT plants appear visibly darker than those of *erf109* mutants [157]. Under these conditions, the total chlorophyll, chlorophyll *a/b* ratios, and the ratios of carotenoid pigments to chlorophyll were similar in both genotypes [157]. Therefore, the visible difference in leaf colour was presumably because protective pigments such as anthocyanins accumulated in the WT but not in the *erf109* mutant leaves. A transcriptome analysis of the leaves of *erf109* mutant plants suggested an association between *ERF109* and *PAP1* (At1g56650) [156], a transcription factor involved in the regulation of anthocyanin biosynthesis. Furthermore, the increased photosensitivity observed in *erf109*

mutants could result from changes in secondary metabolism indicated by the microarray analysis [156]. The lack of functional *ERF109* restricted ROS accumulation in response to stress in mutant plants and conversely overexpression of *ERF109* resulted in an accumulation of ROS [162]. *ERF109* is therefore considered to propagate ROS accumulation in response to ROS-producing abiotic and biotic stress signals.

Transgenic plants overexpressing *ERF109* were impaired in root and shoot development [155, 162], and showed increased light sensitivity [162]. *ERF109* is expressed in low levels in roots [155] but transcripts are upregulated in response to JA [164]. *ERF109* was shown to mediate cross-talk between JA signalling and auxin biosynthesis in the regulation of lateral root formation in *A. thaliana* [155]. *ERF109* binds to the GCC-boxes in the promoters *ASA1* and *YUC2* [155] - two key enzymes in auxin biosynthesis [220-222]. The biosynthesis of auxin, transport of auxin and auxin dependent signalling processes all influence lateral root formation [223-227]. It is plausible that *ERF109* may function alongside a range of other hormones, e.g. auxin, to modulate plant stress responses. Indole-3-acetic acid (IAA) is the most abundant form of auxin natively occurring and functioning in plants [228]. IAA levels were elevated in the roots of *ERF109* overexpression lines relative to WT *A. thaliana* plants [155]. Conversely, IAA levels were reduced in *erf109* mutants. The response of most auxin/IAA genes to IAA is tissue specific and dose dependent [229]. An elevated auxin level within *Arabidopsis* roots increases the levels of auxin response factors (ARF) leading to the degradation of IAA and other auxins [230, 231]. The ARFs promote lateral root formation by activating plant-specific transcriptional regulators such as *LATERAL ORGAN BOUNDARIES-DOMAIN 16* (*At2g42430*) [232]. In contrast to the increased levels of auxins in root tissues, the relative expression levels of *IAA14* and *IAA19* were lower in the shoot tissues of *ERF109* overexpression lines, however there was no difference between *erf109* mutants and WT plants [155]. One explanation for this is that the steady-state mRNA accumulation of auxin/IAA inducible genes may have been inhibited by the constitutively elevated IAA levels in *ERF109* overexpressors, which could have resulted in a different response to what is usually observed from short-term exogenous IAA treatments.

While excellent research into the role of *ERF109* has been performed, its role in the regulation of root and shoot growth has not been fully characterised. The aim of the studies described in this chapter was to characterise the phenotype of *erf109* mutants in the absence and presence of different abiotic stresses to gain greater insights into the role of *ERF109* in plant development and in responses to abiotic stresses.

7.2. Results - Shoot phenotype

7.2.1. Rosette growth in the absence of stress

An *in vitro* phenotyping approach was undertaken to assess the rosette growth of *erf109* mutants. In the absence of stress the WT and *erf109* mutant plants had visibly similar rosettes (Figure 7-1 A). However, digital analysis revealed that the *erf109* mutants had a significantly increased rosette area compared to WT controls after 2 weeks of growth, with WT plants having a mean rosette area of 32.5 mm² while *erf109* mutant plants had a mean rosette area of 34.5 mm² (Figure 7-1 B; P=0.012). Three-week-old WT plants had an average rosette area of 73.8 mm² while the mean rosette area of *erf109* mutants was significantly larger at 79.3 mm² (Figure 7-1 B & C; P=0.003).

7.2.2. Rosette growth in the presence of stress

Rosette growth in the presence of drought, salt and osmotic stress

The same phenotyping approach was used to determine the stress tolerance of *erf109* mutants, as reflected by rosette area. In these experiments, control plates (i.e. the absence of stress) contained ½ MS media alone. Stress conditions were achieved by the inclusion of either sodium chloride (75 mM; salt), mannitol (50 mM; drought), or sorbitol (100 mM; osmotic stress) in the media. A total of 360 plants per genotype were sown in each condition for these experiments - a total of 2880 plants. In all cases, at least 98% of seeds sown germinated.

The rosette area of both the WT and *erf109* mutant plants were visibly smaller when grown in the stress conditions than in the control condition (Figure 7-1 A). After 3 weeks growth in the presence of mannitol, WT plants had a mean rosette area of 35.2 mm² while *erf109* plants had a mean rosette area of 36.9 cm² (Figure 7-1 C). Similarly, after 3 weeks growth in the presence of salt, the mean rosette area of WT plants was 27 mm² while *erf109* was 26.2 mm² (Figure 7-1 C). However, when grown on media containing sorbitol, the average rosette area of *erf109* plants was 54% of the size of those grown in the absence of stress at 43mm². This was significantly larger than WT plants which had an average rosette area 51% of the size of control plants at 37.4 mm² (Figure 7-1 C; P=0.002).

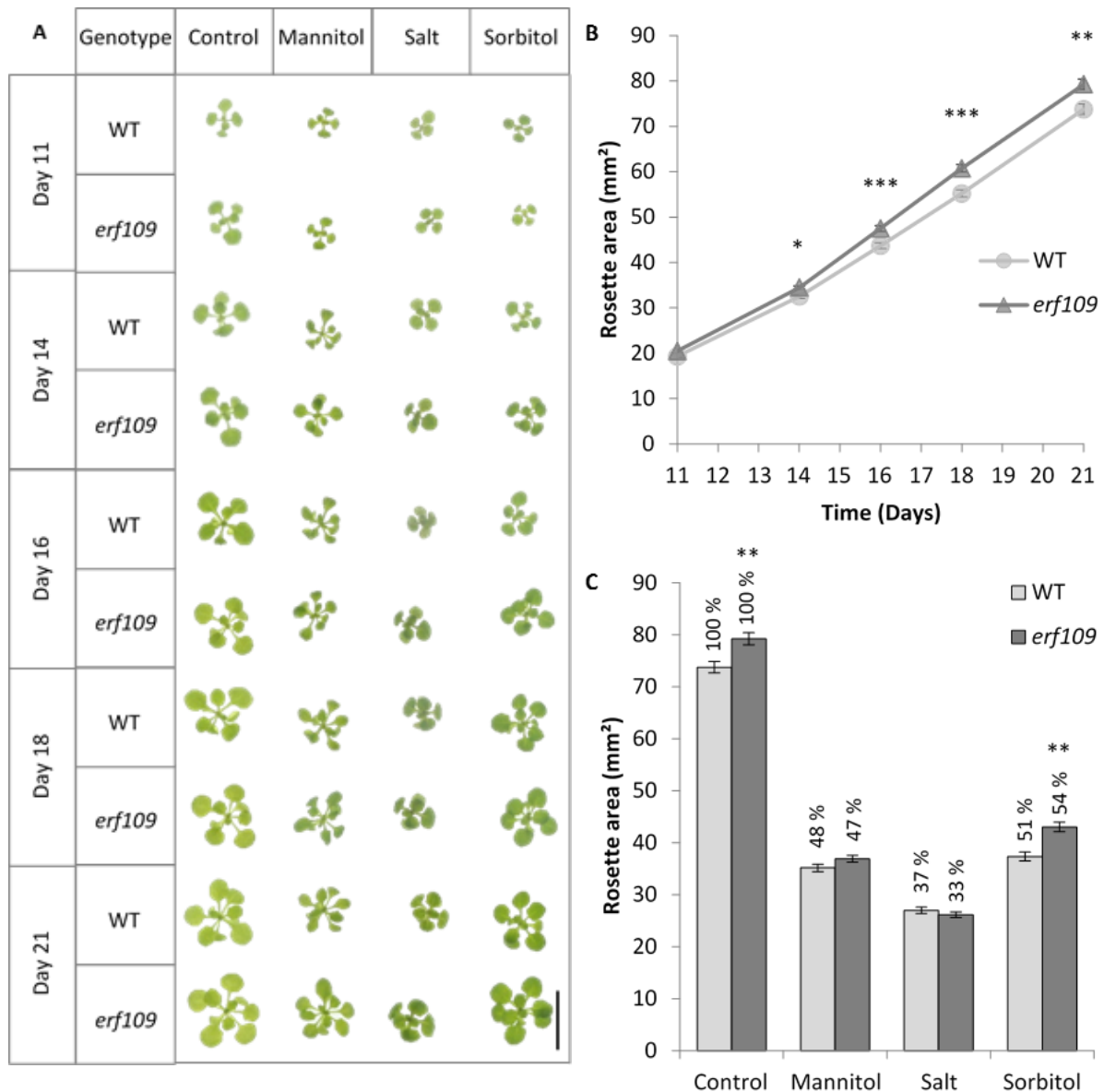


Figure 7-1: The effects of abiotic stress treatments (mannitol, salt, and sorbitol) on the rosette area of wild-type (WT) *A. thaliana* and *erf109* mutants in comparison to plants grown in the absence of stress (control).

Plants were grown under $150 \mu\text{mol}\cdot\text{m}^{-2}\cdot\text{s}^{-1}$ irradiance with a 16 hour photoperiod at $22^\circ\text{C} \pm 2^\circ\text{C}$ for 21 days, either in the absence of stress (control) or presence of abiotic stress caused by inclusion of 50 mM mannitol, 75 mM salt (NaCl) or 100 mM sorbitol to the growth media. A: Phenotypes of WT and *erf109* plants. Scale bar represents 10 mm. B: Rosette area (mm^2) with time for WT and *erf109* plants in the absence of stress. C: Rosette area (mm^2) of WT and *erf109* plants at the end of the experiment (day 21). Error bars represent means \pm standard errors. The asterisks indicate significant differences to WT (* $P < 0.05$, ** $P < 0.01$, *** $P < 0.001$; ANOVA). $N = 360$.

Rosette growth of plants grown on soil in the absence and presence of drought stress

One week old seedlings, germinated on ½ MS media, were grown on soil for 9 weeks. Drought stress was imposed at 5 weeks by withholding water for two weeks to determine the stress tolerance of *erf109* mutants.

The rosette area, number of leaves, and the biomass were similar between the WT and *erf109* mutant plants that were grown in the absence of stress (control). Eight-week-old WT plants had a mean rosette area of 78.6 cm² (Figure 7-2 A), an average of 33.8 leaves (Figure 7-2 B), and mean a dry-weight of 447 mg (Figure 7-2 C), while *erf109* mutants had a mean rosette area of 85.9 cm² (Figure 7-2 A), an average 37.3 leaves (Figure 7-2 B), and a mean dry-weight of 631mg (Figure 7-2 C).

Plants exposed to drought were significantly smaller in terms of rosette area, and biomass (dry-weight) than water replete controls: 8-week-old drought-stressed WT plants had a mean rosette area that was just 64% (50.6 cm²) of the water-replete controls (Figure 7-2 A), with a lower average dry-weight of 219 mg (Figure 7-2 C). However, there was no significant difference in the number of leaves between drought-stressed and water-replete WT plants (Figure 7-2 B). The effects of the drought treatment on the rosette growth of the *erf109* mutants was similar to WT plants, except that the *erf109* mutants also had significantly fewer leaves than their water-replete counterparts. After two weeks exposed to drought, 8-week-old *erf109* mutants had a significantly smaller rosette area (57.1 mm²; Figure 7-2 A), had fewer leaves (34.5 leaves; Figure 7-2 B), and weighed significantly less with a dry-weight of 226mg (Figure 7-2 C) than water-replete *erf109* mutants. However, there were no significant differences in the total rosette area, number of leaves or dry-weight between drought-stressed WT and *erf109* plants.

The light response curves for photosynthetic CO₂ assimilation were measured in the leaves of 4-week-old WT and *erf109* plants. In these experiments, 2-week-old plants were deprived of water for 14 days, and the light response curves were measured. In the absence of stress, the leaves of WT and *erf109* plants had similar light response curves (Figure 7-3 A). The drought treatment led to a decrease in soil water content of ~55% (Figure 7-3 B). This level of drought imposed at the seeding stage had a severe impact on photosynthesis. Photosynthetic CO₂ assimilation did not increase above the compensation point at any of the light levels used in either the WT or *erf109* mutant plants when drought-stressed (Figure 7-3 A)

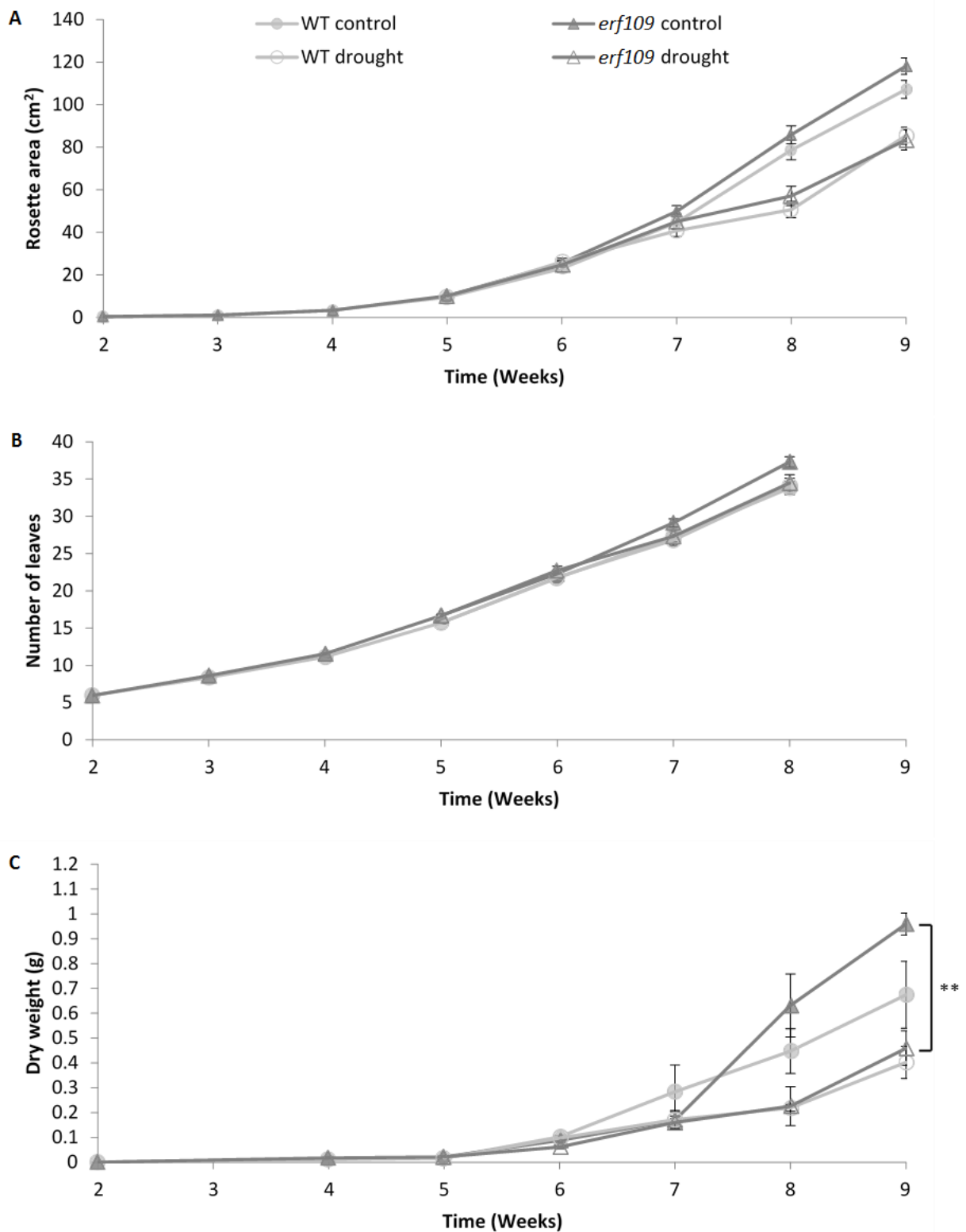


Figure 7-2: The effects of drought on the growth of wild-type (WT) *A. thaliana* and *erf109* mutant plants.

Plants were grown under $100 \mu\text{mol}\cdot\text{m}^{-2}\cdot\text{s}^{-1}$ irradiance with an 8 hour photoperiod, at $22^\circ\text{C} \pm 2^\circ\text{C}$. Water was withheld from plants in the drought treatment from week 5 and resumed at week 7. **A:** Total rosette area (cm^2), **B:** number of leaves, and, **C:** dry weight (g). Error bars represent means \pm standard errors. The asterisks indicate significant differences to WT plants (** $P < 0.01$; ANOVA). $N = 20$.

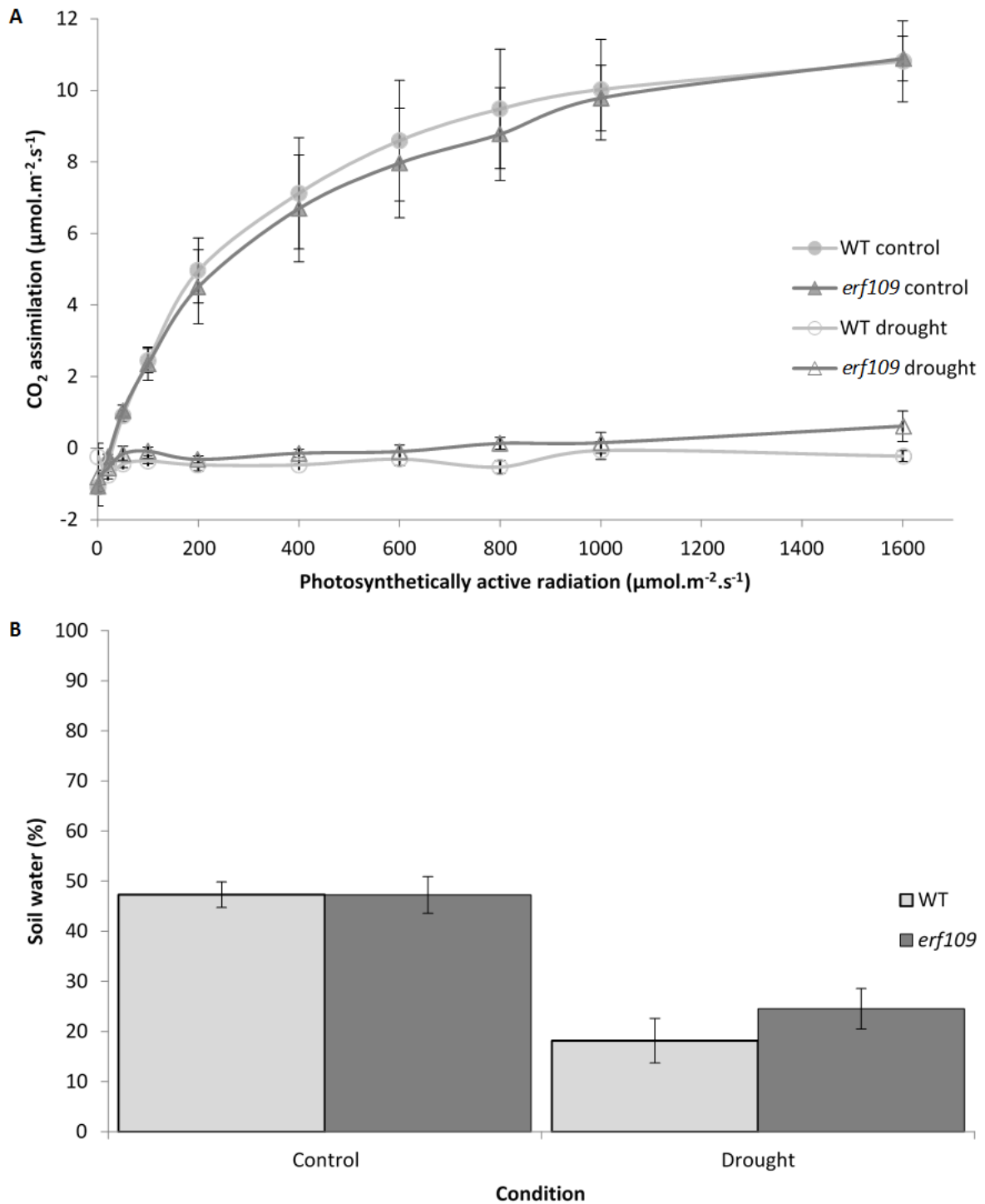


Figure 7-3: Photosynthetic CO₂ assimilation of 4-week-old wild-type (WT) *A. thaliana* and *erf109* mutant plants in optimal and restricted watering regimes.

A: Photosynthetic CO₂ assimilation, measured using a LI-COR LI-6400XT Portable Photosynthesis System.

B: Soil water content. Error bars represent means +/- standard errors.

Rosette growth under high-light

The effects of high-light on rosette growth were also determined using the *in vitro* phenotyping approach. In these experiments, WT and *erf109* mutants were grown in standard conditions for 11 days, after which half were grown for a 10 days under high-light ($600 \mu\text{mol}\cdot\text{m}^{-2}\cdot\text{s}^{-1}$) while the rest remained in control conditions ($100 \mu\text{mol}\cdot\text{m}^{-2}\cdot\text{s}^{-1}$). A total of 960 plants were sown, with a germination rate of 98.8%. 948 plants were measured (480 WT and 468 *erf109* mutants).

Plants grown under high-light were visibly smaller than those grown in the control light condition (Figure 7-4 A). The WT plants had significantly smaller rosette areas when grown under high-light than those grown under control light conditions (Figure 7-4 B; $P < 0.05$). Under control light conditions, the WT plants had a mean rosette area of 102mm^2 after 21 days. The mean rosette area of WT plants grown under high-light were 88mm^2 , 14.3% the size of those grown in control conditions after 21 days. The mean rosette area of *erf109* mutants grown under high-light was 82mm^2 , significantly smaller than the rosettes of WT plants grown in the same conditions (Figure 7-4 B; $P < 0.01$).

Rosette growth in the presence of oxidants

The *in vitro* phenotyping approach was also used to determine the tolerance of *erf109* mutants to oxidative stress, as reflected by the rosette area. In these experiments, control plates contained $\frac{1}{2}$ MS media alone. Stress conditions were achieved by the inclusion of either $0.1 \mu\text{M}$ paraquat (Figure 7-5), or 0.1mM menadione (Figure 7-6) to the media. A total of 2160 plants were sown. The germination rate of both genotypes on control media and on media containing paraquat was $>98\%$. However, on menadione the germination rate of WT plants was 92% and *erf109* mutants was even lower at 52%.

In the absence of stress, the *erf109* mutants had a significantly larger rosette area than WT plants at the end of the experiment (Figure 7-5 B, & C; $P < 0.001$). The presence of paraquat resulted less rosette growth in both genotypes. However, at the end of the experiment, the *erf109* mutants had a mean rosette area of 34.9mm^2 ; significantly larger than WT plants that had a mean rosette area of 28.7mm^2 (Figure 7-5; $P < 0.001$). Like paraquat, menadione caused a significant decrease in the rosette area of both genotypes ($P < 0.001$; Figure 7-6). However, in the presence of menadione 21-day-old *erf109* mutants had a significantly smaller mean rosette area than WT plants ($P < 0.001$; Figure 7-6). After 3 weeks, the *erf109* mutants had a mean rosette area of 19.4mm^2 while WT plants were 45.4mm^2 (Figure 7-6 B & C; $P < 0.001$).

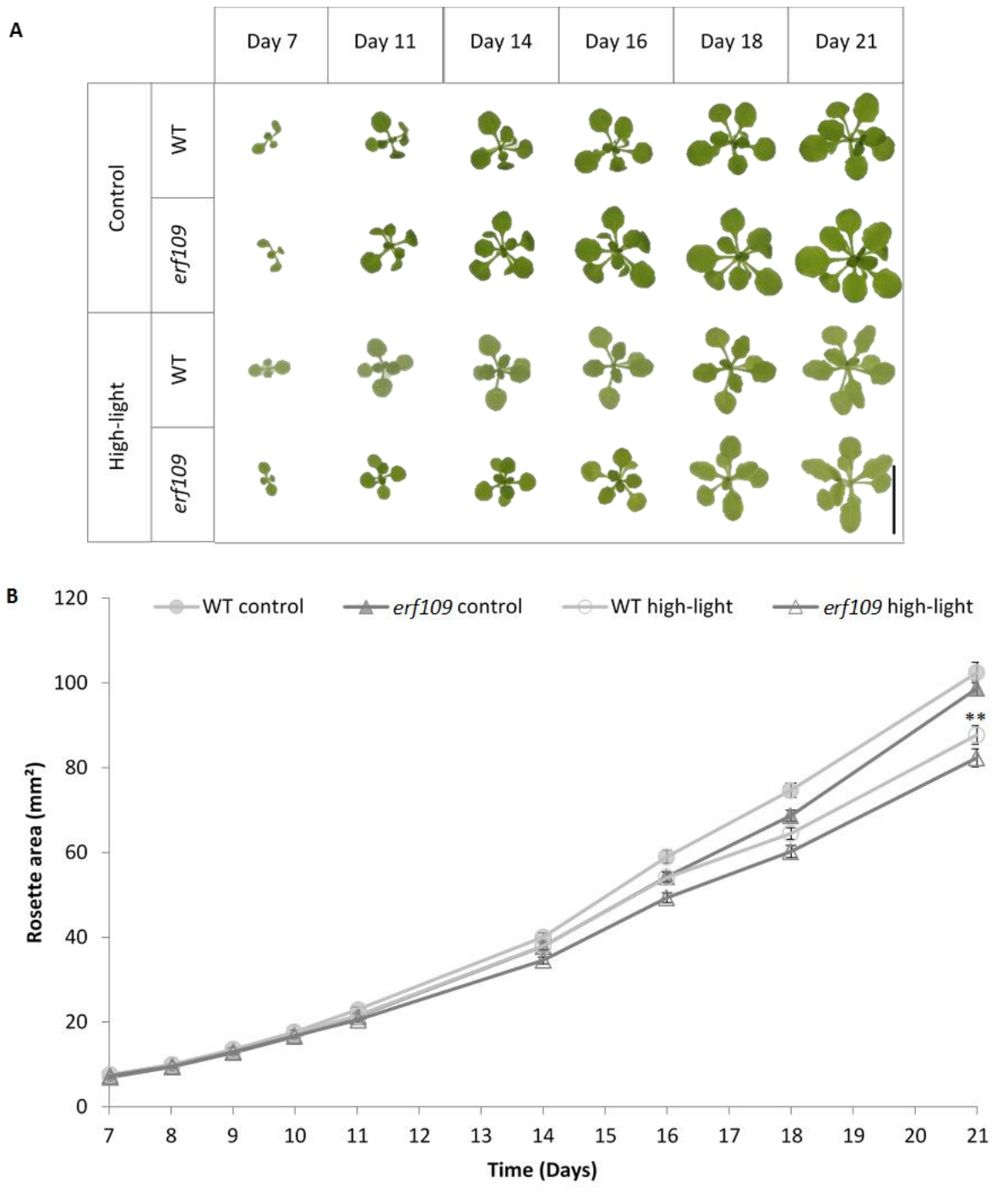


Figure 7-4: The rosette area of wild-type (WT) and *erf109* mutant plants grown under standard (control) light conditions for 11 days and then either under standard light conditions or high-light for 10 days.

Plants were grown for 11 days under $100 \mu\text{mol}\cdot\text{m}^{-2}\cdot\text{s}^{-1}$ irradiance with a 16 hour photoperiod, at which point half were grown under high-light ($600 \mu\text{mol}\cdot\text{m}^{-2}\cdot\text{s}^{-1}$) for the remaining 10 days. All plants were grown for 21 days at $22^\circ\text{C} \pm 2^\circ\text{C}$. Rosette areas were measured at 7, 8, 9, 10, 11, 14, 16, 18 and 21 days either in the standard (control) or high-light conditions. **A:** The phenotype of the WT and *erf109* mutant plants at 21 days. Scale bar represents 10 mm. **B:** Rosette areas (mm^2). Error bars represent means \pm standard errors. The asterisks indicate significant differences to WT plants (** $P < 0.01$; ANOVA). $N = 240$.

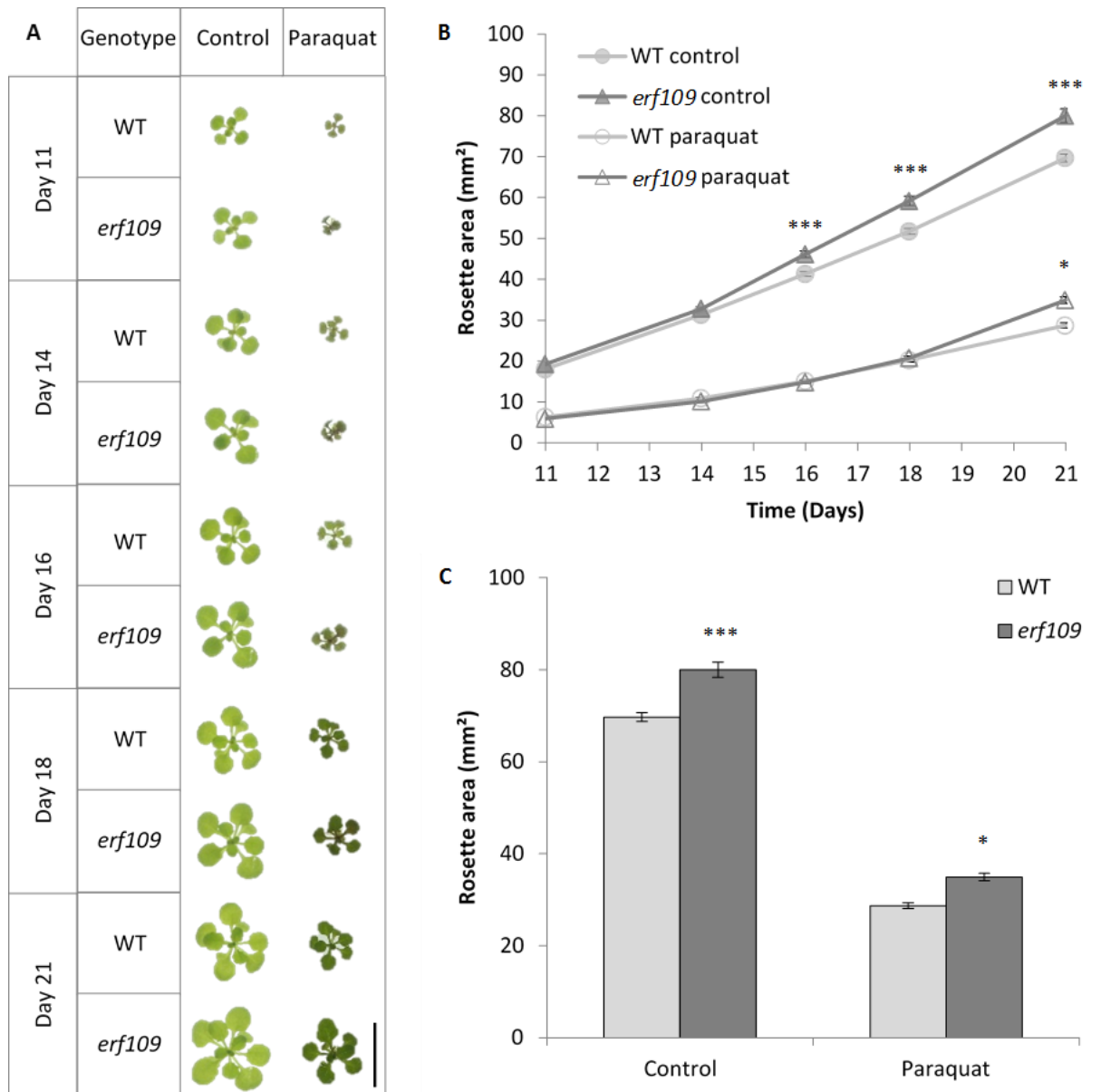


Figure 7-5: The effects of paraquat on rosette area on wild-type (WT) *A. thaliana* and *erf109* mutant plants.

Plants were grown under $150 \mu\text{mol}\cdot\text{m}^{-2}\cdot\text{s}^{-1}$ irradiance with a 16 hour photoperiod at $22^\circ\text{C} \pm 2^\circ\text{C}$ for 21 days, either in the absence (control) or presence of $0.1 \mu\text{M}$ paraquat. **A:** Phenotypes of WT and *erf109* plants. Scale bar represents 10 mm. **B:** Rosette area (mm^2) for WT (circles) and *erf109* mutant (triangles) plants grown in the control condition (shaded shapes) or with the addition of paraquat (non-shaded). **C:** Rosette areas (mm^2) of WT (light bars) and *erf109* mutant (dark bars) plants on day 21 in the conditions described. Error bars represent means \pm standard errors. The asterisks indicate significant differences to WT plants (* $P < 0.05$, *** $P < 0.001$; ANOVA). $N=360$.

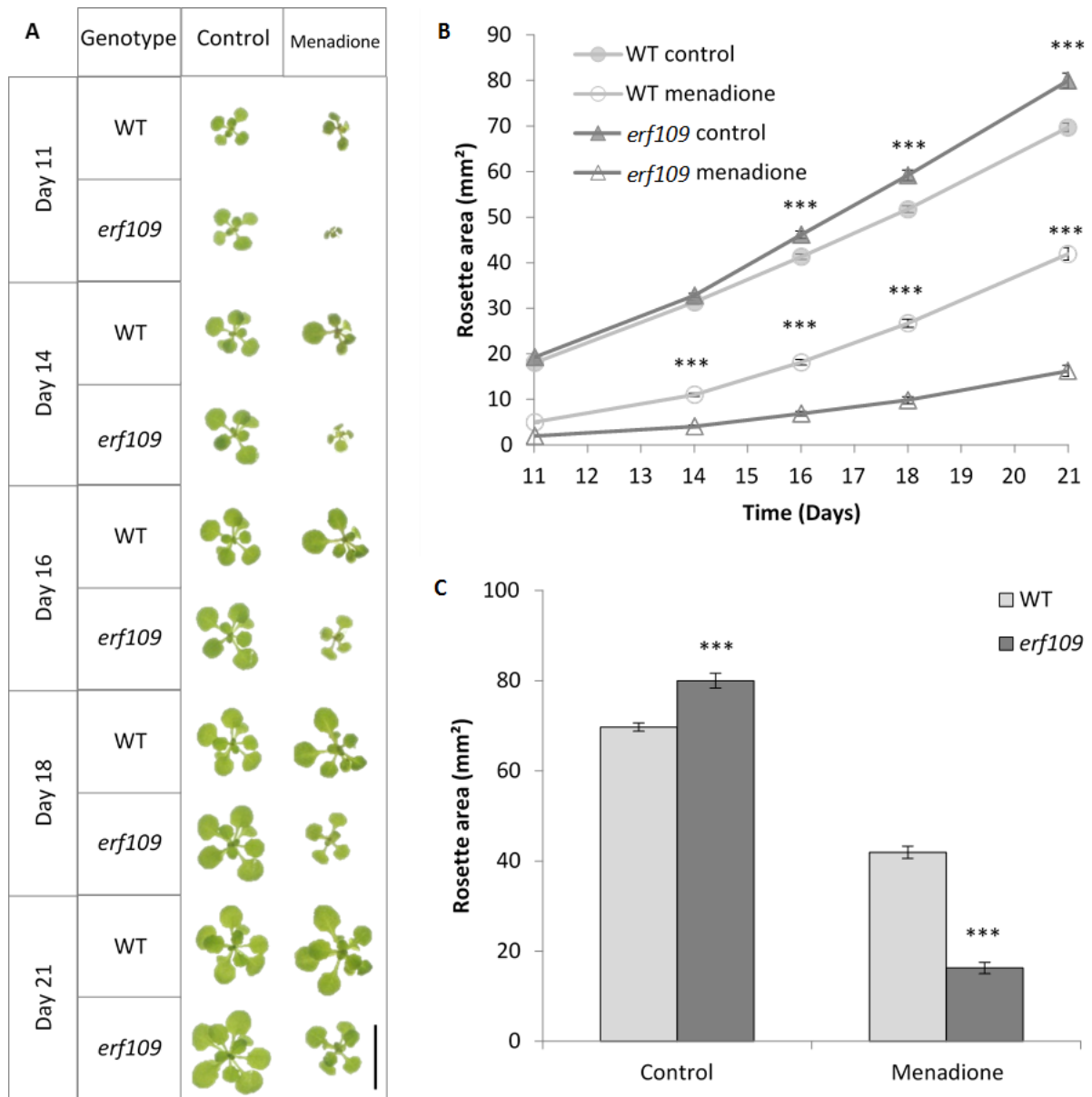


Figure 7-6: The effects of menadione on the rosette area of wild-type (WT) *A. thaliana* and *erf109* mutants.

Plants were grown under $150 \mu\text{mol}\cdot\text{m}^{-2}\cdot\text{s}^{-1}$ irradiance at $22^\circ\text{C} \pm 2^\circ\text{C}$. Rosette areas were measured at 11, 14, 16, 18 and 21 days either in the absence (control) or presence of 0.1 mM menadione. **A:** Phenotypes of WT and *erf109* plants. **B:** Rosette area (mm^2) for WT (squares) and *erf109* (circles) plants in the control condition (shaded shapes) and with the addition of menadione (non-shaded). **C:** Rosette area (mm^2) of WT (white bars) and *erf109* (grey bars) plants on day 21 in the conditions described. Error bars represent means \pm standard errors. The asterisks indicate significant differences to WT plants (***) $P < 0.001$; ANOVA). $N = 360$.

7.2.3. Anthocyanin content of leaves

To investigate the role of *ERF109* in the production of anthocyanins, plants were germinated on ½ MS and then grown on soil until they were 3-weeks-old under 100 $\mu\text{mol.m}^{-2}.\text{s}^{-1}$ irradiance (control). After three-weeks, half of the plants were transferred to a high-light environment (800 $\mu\text{mol.m}^{-2}.\text{s}^{-1}$) while the other half remained in the control condition. Plants were grown for a further 7 days, after which the leaves were harvested and analysed for anthocyanin contents.

In the control light conditions, the anthocyanin content of leaves was similar between both genotypes; WT plants accumulated 16 μg anthocyanin/g FW, while *erf109* mutants accumulated 19 μg anthocyanin/g FW. Growth for 7 days under high-light significantly increased the level of anthocyanins in WT plants (Figure 7-7: $P < 0.001$) but not *erf109* mutants when comparing to controls. Furthermore, the *erf109* mutant leaves accumulated significantly less anthocyanin than WT plants in the high-light conditions (Figure 7-7; $P < 0.001$). WT plants produced an average 124 μg anthocyanin/g FW while *erf109* mutants produced 31 μg anthocyanin/g FW.

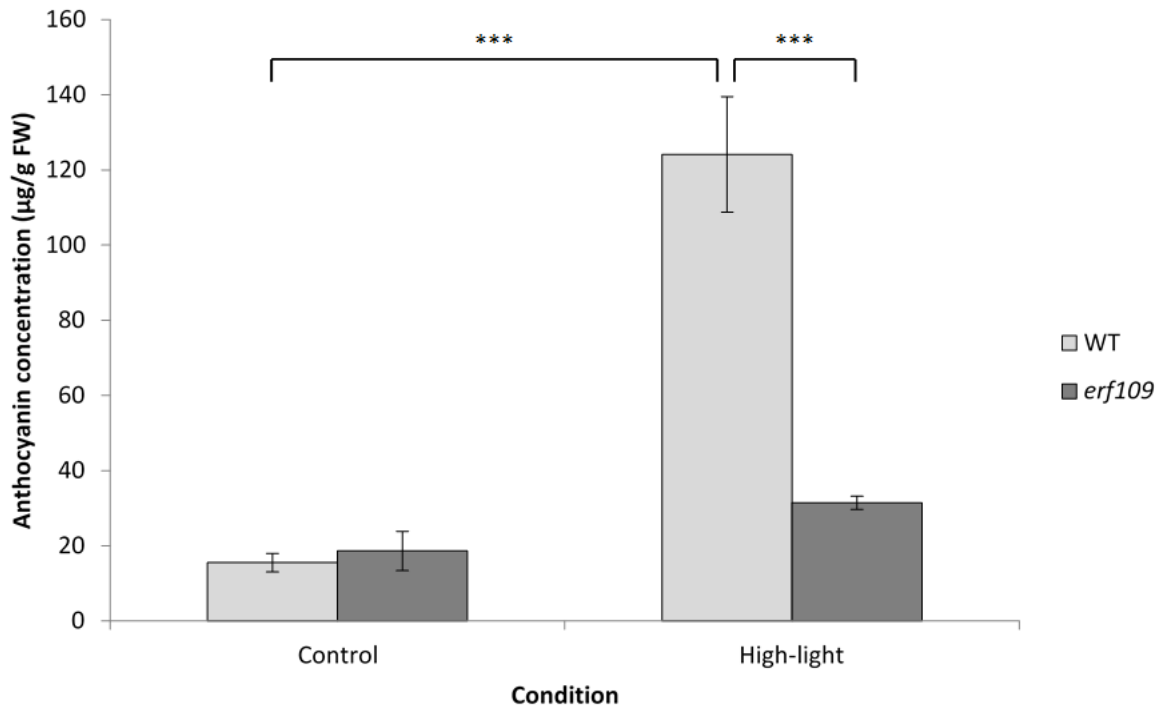


Figure 7-7: Anthocyanin concentration ($\mu\text{g/g FW}$) in 4-week-old wild-type (WT) *A. thaliana* and *erf109* mutant plants grown on soil under standard (control) light conditions for 3 weeks and then either under standard light conditions or high-light for 1 week.

Plants were grown for 3 weeks under standard (control) light irradiance ($100 \mu\text{mol}\cdot\text{m}^{-2}\cdot\text{s}^{-1}$) with a 16 hour photoperiod, then either under standard light conditions or high-light ($600 \mu\text{mol}\cdot\text{m}^{-2}\cdot\text{s}^{-1}$) for 1 week. All plants were grown at $22^\circ\text{C} \pm 2^\circ\text{C}$. Error bars represent means \pm standard errors. The asterisks indicate significant differences to WT plants (***) $P < 0.001$; ANOVA). $N=9$.

7.3. Results - Root phenotype

In these experiments, seeds of WT and *erf109* mutant plants were sown on to either ATS or ½ MS media within vertical plates. The roots grew along the surface of the media for 7 days, at which point the lengths of primary root were measured, the number of lateral roots were counted and lateral root densities were calculated (Figure 7-8).

The *erf109* mutants grown on ATS media for 7 days had significantly shorter primary roots than WT plants (Figure 7-8 A & B; P=0.046). The *erf109* mutant plants had a mean primary root length of 56.3 mm while the WT plants had a mean primary root length of 59.9 mm (Figure 7-8 B; P=0.046). However, there were no significant differences in the number of lateral roots (Figure 7-8 C) or the lateral root densities (Figure 7-8 D) between WT and *erf109* mutant plants.

Root phenotypes were also determined for plants grown on ½ MS media. In these experiments root architecture was determined for a total of 108 plants. There was no difference between WT and *erf109* mutant plants in the primary root length (Figure 7-9 A & B), the number of lateral roots (Figure 7-9 C), or the lateral root density (Figure 7-9 D) when grown on ½ MS media for 10 days.

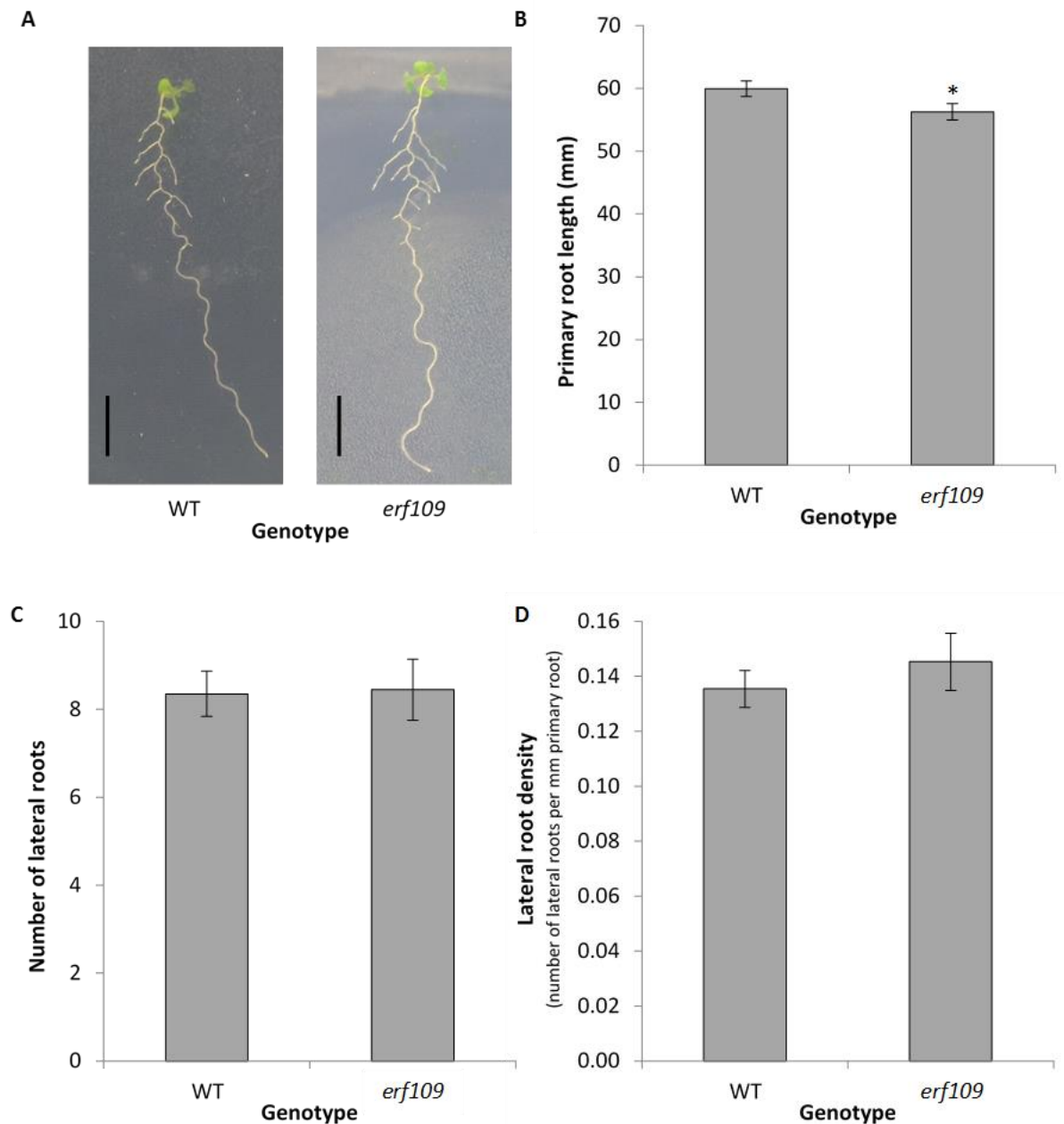


Figure 7-8: The root architecture of 7-day-old wild-type (WT) *A. thaliana* and *erf109* mutant plants.

A: The phenotype of 7-day-old WT and *erf109* mutant plants. Scale bar represents 10 mm. **B:** The primary root length (mm) of WT and *erf109* mutant plants. **C:** The number of lateral roots of WT and *erf109* mutant plants. **D:** The lateral root density (the number of lateral roots per mm primary root) of WT and *erf109* mutant plants. Error bars represent means +/- standard errors. The asterisks indicate significant differences (* $P < 0.05$; T-Test). $N > 30$.

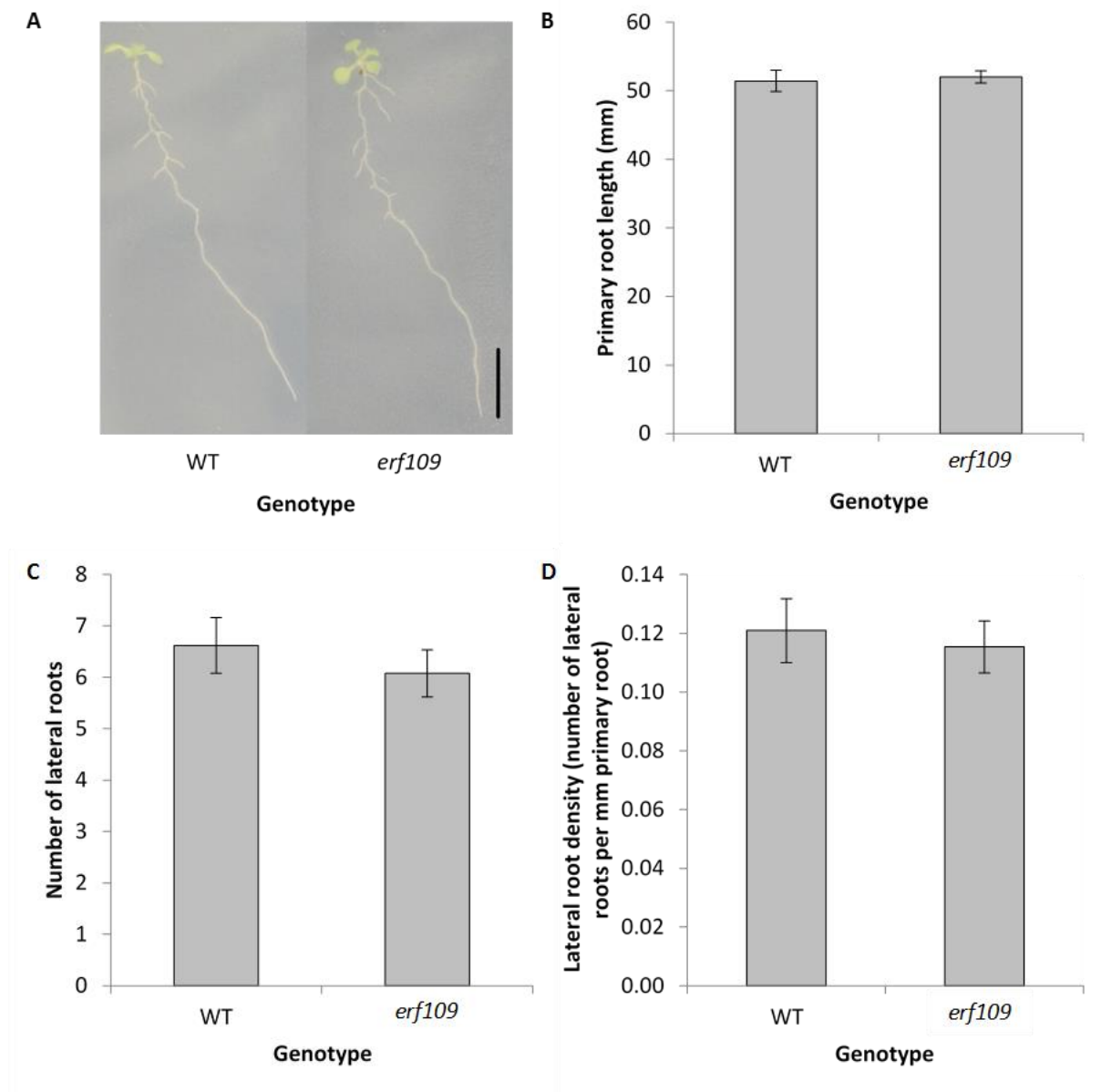


Figure 7-9: The root architecture in 10-day old wild-type (WT) and *erf109* mutant plants grown on ½ MS.

A: The phenotype of 10-day-old WT and *erf109* mutant plants. Scale bar represents 10 mm. **B:** Primary root length (mm). **C:** The number of lateral roots. **D:** The lateral root density (number of lateral roots per mm primary root). Error bars represent means +/- standard errors. N>30.

7.4. Discussion

The studies reported here suggest that *ERF109* has a role in the control of shoot growth in the absence of stress. Although the difference in rosette area between WT and *erf109* mutant plants was small (less than 10%), the *erf109* mutants tended to have a larger rosette area than the WT plants at the later stages of vegetative growth. It was previously shown that overexpression of *ERF109* led to altered leaf morphology, producing leaves that were longer, narrower and curled, similar to auxin overproduction phenotypes [155, 162]. Indeed plants which overexpress *ERF109* had significantly higher auxin levels in the shoot tissues than the WT plants [155]. Conversely, the levels of auxin were reduced in the shoots of *erf109* mutants [155]. The increased rosette area of the *erf109* mutants observed here could result from lower auxin levels. However, the leaf phenotype of the *erf109* mutants was similar to that of WT plants.

Previous studies have shown that by binding to GCC boxes in the promoters of target genes, such as *DREB2A*, ERFs are able to confer drought tolerance in *A. thaliana* [148, 152]. It has also been shown that overexpression *ERF107* enhances tolerance to salt stress [233]. However, the *erf109* mutants showed similar responses to drought stress as the WT plant, except when grown on media containing sorbitol (Figure 7-1). Further studies on soil did not reveal altered growth responses to drought stress, however, the drought-induced repression of growth was greater in the *erf109* mutants than WT plants (Figure 7-2).

The transcripts of *ERF109* are present in all tissues but accumulate in leaves as a result of high-light [158]. Both genotypes, WT and *erf109* mutants, had a similar high-light mediated repression of growth (Figure 7-4). However, the *erf109* mutants accumulated significantly less anthocyanin in their leaves than the WT plants under high-light conditions (Figure 7-7). It has previously been observed that *erf109* mutants do not present a visibly darker phenotype when grown under high-light as WT plants do [157], suggesting that protective pigments such as anthocyanins might not accumulate in the leaves of *erf109* mutant plants as they would in WT plants. The inability to accumulate anthocyanins in the *erf109* mutants explains the increased photosensitivity described previously by Khandelwal *et al.*, 2008 [156]. A leaf transcriptome profile of the *erf109* mutants had suggested an association between *ERF109* and *PAP1* [156] - a transcription factor involved in the regulation of anthocyanin biosynthesis. The results presented here confirm that the WT plants are able to accumulate more anthocyanins under high-light than *erf109* mutants. Taken together, these results confirm that *ERF109* has a role in regulating anthocyanin production, and mediating the response to high-light.

Oxygenic photosynthesis produces superoxide by the univalent reduction of molecular oxygen, a process that is greatly increased in the presence of paraquat. Paraquat is able to inhibit photosynthesis by interfering with electron transfer. Paraquat accepts electrons from photosystem I in light-exposed plants and transfers them to molecular oxygen producing superoxide anions. It is regenerated once the electrons are transferred to oxygen which restarts the cycle, allowing it to again transfer electrons away from photosystem I [234]. Previously it was found that the application of paraquat can induce *ERF109* expression [219]. The data presented here show that the *erf109* mutants had a significantly larger rosette area than WT plants when grown on media containing paraquat (Figure 7-5). This indicates that the *erf109* mutants are less sensitive to paraquat-mediated repression of growth than WT plants. In contrast to paraquat, which acts largely through ROS generation in chloroplast, menadione generates superoxide radicals and hydrogen peroxide via interaction with dehydrogenases, which are present throughout plant cells [235]. It is often used in the study of oxidant stress in plants [236]. The growth of the *erf109* mutants was significantly more inhibited by menadione than the WT plants. One of the functions of *ERF109* is to exacerbate ROS production in response to ROS accumulation or stress signals, and plants that overexpress *ERF109* accumulate much higher levels of ROS than the WT plants [162]. The decreased sensitivity of *erf109* mutants to paraquat can therefore be explained by the lack of accelerated ROS production in the absence of the transcription factor. The effect of menadione is less easy to explain and may be related to dehydrogenase-mediated signalling pathways that are distinct from ROS signalling.

It was previously shown that *ERF109* mediates cross-talk between JA signalling and auxin biosynthesis in the regulation of lateral root formation [155]. Manipulations resulting in an increase in *ERF109* expression were reported to have a marked effect on root phenotype [155]. However, it was also reported that the root phenotype of the *erf109* mutants was similar to that of controls [155]. The experiments described here show that the growth media had an effect on the root phenotype as *erf109* mutants had significantly shorter primary roots than WT plants when grown on ATS media (Figure 7-8) but not on ½MS media (Figure 7-9).

Unlike the roots, the shoots of the *erf109* mutants showed significant differences to the WT in terms of growth in the absence of stress and leaf anthocyanin accumulation, which may be related to oxidative signalling in the shoots. These observations led to an investigation of the *ERF109* interactome that is described in the next chapter.

Chapter 8. The identification of proteins that interact with ERF109

8.1. Introduction

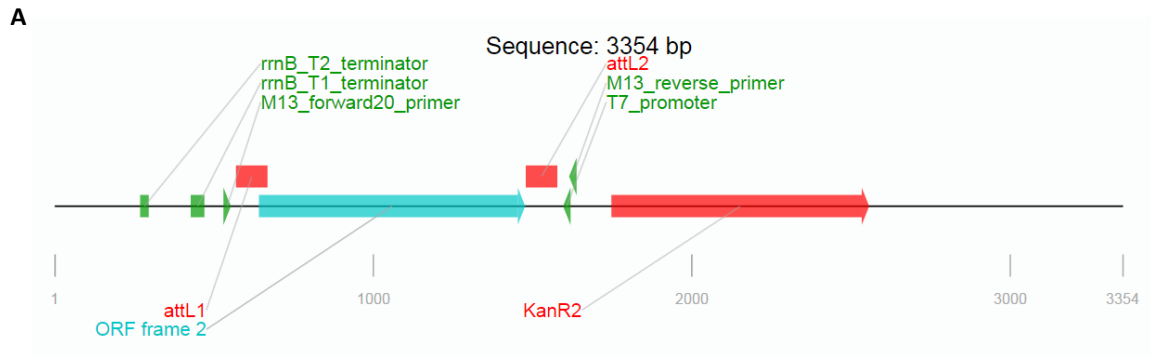
ERF109 encodes a plant specific transcription factor of the Ethylene Responsive Factor family of transcription factors. *ERF109* contains an AP2 domain which is responsible for binding to the promoters of downstream target genes [150, 153, 154]. For example, it was shown to bind to the GCC-boxes in the promoters of *ASA1* (At5g05730) and *YUC2* (At4g13260) in a yeast-one-hybrid assay [155]. The specific binding of ERF109 to the GCC-boxes in the promoters of *ASA1* and *YUC2* was confirmed *in vivo* using transgenic *A. thaliana* plants and chromatin immunoprecipitation assays [155].

The data presented in Chapter 7 suggest that *ERF109* has a role in the control of shoot growth in the absence of stress as the *erf109* mutants tended to have a larger rosette area than WT plants. However, the leaves of *erf109* mutants accumulated less anthocyanin than the WT plants under high-light conditions. The following studies were undertaken to identify proteins that interact with ERF109 in order to gain an insight into the mechanisms that underpin these phenotypes. Proteins can either function as isolated monomeric entities or form multi-protein complexes functioning via interactions with other proteins or molecules (e.g. DNA, RNA, lipids and metabolites) [237]. Analysing protein-protein networks can provide a better understanding of the functional relationships between proteins that facilitate regulatory pathways. A TAP approach was used in combination with mass spectrometry in the following studies to identify proteins that interact with ERF109. The tagged ERF109 protein was expressed in Arabidopsis cell suspension cultures. Tagged proteins were recovered from the host by breaking the cells and retrieving it and associated components through affinity selection and identified using mass-spectrometry analysis [204]. Comprehensive protein sequence repositories were then used to identify purified proteins complexes [205].

8.2. Results

8.2.1. Constructs for TAP experiments

The constructs used for the TAP experiments were prepared using the Gateway® Technology cloning method. 100 ng of pDONR221 plasmid containing *ERF109* was sequenced using primers that covered the *attL1* region of the vector and provided complete coverage of the plasmid insert (*ERF109*; Figure 8-1 A). The sequenced *ERF109* region of the plasmid aligned completely with the *ERF109* ORF (Figure 8-1 B). The *ERF109* fragment, contained in the pDONR221 vector (Figure 8-2), was assembled into pKCTAP destination vector during a single MultiSite LR Clonase reaction to produce an expression clone for use in Agrobacterium mediated transformation. Assembly in to the pKCTAP destination vector was performed at VIB following an established procedure [175]. The pKNTAP destination vector contained the NTAPi tag [176] on the N terminus of *ERF109*, a kanamycin resistance gene for selection of transformed cells, and a GFP expression cassette for use as a visible marker for transformation.



B

ORF	1	ATGCATTATCCTAACAAACAGAACCGAATTCGTCGGAGCTCCAGCCCCAACCCGGTATCAA	60
Seq	671	ATGCATTATCCTAACAAACAGAACCGAATTCGTCGGAGCTCCAGCCCCAACCCGGTATCAA	730
ORF	61	AAGGAGCAGTTGTCCACCGAGCAAGAGCTTTCAGTTATTGTCTCTGCTTTGCAACACGTG	120
Seq	731	AAGGAGCAGTTGTCCACCGAGCAAGAGCTTTCAGTTATTGTCTCTGCTTTGCAACACGTG	790
ORF	121	ATCTCAGGGGAAAACGAAACGGCGCCGTGTCAGGGTTTTCCAGTGACAGCACAGTGATA	180
Seq	791	ATCTCAGGGGAAAACGAAACGGCGCCGTGTCAGGGTTTTCCAGTGACAGCACAGTGATA	850
ORF	181	AGCGCGGAATGCCTCGGTTGGATTCAGACACTTGTCAAGTCTGTAGGATCGAAGGATGT	240
Seq	851	AGCGCGGAATGCCTCGGTTGGATTCAGACACTTGTCAAGTCTGTAGGATCGAAGGATGT	910
ORF	241	CTCGGCTGTAACACTTTTTTCGCGCCAAATCAGAGAATTGAAAAGAATCATCAACAAGAA	300
Seq	911	CTCGGCTGTAACACTTTTTTCGCGCCAAATCAGAGAATTGAAAAGAATCATCAACAAGAA	970
ORF	301	GAAGAGATTACTAGTAGTAGTAACAGAAGAAGAGAGAGCTCTCCCGTGGCGAAGAAAGCG	360
Seq	971	GAAGAGATTACTAGTAGTAGTAACAGAAGAAGAGAGAGCTCTCCCGTGGCGAAGAAAGCG	1030
ORF	361	GAAGTGGCGGGAAAAATCAGGAAGAGGAAGAACAAGAAGATGGTTACAGAGGAGTTAGG	420
Seq	1031	GAAGTGGCGGGAAAAATCAGGAAGAGGAAGAACAAGAAGATGGTTACAGAGGAGTTAGG	1090
ORF	421	CAAAGACCTTGGGGAAAATTTGCAGCTGAGATCAGAGATCCTAAAAGAGCCACACGTGTT	480
Seq	1091	CAAAGACCTTGGGGAAAATTTGCAGCTGAGATCAGAGATCCTAAAAGAGCCACACGTGTT	1150
ORF	481	TGGCTTGGTACTTTTCGAAACCGCCGAAGATGCGGCTCGAGCTTATGATCGAGCCGCGATT	540
Seq	1151	TGGCTTGGTACTTTTCGAAACCGCCGAAGATGCGGCTCGAGCTTATGATCGAGCCGCGATT	1210
ORF	541	GGATTCGCTGGGCAAGGGCTAAACTCAACTTCCCCTTTGTGGATTACACGTCTTCAGTT	600
Seq	1211	GGATTCGCTGGGCAAGGGCTAAACTCAACTTCCCCTTTGTGGATTACACGTCTTCAGTT	1270
ORF	601	TCATCTCCTGTTGCTGCTGATGATATAGGAGCAAAGGCAAGTGCAAGCGCCAGTGTGAGC	660
Seq	1271	TCATCTCCTGTTGCTGCTGATGATATAGGAGCAAAGGCAAGTGCAAGCGCCAGTGTGAGC	1330
ORF	661	GCCACAGATTGAGTTGAGCAGAGCAATGGAACGGAGGAGGAGGGGATTGCAATATGGAG	720
Seq	1331	GCCACAGATTGAGTTGAGCAGAGCAATGGAACGGAGGAGGAGGGGATTGCAATATGGAG	1390
ORF	721	GAGTGGATGAATATGATGATGATGATGGATTTTGGGAATGGAGATTCTTCAGATTCAGGA	780
Seq	1391	GAGTGGATGAATATGATGATGATGATGGATTTTGGGAATGGAGATTCTTCAGATTCAGGA	1450
ORF	781	AATACAATTGCTGATATGTTCCAGTGA	807
Seq	1451	AATACAATTGCTGATATGTTCCAGTGA	1477

Figure 8-1: Linear plasmid map and sequence alignment of the pENTR221 plasmid containing ERF109 DNA.

A: Linear plasmid map of pENTR221 containing ERF109. **B:** The sequence of the ERF109 insert aligned against ERF109 ORF.



Figure 8-2: Circular plasmid map and sequence of pENTR221 plasmid containing *ERF109* DNA.

A: Circular plasmid map of pENTR221 containing ERF109. **B:** The complete sequence of pENTR221 containing ERF109 (highlighted).

8.2.2. The growth of *Arabidopsis thaliana* cell suspension cultures

Arabidopsis thaliana (ecotype Landsberg *erecta*) cell suspension cultures (Plant Systems Biology) were transformed with the pKNTAP-*ERF109* expression vector. The cultures were sub-cultured every 7 days. Growth curves for the cultures grown in the light or in the dark were the same; the exponential phase occurring between 3 and 7 days (data not shown). The presence of the tagged ERF109 protein was detected in extracts of the cell cultures by western blotting. The PAP antibody identified a protein band with a molecular weight between 50-75 kDa. ERF109 has a molecular weight of 29.4 kDa and the GS-tag weighs 21 kDa, thus the tagged ERF109 protein should weigh 50.4 kDa. However, this band was calculated to be about 58 kDa.

8.2.3. The effect of H₂O₂ on ERF109 protein expression in the light and dark

In the following experiments, *Arabidopsis* cell cultures expressing the tagged ERF109 protein were grown either in the dark or in the light with 100 $\mu\text{mol}\cdot\text{m}^{-2}\cdot\text{s}^{-1}$ irradiance and a 16 hour photoperiod for 3 days after sub-culturing.

In the first experiment, concentrations of H₂O₂ up to 20 mM were added to light or dark-grown cultures. Samples were harvested after 1 hour (Figure 8-3 A & B). Western blot analysis showed that in the absence of H₂O₂, extracts from both the light and dark-grown cultures contained a band with a molecular weight between 50-75 kDa band, as well as a protein with a weight close to 37 kDa in approximately equal abundance. There was also a number of other faint bands. The 58 kDa band was present in extracts from light and dark-grown cells incubated at all H₂O₂ concentrations. The intensity of this band appeared to be unchanged with increasing concentrations of H₂O₂. In contrast, the band at 37 kDa was less intense relative to cells not treated with H₂O₂ when in the presence 5, 10, or 20 mM H₂O₂ (Figure 8-3 A & B). The faint bands were present at all concentrations of H₂O₂.

In the second series of experiments, cell cultures were treated with 1 mM H₂O₂, and samples were harvested over a period of 1 hour (Figure 8-4). The abundance of the 58 kDa band in the extracts of light-grown (Figure 8-4 A) and dark-grown (Figure 8-4 B) cultures was similar at all harvest points. At every time point, the 37 kDa band was less intense than the 58 kDa band. However, the intensity of this band increased in the light-grown cultures after 30 minutes of incubation with H₂O₂ (Figure 8-4 A).

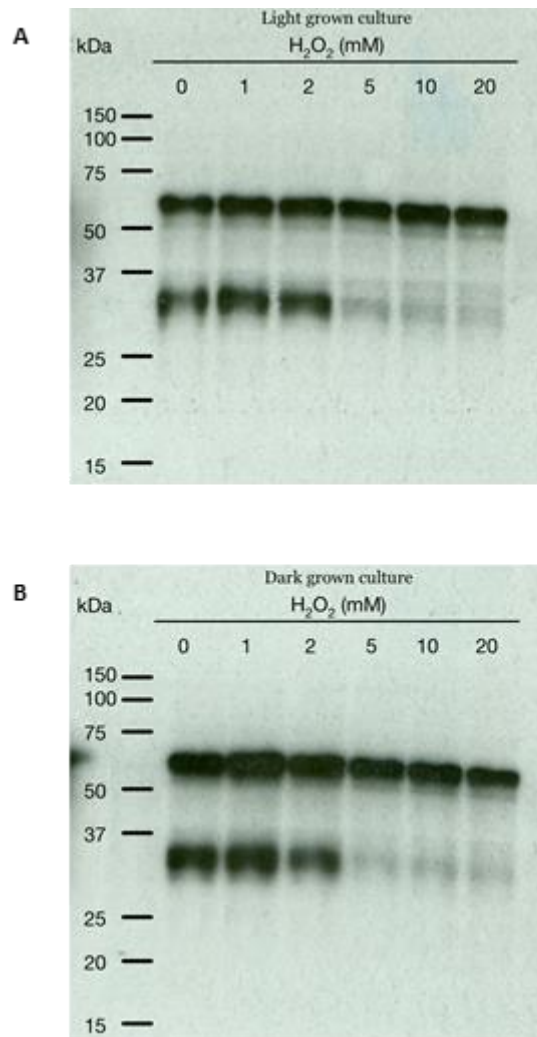


Figure 8-3: Western blots – expression of ERF109 after one hour treatment with H₂O₂ in the light and the dark.

Three-day old *Arabidopsis thaliana* ecotype Landsberg *erecta* cell suspension cultures (Plant Systems Biology), either grown in the light or the dark, were treated with 0, 1, 2, 5, 10, or 20 mM H₂O₂ for 1 hour. **A:** Cultures grown in the light. **B:** Cultures grown in the dark. ERF109 with the GS tag is 50.4 kDa.

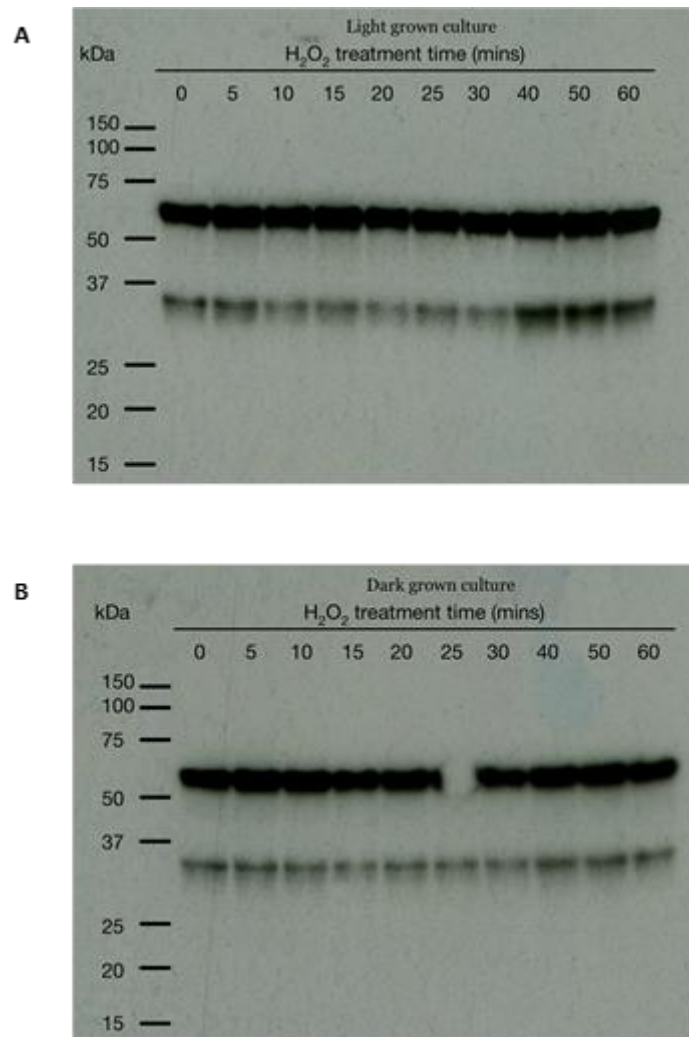


Figure 8-4: Western blots – expression of ERF109 in the light and the dark when treated with 1 mM H₂O₂ for up to 1 hour.

Three-day old *Arabidopsis thaliana* ecotype Landsberg *erecta* cell suspension cultures (Plant Systems Biology), either grown in the light or the dark, were treated with 1 mM H₂O₂ for up to 1 hour. **A:** Cultures grown in the light. **B:** Cultures grown in the dark. ERF109 with the GS tag is 50.4 kDa.

8.2.4. Identification of purified proteins from TAP with ERF109 as bait protein

In these experiments, cultures were grown in the light for 3 days and were either untreated or treated with 1 mM H₂O₂ for 10 minutes. The cells were harvested and homogenised, and protein complexes were extracted and purified by TAP. Protein complexes were separated by SDS PAGE (Figure 8-5) and analysed using mass spectrometry. Identified proteins were checked against a list of proteins known to interact with the GS tag [212]. Proteins that interact with the GS tag were excluded from the list presented in Table 9. In total, 14 proteins were identified as interacting with ERF109 (Table 9). The proteins that interact with ERF109 was changed by the presence of H₂O₂. ERF109 was found to interact with nuclear and cytosolic localised proteins but also one plastid localised protein.

In the absence of oxidative stress, 11 proteins were identified as interacting with ERF109 (Table 9). Two were dead(D/H)-box RNA helicase family proteins: RH20 (encoded by At1g55150) is a nuclear ATP-dependent helicase [238] and RH22 (encoded by At1g59990) is localised to plastids and is essential for apposite accumulation of plastid mRNAs during seed development and seedling growth [214]. Embryo Defective 2762 (EMB2762; encoded by At2g17250) is a nucleolar protein that is a ribosome biogenesis co-factor [239]. SAD2 (super sensitive to ABA and drought 2; encoded by At2g31660) is predominantly nuclear localised and may mediate nuclear transport of ABA signalling proteins [240]. At2g33470 encodes glycolipid transfer protein (GLTP) 1 involved in the intervesicular trafficking of glycosphingolipids [241]. MOB1A (Mps One Binder 1A; encoded by At4g19045) is involved in the co-ordination of tissue patterning and organ growth [242]. EXO70A1 (exocyst subunit EXO70 (exocyst component of 70 kDa) family protein A1; encoded by At5g03540) is the most abundant form of 23 paralogues of EXO70 in *Arabidopsis* and is cytosolic [243, 244]. Replication factor C1 (RFC1; encoded by At5g22010) mediates genomic stability and transcriptional gene silencing [245, 246]. Three of the proteins found to interact with ERF109 in the absence of oxidative stress, encoded by At1g23280, At3g02200, and At5g64420, have not been characterised.

Only 3 proteins were found to interact with ERF109 in cultures were treated with 1 mM H₂O₂; these are encoded by At1g50600, At2g36200 and At3g06400 (Table 9). At1g50600 is a member of GRAS gene family and encodes scarecrow-like 5 [247]. At3g06400 encodes a chromatin remodelling protein that is involved in nuclear proliferation and is required for female gametogenesis [248]. The remaining protein found to interact with ERF109 in the presence of oxidative stress, encoded by At2g36200, has not been functionally characterised.

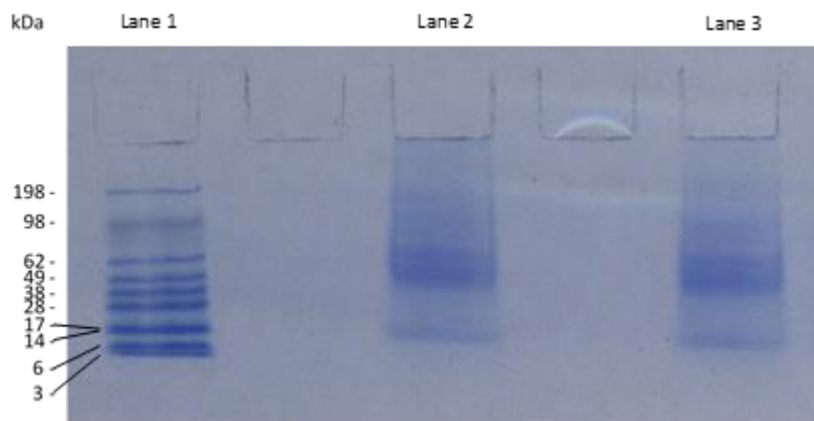


Figure 8-5: SDS-PAGE of purified protein complexes.

Proteins purified by TAP were separated by SDS-PAGE. **Lane 1:** SeeBlue Plus2 MW marker (Invitrogen). **Lane 2:** 35S-ERF109-NGSrhino untreated. **Lane 3:** 35S-ERF109-NGSrhino treated with 1 mM H₂O₂.

Table 12: Proteins that interact with ERF109 in the light when either untreated or treated with 1mM H₂O₂.

A tick indicates that an interaction was observed.

Protein accession	Protein description	No treatment	1mM H ₂ O ₂
At1g23280	MAK16 protein-related	✓	
At1g55150	RH20 DEA(D/H)-box RNA helicase family protein 20	✓	
At1g59990	RH22 DEA(D/H)-box RNA helicase family protein 22	✓	
At2g17250	EMB2762 CCAAT-binding factor	✓	
At2g31660	SAD2 ARM repeat superfamily protein	✓	
At2g33470	GLTP1 glycolipid transfer protein 1	✓	
At3g02200	Proteasome component (PCI) domain protein	✓	
At4g19045; At5g45550	MOB1A MOB1 (Mps One Binder)/phocein family protein	✓	
At5g03540	EXO70A1 exocyst subunit EXO70 family protein A1	✓	
At5g22010	RFC1 replication factor C1	✓	
At5g64420	DNA polymerase V family	✓	
At1g50600	SCL5 scarecrow-like 5		✓
At2g36200	P-loop containing nucleoside triphosphate hydrolases superfamily protein		✓
At3g06400; At5g18620	CHR11 chromatin-remodeling protein 11		✓

8.3. Discussion

The aim of the experiments reported in this chapter was to identify proteins that interact with ERF109. Through the use of an established TAP procedure combined with mass spectrometry, a list of proteins that interact with ERF109 was revealed. ERF109 was found to localise to nuclei in a previous study [155]. The data presented here show that a number of proteins that are localised to nucleus interact with ERF109, as did several proteins that localise to the cytosol. Surprisingly, one protein that localises to the chloroplast, RH22, also interacts with ERF109. Interestingly, the proteins that were found to interact with ERF109, do so either in the absence or presence of oxidative stress but not under both conditions. This finding might suggest that ERF109 protein-protein interactions are determined or responsive to the redox state of the cells. The results of the experiments reported in this chapter help explain some of the phenotypes observed in Chapter 7.

In the absence of oxidation, many of the proteins that interact with ERF109 are involved in RNA processing or related pathways. For example, ERF109 interacts with RH20, a nuclear-localised Dead(D/H)-box RNA helicase family protein involved in the regulation of nonsense-mediated mRNA decay and ribosome biogenesis. ERF109 also interacts with EMB2762, a nucleolar protein that is a ribosome biogenesis co-factor [13]. The *emb2762* mutants display aberrant RNA processing, and homozygous embryos arrest in the globular stage of development. Furthermore, ERF109 was found to interact with EXO70A1, which is the most abundant form of 23 paralogues of EXO70. This cytosolic protein complex involved with pre-mRNA splicing [17, 18].

Other interactions may go some way to explaining the phenotype of the *erf109* mutants reported in Chapter 7. ERF109 was found to interact with SAD2, a predominantly nuclear localised protein, in the absence of oxidants. SAD2 has been found to be involved in nuclear transport as well as in ABA signalling [240]. The *sad2* mutants are more tolerant to UV-B radiation than the WT plants [249]. SAD2 is required for the nuclear trafficking of MYB4 [249], which has previously been shown to negatively regulate the transcription of cinnamate 4-hydroxylase (C4H) [250], a component of the anthocyanin biosynthetic pathway. The MYB4 protein also specifically binds to the promoter of *MYB4* and represses its own expression [249]. In this way the MYB4 protein and mRNA are part of a negative autoregulatory loop. MYB4 is therefore able to regulate expression of both MYB4 and C4H, and the accumulation of UV-absorbing compounds. The negative autoregulatory feedback loop is altered in the *sad2* mutant due to the

absence of MYB4 protein in the nucleus, leading to the constitutive expression of MYB4 and C4H and resulting in accumulation of UV-absorbing pigments [249]. As discussed in Chapter 7, *erf109* mutants produce significantly less anthocyanins than WT plants, which is in contrast to *sad2* mutants, which accumulate more anthocyanins than the WT. This finding might suggest that ERF109 interacts with SAD2 in the absence of oxidants to alter this pathway.

The interaction of ERF109 with MOB1A might also explain some of the phenotypic characteristics of the *erf109* mutants described in Chapter 7, and in previous studies [155]. In a previous study, the root meristems of *mob1a* mutants were significantly reduced in size [242], similar to the root phenotype of plants that overexpress *ERF109* [155]. *MOB1A* transcript levels are high in columella and lateral root cap cells of WT plants. Moreover, *MOB1A* expression was upregulated by several stress conditions as well as by ABA and salicylic acid [242]. Reduced levels of *MOB1A* expression in the primary root brought about severe defects in tissue patterning of the stem cell niche and columella and led to a decrease in meristem size [242]. *MOB1A* also regulates the expression of PINNATE (PIN)4, which is an auxin efflux carrier [251]. The *pin4* mutants are defective in establishment and maintenance of endogenous auxin gradients, and fail to canalise externally applied auxin [251]. Transport of auxin through PIN4 generates a sink for auxin below the quiescent centre of the root meristem that is essential for auxin distribution and patterning [251]. The expression of *PIN4* in WT columella initials was altered in *MOB1A* knocked-down lines [242]. In addition, *MOB1A* RNAi plants showed a misalignment of *PIN4*-labelled cell files around the quiescent centre. The observation that *ERF109* overexpression causes a root phenotype that resembles those of auxin overproduction [155], is consistent with the observations reported here.

Three proteins were found to interact with ERF109 in cultures exposed to oxidants; these are encoded by At1g50600, At2g36200 and At3g06400 (Table 1). Interestingly, the proteins that were found to interact with ERF109 in the presence of oxidative stress, did not do so in the absence of oxidative stress. This finding might suggest that ERF109 protein-protein interactions are determined or responsive to the redox state of the cells. It is likely that ERF109 interactome is condition-dependent, and this influences interaction with other proteins that have not been identified in this study.

As discussed in Chapter 5, other approaches should be used to verify the results of the protein interaction studies. For example, a split-YFP approach, used in Chapter 5, is a well-established procedure in plants [207-211] and could be used to verify the results presented here.

The western blot analysis reported here, provides insights into the expression and stability of the tagged ERF109 protein. The tagged ERF109 protein was always detected in the cells, whether they were grown in the dark or the light, in the absence or the presence of oxidant. Another band containing the tag weighing about 37 kDa was also apparent in blots of proteins extracted from both light- and dark-grown 3-day-old cultures. There was no discernible difference in the pattern of bands observed on western blots of protein extracts from light- or dark-grown cultures. However, in the presence 5, 10, or 20 mM H₂O₂, the 37 kDa band was less intense relative to cells not treated with H₂O₂. This finding would suggest that the tagged ERF109 protein is more stable in the presence of oxidative stress than the 37 kDa protein.

The results of the experiments performed in this chapter help explain some of the phenotypes observed in Chapter 7. Furthermore, the western blots and TAP results taken together suggest that the ERF109 interactome is complex, and alters with cell oxidation conditions.

Chapter 9. General discussion and conclusions

9.1. The challenge

The focus of the studies in this thesis was on two genes putatively involved in the regulation of plant redox processes. These were *LEA5*, which was found to provide tolerance to oxidative stress, and *ERF109*, a transcription factor that is part of a regulatory network that plays role in the adjustment of leaves to homeostasis after high-light stress. The general aim of the studies was to find the role that these to genes play in plant growth and stress responses.

Current and predicted climate conditions, such as prolonged drought and heatwaves, present a challenge for agricultural production worldwide by affecting plant growth and yield, and causing annual losses estimated to cost £billions [252, 253]. Climate change and global warming are generating rapid changes in global temperature that are not matched by any global temperature increase of the past 50 million years [254]. Models tend to agree in their predictions of increased frequencies of heatwaves, tropical cyclones, floods, and prolonged drought episodes [255]. There is a general consensus supporting the notion that changes in atmospheric CO₂ concentrations, an increase in the ambient temperature, and regional changes in annual precipitation will significantly influence future agricultural production.

Transgenic crops provide a promising avenue to reduce yield losses, improve growth, and provide a secure food supply for a growing world population [256, 257]. Various strategies can be used to enhance the tolerance of plants to abiotic stress by genetic engineering. However, a detailed understanding of the response of plants to abiotic stress is a prerequisite to the identification and use of transgenes or upstream regulators to activate an acclimation response that will enhance the tolerance of plants to different stresses. A major objective of abiotic stress research in plants is to study how plants sense and acclimate to abiotic stress conditions, and then use this knowledge to develop plants and crops with enhanced tolerance to abiotic stresses.

9.2. The role of LEA5 in plant growth and stress responses

The aims of the studies on LEA5 were to determine its effects on the plant phenotype in optimal and stress conditions, characterise its functions in mitochondria, and to determine whether the protein interactions with LEA5 are important in the control of growth and stress tolerance.

LEA proteins are frequently associated with stress tolerance [12, 13]. LEA5 is novel as it was found to provide tolerance to oxidative stress [43, 51]. Homologues of LEA5 exist throughout the plant kingdom (Figure 9-1). Previous studies using transgenic *A. thaliana* found that the over-expression of *LEA5* resulted in plants with a greater biomass [43, 51]. However, the results presented in Chapter 3 which used the same transgenic lines as previous studies, but were of a different generation, were similar to WT plants. This is likely because expression of *LEA5* in these lines was not as previously described [43, 51]. A possible explanation for this discrepancy lies in loss of transgene expression. It could be that, in successive generations, the transgene has been silenced. However, transgenic barley plants that express *LEA5* analysed in Chapter 6, do have a greater biomass, as observed in the Arabidopsis lines in previously published studies [43, 51]. Three independently transformed lines of barley that express *LEA5* were selected for homozygosity. These transgenic barley plants had more biomass on average than WT plants ($P < 0.05$ for line 11.2.2). Also, after 8 weeks of growth, the LEA5-YFP line 11.2.2 had 96 leaves whilst WT plants which had 81 leaves ($P < 0.05$). Furthermore, the expression of *LEA5* resulted in the production of significantly more tillers in line 4.1.2 ($P < 0.05$), however the tillers weighed less than those of WT plants.

Given these findings, a pertinent question concerns the mechanisms by which *LEA5* might confer an increase in biomass. One clue might be found in the localisation of this protein. Earlier studies had shown that LEA5 is localised to mitochondria [44, 51]. While no significant differences were found in the assays performed on the ETC in Chapter 4, there was a tendency towards higher cytochrome *c* oxidase activity in isolated mitochondria from the *LEA5* OEX line compared to from the WT plants. Further investigation is still necessary to determine how these parameters might contribute to the greater biomass observed in the OEX lines. Alternatively, LEA5 could be involved in retrograde signalling from the mitochondria to the nucleus, which has been proposed to mediate abiotic stress perception [190]. Many abiotic stresses will influence mitochondrial metabolism and could generate signals such as the over-reduction of the ETC, enhanced accumulation of ROS, or altered redox potential that will, in turn, trigger nuclear gene expression and acclimation responses. It is possible that LEA5 is

involved in the adjustment of the redox state of mitochondria. For this purpose, transgenic plants that express roGFP in either the mitochondria or the cytosol were produced in plants with altered expression of LEA5. The roGFP emission spectrum changes in a more reduced environment [172]. Homozygous plants expressing either mitochondrial-roGFP or cytosolic-roGFP were produced in plants with altered expression of *LEA5* and seeds of these lines are now available for further study. An understanding of how LEA5 alters the redox state in mitochondria could provide insights into plant growth and stress tolerance.

A crucial step towards understanding cellular systems is mapping networks of physical protein-protein interactions. Knowledge of the interactome of LEA5 increases our understanding of plant growth and development. In Chapter 5 protein interactions with LEA5 were explored using TAP combined with mass spectrometry. The TAP isolated protein complexes from suspension-cultured *A. thaliana* cells. TAP uses a combination of two high-affinity handles to reduce background interactions caused by spurious and promiscuous proteins, while maintaining a high protein complex purification yield [175]. RH22 was shown to interact with LEA5 in the protein-protein experiments, but was not verified in the split-YFP experiments. However, the functions of this protein merit further consideration. RH22 is essential for apposite accumulation of plastid mRNAs during seed development and seedling growth, ensuring seed oil biosynthesis by maintaining plastid mRNA levels [214]. It is possible that LEA5 interacts with RH22 under certain conditions, or when cells are damaged. In this way, LEA5 might interact with RH22 to regulate plastid gene expression, a possibility that can be explored in future work. Another Dead(D/H)-box RNA helicase family protein, RH20 also interacted with LEA5. It is possible that the interaction of LEA5 with RH22 occurs via a similar domain to RH20. This interaction occurred in the dark but not in the light which is interesting as *LEA5* transcripts are also abundant in the dark [43], possibly indicating circadian regulation. Additionally, the growth of a fungal (*Botrytis cinerea*), and a bacterial pathogen (*Pseudomonas syringae*) was previously shown to be altered in *LEA5* over-expression lines [51]. The interaction of LEA5 with PDF2.2, which is located in the cell wall and is often used a marker for ethylene and jasmonate dependent pathogen defence induction, could help explain these results. Further investigation of the LEA5 interactome could advance understanding of the role of LEA5 in plant growth and stress tolerance. An understanding of the functions of LEA5 could provide insights into the control of plant growth and stress tolerance. This information could be used in breeding programmes to improve the predictability and sustainability of crop yields by enhancing stress tolerance which is of interest to biotechnology companies [1].

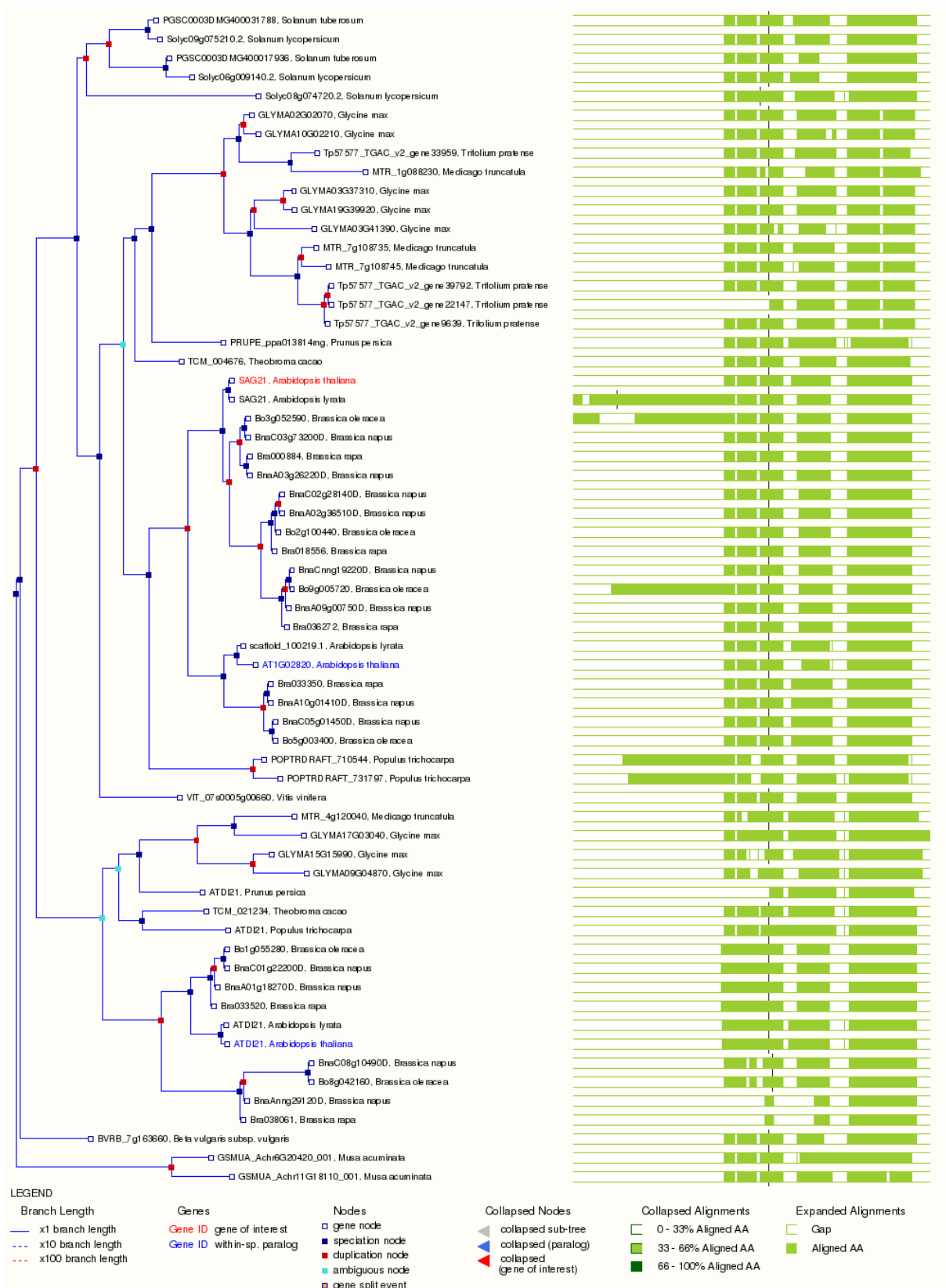


Figure 9-1: Plant compara gene tree of all known orthologues of LEA5 in Ensembl Plants (plants.ensembl.org).

Left: Dendrogram of orthologues. **Right:** Alignment structures of LEA5 orthologues.

9.3. Future prospects for LEA5

LEA5 is predominantly expressed in non-photosynthetic tissues such as roots. For this reason, *LEA5* is thought to be involved in the protection of roots against stress. Under conditions of dehydration and oxidative stresses, root-to-shoot signalling leads to the expression of *LEA5* in vegetative tissues [51]. The over-expression of *LEA5* conferred tolerance to H₂O₂ [43]. Many of the proteins found to interact with *LEA5* in Chapter 5 have been associated with various stresses. Verifying these interactions *in vivo* by split-YFP could provide new information on important pathways. Furthermore, while predominant expression in non-photosynthetic tissues might preclude a direct antioxidant role in photosynthesis, the interaction of *LEA5* with RH22, in addition to the up-regulation of *LEA5* transcripts in response to oxidants and the reduced sensitivity to H₂O₂ in *LEA5* over-expressing plants, suggest a potential role in ROS mediated signalling. Transgenic *A. thaliana* plants that express roGFP in either the mitochondria or cytosol were produced for further analysis of the involvement of *LEA5* in moderating the cell redox state and in oxidative stress tolerance. An understanding of how *LEA5* alters the redox state in mitochondria could provide insights into plant growth and stress tolerance.

Finally, the production of homozygous transgenic barley plants expressing *LEA5* will allow the exploration of bestowed stress tolerance by analysing these plants under a range of biotic and abiotic stresses. A reasonable starting point would be to investigate tolerance of these plants to H₂O₂ as *LEA5* has been shown to be upregulated by oxidants and provide tolerance to H₂O₂ [43]. *LEA5* was also found to be involved in the control of root architecture [43, 51], and so the analysis of the effects of *LEA5* on barley roots could also provide further insights in to root growth. If *LEA5* confers increased stress tolerance and altered root structures into a crop species such as barley then it could have a major effect in the agriculture industry [1].

9.4. The role of ERF109 in plant growth and stress responses

Like *LEA5*, *ERF109* is considered to have a role in the regulation of plant redox processes. Studies have shown that *ERF109* propagates ROS accumulation in response to ROS-producing abiotic and biotic stress signals [162]. A further aim of studies performed in this thesis was to characterise the phenotypes of *erf109* mutants and to determine *ERF109* protein interactions.

The combination and cross-regulation of transcription factors defines the core regulatory network of a cell. Understanding the roles of transcriptional regulatory networks and their effects on downstream target genes will aid in the development of stress tolerant crops. The

transcription factor, *ERF109*, is part of a regulatory network that has a major role in the adjustment of *A. thaliana* leaves to reach homeostasis after high-light stress [156]. Much of the current understanding of the functions of *ERF109* comes from the analysis of *A. thaliana erf109* mutants. These mutants have no visible phenotypic differences to the WT when grown under low-light [157]. However, they show a markedly different phenotype when grown for two weeks under high-light as the leaves of WT plants appear visibly darker than those of the *erf109* mutants [157]. The results in Chapter 7 reflect this, as the *erf109* mutant leaves accumulated significantly less anthocyanin than WT plants in the high-light conditions. The studies presented in Chapter 7 suggest that *ERF109* has a role in the control of shoot growth in the absence of stress. Although the difference in rosette area between WT and *erf109* mutant plants was small, the *erf109* mutants tended to have a larger rosette area than the WT plants at the later stages of vegetative growth. It was previously shown that overexpression of *ERF109* led to altered leaf morphology, producing leaves that were longer, narrower and curled, similar to auxin overproduction phenotypes [155, 162]. Moreover, plants that overexpress *ERF109* were found to have significantly higher auxin levels in the shoot tissues than the WT plants [155]. Conversely, the levels of auxin were reduced the shoots of *erf109* mutants [155]. The increased rosette area of the *erf109* mutants observed here could result from lower auxin levels.

Knowledge of the ERF109 interactome improves our understanding of the role ERF109 has in plant growth and response to stress. In Chapter 8 protein interactions with ERF109 were investigated using TAP, and proteins that interact with ERF109 were revealed. The interactions reported in Chapter 8 explain some of the phenotypic characteristics of the *erf109* mutants described in Chapter 7, and in previous studies [155]. ERF109 was found to interact with SAD2, a predominantly nuclear localised protein. SAD2 is involved in nuclear transport as well as ABA signalling [240]. The *sad2* mutants are more tolerant to UV-B radiation than WT plants [249]. SAD2 is required for the nuclear trafficking of MYB4 [249], which has previously been shown to negatively regulate the transcription of C4H [250], a component of the anthocyanin biosynthetic pathway. This could help explain why the leaves of *erf109* mutants accumulated significantly less anthocyanin than WT plants in high-light conditions. Furthermore, ERF109 was found to interact with MOB1A. Reduced levels of *MOB1A* expression in the primary root brought about severe defects in tissue patterning of the stem cell niche and columella and led to a decrease in meristem size [242]. MOB1A regulates the expression of PIN4, which is an auxin efflux carrier, and *pin4* mutants are defective in establishment and maintenance of endogenous auxin gradients, and fail to canalise externally applied auxin [251]. The observation

that *ERF109* overexpression causes a root phenotype that resembles those of auxin overproduction [155], is consistent with the observations reported here.

9.5. Future prospects for ERF109

The interactions reported in Chapter 8 help to explain some of the phenotypic characteristics of the *erf109* mutants described in Chapter 7, and in previous studies [155]. Other approaches should be used to verify the results of the protein interaction studies. For example, a split-YFP approach, as performed in Chapter 5, could be used here. Verifying these interactions *in vivo* by split-YFP would validate these experiments and show the location of these interactions.

The *erf109* mutants tended to have a larger rosette area than the WT plants at the later stages of vegetative growth. This could be due to lower photo-respiration rates and so investigating the rates of photorespiration of these mutants, as well as of *ERF109* over-expression lines, in environments with altered CO₂ might indicate if this is the case. Further experiments to understand why *erf109* mutants accumulated less anthocyanin than WT plants in high-light conditions could reveal the role of ERF109 in regulating this pathway. Norflurazon and lincomycin induce retrograde signalling in WT plants resulting in altered anthocyanin accumulation [258]. Treating *erf109* mutants with these compounds, might indicate if ERF109 has a role in ROS signalling. This could be particularly interesting as ERF109 is considered to propagate ROS accumulation in response to ROS-producing abiotic and biotic stress signals.

Once an improved understanding of the role ERF109 plays in growth and stress responses is developed, then it would be useful to apply this knowledge to a crop species which could have tangible outcomes and a major effect in the agriculture industry.

9.6. Conclusion

The challenges of food security, adequate nutrition and sustainable agriculture require innovative approaches to crop improvement. Next generation crops are needed to mitigate future food shortages and to make agricultural industries more competitive [256, 257]. However, a detailed understanding of the response of plants to abiotic stress is a prerequisite to the identification and use of transgenes or upstream regulators to activate an acclimation response that will enhance the tolerance of plants to different stresses. While further work is required, the results presented in this thesis have provided insights and will help elucidate the roles of LEA5 and ERF109 in plant growth and stress responses.

Chapter 10. References

1. Mittler, R. and Blumwald, E. Genetic engineering for modern agriculture: challenges and perspectives. *Annu Rev Plant Biol.* 2010, **61**, pp.443-62.
2. Mittler, R. Oxidative stress, antioxidants and stress tolerance. *Trends Plant Sci.* 2002, **7**(9), pp.405-10.
3. Tunnacliffe, A. and Wise, M.J. The continuing conundrum of the LEA proteins. *Naturwissenschaften.* 2007, **94**(10), pp.791-812.
4. Tunnacliffe, A., Hinch, D.K., Leprince, O. and Macherel, D. LEA proteins: versatility of form and function. In: Lubzens, E. et al. eds. *Sleeping Beauties: Dormancy and Resistance in Harsh Environments.* Berlin, Germany: Springer, 2010, pp.91-108.
5. Dure, L., Greenway, S.C. and Galau, G.A. Developmental biochemistry of cottonseed embryogenesis and germination: changing messenger ribonucleic acid populations as shown by in vitro and in vivo protein synthesis. *Biochemistry.* 1981, **20**(14), pp.4162-4168.
6. Grzelczak, Z.F., Sattolo, M.H., Hanley-Bowdoin, L.K., Kennedy, T.D. and Lane, B.G. Synthesis and turnover of proteins and mRNA in germinating wheat embryos. *Can J Biochem.* 1982, **60**(3), pp.389-97.
7. Browne, J., Tunnacliffe, A. and Burnell, A. Anhydrobiosis: plant desiccation gene found in a nematode. *Nature.* 2002, **416**(6876), p.38.
8. Mtwisha, L., Brandt, W., McCreedy, S. and Lindsey, G.G. HSP 12 is a LEA-like protein in *Saccharomyces cerevisiae*. *Plant Mol Biol.* 1998, **37**(3), pp.513-21.
9. Sales, K., Brandt, W., Rumbak, E. and Lindsey, G. The LEA-like protein HSP 12 in *Saccharomyces cerevisiae* has a plasma membrane location and protects membranes against desiccation and ethanol-induced stress. *Biochim Biophys Acta.* 2000, **1463**(2), pp.267-78.

10. Solomon, A., Salomon, R., Paperna, I. and Glazer, I. Desiccation stress of entomopathogenic nematodes induces the accumulation of a novel heat-stable protein. *Parasitology*. 2000, **121** (Pt 4), pp.409-16.
11. Stacy, R.A. and Aalen, R.B. Identification of sequence homology between the internal hydrophilic repeated motifs of group 1 late-embryogenesis-abundant proteins in plants and hydrophilic repeats of the general stress protein GsiB of *Bacillus subtilis*. *Planta*. 1998, **206**(3), pp.476-8.
12. Dure, L., 3rd, Crouch, M., Harada, J., Ho, T.H., Mundy, J., Quatrano, R., Thomas, T. and Sung, Z.R. Common amino acid sequence domains among the LEA proteins of higher plants. *Plant Mol Biol*. 1989, **12**(5), pp.475-86.
13. Cuming, A. LEA proteins. In: Shewry, P.R. and Casey, R. eds. *Seed Proteins*. Springer Netherlands, 1999, pp.753-780.
14. Xu, D., Duan, X., Wang, B., Hong, B., Ho, T. and Wu, R. Expression of a late embryogenesis abundant protein gene, HVA1, from barley confers tolerance to water deficit and salt stress in transgenic rice. *Plant Physiol*. 1996, **110**(1), pp.249-257.
15. Sivamani, E., Bahieldin, A., Wraith, J.M., Al-Niemi, T., Dyer, W.E., Ho, T.D. and Qu, R. Improved biomass productivity and water use efficiency under water deficit conditions in transgenic wheat constitutively expressing the barley HVA1 gene. *Plant Sci*. 2000, **155**(1), pp.1-9.
16. Hara, M., Terashima, S., Fukaya, T. and Kuboi, T. Enhancement of cold tolerance and inhibition of lipid peroxidation by citrus dehydrin in transgenic tobacco. *Planta*. 2003, **217**(2), pp.290-8.
17. Houde, M., Dallaire, S., N'Dong, D. and Sarhan, F. Overexpression of the acidic dehydrin WCOR410 improves freezing tolerance in transgenic strawberry leaves. *Plant Biotechnol J*. 2004, **2**(5), pp.381-7.
18. Kaye, C., Neven, L., Hofig, A., Li, Q.B., Haskell, D. and Guy, C. Characterization of a gene for spinach CAP160 and expression of two spinach cold-acclimation proteins in tobacco. *Plant Physiol*. 1998, **116**(4), pp.1367-77.

19. Bies-Etheve, N., Gaubier-Comella, P., Debures, A., Lasserre, E., Jobet, E., Raynal, M., Cooke, R. and Delseny, M. Inventory, evolution and expression profiling diversity of the LEA (late embryogenesis abundant) protein gene family in *Arabidopsis thaliana*. *Plant Mol Biol.* 2008, **67**(1-2), pp.107-24.
20. Garay-Arroyo, A., Colmenero-Flores, J.M., Garcarrubio, A. and Covarrubias, A.A. Highly hydrophilic proteins in prokaryotes and eukaryotes are common during conditions of water deficit. *J Biol Chem.* 2000, **275**(8), pp.5668-74.
21. Wise, M.J. LEAping to conclusions: a computational reanalysis of late embryogenesis abundant proteins and their possible roles. *BMC Bioinformatics.* 2003, **4**, p.52.
22. Uversky, V.N., Gillespie, J.R. and Fink, A.L. Why are "natively unfolded" proteins unstructured under physiologic conditions? *Proteins.* 2000, **41**(3), pp.415-27.
23. Dunker, A.K., Lawson, J.D., Brown, C.J., Williams, R.M., Romero, P., Oh, J.S., Oldfield, C.J., Campen, A.M., Ratliff, C.M., Hipps, K.W., Ausio, J., Nissen, M.S., Reeves, R., Kang, C., Kissinger, C.R., Bailey, R.W., Griswold, M.D., Chiu, W., Garner, E.C. and Obradovic, Z. Intrinsically disordered protein. *J Mol Graph Model.* 2001, **19**(1), pp.26-59.
24. Tompa, P. Intrinsically unstructured proteins. *Trends Biochem Sci.* 2002, **27**(10), pp.527-33.
25. Wolkers, W.F., McCready, S., Brandt, W.F., Lindsey, G.G. and Hoekstra, F.A. Isolation and characterization of a D-7 LEA protein from pollen that stabilizes glasses in vitro. *Biochim Biophys Acta.* 2001, **1544**(1-2), pp.196-206.
26. Shih, M.D., Lin, S.C., Hsieh, J.S., Tsou, C.H., Chow, T.Y., Lin, T.P. and Hsing, Y.I. Gene cloning and characterization of a soybean (*Glycine max* L.) LEA protein, GmPM16. *Plant Mol Biol.* 2004, **56**(5), pp.689-703.
27. Goyal, K., Walton, L.J. and Tunnacliffe, A. LEA proteins prevent protein aggregation due to water stress. *Biochem J.* 2005, **388**(Pt 1), pp.151-7.
28. Tolleter, D., Jaquinod, M., Mangavel, C., Passirani, C., Saulnier, P., Manon, S., Teyssier, E., Payet, N., Avelange-Macherel, M.H. and Macherel, D. Structure and function of a mitochondrial late embryogenesis abundant protein are revealed by desiccation. *Plant Cell.* 2007, **19**(5), pp.1580-9.

29. Li, D. and He, X. Desiccation induced structural alterations in a 66-amino acid fragment of an anhydrobiotic nematode late embryogenesis abundant (LEA) protein. *Biomacromolecules*. 2009, **10**(6), pp.1469-77.
30. Hundertmark, M., Popova, A.V., Rausch, S., Seckler, R. and Hinch, D.K. Influence of drying on the secondary structure of intrinsically disordered and globular proteins. *Biochem Biophys Res Commun*. 2012, **417**(1), pp.122-8.
31. Hand, S.C., Menze, M.A., Toner, M., Boswell, L. and Moore, D. LEA proteins during water stress: not just for plants anymore. *Annu Rev Physiol*. 2011, **73**, pp.115-34.
32. Goyal, K., Tisi, L., Basran, A., Browne, J., Burnell, A., Zurdo, J. and Tunnacliffe, A. Transition from natively unfolded to folded state induced by desiccation in an anhydrobiotic nematode protein. *J Biol Chem*. 2003, **278**(15), pp.12977-84.
33. Goldgur, Y., Rom, S., Ghirlando, R., Shkolnik, D., Shadrin, N., Konrad, Z. and Bar-Zvi, D. Desiccation and zinc binding induce transition of tomato abscisic acid stress ripening 1, a water stress- and salt stress-regulated plant-specific protein, from unfolded to folded state. *Plant Physiol*. 2007, **143**(2), pp.617-28.
34. Boucher, V., Buitink, J., Lin, X., Boudet, J., Hoekstra, F.A., Hundertmark, M., Renard, D. and Leprieux, O. MtPM25 is an atypical hydrophobic late embryogenesis-abundant protein that dissociates cold and desiccation-aggregated proteins. *Plant Cell Environ*. 2010, **33**(3), pp.418-30.
35. Chakrabortee, S., Boschetti, C., Walton, L.J., Sarkar, S., Rubinsztein, D.C. and Tunnacliffe, A. Hydrophilic protein associated with desiccation tolerance exhibits broad protein stabilization function. *Proc Natl Acad Sci U S A*. 2007, **104**(46), pp.18073-8.
36. Pouchkina-Stantcheva, N.N., McGee, B.M., Boschetti, C., Tolleter, D., Chakrabortee, S., Popova, A.V., Meersman, F., Macherel, D., Hinch, D.K. and Tunnacliffe, A. Functional divergence of former alleles in an ancient asexual invertebrate. *Science*. 2007, **318**(5848), pp.268-71.
37. Reyes, J.L., Rodrigo, M.J., Colmenero-Flores, J.M., Gil, J.V., Garay-Arroyo, A., Campos, F., Salamini, F., Bartels, D. and Covarrubias, A.A. Hydrophilins from distant organisms can protect enzymatic activities from water limitation effects in vitro. *Plant Cell and Environment*. 2005, **28**(6), pp.709-718.

38. Nakayama, K., Okawa, K., Kakizaki, T., Honma, T., Itoh, H. and Inaba, T. Arabidopsis Cor15am is a chloroplast stromal protein that has cryoprotective activity and forms oligomers. *Plant Physiol.* 2007, **144**(1), pp.513-23.
39. Grelet, J., Benamar, A., Teyssier, E., Avelange-Macherel, M.H., Grunwald, D. and Macherel, D. Identification in pea seed mitochondria of a late-embryogenesis abundant protein able to protect enzymes from drying. *Plant Physiol.* 2005, **137**(1), pp.157-67.
40. Honjoh, K.I., Matsumoto, H., Shimizu, H., Ooyama, K., Tanaka, K., Oda, Y., Takata, R., Joh, T., Suga, K., Miyamoto, T., Iio, M. and Hatano, S. Cryoprotective activities of group 3 late embryogenesis abundant proteins from *Chlorella vulgaris* C-27. *Biosci Biotechnol Biochem.* 2000, **64**(8), pp.1656-63.
41. Hundertmark, M. and Hinch, D.K. LEA (late embryogenesis abundant) proteins and their encoding genes in *Arabidopsis thaliana*. *BMC Genomics.* 2008, **9**, p.118.
42. Weaver, L.M., Gan, S., Quirino, B. and Amasino, R.M. A comparison of the expression patterns of several senescence-associated genes in response to stress and hormone treatment. *Plant Mol Biol.* 1998, **37**(3), pp.455-69.
43. Mowla, S.B., Cuypers, A., Driscoll, S.P., Kiddle, G., Thomson, J., Foyer, C.H. and Theodoulou, F.L. Yeast complementation reveals a role for an *Arabidopsis thaliana* late embryogenesis abundant (LEA)-like protein in oxidative stress tolerance. *Plant J.* 2006, **48**(5), pp.743-56.
44. Candat, A., Paszkiewicz, G., Neveu, M., Gautier, R., Logan, D.C., Avelange-Macherel, M.H. and Macherel, D. The ubiquitous distribution of late embryogenesis abundant proteins across cell compartments in *Arabidopsis* offers tailored protection against abiotic stress. *Plant Cell.* 2014, **26**(7), pp.3148-66.
45. Babiychuk, E., Kushnir, S., Belles-Boix, E., Van Montagu, M. and Inze, D. Arabidopsis thaliana NADPH oxidoreductase homologs confer tolerance of yeasts toward the thiol-oxidizing drug diamide. *J Biol Chem.* 1995, **270**(44), pp.26224-31.
46. Belles-Boix, E., Babiychuk, E., Montagu, M.V., Inze, D. and Kushnir, S. CEF, a sec24 homologue of *Arabidopsis thaliana*, enhances the survival of yeast under oxidative stress conditions. *J Exp Bot.* 2000, **51**(351), pp.1761-2.

47. Kushnir, S., Babiychuk, E., Kampfenkel, K., Belles-Boix, E., Van Montagu, M. and Inze, D. Characterization of *Arabidopsis thaliana* cDNAs that render yeasts tolerant toward the thiol-oxidizing drug diamide. *Proc Natl Acad Sci U S A*. 1995, **92**(23), pp.10580-4.
48. Mano, J., Babiychuk, E., Belles-Boix, E., Hiratake, J., Kimura, A., Inze, D., Kushnir, S. and Asada, K. A novel NADPH:diamide oxidoreductase activity in *Arabidopsis thaliana* P1 zeta-crystallin. *Eur J Biochem*. 2000, **267**(12), pp.3661-71.
49. Desikan, R., Neill, S.J. and Hancock, J.T. Hydrogen peroxide-induced gene expression in *Arabidopsis thaliana*. *Free Radic Biol Med*. 2000, **28**(5), pp.773-8.
50. Vanderauwera, S., Zimmermann, P., Rombauts, S., Vandenabeele, S., Langebartels, C., Gruissem, W., Inze, D. and Van Breusegem, F. Genome-wide analysis of hydrogen peroxide-regulated gene expression in *Arabidopsis* reveals a high light-induced transcriptional cluster involved in anthocyanin biosynthesis. *Plant Physiol*. 2005, **139**(2), pp.806-21.
51. Salleh, F.M., Evans, K., Goodall, B., Machin, H., Mowla, S.B., Mur, L.A., Runions, J., Theodoulou, F.L., Foyer, C.H. and Rogers, H.J. A novel function for a redox-related LEA protein (SAG21/AtLEA5) in root development and biotic stress responses. *Plant Cell Environ*. 2012, **35**(2), pp.418-29.
52. Zimmermann, P., Hirsch-Hoffmann, M., Hennig, L. and Gruissem, W. GENEVESTIGATOR. *Arabidopsis* microarray database and analysis toolbox. *Plant Physiol*. 2004, **136**(1), pp.2621-32.
53. Miller, J.D., Arteca, R.N. and Pell, E.J. Senescence-associated gene expression during ozone-induced leaf senescence in *Arabidopsis*. *Plant Physiol*. 1999, **120**(4), pp.1015-24.
54. Seki, M., Narusaka, M., Abe, H., Kasuga, M., Yamaguchi-Shinozaki, K., Carninci, P., Hayashizaki, Y. and Shinozaki, K. Monitoring the expression pattern of 1300 *Arabidopsis* genes under drought and cold stresses by using a full-length cDNA microarray. *Plant Cell*. 2001, **13**(1), pp.61-72.
55. Wang, R., Guegler, K., LaBrie, S.T. and Crawford, N.M. Genomic analysis of a nutrient response in *Arabidopsis* reveals diverse expression patterns and novel metabolic and potential regulatory genes induced by nitrate. *Plant Cell*. 2000, **12**(8), pp.1491-509.

56. Liu, G., Kennedy, R., Greenshields, D.L., Peng, G., Forseille, L., Selvaraj, G. and Wei, Y. Detached and attached Arabidopsis leaf assays reveal distinctive defense responses against hemibiotrophic Colletotrichum spp. *Mol Plant Microbe Interact.* 2007, **20**(10), pp.1308-19.
57. Xiao, W., Sheen, J. and Jang, J.C. The role of hexokinase in plant sugar signal transduction and growth and development. *Plant Mol Biol.* 2000, **44**(4), pp.451-61.
58. De Paepe, A., Vuylsteke, M., Van Hummelen, P., Zabeau, M. and Van Der Straeten, D. Transcriptional profiling by cDNA-AFLP and microarray analysis reveals novel insights into the early response to ethylene in Arabidopsis. *Plant J.* 2004, **39**(4), pp.537-59.
59. Jung, C., Lyou, S.H., Yeu, S., Kim, M.A., Rhee, S., Kim, M., Lee, J.S., Choi, Y.D. and Cheong, J.J. Microarray-based screening of jasmonate-responsive genes in *Arabidopsis thaliana*. *Plant Cell Rep.* 2007, **26**(7), pp.1053-63.
60. Zhu, J.K. Salt and drought stress signal transduction in plants. *Annu Rev Plant Biol.* 2002, **53**, pp.247-73.
61. Seo, M. and Koshiba, T. Complex regulation of ABA biosynthesis in plants. *Trends Plant Sci.* 2002, **7**(1), pp.41-8.
62. Fournier-Level, A., Korte, A., Cooper, M.D., Nordborg, M., Schmitt, J. and Wilczek, A.M. A map of local adaptation in *Arabidopsis thaliana*. *Science.* 2011, **334**(6052), pp.86-9.
63. Henze, K. and Martin, W. Evolutionary biology: essence of mitochondria. *Nature.* 2003, **426**(6963), pp.127-8.
64. McBride, H.M., Neuspiel, M. and Wasiak, S. Mitochondria: more than just a powerhouse. *Curr Biol.* 2006, **16**(14), pp.R551-60.
65. Douce, R. General organization of plant mitochondria. In: Douce, R. ed. *Mitochondria in Higher Plants: Structure, Function and Biogenesis.* Orlando, Florida: Academic Press, 1985, pp.1-44.
66. Hood, D.A. and Joseph, A.M. Mitochondrial assembly: protein import. *Proc Nutr Soc.* 2004, **63**(2), pp.293-300.
67. Fox, T.D. Mitochondrial protein synthesis, import, and assembly. *Genetics.* 2012, **192**(4), pp.1203-34.

68. Neupert, W. and Herrmann, J.M. Translocation of proteins into mitochondria. *Annu Rev Biochem.* 2007, **76**, pp.723-49.
69. Ryan, M.T. and Hoogenraad, N.J. Mitochondrial-nuclear communications. *Annu Rev Biochem.* 2007, **76**(1), pp.701-22.
70. Kellems, R.E., Allison, V.F. and Butow, R.A. Cytoplasmic type 80S ribosomes associated with yeast mitochondria. IV. Attachment of ribosomes to the outer membrane of isolated mitochondria. *J Cell Biol.* 1975, **65**(1), pp.1-14.
71. Ades, I.Z. and Butow, R.A. The products of mitochondria-bound cytoplasmic polysomes in yeast. *J Biol Chem.* 1980, **255**(20), pp.9918-24.
72. Suissa, M. and Schatz, G. Import of proteins into mitochondria. Translatable mRNAs for imported mitochondrial proteins are present in free as well as mitochondria-bound cytoplasmic polysomes. *J Biol Chem.* 1982, **257**(21), pp.13048-55.
73. Garcia, M., Darzacq, X., Delaveau, T., Jourden, L., Singer, R.H. and Jacq, C. Mitochondria-associated yeast mRNAs and the biogenesis of molecular complexes. *Mol Biol Cell.* 2007, **18**(2), pp.362-8.
74. Corral-Debrinski, M., Blugeon, C. and Jacq, C. In yeast, the 3' untranslated region or the presequence of ATM1 is required for the exclusive localization of its mRNA to the vicinity of mitochondria. *Mol Cell Biol.* 2000, **20**(21), pp.7881-92.
75. Truscott, K.N., Brandner, K. and Pfanner, N. Mechanisms of protein import into mitochondria. *Curr Biol.* 2003, **13**(8), pp.R326-37.
76. Bolender, N., Sickmann, A., Wagner, R., Meisinger, C. and Pfanner, N. Multiple pathways for sorting mitochondrial precursor proteins. *EMBO Rep.* 2008, **9**(1), pp.42-9.
77. Young, J.C., Hoogenraad, N.J. and Hartl, F.U. Molecular chaperones Hsp90 and Hsp70 deliver preproteins to the mitochondrial import receptor Tom70. *Cell.* 2003, **112**(1), pp.41-50.
78. Abe, Y., Shodai, T., Muto, T., Mihara, K., Torii, H., Nishikawa, S., Endo, T. and Kohda, D. Structural basis of presequence recognition by the mitochondrial protein import receptor Tom20. *Cell.* 2000, **100**(5), pp.551-60.

79. Sirrenberg, C., Bauer, M.F., Guiard, B., Neupert, W. and Brunner, M. Import of carrier proteins into the mitochondrial inner membrane mediated by Tim22. *Nature*. 1996, **384**(6609), pp.582-5.
80. Glaser, S.M., Miller, B.R. and Cumsky, M.G. Removal of a hydrophobic domain within the mature portion of a mitochondrial inner membrane protein causes its mislocalization to the matrix. *Mol Cell Biol*. 1990, **10**(5), pp.1873-81.
81. Hartl, F.U., Schmidt, B., Wachter, E., Weiss, H. and Neupert, W. Transport into mitochondria and intramitochondrial sorting of the Fe/S protein of ubiquinol-cytochrome c reductase. *Cell*. 1986, **47**(6), pp.939-51.
82. Hartl, F.U., Pfanner, N. and Neupert, W. Translocation intermediates on the import pathway of proteins into mitochondria. *Biochem Soc Trans*. 1987, **15**(1), pp.95-7.
83. Mihara, K. and Omura, T. Cytoplasmic chaperones in precursor targeting to mitochondria: the role of MSF and hsp 70. *Trends Cell Biol*. 1996, **6**(3), pp.104-8.
84. Hell, K., Herrmann, J., Pratje, E., Neupert, W. and Stuart, R.A. Oxa1p mediates the export of the N- and C-termini of pCoxII from the mitochondrial matrix to the intermembrane space. *FEBS Lett*. 1997, **418**(3), pp.367-70.
85. Hell, K., Herrmann, J.M., Pratje, E., Neupert, W. and Stuart, R.A. Oxa1p, an essential component of the N-tail protein export machinery in mitochondria. *Proc Natl Acad Sci U S A*. 1998, **95**(5), pp.2250-5.
86. Fernie, A.R., Carrari, F. and Sweetlove, L.J. Respiratory metabolism: glycolysis, the TCA cycle and mitochondrial electron transport. *Curr Opin Plant Biol*. 2004, **7**(3), pp.254-261.
87. Plaxton, W.C. The organization and regulation of plant glycolysis. *Annu Rev Plant Physiol Plant Mol Biol*. 1996, **47**, pp.185-214.
88. Kennedy, R.A., Rumpho, M.E. and Fox, T.C. Anaerobic metabolism in plants. *Plant Physiol*. 1992, **100**(1), pp.1-6.
89. Ricard B, C.I., Raymond P, Saglio P, Saint-Ges V, Pradet A. Plant metabolism under hypoxia and anoxia. *Plant Physiol Biochem*. 1994, **32**, pp.1–10.

90. Krebs, H.A. and Johnson, W.A. Metabolism of ketonic acids in animal tissues. *Biochem J.* 1937, **31**(4), pp.645-60.
91. La Cognata, U., Landschutze, V., Willmitzer, L. and Muller-Rober, B. Structure and expression of mitochondrial citrate synthases from higher plants. *Plant Cell Physiol.* 1996, **37**(7), pp.1022-9.
92. Figueroa, P., Leon, G., Elorza, A., Holuigue, L., Araya, A. and Jordana, X. The four subunits of mitochondrial respiratory complex II are encoded by multiple nuclear genes and targeted to mitochondria in *Arabidopsis thaliana*. *Plant Mol Biol.* 2002, **50**(4-5), pp.725-34.
93. Stiban, J., So, M. and Kaguni, L.S. Iron-sulfur clusters in mitochondrial metabolism: multifaceted roles of a simple cofactor. *Biochemistry (Mosc).* 2016, **81**(10), pp.1066-1080.
94. Efremov, R.G. and Sazanov, L.A. The coupling mechanism of respiratory complex I - a structural and evolutionary perspective. *Biochim Biophys Acta.* 2012, **1817**(10), pp.1785-95.
95. Rasmusson, A.G., Geisler, D.A. and Moller, I.M. The multiplicity of dehydrogenases in the electron transport chain of plant mitochondria. *Mitochondrion.* 2008, **8**(1), pp.47-60.
96. Iverson, T. "Catalytic mechanisms of Complex II enzymes: A structural perspective". *Biochim Biophys Acta.* 2013, **1827**(5), pp.648-57.
97. Zhang, Z., Huang, L., Shulmeister, V.M., Chi, Y.-I., Kim, K.K., Hung, L.-W., Crofts, A.R., Berry, E.A. and Kim, S.-H. Electron transfer by domain movement in cytochrome bc1. *Nature.* 1998, **392**(6677), pp.677-684.
98. Xia, D., Esser, L., Tang, W.-K., Zhou, F., Zhou, Y., Yu, L. and Yu, C.-A. Structural analysis of cytochrome *bc*(1) complexes: implications to the mechanism of function. *Biochim Biophys Acta.* 2013, **1827**(0), pp.1278-1294.
99. Welchen, E. and Gonzalez, D.H. Cytochrome c, a hub linking energy, redox, stress and signaling pathways in mitochondria and other cell compartments. *Physiol Plant.* 2016, **157**(3), pp.310-21.
100. Wikstrom, M.K. Proton pump coupled to cytochrome c oxidase in mitochondria. *Nature.* 1977, **266**(5599), pp.271-3.

101. Hosler, J.P., Ferguson-Miller, S. and Mills, D.A. Energy transduction: proton transfer through the respiratory complexes. *Annu Rev Biochem.* 2006, **75**, pp.165-87.
102. Millenaar, F.F. and Lambers, H. The alternative oxidase: in vivo regulation and function. *Plant Biology.* 2003, **5**(1), pp.2-15.
103. Sweetlove LJ and CH, F. Roles for reactive oxygen species and antioxidants in plant mitochondria. In: DA Day, A.M., J Whelan ed. *Plant Mitochondria: From Genome to Function, Vol. 1 Advances in Photosynthesis and Respiration.* . Dordrecht, The Netherlands: Kluwer Academic Press, 2004, pp.307–320.
104. Turrens, J.F. and Boveris, A. Generation of superoxide anion by the NADH dehydrogenase of bovine heart mitochondria. *Biochem J.* 1980, **191**(2), pp.421-7.
105. Turrens, J.F., Alexandre, A. and Lehninger, A.L. Ubisemiquinone is the electron donor for superoxide formation by complex III of heart mitochondria. *Arch Biochem Biophys.* 1985, **237**(2), pp.408-14.
106. Cadenas, E., Boveris, A., Ragan, C.I. and Stoppani, A.O. Production of superoxide radicals and hydrogen peroxide by NADH-ubiquinone reductase and ubiquinol-cytochrome c reductase from beef-heart mitochondria. *Arch Biochem Biophys.* 1977, **180**(2), pp.248-57.
107. Boveris, A., Cadenas, E. and Stoppani, A.O. Role of ubiquinone in the mitochondrial generation of hydrogen peroxide. *Biochem J.* 1976, **156**(2), pp.435-44.
108. Kagawa, Y. and Racker, E. Partial resolution of the enzymes catalyzing oxidative phosphorylation. 8. Properties of a factor conferring oligomycin sensitivity on mitochondrial adenosine triphosphatase. *J Biol Chem.* 1966, **241**(10), pp.2461-6.
109. McCarty, R.E. A plant biochemist's view of h⁺-ATPases and ATP synthases. *J Exp Biol.* 1992, **172**(Pt 1), pp.431-441.
110. Fernandez Moran, H., Oda, T., Blair, P.V. and Green, D.E. A macromolecular repeating unit of mitochondrial structure and function. correlated electron microscopic and biochemical studies of isolated mitochondria and submitochondrial particles of beef heart muscle. *J Cell Biol.* 1964, **22**, pp.63-100.

111. Fischer, S. and Graber, P. Comparison of ΔpH - and $\Delta\phi$ -driven ATP synthesis catalyzed by the H(+)-ATPases from *Escherichia coli* or chloroplasts reconstituted into liposomes. *FEBS Lett.* 1999, **457**(3), pp.327-32.
112. Boyer, P.D. The ATP synthase--a splendid molecular machine. *Annu Rev Biochem.* 1997, **66**, pp.717-49.
113. Hakulinen, J.K., Klyszejko, A.L., Hoffmann, J., Eckhardt-Strelau, L., Brutschy, B., Vonck, J. and Meier, T. Structural study on the architecture of the bacterial ATP synthase Fo motor. *Proc Natl Acad Sci U S A.* 2012, **109**(30), pp.E2050-6.
114. Jiang, W. and Fillingame, R.H. Interacting helical faces of subunits a and c in the F1Fo ATP synthase of *Escherichia coli* defined by disulfide cross-linking. *Proc Natl Acad Sci U S A.* 1998, **95**(12), pp.6607-12.
115. Stock, D., Leslie, A.G. and Walker, J.E. Molecular architecture of the rotary motor in ATP synthase. *Science.* 1999, **286**(5445), pp.1700-5.
116. Sielaff, H. and Börsch, M. Twisting and subunit rotation in single F(O)F(1)-ATP synthase. *Philos Trans R Soc Lond B Biol Sci.* 2013, **368**(1611).
117. Junge, W., Sielaff, H. and Engelbrecht, S. Torque generation and elastic power transmission in the rotary F(O)F(1)-ATPase. *Nature.* 2009, **459**(7245), pp.364-70.
118. von Ballmoos, C., Cook, G.M. and Dimroth, P. Unique rotary ATP synthase and its biological diversity. *Annu Rev Biophys.* 2008, **37**, pp.43-64.
119. von Ballmoos, C., Wiedenmann, A. and Dimroth, P. Essentials for ATP synthesis by F1F0 ATP synthases. *Annu Rev Biochem.* 2009, **78**, pp.649-72.
120. Junge, W. and Nelson, N. ATP synthase. *Annu Rev Biochem.* 2015, **84**, pp.631-57.
121. Tripathy, B.C. and Oelmüller, R. Reactive oxygen species generation and signaling in plants. *Plant Signal Behav.* 2012, **7**(12), pp.1621-33.
122. Drose, S. and Brandt, U. Molecular mechanisms of superoxide production by the mitochondrial respiratory chain. *Adv Exp Med Biol.* 2012, **748**, pp.145-69.
123. Boveris, A. and Chance, B. The mitochondrial generation of hydrogen peroxide. General properties and effect of hyperbaric oxygen. *Biochem J.* 1973, **134**(3), pp.707-16.

124. Dickinson, B.C. and Chang, C.J. Chemistry and biology of reactive oxygen species in signaling or stress responses. *Nat Chem Biol.* 2011, **7**(8), pp.504-11.
125. Ray, P.D., Huang, B.W. and Tsuji, Y. Reactive oxygen species (ROS) homeostasis and redox regulation in cellular signaling. *Cell Signal.* 2012, **24**(5), pp.981-90.
126. Jain, M., Rivera, S., Monclus, E.A., Synenki, L., Zirk, A., Eisenbart, J., Feghali-Bostwick, C., Mutlu, G.M., Budinger, G.R. and Chandel, N.S. Mitochondrial reactive oxygen species regulate transforming growth factor-beta signaling. *J Biol Chem.* 2013, **288**(2), pp.770-7.
127. Berkowitz, O., De Clercq, I., Van Breusegem, F. and Whelan, J. Interaction between hormonal and mitochondrial signalling during growth, development and in plant defence responses. *Plant Cell Environ.* 2016, **39**(5), pp.1127-39.
128. Liu, Z. and Butow, R.A. A transcriptional switch in the expression of yeast tricarboxylic acid cycle genes in response to a reduction or loss of respiratory function. *Mol Cell Biol.* 1999, **19**(10), pp.6720-8.
129. Puigserver, P., Wu, Z., Park, C.W., Graves, R., Wright, M. and Spiegelman, B.M. A cold-inducible coactivator of nuclear receptors linked to adaptive thermogenesis. *Cell.* 1998, **92**(6), pp.829-39.
130. Amuthan, G., Biswas, G., Ananadatheerthavarada, H.K., Vijayasarathy, C., Shephard, H.M. and Avadhani, N.G. Mitochondrial stress-induced calcium signaling, phenotypic changes and invasive behavior in human lung carcinoma A549 cells. *Oncogene.* 2002, **21**(51), pp.7839-49.
131. Zhao, Q., Wang, J., Levichkin, I.V., Stasinopoulos, S., Ryan, M.T. and Hoogenraad, N.J. A mitochondrial specific stress response in mammalian cells. *EMBO J.* 2002, **21**(17), pp.4411-9.
132. Maxwell, D.P., Nickels, R. and McIntosh, L. Evidence of mitochondrial involvement in the transduction of signals required for the induction of genes associated with pathogen attack and senescence. *Plant J.* 2002, **29**(3), pp.269-79.

133. Maxwell, D.P., Wang, Y. and McIntosh, L. The alternative oxidase lowers mitochondrial reactive oxygen production in plant cells. *Proc Natl Acad Sci U S A*. 1999, **96**(14), pp.8271-6.
134. Yao, N., Tada, Y., Sakamoto, M., Nakayashiki, H., Park, P., Tosa, Y. and Mayama, S. Mitochondrial oxidative burst involved in apoptotic response in oats. *Plant J*. 2002, **30**(5), pp.567-79.
135. Han, D., Antunes, F., Canali, R., Rettori, D. and Cadenas, E. Voltage-dependent anion channels control the release of the superoxide anion from mitochondria to cytosol. *J Biol Chem*. 2003, **278**(8), pp.5557-63.
136. Raven, J.A. and Allen, J.F. Genomics and chloroplast evolution: what did cyanobacteria do for plants? *Genome Biology*. 2003, **4**(3), p.209.
137. Bobik, K. and Burch-Smith, T.M. Chloroplast signaling within, between and beyond cells. *Front Plant Sci*. 2015, **6**(781).
138. Whitney, S.M. and Andrews, T.J. Plastome-encoded bacterial ribulose-1,5-bisphosphate carboxylase/oxygenase (RubisCO) supports photosynthesis and growth in tobacco. *Proc Natl Acad Sci U S A*. 2001, **98**(25), pp.14738-43.
139. Dhingra, A., Portis, A.R., Jr. and Daniell, H. Enhanced translation of a chloroplast-expressed RbcS gene restores small subunit levels and photosynthesis in nuclear RbcS antisense plants. *Proc Natl Acad Sci U S A*. 2004, **101**(16), pp.6315-20.
140. Mayfield, S.P. and Taylor, W.C. Carotenoid-deficient maize seedlings fail to accumulate light-harvesting chlorophyll a/b binding protein (LHCP) mRNA. *Eur J Biochem*. 1984, **144**(1), pp.79-84.
141. Burgess, D.G. and Taylor, W.C. The chloroplast affects the transcription of a nuclear gene family. *Molecular and General Genetics MGG*. 1988, **214**(1), pp.89-96.
142. Taylor, W.C. Regulatory interactions between nuclear and plastid genomes. *Annual review of plant biology*. 1989, **40**(1), pp.211-233.
143. Susek, R.E., Ausubel, F.M. and Chory, J. Signal transduction mutants of Arabidopsis uncouple nuclear CAB and RBCS gene expression from chloroplast development. *Cell*. 1993, **74**(5), pp.787-99.

144. Beck, C.F. Signaling pathways from the chloroplast to the nucleus. *Planta*. 2005, **222**(5), pp.743-56.
145. Nott, A., Jung, H.S., Koussevitzky, S. and Chory, J. Plastid-to-nucleus retrograde signaling. *Annu Rev Plant Biol*. 2006, **57**, pp.739-59.
146. Sullivan, J.A. and Gray, J.C. Multiple plastid signals regulate the expression of the pea plastocyanin gene in pea and transgenic tobacco plants. *Plant J*. 2002, **32**(5), pp.763-74.
147. Strand, A., Asami, T., Alonso, J., Ecker, J.R. and Chory, J. Chloroplast to nucleus communication triggered by accumulation of Mg-protoporphyrinIX. *Nature*. 2003, **421**(6918), pp.79-83.
148. Sakuma, Y., Liu, Q., Dubouzet, J.G., Abe, H., Shinozaki, K. and Yamaguchi-Shinozaki, K. DNA-binding specificity of the ERF/AP2 domain of Arabidopsis DREBs, transcription factors involved in dehydration- and cold-inducible gene expression. *Biochem Biophys Res Commun*. 2002, **290**(3), pp.998-1009.
149. Wu, G., Ortiz-Flores, G., Ortiz-Lopez, A. and Ort, D.R. A point mutation in atpC1 raises the redox potential of the Arabidopsis chloroplast ATP synthase gamma-subunit regulatory disulfide above the range of thioredoxin modulation. *J Biol Chem*. 2007, **282**(51), pp.36782-9.
150. Ohme-Takagi, M. and Shinshi, H. Ethylene-inducible DNA binding proteins that interact with an ethylene-responsive element. *Plant Cell*. 1995, **7**(2), pp.173-82.
151. Licausi, F., Ohme-Takagi, M. and Perata, P. APETALA2/Ethylene Responsive Factor (AP2/ERF) transcription factors: mediators of stress responses and developmental programs. *New Phytol*. 2013, **199**(3), pp.639-49.
152. Sakuma, Y., Maruyama, K., Osakabe, Y., Qin, F., Seki, M., Shinozaki, K. and Yamaguchi-Shinozaki, K. Functional analysis of an Arabidopsis transcription factor, DREB2A, involved in drought-responsive gene expression. *Plant Cell*. 2006, **18**(5), pp.1292-309.
153. Hao, D., Ohme-Takagi, M. and Sarai, A. Unique mode of GCC box recognition by the DNA-binding domain of ethylene-responsive element-binding factor (ERF domain) in plant. *J Biol Chem*. 1998, **273**(41), pp.26857-61.
154. Riechmann, J.L. and Meyerowitz, E.M. The AP2/EREBP family of plant transcription factors. *Biol Chem*. 1998, **379**(6), pp.633-46.

155. Cai, X.T., Xu, P., Zhao, P.X., Liu, R., Yu, L.H. and Xiang, C.B. Arabidopsis ERF109 mediates cross-talk between jasmonic acid and auxin biosynthesis during lateral root formation. *Nat Commun.* 2014, **5**, p.5833.
156. Khandelwal, A., Elvitigala, T., Ghosh, B. and Quatrano, R.S. Arabidopsis transcriptome reveals control circuits regulating redox homeostasis and the role of an AP2 transcription factor. *Plant Physiol.* 2008, **148**(4), pp.2050-8.
157. Foyer, C.H., Karpinska, B. and Krupinska, K. The functions of WHIRLY1 and REDOX-RESPONSIVE TRANSCRIPTION FACTOR 1 in cross tolerance responses in plants: a hypothesis. *Philos Trans R Soc Lond B Biol Sci.* 2014, **369**(1640), p.20130226.
158. Gordon, M.J., Carmody, M., Albrecht, V. and Pogson, B. Systemic and local responses to repeated HL stress-induced retrograde signaling in Arabidopsis. *Front Plant Sci.* 2012, **3**, p.303.
159. Triantaphylides, C. and Havaux, M. Singlet oxygen in plants: production, detoxification and signaling. *Trends Plant Sci.* 2009, **14**(4), pp.219-28.
160. Triantaphylides, C., Krischke, M., Hoerberichts, F.A., Ksas, B., Gresser, G., Havaux, M., Van Breusegem, F. and Mueller, M.J. Singlet oxygen is the major reactive oxygen species involved in photooxidative damage to plants. *Plant Physiol.* 2008, **148**(2), pp.960-8.
161. Gonzalez-Perez, S., Gutierrez, J., Garcia-Garcia, F., Osuna, D., Dopazo, J., Lorenzo, O., Revuelta, J.L. and Arellano, J.B. Early transcriptional defense responses in Arabidopsis cell suspension culture under high-light conditions. *Plant Physiol.* 2011, **156**(3), pp.1439-56.
162. Matsuo, M., Johnson, J.M., Hieno, A., Tokizawa, M., Nomoto, M., Tada, Y., Godfrey, R., Obokata, J., Sherameti, I., Yamamoto, Y.Y., Bohmer, F.D. and Oelmuller, R. High REDOX RESPONSIVE TRANSCRIPTION FACTOR1 levels result in accumulation of reactive oxygen species in *Arabidopsis thaliana* shoots and roots. *Mol Plant.* 2015, **8**(8), pp.1253-73.
163. Kerchev, P.I., Karpinska, B., Morris, J.A., Hussain, A., Verrall, S.R., Hedley, P.E., Fenton, B., Foyer, C.H. and Hancock, R.D. Vitamin C and the abscisic acid-insensitive 4 transcription factor are important determinants of aphid resistance in Arabidopsis. *Antioxid Redox Signal.* 2013, **18**(16), pp.2091-105.

164. Wang, Z., Cao, G., Wang, X., Miao, J., Liu, X., Chen, Z., Qu, L.J. and Gu, H. Identification and characterization of COI1-dependent transcription factor genes involved in JA-mediated response to wounding in Arabidopsis plants. *Plant Cell Rep.* 2008, **27**(1), pp.125-35.
165. McGrath, K.C., Dombrecht, B., Manners, J.M., Schenk, P.M., Edgar, C.I., Maclean, D.J., Scheible, W.R., Udvardi, M.K. and Kazan, K. Repressor- and activator-type ethylene response factors functioning in jasmonate signaling and disease resistance identified via a genome-wide screen of Arabidopsis transcription factor gene expression. *Plant Physiol.* 2005, **139**(2), pp.949-59.
166. Shinozaki, K., Yamaguchi-Shinozaki, K. and Seki, M. Regulatory network of gene expression in the drought and cold stress responses. *Curr Opin Plant Biol.* 2003, **6**(5), pp.410-7.
167. de Ollas, C., Arbona, V. and Gomez-Cadenas, A. Jasmonic acid interacts with abscisic acid to regulate plant responses to water stress conditions. *Plant Signal Behav.* 2015, **10**(12), p.e1078953.
168. Schindelin, J., Arganda-Carreras, I., Frise, E., Kaynig, V., Longair, M., Pietzsch, T., Preibisch, S., Rueden, C., Saalfeld, S., Schmid, B., Tinevez, J.Y., White, D.J., Hartenstein, V., Eliceiri, K., Tomancak, P. and Cardona, A. Fiji: an open-source platform for biological-image analysis. *Nat Methods.* 2012, **9**(7), pp.676-82.
169. Hornik, K. *The RFAQ*. [Online]. 2013. [Accessed]. Available from: <http://cran.r-project.org/doc/FAQ/R-FAQ.html>
170. Lichtenthaler, H.K. Chlorophylls and carotenoids: Pigments of photosynthetic biomembranes. In: *Methods in Enzymology*. Academic Press, 1987, pp.350-382.
171. Neff, M.M. and Chory, J. Genetic interactions between phytochrome A, phytochrome B, and cryptochrome 1 during Arabidopsis development. *Plant Physiol.* 1998, **118**(1), pp.27-36.
172. Wierer, S., Peter, S., Elgass, K., Mack, H.G., Bieker, S., Meixner, A.J., Zentgraf, U. and Schleifenbaum, F. Determination of the in vivo redox potential by one-wavelength spectro-microscopy of roGFP. *Anal Bioanal Chem.* 2012, **403**(3), pp.737-44.

173. Inoue, H., Nojima, H. and Okayama, H. High efficiency transformation of *Escherichia coli* with plasmids. *Gene*. 1990, **96**(1), pp.23-8.
174. Kozak, M. An analysis of 5'-noncoding sequences from 699 vertebrate messenger RNAs. *Nucleic Acids Res.* 1987, **15**(20), pp.8125-48.
175. Van Leene, J., Stals, H., Eeckhout, D., Persiau, G., Van De Slijke, E., Van Isterdael, G., De Clercq, A., Bonnet, E., Laukens, K., Remmerie, N., Henderickx, K., De Vijlder, T., Abdelkrim, A., Pharazyn, A., Van Onckelen, H., Inze, D., Witters, E. and De Jaeger, G. A tandem affinity purification-based technology platform to study the cell cycle interactome in *Arabidopsis thaliana*. *Mol Cell Proteomics*. 2007, **6**(7), pp.1226-38.
176. Vandepoele, K., Raes, J., De Veylder, L., Rouze, P., Rombauts, S. and Inze, D. Genome-wide analysis of core cell cycle genes in Arabidopsis. *Plant Cell*. 2002, **14**(4), pp.903-16.
177. Menges, M. and Murray, J.A. Synchronous Arabidopsis suspension cultures for analysis of cell-cycle gene activity. *Plant J*. 2002, **30**(2), pp.203-12.
178. Van Leene, J., Eeckhout, D., Persiau, G., Van De Slijke, E., Geerinck, J., Van Isterdael, G., Witters, E. and De Jaeger, G. Isolation of transcription factor complexes from Arabidopsis cell suspension cultures by tandem affinity purification. *Methods Mol Biol*. 2011, **754**, pp.195-218.
179. Shevchenko, A., Wilm, M., Vorm, O. and Mann, M. Mass spectrometric sequencing of proteins silver-stained polyacrylamide gels. *Anal Chem*. 1996, **68**(5), pp.850-8.
180. Rice, P., Longden, I. and Bleasby, A. EMBOSS: the European molecular biology open software suite. *Trends Genet*. 2000, **16**(6), pp.276-7.
181. Wu, F.H., Shen, S.C., Lee, L.Y., Lee, S.H., Chan, M.T. and Lin, C.S. Tape-Arabidopsis Sandwich - a simpler Arabidopsis protoplast isolation method. *Plant Methods*. 2009, **5**, p.16.
182. Yoo, S.D., Cho, Y.H. and Sheen, J. Arabidopsis mesophyll protoplasts: a versatile cell system for transient gene expression analysis. *Nat Protoc*. 2007, **2**(7), pp.1565-72.
183. Altenhoff, A.M., Skunca, N., Glover, N., Train, C.M., Sueki, A., Pilizota, I., Gori, K., Tomiczek, B., Muller, S., Redestig, H., Gonnet, G.H. and Dessimoz, C. The OMA orthology database in 2015: function predictions, better plant support, synteny view and other improvements. *Nucleic Acids Res*. 2015, **43**(Database issue), pp.D240-9.

184. Verslues, P.E., Agarwal, M., Katiyar-Agarwal, S., Zhu, J. and Zhu, J.K. Methods and concepts in quantifying resistance to drought, salt and freezing, abiotic stresses that affect plant water status. *Plant J.* 2006, **45**(4), pp.523-39.
185. Schnaubelt, D., Schulz, P., Hannah, M.A., Yocgo, R.E. and Foyer, C.H. A phenomics approach to the analysis of the influence of glutathione on leaf area and abiotic stress tolerance in *Arabidopsis thaliana*. *Front Plant Sci.* 2013, **4**, p.416.
186. Munns, R. and Tester, M. Mechanisms of salinity tolerance. *Annu Rev Plant Biol.* 2008, **59**, pp.651-81.
187. Lawlor, D.W. Genetic engineering to improve plant performance under drought: physiological evaluation of achievements, limitations, and possibilities. *J Exp Bot.* 2013, **64**(1), pp.83-108.
188. Gill, S.S. and Tuteja, N. Reactive oxygen species and antioxidant machinery in abiotic stress tolerance in crop plants. *Plant Physiol Biochem.* 2010, **48**(12), pp.909-30.
189. Deikman, J., Petracek, M. and Heard, J.E. Drought tolerance through biotechnology: improving translation from the laboratory to farmers' fields. *Curr Opin Biotechnol.* 2012, **23**(2), pp.243-50.
190. Pogson, B.J., Woo, N.S., Forster, B. and Small, I.D. Plastid signalling to the nucleus and beyond. *Trends Plant Sci.* 2008, **13**(11), pp.602-9.
191. Day, D.A., Neuburger, M. and Douce, R. Biochemical-characterization of chlorophyll-free mitochondria from pea leaves. *Australian Journal of Plant Physiology.* 1985, **12**(3), pp.219-228.
192. Bykova, N.V., Keerberg, O., Parnik, T., Bauwe, H. and Gardestrom, P. Interaction between photorespiration and respiration in transgenic potato plants with antisense reduction in glycine decarboxylase. *Planta.* 2005, **222**(1), pp.130-40.
193. Kearns, A., Whelan, J., Young, S., Elthon, T.E. and Day, D.A. Tissue-specific expression of the alternative oxidase in soybean and siratro. *Plant Physiol.* 1992, **99**(2), pp.712-7.
194. Clark, L.C., Jr., Wolf, R., Granger, D. and Taylor, Z. Continuous recording of blood oxygen tensions by polarography. *J Appl Physiol.* 1953, **6**(3), pp.189-93.

195. Severinghaus, J.W. and Astrup, P.B. History of blood gas analysis. IV. Leland Clark's oxygen electrode. *J Clin Monit.* 1986, **2**(2), pp.125-39.
196. Shaw, D.S., Meitha, K., Considine, M.J. and Foyer, C.H. Mitochondrial respiration and oxygen tension. *in press.* 2016.
197. Degli Esposti, M. Assessing functional integrity of mitochondria in vitro and in vivo. *Methods Cell Biol.* 2001, **65**, pp.75-96.
198. Sanchez, C., Lachaize, C., Janody, F., Bellon, B., Röder, L., Euzenat, J., Rechenmann, F. and Jacq, B. Grasping at molecular interactions and genetic networks in *Drosophila melanogaster* using FlyNets, an Internet database. *Nucleic Acids Res.* 1999, **27**(1), pp.89-94.
199. Rigaut, G., Shevchenko, A., Rutz, B., Wilm, M., Mann, M. and Seraphin, B. A generic protein purification method for protein complex characterization and proteome exploration. *Nat Biotechnol.* 1999, **17**(10), pp.1030-2.
200. Burckstummer, T., Bennett, K.L., Preradovic, A., Schutze, G., Hantschel, O., Superti-Furga, G. and Bauch, A. An efficient tandem affinity purification procedure for interaction proteomics in mammalian cells. *Nat Methods.* 2006, **3**(12), pp.1013-9.
201. Rohila, J.S., Chen, M., Cerny, R. and Fromm, M.E. Improved tandem affinity purification tag and methods for isolation of protein heterocomplexes from plants. *Plant J.* 2004, **38**(1), pp.172-81.
202. Van Leene, J., Witters, E., Inze, D. and De Jaeger, G. Boosting tandem affinity purification of plant protein complexes. *Trends Plant Sci.* 2008, **13**(10), pp.517-20.
203. Rubio, V., Shen, Y., Saijo, Y., Liu, Y., Gusmaroli, G., Dinesh-Kumar, S.P. and Deng, X.W. An alternative tandem affinity purification strategy applied to Arabidopsis protein complex isolation. *Plant J.* 2005, **41**(5), pp.767-78.
204. Chang, I.F. Mass spectrometry-based proteomic analysis of the epitope-tag affinity purified protein complexes in eukaryotes. *Proteomics.* 2006, **6**(23), pp.6158-66.
205. Feng, X., Liu, X., Luo, Q. and Liu, B.F. Mass spectrometry in systems biology: an overview. *Mass Spectrom Rev.* 2008, **27**(6), pp.635-60.

206. Horstman, A., Nougalli Tonaco, I.A., Boutilier, K. and Immink, R.G.H. A Cautionary Note on the Use of Split-YFP/BiFC in Plant Protein-Protein Interaction Studies. *Int J Mol Sci.* 2014, **15**(6), pp.9628-43.
207. Bracha-Drori, K., Shichrur, K., Katz, A., Oliva, M., Angelovici, R., Yalovsky, S. and Ohad, N. Detection of protein-protein interactions in plants using bimolecular fluorescence complementation. *Plant J.* 2004, **40**(3), pp.419-27.
208. Citovsky, V., Lee, L.Y., Vyas, S., Glick, E., Chen, M.H., Vainstein, A., Gafni, Y., Gelvin, S.B. and Tzfira, T. Subcellular localization of interacting proteins by bimolecular fluorescence complementation in planta. *J Mol Biol.* 2006, **362**(5), pp.1120-31.
209. Ohad, N., Shichrur, K. and Yalovsky, S. The analysis of protein-protein interactions in plants by bimolecular fluorescence complementation. *Plant Physiol.* 2007, **145**(4), pp.1090-9.
210. Citovsky, V., Gafni, Y. and Tzfira, T. Localizing protein-protein interactions by bimolecular fluorescence complementation in planta. *Methods.* 2008, **45**(3), pp.196-206.
211. Waterworth, W.M., Drury, G.E., Blundell-Hunter, G. and West, C.E. Arabidopsis TAF1 is an MRE11-interacting protein required for resistance to genotoxic stress and viability of the male gametophyte. *Plant J.* 2015, **84**(3), pp.545-57.
212. Van Leene, J., Eeckhout, D., Cannoot, B., De Winne, N., Persiau, G., Van De Slijke, E., Vercruyssen, L., Dedeker, M., Verkest, A., Vandepoele, K., Martens, L., Witters, E., Gevaert, K. and De Jaeger, G. An improved toolbox to unravel the plant cellular machinery by tandem affinity purification of Arabidopsis protein complexes. *Nat Protoc.* 2015, **10**(1), pp.169-87.
213. Emanuelsson, O., Nielsen, H., Brunak, S. and von Heijne, G. Predicting subcellular localization of proteins based on their N-terminal amino acid sequence. *J Mol Biol.* 2000, **300**(4), pp.1005-16.
214. Kanai, M., Hayashi, M., Kondo, M. and Nishimura, M. The plastidic DEAD-box RNA helicase 22, HS3, is essential for plastid functions both in seed development and in seedling growth. *Plant Cell Physiol.* 2013, **54**(9), pp.1431-40.

215. Konishi, T., Shinohara, K., Yamada, K. and Sasaki, Y. Acetyl-CoA carboxylase in higher plants: Most plants other than gramineae have both the prokaryotic and the eukaryotic forms of this enzyme. *Plant and Cell Physiology*. 1996, **37**(2), pp.117-122.
216. Ke, J., Wen, T.N., Nikolau, B.J. and Wurtele, E.S. Coordinate regulation of the nuclear and plastidic genes coding for the subunits of the heteromeric acetyl-coenzyme A carboxylase. *Plant Physiol*. 2000, **122**(4), pp.1057-71.
217. Sasaki, Y. and Nagano, Y. Plant acetyl-CoA carboxylase: structure, biosynthesis, regulation, and gene manipulation for plant breeding. *Biosci Biotechnol Biochem*. 2004, **68**(6), pp.1175-84.
218. Cahoon, E.B., Shockey, J.M., Dietrich, C.R., Gidda, S.K., Mullen, R.T. and Dyer, J.M. Engineering oilseeds for sustainable production of industrial and nutritional feedstocks: solving bottlenecks in fatty acid flux. *Curr Opin Plant Biol*. 2007, **10**(3), pp.236-44.
219. Mehterov, N., Balazadeh, S., Hille, J., Toneva, V., Mueller-Roeber, B. and Gechev, T. Oxidative stress provokes distinct transcriptional responses in the stress-tolerant *atr7* and stress-sensitive *loh2* *Arabidopsis thaliana* mutants as revealed by multi-parallel quantitative real-time PCR analysis of ROS marker and antioxidant genes. *Plant Physiol Biochem*. 2012, **59**, pp.20-9.
220. Sun, J., Xu, Y., Ye, S., Jiang, H., Chen, Q., Liu, F., Zhou, W., Chen, R., Li, X., Tietz, O., Wu, X., Cohen, J.D., Palme, K. and Li, C. Arabidopsis ASA1 is important for jasmonate-mediated regulation of auxin biosynthesis and transport during lateral root formation. *Plant Cell*. 2009, **21**(5), pp.1495-511.
221. Zhao, Y., Christensen, S.K., Fankhauser, C., Cashman, J.R., Cohen, J.D., Weigel, D. and Chory, J. A role for flavin monooxygenase-like enzymes in auxin biosynthesis. *Science*. 2001, **291**(5502), pp.306-9.
222. Cheng, Y., Dai, X. and Zhao, Y. Auxin biosynthesis by the YUCCA flavin monooxygenases controls the formation of floral organs and vascular tissues in Arabidopsis. *Genes Dev*. 2006, **20**(13), pp.1790-9.
223. Petricka, J.J., Winter, C.M. and Benfey, P.N. Control of Arabidopsis root development. *Annu Rev Plant Biol*. 2012, **63**, pp.563-90.

224. De Smet, I., White, P.J., Bengough, A.G., Dupuy, L., Parizot, B., Casimiro, I., Heidstra, R., Laskowski, M., Lepetit, M., Hochholdinger, F., Draye, X., Zhang, H., Broadley, M.R., Peret, B., Hammond, J.P., Fukaki, H., Mooney, S., Lynch, J.P., Nacry, P., Schurr, U., Laplaze, L., Benfey, P., Beeckman, T. and Bennett, M. Analyzing lateral root development: how to move forward. *Plant Cell*. 2012, **24**(1), pp.15-20.
225. Marhavy, P., Vanstraelen, M., De Rybel, B., Zhaojun, D., Bennett, M.J., Beeckman, T. and Benkova, E. Auxin reflux between the endodermis and pericycle promotes lateral root initiation. *EMBO J*. 2013, **32**(1), pp.149-58.
226. Lavenus, J., Goh, T., Roberts, I., Guyomarc'h, S., Lucas, M., De Smet, I., Fukaki, H., Beeckman, T., Bennett, M. and Laplaze, L. Lateral root development in Arabidopsis: fifty shades of auxin. *Trends Plant Sci*. 2013, **18**(8), pp.450-8.
227. Fukaki, H. and Tasaka, M. Hormone interactions during lateral root formation. *Plant Mol Biol*. 2009, **69**(4), pp.437-49.
228. Simon, S. and Petrasek, J. Why plants need more than one type of auxin. *Plant Sci*. 2011, **180**(3), pp.454-60.
229. Abel, S., Nguyen, M.D. and Theologis, A. The PS-IAA4/5-like family of early auxin-inducible mRNAs in *Arabidopsis thaliana*. *J Mol Biol*. 1995, **251**(4), pp.533-49.
230. Calderon Villalobos, L.I., Lee, S., De Oliveira, C., Ivetac, A., Brandt, W., Armitage, L., Sheard, L.B., Tan, X., Parry, G., Mao, H., Zheng, N., Napier, R., Kepinski, S. and Estelle, M. A combinatorial TIR1/AFB-Aux/IAA co-receptor system for differential sensing of auxin. *Nat Chem Biol*. 2012, **8**(5), pp.477-85.
231. Kelley, D.R. and Estelle, M. Ubiquitin-mediated control of plant hormone signaling. *Plant Physiol*. 2012, **160**(1), pp.47-55.
232. Goh, T., Joi, S., Mimura, T. and Fukaki, H. The establishment of asymmetry in Arabidopsis lateral root founder cells is regulated by LBD16/ASL18 and related LBD/ASL proteins. *Development*. 2012, **139**(5), pp.883-93.
233. Sun, Z.M., Zhou, M.L., Dan, W., Tang, Y.X., Lin, M. and Wu, Y.M. Overexpression of the *Lotus corniculatus* soloist gene LcAP2/ERF107 enhances tolerance to salt stress. *Protein Pept Lett*. 2016, **23**(5), pp.442-9.

234. Summers, L.A. *The Bipyridinium Herbicides*. New York, NY: Academic Press, 1980.
235. Hassan, H.M. and Fridovich, I. Intracellular production of superoxide radical and of hydrogen peroxide by redox active compounds. *Arch Biochem Biophys*. 1979, **196**(2), pp.385-95.
236. Sun, Y.L., Zhao, Y., Hong, X. and Zhai, Z.H. Cytochrome *c* release and caspase activation during menadione-induced apoptosis in plants. *FEBS Lett*. 1999, **462**(3), pp.317-21.
237. Alberts, B. The cell as a collection of protein machines: preparing the next generation of molecular biologists. *Cell*. 1998, **92**(3), pp.291-4.
238. Mingam, A., Toffano-Nioche, C., Brunaud, V., Boudet, N., Kreis, M. and Lecharny, A. DEAD-box RNA helicases in *Arabidopsis thaliana*: establishing a link between quantitative expression, gene structure and evolution of a family of genes. *Plant Biotechnol J*. 2004, **2**(5), pp.401-15.
239. Missbach, S., Weis, B.L., Martin, R., Simm, S., Bohnsack, M.T. and Schleiff, E. 40S ribosome biogenesis co-factors are essential for gametophyte and embryo development. *PLoS One*. 2013, **8**(1), p.e54084.
240. Verslues, P.E., Guo, Y., Dong, C.H., Ma, W. and Zhu, J.K. Mutation of *SAD2*, an importin beta-domain protein in *Arabidopsis*, alters abscisic acid sensitivity. *Plant J*. 2006, **47**(5), pp.776-87.
241. West, G., Viitanen, L., Alm, C., Mattjus, P., Salminen, T.A. and Edqvist, J. Identification of a glycosphingolipid transfer protein GLTP1 in *Arabidopsis thaliana*. *Febs j*. 2008, **275**(13), pp.3421-37.
242. Pinosa, F., Begheldo, M., Pasternak, T., Zermiani, M., Paponov, I.A., Dovzhenko, A., Barcaccia, G., Ruperti, B. and Palme, K. The *Arabidopsis thaliana Mob1A* gene is required for organ growth and correct tissue patterning of the root tip. *Ann Bot*. 2013, **112**(9), pp.1803-14.
243. Synek, L., Schlager, N., Elias, M., Quentin, M., Hauser, M.T. and Zarsky, V. AtEXO70A1, a member of a family of putative exocyst subunits specifically expanded in land plants, is important for polar growth and plant development. *Plant J*. 2006, **48**(1), pp.54-72.
244. Zarsky, V., Cvrckova, F., Potocky, M. and Hala, M. Exocytosis and cell polarity in plants - exocyst and recycling domains. *New Phytol*. 2009, **183**(2), pp.255-72.

245. Liu, Y., Deng, Y., Li, G. and Zhao, J. Replication factor C1 (RFC1) is required for double-strand break repair during meiotic homologous recombination in Arabidopsis. *Plant J.* 2013, **73**(1), pp.154-65.
246. Liu, Q., Wang, J., Miki, D., Xia, R., Yu, W., He, J., Zheng, Z., Zhu, J.K. and Gong, Z. DNA replication factor C1 mediates genomic stability and transcriptional gene silencing in Arabidopsis. *Plant Cell.* 2010, **22**(7), pp.2336-52.
247. Bolle, C. The role of GRAS proteins in plant signal transduction and development. *Planta.* 2004, **218**(5), pp.683-92.
248. Huanca-Mamani, W., Garcia-Aguilar, M., Leon-Martinez, G., Grossniklaus, U. and Vielle-Calzada, J.P. CHR11, a chromatin-remodeling factor essential for nuclear proliferation during female gametogenesis in *Arabidopsis thaliana*. *Proc Natl Acad Sci U S A.* 2005, **102**(47), pp.17231-6.
249. Zhao, J., Zhang, W., Zhao, Y., Gong, X., Guo, L., Zhu, G., Wang, X., Gong, Z., Schumaker, K.S. and Guo, Y. SAD2, an importin -like protein, is required for UV-B response in Arabidopsis by mediating MYB4 nuclear trafficking. *Plant Cell.* 2007, **19**(11), pp.3805-18.
250. Jin, H., Cominelli, E., Bailey, P., Parr, A., Mehrrens, F., Jones, J., Tonelli, C., Weisshaar, B. and Martin, C. Transcriptional repression by AtMYB4 controls production of UV-protecting sunscreens in Arabidopsis. *EMBO J.* 2000, **19**(22), pp.6150-61.
251. Friml, J., Benkova, E., Blilou, I., Wisniewska, J., Hamann, T., Ljung, K., Woody, S., Sandberg, G., Scheres, B., Jurgens, G. and Palme, K. AtPIN4 mediates sink-driven auxin gradients and root patterning in Arabidopsis. *Cell.* 2002, **108**(5), pp.661-73.
252. Boyer, J.S. Plant productivity and environment. *Science.* 1982, **218**(4571), pp.443-8.
253. Mittler, R. Abiotic stress, the field environment and stress combination. *Trends Plant Sci.* 2006, **11**(1), pp.15-9.
254. Kerr, R.A. Climate change. Global warming is changing the world. *Science.* 2007, **316**(5822), pp.188-90.
255. Bates, B.C., Kundzewicz, Z.W., Wu, S. and Palutikof, J.P. *Climate change and water: IPCC Technical Paper VI.* 2008.

256. Lemaux, P.G. Genetically engineered plants and foods: a scientist's analysis of the issues (part I). *Annu Rev Plant Biol.* 2008, **59**, pp.771-812.
257. Lemaux, P.G. Genetically engineered plants and foods: a scientist's analysis of the issues (part II). *Annu Rev Plant Biol.* 2009, **60**, pp.511-59.
258. Cottage, A., Mott, E.K., Kempster, J.A. and Gray, J.C. The Arabidopsis plastid-signalling mutant *gun1* (genomes uncoupled1) shows altered sensitivity to sucrose and abscisic acid and alterations in early seedling development. *J Exp Bot.* 2010, **61**(13), pp.3773-86.